

**FORM AND FUNCTION IN HUMMINGBIRD FLIGHT**

by

DIMITRI ARIEL SKANDALIS

B.Sc., Brock University, 2007

M.Sc., University of Ottawa, 2010

A THESIS SUBMITTED IN PARTIAL FULFILLMENT OF  
THE REQUIREMENTS FOR THE DEGREE OF

DOCTOR OF PHILOSOPHY

in

THE FACULTY OF GRADUATE AND POSTDOCTORAL STUDIES

(Zoology)

THE UNIVERSITY OF BRITISH COLUMBIA

(Vancouver)

December 2017

© Dimitri Ariel Skandalis, 2017

## **Abstract**

The extent to which locomotor adaptations depend on evolution of morphological form or kinematic function remains an open question. Hummingbirds are a speciose group with exceptional aerial abilities across a large range of habitats, making them attractive models for biomechanical studies of coupled form and function. Here, I investigate the origin of hummingbird flight performance among and within species, and within individuals. I develop a novel biomechanical framework adapted from aerodynamic principles, and find that a weight-support strategy thus far only identified among hummingbird species is likely a response to selection for constant, mass-independent hovering and burst performance. Within species, hummingbirds exhibit an alternative weight-support strategy that instead results in reduced flight performance in larger individuals. I next develop experimental and analytical techniques to investigate the time- and behaviour-dependence of wing morphology and kinematics. Within individuals, flight performance depends on fine adjustments to wing kinematics and wing morphology, including wing twisting and cambering. I suggest that individual hummingbirds dynamically control their wing morphology to minimise the cost of flight rather than maximise force production, but can sacrifice flight efficiency to enable challenging flight behaviours. Wing morphing therefore offers flight control degrees of freedom that can be called upon as required. Taken together, I propose that evolution of wing form maximises average performance, but also maximises the scope for dynamic wing control.

## **Lay Summary**

Hummingbirds possess remarkable aerial agility and many unique traits for high-performance flight. I examine the mechanisms that have evolved to support hummingbirds' extreme flight behaviours, and ask whether specialising in one aspect of flight performance comes at the cost of another. I find that hummingbirds have evolved an unexpected and novel flight strategy that results in size-independent flight performance. I also find that despite convergence on insect-like flight, hummingbirds have retained a crucial feature of vertebrate flight, the ability to morph their wing shape on the fly. Taken together, I suggest that hummingbird evolution has favoured adaptations that not only minimise the cost of flight, but maximise behavioural flexibility.

## Preface

This work was conducted with the approval of the UBC Animal Care Committee, certificate A15-0116, in the laboratory of Douglas L. Altshuler (DLA) at UBC Point Grey campus.

Chapters 1 and 4 are original and were written by me (DAS). Chapter 2 is published in *Nature Communications* (Skandalis et al. *Nat. Comm.* 8(1):1047) and was completed in collaboration with an international team of researchers: Paolo S. Segre (PSS), Joseph W. Bahlman (JWB), Derrick Groom (DG), Kenneth C. Welch, Jr. (KCW), Christopher C. Witt (CCW), Jimmy A. McGuire (JAM), Robert Dudley (RD), David Lentink (DL), and Douglas L. Altshuler (DLA). I was the lead investigator, responsible for the majority of conception and design of the aerodynamic framework, development and implementation of the analytical methods, quality control of the data, and the majority of writing and figure creation. Overall, DAS and DLA conceived of the study; DAS, DL, DLA, JWB, and RD developed the modeling and aerodynamic framework; RD contributed criticisms; DLA, JAM, PSS, CCW, DG, and KCW collected field measurements; DAS analysed data; and DAS and DLA wrote the text. All authors edited the text. Chapter 3 is original and unpublished, and was completed in collaboration with Benny Goller (BG), Vikram Baliga (VB), and DLA. I conceived of the marker capture method, treatment conditions, and surface reconstruction techniques, digitised all high-speed marker data, implemented all analyses, and wrote the text. DAS and BG developed the animal handling and marking techniques; DAS and DLA developed the research questions; and VB contributed the anatomical drawing of the hummingbird wing, with direction and editing by DAS.

# Table of Contents

<b>Abstract.....</b>	<b>ii</b>
<b>Lay Summary .....</b>	<b>iii</b>
<b>Preface.....</b>	<b>iv</b>
<b>Table of Contents .....</b>	<b>v</b>
<b>List of Tables .....</b>	<b>viii</b>
<b>List of Figures.....</b>	<b>ix</b>
<b>List of Statistical Symbols and Distributions .....</b>	<b>xi</b>
<b>List of Physical Symbols.....</b>	<b>xii</b>
<b>List of Abbreviations .....</b>	<b>xiv</b>
<b>Glossary .....</b>	<b>xv</b>
<b>Acknowledgements .....</b>	<b>xvii</b>
<b>Chapter 1: Introduction .....</b>	<b>1</b>
1.1 The form-function-fitness paradigm.....	1
1.2 Hummingbirds in the form-function-fitness paradigm.....	7
1.2.1 Behaviour and reproduction.....	8
1.2.2 Form and function.....	16
1.2.3 Ecological context.....	27
1.3 Allometry and the origin of the hummingbird performance envelope .....	30
1.4 Thesis objectives and outline .....	35
<b>Chapter 2: The biomechanical origin of extreme wing allometry in hummingbirds .....</b>	<b>42</b>
2.1 Introduction.....	42

2.2	Methods.....	45
2.2.1	Data collection .....	45
2.2.2	Phylogenetic uncertainty.....	47
2.2.3	Regressions and hierarchical Bayesian modeling.....	49
2.2.4	Force equation for flapping flight.....	51
2.2.5	Allometry of aerodynamic force.....	53
2.2.6	Induced power calculation .....	56
2.2.7	Data analysis .....	59
2.3	Results.....	60
2.4	Discussion.....	65
<b>Chapter 3: Hummingbirds dynamically control wing shape to tune flight efficiency and modulate aerodynamic force.....</b>		<b>82</b>
3.1	Introduction.....	82
3.2	Methods.....	86
3.2.1	Wing anatomy.....	86
3.2.2	Hovering flight challenges .....	86
3.2.3	Wing and body marking.....	88
3.2.4	Marker tracking.....	89
3.2.5	Mesh reconstruction.....	91
3.2.6	Kinematics and morphology in flight .....	92
3.2.7	Aerodynamic forces .....	94
3.2.8	Function of the dynamic wing .....	96
3.2.9	Statistical analysis of flight performance.....	97

3.3	Results.....	98
3.3.1	Anatomy of the wing .....	98
3.3.2	Geometric morphometric analysis of dynamic morphology .....	99
3.3.3	Aerodynamic analysis of dynamic morphology .....	101
3.3.4	Dynamic morphology during flight challenges .....	102
3.3.5	Performance of morphing wings.....	104
3.4	Discussion.....	106
<b>Chapter 4: Conclusion.....</b>		<b>120</b>
4.1	What drives body size evolution in hummingbirds?.....	121
4.2	How do hummingbirds adapt to montane habitats?.....	131
4.3	Is there an allometry of biomechanical innovation?.....	135
4.3.1	Functional evolution in bats.....	135
4.3.2	Functional evolution of adhesive pads.....	138
4.3.3	Functional evolution of leaf flexibility .....	140
4.3.4	Allometry and estimates of maximum size.....	142
4.4	Can the force allometry approach guide allometric research?.....	145
4.4.1	Interpretation of body mass .....	145
4.4.2	A formal basis for scaling and allometry .....	146
4.4.3	The importance of the evolutionary framework .....	148
4.5	Summary and prospects .....	151
<b>References.....</b>		<b>160</b>
<b>Appendix A Species naming decisions .....</b>		<b>191</b>

## List of Tables

Table 2.1 Sample sizes, exponents, and 95% credible intervals for variables studied in Chapter 2. .....	81
Table 3.1 Mean and standard deviation for selected kinematic parameters in Chapter 3. ....	119

## List of Figures

Figure 1.1 Hierarchical paradigm of form, function, and fitness.....	38
Figure 1.2 Biomechanics of hummingbird hovering flight. ....	40
Figure 1.3 Allometric relationships in flying animals. ....	41
Figure 2.1 Biogeographic and phylogenetic sampling of hummingbirds.....	69
Figure 2.2 Impact of data subsets on the estimated slope of air density on body weight.....	70
Figure 2.3 No association between literature-derived species mean body mass and elevation....	71
Figure 2.4 Concordance between sampled and theoretical species mean elevations. ....	72
Figure 2.5 Comparison of collector data sets for systematic bias.....	73
Figure 2.6 Uncertainty in phylogenetic relationships among species in this study.....	74
Figure 2.7 Allometric divergence among and within species.....	75
Figure 2.8 Comparison of allometric variation among and within species. ....	76
Figure 2.9 Comparison of different methods of reconstructing the allometry of force and specific induced power.....	77
Figure 2.10 Effect of modelling assumptions on estimated allometric exponents and sum of exponents. ....	78
Figure 2.11 Effect of force coefficient calculation on sum-to-one constraint.....	79
Figure 2.12 Force allometry and mass variation in individual hummingbird clades.....	80
Figure 3.1 Coordinate system in this study.....	111
Figure 3.2 Feather and bone anatomy of the hummingbird wing (dorsal view).....	112
Figure 3.3 Marker paths through the stroke cycle. ....	113
Figure 3.4 Changes in wing surface area through the stroke cycle and among treatments. ....	114

Figure 3.5 Twist and camber profiles of the wing throughout the stroke cycle. ....	115
Figure 3.6 Twisting and cambering of the wing during the downstroke and upstroke. ....	116
Figure 3.7 Force and power profiles of real and simulated wings.....	117
Figure 3.8 Aerodynamic performance of real and flat plate model wings. ....	118
Figure 4.1 Contrasting consequences of selection for larger and smaller body sizes, based on extrapolation of intraspecific allometry. ....	155
Figure 4.2 Evolution of body size among hummingbirds.....	156
Figure 4.3 Consequences of selection on different measures contributing to flight performance. .....	157
Figure 4.4 Proposed model for correlated selection on body weight and wing area in hummingbirds. ....	158
Figure 4.5 A network integrative perspective reveals wing area is a key morphological trait in hummingbird diversification.....	159

## List of Statistical Symbols and Distributions

$\alpha$	Regression intercept
$\beta$	Regression slope
$a$	Allometric intercept
$b$	Allometric exponent
$Y, X$	Species means
$y, x$	Individual observations
$\sigma_Y^2$	Phylogenetic variances
$\sigma_y^2$	Observational variances
$\tau$	Precision
$\Sigma$	Posterior distribution of covariance matrices
$\mathbf{I}$	Identity matrix (star phylogeny)
$\lambda$	Pagel's lambda
$\mathcal{N}(\mu, \tau)$	Normal distribution with mean and precision $\mu, \tau$
$\mathcal{N}(\boldsymbol{\mu}, \boldsymbol{\tau})$	Multivariate normal distribution with multivariate mean and precision $\boldsymbol{\mu}, \boldsymbol{\tau}$
$\mathcal{U}(n, m)$	Uniform distribution with bounds $n, m$
$\mathcal{W}^{-1}(\boldsymbol{\Psi}/k_\psi, \nu)$	Inverse Wishart distribution with prior covariance $\boldsymbol{\Psi}$ , prior scale factor $k_\psi$ , and degrees of freedom $\nu$

## List of Physical Symbols

$\alpha$	Aerodynamic angle of attack
$\beta, \dot{\beta}, \ddot{\beta}$	Geometric angle of angle of attack (pitching angle), angular velocity and acceleration
$\gamma$	Flapping amplitude asymmetry
$\theta, \dot{\theta}, \ddot{\theta}$	Elevation angle, angular velocity and acceleration
$\Theta$	Wing twist
$\rho$	Air density
$\lambda$	Inflow ratio
$\varphi, \dot{\varphi}, \ddot{\varphi}$	Excursion angle, angular velocity and acceleration
$\Phi$	Stroke amplitude
$\omega$	Angular velocity vector
$\dot{\omega}$	Angular acceleration vector
$\dot{\omega}_a$	Active torque angular acceleration
$\dot{\omega}_{FCT}$	Flapping counter-torque angular acceleration
$AR$	Wing aspect ratio
$c$	Chord length
$\hat{c}$	Unit chord vector
$C_D$	Drag coefficient
$C_F$	Force coefficient
$C_H$	Horizontal force coefficient
$C_L$	Lift coefficient
$C_{rot}$	Rotational force coefficient
$C_P$	Power coefficient
$C_T$	Thrust coefficient
$C_V$	Vertical force coefficient
$h_{max}$	Maximum camber height
$f$	Stroke frequency
$F$	Force
$F_h$	Horizontal force
$F_v$	Vertical force
$F_{aero}$	Aerodynamic force vector
$F_{acc}$	Inertial/added mass force vector
$F_{rot}$	Rotational force vector
$F_{trans}$	Translational force vector

$h_{\max}$	Maximum camber height
$I$	Moment of inertia
$M_T$	Total lifted mass
$n$	Load factor
$\hat{n}$	Unit normal vector
$P_{\text{aero}}$	Aerodynamic power
$P_{\text{ind}}^*$	Induced power (* = specific)
$P_{\text{pro}}^*$	Profile power (* = specific)
$P_{\text{acc}}^*$	Inertial power (* = specific)
$P_{\text{per}}^*$	Total power (Ellington) – perfect (* = specific)
$P_{\text{zero}}^*$	Total power (Ellington) – zero (* = specific)
$PF$	Power factor
$r$	Radius
$\hat{r}$	Non-dimensional radius
$\hat{r}_2$	Non-dimensional second moment of area
$\hat{r}_3$	Non-dimensional third moment of area
$R$	Wing length
$R_2$	Wing length corrected for $\hat{r}_2$
$s_{\max}$	Maximum spanwise camber
$S$	Wing surface area
$t$	Time step
$T$	Stroke period
$U$	Wing velocity
$U_2$	Wing velocity corrected for $\hat{r}_2$
$v_{\text{tip}}$	Wing tip velocity
$w_m$	Wing mass
$Re$	Reynolds number
$\hat{s}$	Unit spanwise vector
$\hat{v}$	Unit velocity vector
$w_m$	Wing mass
$W$	Body weight

## List of Abbreviations

DEE	Daily energy expenditure
JAGS	Just Another Gibbs Sampler (Software for Bayesian inference)
MCMC	Markov-chain Monte Carlo
PC(A)	Principal component (analysis)
PGLS	Phylogenetic generalised least squares
RMA	Reduced major axis
WDL	Wing disc loading

## Glossary

Allometry	Method for identifying consistent power-law changes in morphology or behaviour with changes in body mass
Angle of attack (aerodynamic)	Angle formed by wing chord and chord direction of travel
Angle of attack (geometric)	Angle formed by wing chord and horizontal plane ( <i>XY</i> )
Chord	Vector pointing from trailing to leading edge, magnitude gives chord length
Drag	Aerodynamic resistance to wing motion. Vertical component contributes to weight support.
Efficiency	A measure of performance relative to cost, typically expressed as a ratio, like lift/drag, vertical/horizontal force, or $\text{force}^{3/2}/\text{power}$
Feeder mask	A visual barrier placed over a sugar-feeder to constrain stroke kinematics
Kinematics	Movement of the wing described by parameters like stroke amplitude, frequency, and wing angle of attack
Lift	Aerodynamic force generated normal to the wing surface. Vertical component contributes to weight support.
Load factor	Amount of force an animal can generate in excess of body weight, i.e., total force/body weight
Load-lifting	Method for experimental determination of force production in flying animals. Asymptotic load lifting (Chapter 2): maximum power and force. Submaximum load lifting (Chapter 3): sustained power and force.
Morphing	Changes in two- and three-dimensional wing form, such as length and area or twisting and camber. Due to joint and feather movements, in birds.
Stroke amplitude	Angle (degrees) between the reversal points of the stroke cycle
Stroke frequency	Number of wing stroke cycles per second, or the inverse of stroke period
Stroke plane	Average plane through which the wing moves during the stroke cycle
Performance	An ecologically- or phylogenetically-relevant trait for which animals can be compared, such as load factor or turning rate
Performance envelope	Bounds of performance for a given animal in a given condition, such as maximum load factor at high and low elevation
Posterior distribution	Distribution of hypotheses updated to include observed evidence, i.e., the prior distribution multiplied by the likelihood of the data
Power (aerodynamic)	Sum of induced, profile, and parasite (body drag) powers

Power (induced)	Power expended at the stroke plane to accelerate air in the wake
Power (inertial)	Power expended to accelerate the wing
Power (profile)	Power expended to overcome wing drag
Prior distribution	Distribution of hypotheses before any evidence is observed, here ‘flat’ in the sense that all hypotheses are equally likely
Twist	Difference in angle of attack from wing tip to wing base

## Acknowledgements

I am sincerely appreciative to Dr. Douglas Altshuler for taking me in from the academic cold, giving me the resources, patience, and guidance to pursue my research independently, and the freedom to barge into his office and just start talking. Special thanks are owed to my supervisory committee of Drs. Michael Gordon, Darren Irwin, and Robert Shadwick for keeping me on track, for rich discussions that greatly influenced the development of these chapters, and for catching numerous errors just in the nick of time. I am indebted to Dr. Sheldon Green and Justin Roberts for the loan of high-speed cameras to facilitate Chapter 3, and to the Zoology Computing Unit for calm technical support and troubleshooting ('Have you tried turning it off and on?'). I am grateful to Drs. David Lentink and John M. Gosline for investing so much time and patience to explain biomechanical and aerodynamic concepts, and Dr. F. Gary Stiles for hosting me and for the accidental theft of his ruler. I greatly profited from interactions with the Comparative Physiology, Biodiversity, and Biomechanics groups, particularly Dr. Joseph W. Bahlman, who was instrumental in developing the framework of Chapter 2. Dr. Benny Goller made Chapter 3 achievable and Brazil's 7-1 loss memorable. This research would not have been conducted without graduate fellowship support from the National Science and Engineering Research Council. I am extremely grateful to my whole family, and not least Isabel Skandalis Duarte for unwavering moral support. I am most especially grateful to my wife Dr. Paula Duarte Guterman as my inspiration to do better and work harder, and for indispensable life support without which, it is clear, things would go fairly disastrously.

## Chapter 1: Introduction

### 1.1 The form-function-fitness paradigm

Locomotion underlies the success of modern animals, driving diversification through exploitation of new niches and resources and through behaviours such as dispersal and mate finding. Specialisation of locomotor modes and habitats is common because the environment mechanically links body form and function, and evolution tinkers with the pieces. Character trait frequencies and distributions shift in accordance with organismal fitness, but the probability of passing genes to the next generation is dependent on many factors encompassing animal behaviour and energetics, many of which are not related to locomotion at all. Accordingly, any single component of organismal biology does not exist in isolation, and an integrative perspective is needed to understand morphological, physiological, and behavioural diversification. Understanding the evolutionary context of hummingbird flight performance requires understanding the array of behaviours that drives their evolution, along with the anatomical and physiological foundations on which performance has evolved.

A comprehensive evolutionary framework unifying form, function, and fitness has been developed over several decades [(Arnold, 1983; Careau and Garland, 2012; Garland and Losos, 1994); Figure 1.1a, modelled on (Careau and Garland, 2012)]. The paradigm was proposed to guide the division of research effort into laboratory and field studies: mapping morphology and physiology to performance in the lab, and then mapping performance to fitness in the field (Arnold, 1983). It has since been modified and expanded into general categories of morphology and physiology, performance, energetics, behaviour, and fitness, represented by boxes in a path diagram (Figure 1.1a). Though represented simply in Figure 1.1, the actual links between categories will typically be complex transfer functions describing multidimensional relationships

among parameters, such as the phenome, the space of all phenotypes (Houle et al., 2010). A major challenge of organismal research is therefore to develop a framework which can adequately, but as simply as possible, map morphology and physiology to fitness and adaptation. Here, I describe the established paradigm, and contribute some generalisations of the paradigm that will allow a broader integrative perspective. I then discuss form, function, and fitness in hummingbirds, and how hummingbird behaviour has driven their adaptations for agile and efficient flight.

**Morphology, physiology, and performance** Morphological traits, such as limb lengths or wing area, and physiological capacities, such as blood gas tension or enzyme flux rates, define the envelope of animal performance (Arnold, 1983; Irschick et al., 2008) within which animals behave (Careau and Garland, 2012; Garland and Losos, 1994; Husak, 2006). In this paradigm, performance is an ecologically or phylogenetically relevant ‘dynamic’ trait, such as maximal sprint speed or endurance, or ‘regulatory’ trait, such as thermoregulatory capacity or ionic homeostasis (Careau and Garland, 2012; Husak et al., 2009). The performance envelope in the strict sense (Arnold, 1983; Careau and Garland, 2012) is a function of morphological and physiological factors within an environment. The dynamic functional envelope is set absolutely by the maximum and sustained power expenditure, whereas the regulatory functional envelope is set by homeostatic physiological capabilities, such as the ability to maintain cardiac function and oxygen unloading [e.g., (Eliason et al., 2011; Rummer et al., 2013)]. Plasticity and the capacity to modify regulatory traits, such as through acclimation, is not explicitly represented in Figure 1.1, which omits backwards-pointing arrows that would represent feedback.

**Behavioural filter** In the strict sense of the performance envelope, only the limits of capacities are considered (Arnold, 1983), so Garland and Losos introduced behaviour as a filter between

what is possible and what is observed (Careau and Garland, 2012; Garland and Losos, 1994). An animal might have great sprint capacity in the laboratory, but freeze and hide from a predator in the wild. How an animal routinely behaves, and the fitness consequences of this behaviour, is at least as important as the limits of performance. Whereas maximum capacities may determine a performance envelope, the performance space inside the envelope is dependent on the functioning of the whole organism (Husak et al., 2009; Irschick et al., 2008) (Figure 1.1).

Behaviour is the organism's current state, out of all its possible states. This satisfies the behavioural sense of Careau, Garland, and Losos, providing a filter between what is possible in the laboratory, and what is observed in a natural setting.

**Energy balance** Energy balance mediates fitness independently of direct behavioural impacts by accounting for factors such as developmental costs (Figure 1.1) (Oufiero and Garland, 2007).

The concept of a performance space, rather than an envelope, more easily links the energetic consequences of normal behaviour to measures of energy balance. Inside the performance space, the topology of energy balance is not necessarily known, and may help explain why animals exhibit a given range of behaviours. For instance, a single optimum could correspond to the minimum cost of transport of a migratory animal [i.e., maximum migration efficiency, (Irschick and Garland, 2001)], and behaving near this optimum might enhance fitness by maximising the energy available for reproduction after arriving at the breeding grounds. The energetic landscape might be mostly flat if many behaviours have similar cost, such as the metabolic power exchangeability of frequency and amplitude modulation during *Drosophila* weight support (Lehmann and Dickinson, 1997) or the flat power curve of forward flight speed in bumblebees (Ellington et al., 1990). Multiple energetic optima can exist if distinct behaviours have similar energetic costs; such optima might be particularly prevalent where the combined

effects of mechanical linkages result in multiple morphological and kinematic strategies.

Understanding the energetic landscape and associated behaviours is critical because animals frequently behave very differently than expected by a given energetic theory (Irschick and Garland, 2001). Among individuals with a similar performance and energetic space, differences in animal personality (Careau and Garland, 2012; Duckworth and Badyaev, 2007) can lead to variation in the portion of the space that is actually used, and so variation in life history.

**Darwinian fitness** Ultimately, natural selection maximises lifetime reproductive success, principally as a function of fecundity, survivorship, and age at first reproduction (Oufiero and Garland, 2007). Age at first reproduction is favoured even for the same lifetime reproductive success, because then offspring too reproduce earlier. Fitness is typically difficult to link to performance directly because traits can have opposite effects on reproductive success, such as development of a sexually-selected ornament (positive effect on success) that delays the age at first reproduction (negative effect on success) (Oufiero and Garland, 2007). Complex animal behaviours, such as cooperation, yield greater potential fitness benefits than predicted by the individual on its own (Nowak, 2006). Although generally solitary, hummingbirds are known to mob predators (Stiles, 1978; Zenzal et al., 2013) and groups of immature hummingbirds will work together to wear down adults and take their territories (Stiles, 1973). Reproduction and offspring care entail substantial energetic input (pers. obs.), so in many cases choosy females may be directly evaluating motor performance through sexual displays as an indirect measure of genetic quality. Vigorous or long-lasting displays should better signal males with good energetics than morphological ornaments (Byers et al., 2010), leading to direct fitness benefits in individuals with those traits, though compensatory evolution of other character traits means fitness is not easily predicted (Oufiero and Garland, 2007). Perhaps because of the inherent

costliness of flight and the intimate link between body shape and flight performance, sexual selection of male traits by females seems to be particularly important in birds (Møller and Alatalo, 1999).

A critical feature of the fitness landscape is that it may exhibit distinct adaptive peaks for males and females. Male Willow Warblers migrating in Scandinavia have longer and pointier wings that may be adaptive for fast flight to establish territories prior to females' arrivals, whereas females instead have shorter and blunter wings that favour agility and maneuverability, likely for hunting aerial prey and for quick escapes (Hedenström and Pettersson, 1986). Contrasting requirements in wing morphology can cause sexual conflict if the loci determining size and shape are the same in both sexes, such as longer male wings being associated with negative fitness in female offspring (Tarka et al., 2014).

**Ecological context** In every case, the links between boxes in Figure 1.1a depend on ecological context. In the sense of Careau and Garland (Careau and Garland, 2012), ecological context comprises biotic factors, such as parasitism and competition, and abiotic factors such as temperature and oxygen availability. However, the biomechanical perspective of ecological context is much broader, because the environment is the mechanical link between morphology and function. Fins and wings cannot generate propulsion in the absence of fluid viscosity, and each is adapted to the special demands of the respective fluid densities. The general dependence of the mechanical linkage on characteristic scales explains fundamental differences, such as why bacterial locomotion must be intrinsically different from any larger organism (Purcell, 1977). Specific mechanisms of the mechanical linkage between form and function, such as the running substrate, can interact with biotic context to favour different forms through selection on performance. In the aftermath of an introduced predator, long legs are initially favoured because

they confer an advantage in ground running speed, but short legs are subsequently favoured for running on branches as the species becomes arboreal (Losos et al., 2006). Biotic ecological context in the form of competition can drive diversification through resource partitioning [character displacement, (Schluter, 1994; Temeles and Kress, 2003)] and directly or indirectly impacting biomechanical performance, such as (possibly) correlated changes in beak size, body weight, and wing length (Grant and Grant, 2006).

An illustrative example of the form-function-fitness paradigm, and the crucial role of detailed biomechanics, is the sexually-exaggerated elongated streamer tail feathers of barn swallows. Females prefer males with longer and more symmetrical streamers, suggesting sexual selection (Møller, 1988; Møller, 1992). Experimental manipulation of tail length is correlated with both male and female reproductive success (Cuervo et al., 2003; Møller, 1988), though in females the impact lags to the following year, pointing to the complexity of behavioural interactions. The costliness of the streamer is supported by reduced foraging efficiency after experimental tail lengthening, as birds switch from capturing a few large insects to many smaller ones (Møller et al., 1995b). The longer tail streamer will have a longer moment arm to rotate (Evans and Thomas, 1992), suggesting that the differences in foraging efficiency and reproductive success are due compromised maneuverability. In fact, male swallows have numerous morphological compensatory mechanisms, such as a change in the streamer shape, potentially to mitigate drag, and an elongation of the central feathers to reduce the tail asymmetry and aerodynamic cost of the streamers (Møller et al., 1995a; Thomas, 1993). It is noteworthy that males increase wing area relative to body weight (Møller et al., 1995a), which should provide more aerodynamic force to overcome extra drag on the tail. Larger wing areas will likely also affect kinematics (the set of wing and body motions used in flight) and thus

aerodynamic and inertial moments (Bahlman et al., 2013; Ellington, 1984a; Evans and Thomas, 1992; Hedrick et al., 2009; Riskin et al., 2012), which can increase flight costs and constrain maneuverability. Thus, the true cost of a given adaptation is obscured by knock-on effects to covarying traits and their respective trade-offs (Oufiero and Garland, 2007).

Despite extensive research, the role of selection in the evolution of the barn swallow tail feather remains contentious for a simple biomechanical reason that is important for this thesis: the tail's shape and use in flight remains largely unknown (Barbosa and Møller, 1999; Evans, 1998). Significant insight into ornaments with potential aerodynamic function requires an examination of their dynamic morphology, i.e., their shape in flight and response to flow. In wind tunnel tests, the tail geometry is reconfigured through automatic aeroelastic mechanisms, increasing tail lift and decreasing turn radius (Norberg, 1994). Streamers might, therefore, have arisen through natural selection on flight performance and were secondarily pushed beyond their optimum by sexual selection (Norberg, 1994). Norberg inferred the aerodynamic function of the tail by analogy to aircraft slats, rather than through a direct test. In general, ornaments such as elongated tail feathers may be costly only in specific contexts (Askew, 2014; Clark and Dudley, 2009; Evans and Thomas, 1992). In fact, the barn swallow tail sexual dimorphism exhibits a latitudinal gradient, and appears not to be maintained when the local environment imposes too great a cost (Møller, 1995).

## **1.2 Hummingbirds in the form-function-fitness paradigm**

Substantial research effort has been directed into understanding hummingbird natural history, physiological ecology, and comparative biomechanics. Hummingbirds' success is propelled by their extraordinary behaviours, including putative juvenile play and aerial jousting

(Rico-Guevara and Araya-Salas, 2015; Stiles, 1971; Stiles, 1973). Hummingbird ecology is a major factor in their speciose radiation, where competition, insect and flower foraging, and colonisation of high altitudes have been central processes (Altshuler et al., 2004c; Graham et al., 2009; McGuire et al., 2014; Temeles and Kress, 2003; Wolf et al., 1972; Yanega and Rubega, 2004). Hummingbirds have a large aerial performance envelope including hovering, long-distance migration, and sexual displays. Their impressive aerial abilities are not explained by any one morphological or physiological trait, but are supported by numerous adaptations in anatomy and wing design, muscle design and fuel use, circulation, and sensory processing (Altshuler et al., 2015; Clark, 2009; Gaede et al., 2017; Opazo et al., 2005; Projecto-Garcia et al., 2013; Suarez and Gass, 2002; Suarez et al., 1991; Warrick et al., 2012). In this section, I offer a broad overview of hummingbird biology and biomechanics, which provides a framework for understanding both the present investigations and directions for future work.

### **1.2.1 Behaviour and reproduction**

Fitness and adaptive significance in hummingbirds is generally inferred through behavioural observations. Males, and in many cases females, defend breeding and feeding territories (Kodric-Brown and Brown, 1978; Stiles, 1971; Wolf, 1969). Competitive interactions among hummingbirds are frequently aggressive, involving high-speed chases at a minimum (Altshuler, 2006; Kodric-Brown and Brown, 1978; Stiles and Wolf, 1979), but potentially escalating to vigorous aerial combat such as jousting (Rico-Guevara and Araya-Salas, 2015) or to birds locked together and grappling on the ground (Kodric-Brown and Brown, 1978; Stiles, 1973). Males attract females to their territories through acrobatic displays (Clark, 2009; Stiles,

1982; Stiles and Wolf, 1979) and through vocal (Stiles and Wolf, 1979) and tail- and wing-based acoustic signals (Clark et al., 2011; Hunter, 2008; Hunter and Picman, 2005).

In the overall locomotor context of this review, some species' innovation of wing acoustic signalling during flight are most interesting. The whistling likely derives from structural modification of the distal primary flight feathers to allow aeroelastic flutter [(Clark et al., 2016), studied in broadbills, but the mechanism would be the same], or from air whistling through notches in the wing [see wing morphology drawn in (Banks and Johnson, 1961)]. The signal is created by impressive modulation of stroke kinematics (wing flapping movements) to a transient 30% increase in wing stroke frequency (Hunter, 2008; Hunter and Picman, 2005). The mechanical evolution, together with the sexual dimorphism of the signals (Hunter, 2008; Hunter and Picman, 2005), suggests that wing acoustic signalling will be an interesting avenue to explore the locomotor and performance costs of a signalling innovation.

It should also be interesting to examine the apparently common hybridisation among hummingbird species (Banks and Johnson, 1961; Graves et al., 2016; McCarthy, 2006). Hybrids exhibit intermediate morphological forms to the parents, including wing and tail lengths, and to derived morphological features like wing tip notches that contribute to wing acoustic signalling [(Banks and Johnson, 1961), note hybrids have not usually been genotyped, but see Graves and references: (Graves et al., 2016)]. Hybrid behaviour, such as male sexual displays, may be intermediate to the parents, or sometimes different altogether (Wells and Baptista, 1979; Wells et al., 1978). Studies of hybrids could therefore also provide insight into how genetic factors influence locomotor behaviours.

The physical demands of holding territories are energetically wearing. In a lekking species, where males establish territories in close proximity to each other, holding territories for

a longer period of the year may offer more mating opportunities, but is adversely associated with survivorship to the next year (Stiles and Wolf, 1979). Nonetheless, the average fitness of males in a lek is greater than when displaying alone (Stiles and Wolf, 1979), an example of how behaviour and reproductive success push hummingbirds toward mating systems that increase conflict and individual costs. Similarly, hummingbirds may select a resource-poor territory if it brings them closer to a female nesting area (Armstrong, 1987).

Because of the energetic cost of defending territories, individuals rely on an economical model to scale their efforts to available energy, including adjustment of territory size to floral nectar rewards (Carpenter et al., 1983; Ewald and Bransfield, 1987; Ewald and Orians, 1983; Gass, 1978; Kodric-Brown and Brown, 1978; Powers, 1987; Tamm, 1985) and budgeting their time among behaviours with different costs to maintain similar overall expenditure (Stiles, 1971). A clever solution to maximise resource defense and minimise energetic costs is the selective draining of floral resources in patches of the territory where intrusions occur (Paton and Carpenter, 1984). Although renowned for their flight, resident hummingbirds in fact spend most of their time perching (Kodric-Brown and Brown, 1978; Stiles, 1971). The time spent perching is plastic and adaptive (in the sense of variation among species), an example of the behavioural filter between fitness and performance (Figure 1.1). In response to experimental manipulations of territory quality by introducing artificial feeders, *Calypte anna* increase their aggression toward intruders, whereas *Archilochus alexandri* increase aggression but also spend more of their time on inexpensive threat vocalisations (Ewald and Bransfield, 1987). Variation in energy balance due to the costs of resource acquisition and expenditure on defense has led to divergence of the hummingbirds into behavioural guilds, such as territorialists, trappliners (visiting successive

flower patches along a path), territory-parasites, and generalists (Altshuler, 2006; Feinsinger and Colwell, 1978; Feinsinger et al., 1979).

Hummingbird territorial behaviour has received the majority of attention because it is a key element of hummingbird evolution and community organisation (Graham et al., 2009) and because it can be readily studied and manipulated. There is, though, the potential for alternative behavioural and reproductive tactics. An example is the territory establishment of migratory *Selasphorus rufus*, where nonterritorial birds are common and divided into categories of challengers and robbers (Kodric-Brown and Brown, 1978). Challengers are especially noisy and violent, and may persistently attack a territory resident over a whole day, until driving him or her away. Speculatively, a challenger phenotype could be adaptive for some individuals in migratory species, where a relatively slower migration speed results in a reliance on stealing good established territories. This may occur when migration and territorial pressures lead to conflicting morphological optima [(Kodric-Brown and Brown, 1978), discussed below], and may be supported by the observation of multiple pre-migratory fueling strategies (Hou and Welch, 2016). In contrast to challengers, robbers rely on being inconspicuous, to raid flowers out of sight of the resident and flee if caught (Ewald and Rohwer, 1980; Kodric-Brown and Brown, 1978). This works well for dull-coloured females and juveniles, but may also be attempted by a few bright adult males (Ewald and Rohwer, 1980; Kodric-Brown and Brown, 1978). What determines if an adult will be a nonterritorial, or how long that behaviour persists, is not yet established, but could be related to smaller body size or morphological differences that reduce holding capacity (Stiles and Wolf, 1979).

What evolutionary forces actually drive hummingbirds' extreme performance, and is selection equal between males and females? The majority of hummingbird research has focused

on easily observed and captured males, which may skew our perception of hummingbird evolution. It is clear that locomotor capacity is involved in male success, including chases and combat, but also for hovering for specialized gape and face pattern displays (Stiles and Wolf, 1979). It seems likely that flight efficiency should be favoured in males, to maximise the potential for expensive displays and competitions even with poor resource availability, which could collectively drive hummingbirds' morphological and physiological adaptations. On the other hand, the notion of efficient flight must be carefully defined, and some aspects of efficiency, such as very large wings, could be detrimental to performance (Hedrick, 2011). This might be true on an individual level, if males favour inefficient flight that increases maneuverability (Kodric-Brown and Brown, 1978).

We have limited knowledge of the morphological and flight competitive abilities that determine successful territory holding, which in many species determine male reproductive success. This is due to a lack of aerodynamically meaningful parameters to characterise morphological variation (Altshuler et al., 2004a; Epting and Casey, 1973; Feinsinger et al., 1979; Lockwood et al., 1998), exacerbated by conflict between aerodynamic and ornithological body size measurements (Stiles et al., 2004) and the suspect conversion factors between them. Overall body size seems an attractive predictor, but is only a clear determinant of competitive success when there are large differences among species (Dearborn, 1998; Stiles and Wolf, 1979). Within mating systems such as a lek, morphological characteristics at best are only weak predictors of dominance and territory quality; males at the center and periphery may be the same size (Stiles and Wolf, 1979). Relative muscle mass should be a major contributor to performance through the ability to generate burst forces (Segre et al., 2015; Sholtis et al., 2015). In dragonflies, relative muscle mass has been directly linked to fitness (Marden, 1989), but thus far in hummingbirds the

relative contributions of wing morphology and muscle mass (which requires dissection) have not been satisfactorily disentangled. The ability to establish and hold central territories and to advertise them to females by singing may instead be a function of individual aggressiveness rather than morphological traits, a potentially interesting example of animal personalities as a behavioural filter to fitness (Careau and Garland, 2012; Duckworth and Badyaev, 2007). Experience also plays a role, as younger and less established males get pushed out of lek territories that are then taken over by dominant males (Stiles and Wolf, 1979).

Flight performance of females has received little attention overall, but could be under intense selective pressure for flight efficiency because of energetic and reproductive demands. In a few species, females as well as males hold territories around their nests and flower patches (Kodric-Brown and Brown, 1978; Wolf, 1969), which could drive even greater selection on flight performance in the species. However, males are mostly territorial to the point of even chasing females from their flower patches. In an extreme case, this has apparently driven sexual dimorphism in bill shape and sexual preferences for distinct flower species (Temeles and Kress, 2003). Because conflict with males usually pushes females into resource-poor areas (Temeles and Kress, 2003; Wolf, 1975), pressures for flight efficiency could be even higher. In a memorable example, females have been proposed to ‘prostitute’ themselves to access males’ flower patches (Wolf, 1975).

The cost of reproduction to females could be a major factor in female flight performance and fitness. This can include the need to guard the territory around her nest (Wolf, 1969), to carry eggs reaching up to 45% of female weight (Lislevand et al., 2007), and to feed herself and her young (Fierro-Calderón and Martin, 2007). A markedly great energetic burden may be that to brood her eggs and young (Wolf and Stiles, 1970), the female may have to sacrifice torpor,

which saves up to 90% of night-time metabolism (Hainsworth and Wolf, 1970). Taken together, this suggests that females should face strong selection for energetic efficiency, potentially causing sexual conflict in hummingbird form and function. For instance, females could favour increased wing lengths and areas, and greater efficiency, whereas males may favour decreases in the same, for greater maneuverability (Tarka et al., 2014).

Females generally build nests, incubate, and provision offspring on their own. Ironically, lack of male investment in offspring favours choosy females (Byers et al., 2010), which may drive males toward greater aggressiveness and competition (Duckworth and Badyaev, 2007). The cost of male competitions may be higher mortality rates and lower life expectancies in males than in females (Miller and Gass, 1985). Because Darwinian fitness acts through lifetime reproductive success, there is thus the potential for selection in favour of alternative strategies. In rare cases, males have been observed to contribute indirectly to offspring rearing and welfare, and possibly even help incubate eggs (Moore, 1947; Wolf and Stiles, 1970). Incipient parental care may thus have arisen in these species precisely because it favours lifetime reproductive productivity (Sibly et al., 2012). Increased parental care is associated with reduced aggressiveness in some species (Duckworth and Badyaev, 2007), potentially further increasing expected male life span. Because of the female's greater investment in the offspring, her lifetime fitness should be strongly associated with fledgling success. Nest predation is a major factor, with fledgling success in some cases only around 40% (Baltosser, 1986). However, male fitness is also increased by fledgling success, and in some species it is suggested that males guard the nest (Moore, 1947).

Selection may also act on behaviours that influence the success of juveniles.

Development is a critical period for establishing context-specificity of the link between

locomotor performance and fitness (Le Galliard et al., 2004). Currently, we have limited understanding of the ontogeny of flight performance (Crino et al., 2017; Dial et al., 2012; Heers et al., 2011). For instance, wing and body size at fledging declines with increasing predation (Martin, 2015), which may contribute to evolution of escape behaviours aided by underdeveloped wings (Dial, 2003; Dial et al., 2008). This strategy is unlikely to be available to hummingbird nestlings with their underdeveloped leg muscles, which could mean that there is strong pressure on rapid growth to fledging. Like in other birds, morphology of immatures differs from adults. Immatures of both sexes have larger wings than adult males (Stiles et al., 2005), contrary to the passerines, where immature wing lengths are usually shorter (Alatalo et al., 1984). In the latter, it is thought the shorter wings aid maneuverability for escapes. It could be that the longer wings of immature hummingbirds are more energetically efficient, though the aerodynamic mechanisms of this are not yet clear (Stiles et al., 2005). To what extent hummingbirds' complex motor skills are innate or gained through experience is, to my knowledge, unknown. Based on his extensive observations of hummingbird behaviour, Stiles hypothesised that immature hummingbirds play in pairs (possibly nestmates), practicing the elements of social behaviour that will be required for territorial and mating success, including displays and chases, (Stiles, 1973, 66). For instance, flight experience is involved in the gain of steering precision in *Drosophila* (Hesselberg and Lehmann, 2009).

Finally, hummingbirds have a variety of predators that affect both sexes throughout their life spans, including birds, arthropods, frogs, and fish (Miller and Gass, 1985; Zenzal et al., 2013). Whether hummingbirds are regularly taken on the wing is doubtful and many predation records may be opportunistic attacks (Miller and Gass, 1985), but a few predators have adapted to hummingbirds' predictable lifestyle. Tiny Hawks exploit males' predictability in perch

selection and daily behaviours (Stiles, 1978), and mantids capture hummingbirds at hummingbird-pollinated plants and at feeders (Nyffeler et al., 2017). It is possible that females' and juveniles' drab colours may be adaptive in these situations, avoiding the adult male flashiness that might attract a predator [see also, (Dale et al., 2015)]. These behavioural and ecological factors suggest additional ways in which selection could converge or diverge between the sexes.

### **1.2.2 Form and function**

Hummingbird flight is supported by a large number of morphological and physiological innovations. The most startling of these, of course, is the ability to sustain hovering flight, specifically defined by a very low ratio of forward velocity to wing tip velocity [(Ellington, 1984b), advance ratio,  $J < 0.4$ ], but more generally defined by station-holding capacity. The ability to sustain hovering was likely a crucial adaptation underlying hummingbird success, allowing arthropod foraging in foliage (Mayr, 2003; Stiles, 1995; Stiles and Wolf, 1979) and uninterrupted feeding at flowers that are possibly moving in the wind (Goller and Altshuler, 2014). Hummingbirds also collect silk to make their nests (Calder, 1973). Speculatively, this may be a delicate operation (i.e., careful control of hovering) because hummingbirds develop a positive electric charge in flight (Badger et al., 2015), which could deform a spiderweb and enhance the possibility of capture (Ortega-Jimenez and Dudley, 2013).

Sustained hovering flight evolved from existing avian capacities for transient hovering [for a fossil record perspective, see (Bochenski and Bochenski, 2008; Mayr, 2003; Mayr, 2004)]. Many birds can hover briefly, or maintain very slow flight, at greatly increased flight costs (Tobalske et al., 2003; Wester, 2014). Even in cases where other birds can hover, they primarily

generate forces in the downstroke (also called the power stroke), then flex their wing against the body (upstroke, or recovery stroke) to avoid generating counterproductive forces, and to minimise the inertial cost of returning the wing to the downstroke start position. Besides the energetic costs, this type of stroke cannot maintain a constant body and head position to execute useful behaviours (Warrick et al., 2002; Warrick et al., 2012). Thus, hummingbirds have evolved an aerodynamically active upstroke to contribute weight support (Pournazeri et al., 2013; Song et al., 2014; Song et al., 2016; Warrick et al., 2005), and the musculature to support it (Reiser et al., 2013; Warrick et al., 2012; Welch and Altshuler, 2009).

Hummingbird hovering flight involves exploitation of unconventional aerodynamic mechanisms to generate more force than possible just by laminar, attached flow over the wing. These high-lift mechanisms may enable numerous behaviours by augmenting force production, but greatly increase power expenditure (Ellington, 1984a) (Figure 1.2). One such mechanism is the leading-edge vortex, a region of rapidly moving air that reduces pressure above the wing [or equivalently, increases circulation, (Ellington et al., 1996)], but substantially increases drag and therefore aerodynamic power costs. The presence of a leading-edge vortex in hummingbird flight was initially considered a sign of aerodynamic convergence with insects (Warrick et al., 2005; Warrick et al., 2009), but this mechanism has since been discovered or proposed in numerous animals (Henningson et al., 2011; Hubel and Tropea, 2010; Lentink and Dickinson, 2009a; Muijres et al., 2008; Muijres et al., 2012b). Perhaps surprisingly, the leading-edge vortex is relatively weak compared even to other birds (Muijres et al., 2008; Muijres et al., 2012b; Warrick et al., 2005), although this could be adaptive to minimise its associated energetic costs when more conventional aerodynamics are sufficient. An unexplored possibility is that hummingbirds may limit the recruitment of high-lift mechanisms in order to minimise the cost

for routine flight, but rely on stronger unsteady effects to enable a broader range of behaviours. There is little evidence that hummingbirds exploit to any great degree some other known sources of unconventional lift production, like wake capture and rotational lift (Song et al., 2014; Song et al., 2015b), but it has not been ruled out that they could do so during different behaviours.

The exact nature of hummingbird flight aerodynamics remains unclear, because of difficulty precisely reconstructing the flow field (air velocity) around the wings, tail, and wake (Altshuler et al., 2009; Pournazeri et al., 2013; Song et al., 2014; Warrick et al., 2005; Warrick et al., 2009; Wolf et al., 2013). A key question has been whether hummingbirds utilise a single leading edge vortex spanning from wing to wing and shed into the wake as a single loop, or bilateral loops independently shed from each wing. The single loop should maximise the efficiency of lift production (span efficiency), whereas the latter should offer greater aerodynamic control, and so greater maneuverability, at the cost of greater aerodynamic power (Bomphrey et al., 2009; Muijres et al., 2012a; Wolf et al., 2013). Recent experiments have favoured the bilateral vortex loop model (Altshuler et al., 2009; Kim et al., 2014; Wolf et al., 2013), which would be consistent with an evolutionary strategy of favouring maneuverability over energetic efficiency.

Nonetheless, it is entirely possible that hummingbirds can transition between aerodynamic states (e.g., single to bilateral loops) between successive strokes, as has been found in other animals (Srygley and Thomas, 2002). This may explain some variation among individuals and species and differing conclusions among studies, particularly when only a few stroke cycles are examined, or the aerodynamic reconstruction is averaged over multiple stroke cycles. As well, aerodynamic reconstruction by wake visualisation assumes the vortex topology and strength is unchanged (frozen) as it is advected downstream, which is typically untrue

[(Gutierrez et al., 2017), who also discuss further challenges to aerodynamic analyses of flapping flight]. A second notable proposal is that hummingbirds can use their tails to deflect the wing wake, and so enhance their maneuverability over what is possible by the wings alone (Altshuler et al., 2009). To date, all flow-field measurements have been done on the small hummingbirds of the Bee clade, so whether other clades and larger hummingbirds adhere to similar patterns is unknown.

The morphology and physiology enabling the evolution of hummingbird flight further shows adaptation of preexisting structures. The bones of the wing have been fused and generally shortened (Figure 1.2), a character trait delineating stem hummingbirds (Mayr, 2004). A key feature of the anatomical modifications appears to be a repurposing of the humerus from its function of transitioning between stroke postures (upstroke and downstroke), to driving the wing through the power phase of the stroke (Hedrick et al., 2012). The adapted functionality of the humerus increases flight efficiency by allowing more of the muscle strain to be directed into the aerodynamically most active part of the stroke cycle, in an insect-like manner [increased transmission ratio from muscle to wing, (Hedrick et al., 2012)]. An additionally insect-like feature of the hummingbird stroke is that both experimental and theoretical analyses reveal that wing rotation at supination, the reversal of the wing into the upstroke, cannot be solely explained by twisting of the wrist (Hedrick et al., 2012; Song et al., 2015a), but must involve some inertial and aerodynamic mechanisms.

Concurrent with the shortening of the arm bones is a large expansion of the wing surface area covered by primary flight feathers, and a reduction in the number and size of the secondary flight feathers (Warrick et al., 2012). This allows hummingbirds to control the wing surface primarily through twisting of the wrist and long-axis rotation of the humerus, enabling the

inversion of the wing during the upstroke, and thus enabling upstroke lift. An unresolved aspect of hummingbird comparative morphology is that although wing surface areas are smaller than expected if hummingbirds shared a common body plan with other birds [see (Warrick et al., 2012) for an illustration of comparative wing designs], the rate at which proportional wing area changes with increasing species size is much greater than in other birds or insects (Greenewalt, 1962; Rayner, 1988) (Figure 1.3). The evolutionary origin and significance of this trend is unknown, nor does there exist a paradigm to validate the statistical robustness, functional significance, or likely evolutionary origin of this observation. To my knowledge, it has also not been acknowledged that this might not be a pattern unique to hummingbirds, but a taxonomic artefact of comparing trends within a family (Trochilidae) to a trend within classes (Aves and various groupings of Insecta) (Figure 1.3). Similarly high rates of wing area increase have been reported in other high-performance taxa, such as insects and bats (Bolstad et al., 2015; Darveau et al., 2005a; Riskin et al., 2010). Within birds, I suggest that other taxa may also exhibit this trend [Figure 1.3, trends within families and Aves overall analysed by a generalised linear model using the avian phylogeny of (Jetz et al., 2012)]. As for hummingbirds, understanding why this trend appears in some clades requires more detailed biomechanical evolutionary models.

The principle constraint on hummingbird wing shape identified so far appears to be on aspect ratio (wing length<sup>2</sup>/surface area). Aspect ratio must be high enough for aerodynamic efficiency, but low enough that the leading edge vortex does not separate from the wing (wing stall), which greatly decreases lift and increases drag (Kruyt et al., 2015). For the high aerodynamic angles of attack typical of animal flight (angle between the wing and the air flow), this condition coincides with wings in which the local wing radius is about four chord widths (local aspect ratio). Thus, the lift distribution from root to the tip appears to explain why

hummingbird aspect ratios fall into the range 3.5–4 (Kruyt et al., 2014; Kruyt et al., 2015; Lentink and Dickinson, 2009a). Nonetheless, with the exception of some theoretical computational studies (Song et al., 2014; Song et al., 2016), changes in wing shape during the stroke cycle have not been extensively considered in aerodynamics studies (which typically consider downstroke-like wing shapes). Shape variation may contribute to greater downstroke lift production than upstroke (Warrick et al., 2005; Warrick et al., 2009), including asymmetry in wing twisting, camber, and surface area between the strokes (Song et al., 2014; Tanaka et al., 2013; Warrick et al., 2005). Constraints on wing shape between the stroke cycles may explain why hovering remains relatively metabolically costly for hummingbirds compared to intermediate forward flight speeds [like for other birds, (Clark and Dudley, 2010; Dial et al., 1997; Tobalske et al., 2003; Tobalske et al., 2010), despite the overall similarity to insect-like flight (Ellington, 2006; Ellington et al., 1990; Warrick et al., 2005)].

Physiologically, flight seems to be supported by maximisation of existing capacities rather than evolution of novel mechanisms. Hummingbirds depend on dense mitochondrial and enzymatic packing, and maximising flux rates through biochemical pathways (Suarez et al., 1990; Suarez et al., 1991). Hummingbirds metabolise nectar for short flights and fats for long flights (Chen and Welch, 2014; Suarez and Gass, 2002). Carbohydrate metabolism is advantageous for maintaining high-performance behaviours because newly-ingested sugars are rapidly recruited to fuel flight [‘aerial refueling’, (Suarez and Welch, 2017; Suarez et al., 2011)], but could have other energetic implications, such as reducing respiratory costs by minimising oxygen consumption rates relative to fat metabolism (Welch et al., 2007). The preference for sugar-powered flight is nonetheless constraining because fat metabolism is recruited after only a

few minutes of continuous flight; hummingbirds therefore avoid flying for more than a few minutes continuously [except in migration, (Suarez and Gass, 2002)].

The discovery of novel fructose metabolism in vertebrates capable of hovering [hummingbirds and bats, (Chen and Welch, 2014)] or that are subterranean [naked mole rats, (Park et al., 2017)], suggests that oxidation of other carbohydrates may arise repeatedly in response to challenged oxygen demands (hypoxia in naked mole rats, oxygen flux in hovering flight)[see (Suarez and Gass, 2002) for a more extensive review of adaptations for oxygen delivery in hummingbirds]. The evolutionary switch for this ability may be a straightforward expansion of tissue distributions of glucose transporters (GLUT), such as GLUT5 in naked mole rats (Park et al., 2017) or other GLUTs in hummingbirds (Welch et al., 2013). Overall, hummingbirds have a highly optimised fuel delivery system, termed the ‘sugar oxidation cascade’ [reviewed in, (Suarez and Welch, 2017; Suarez et al., 2011; Welch et al., 2014)]. A persistent physiological question has been how hummingbirds can maintain such high levels of circulating sugars even though persistent hyperglycemia is toxic to vertebrates. That hummingbirds do not develop diseases such as diabetes may be due to their intense daily exercise (Suarez and Welch, 2017). Hummingbird adaptations therefore not only enable constant intensive flight activity, but may actually require it as well.

Hummingbird muscles are greatly enlarged to power the demands of hovering flight. They also exhibit a unique motor unit design in which the motor endplates are organised in highly structured lines compared to the dispersed distribution in other birds (Donovan et al., 2013) (Figure 1.2). This may serve to facilitate more coordinated electrical signalling and contraction of the flight muscle. It would be interesting to examine whether hummingbird

myofibrils exhibit the long-range order (crystallinity) associated with high-performance insect muscles (Iwamoto et al., 2006).

Hummingbird neurobiology likewise exhibits maximisation and tweaking of capacities to support the specific visual requirements of hovering and fast forward flight (Dakin et al., 2016; Goller and Altshuler, 2014), including hypertrophy of brain visual centers and shifting of neuron tuning frequencies (Gaede et al., 2017; Iwaniuk and Wylie, 2007). Some of these features might be present in other birds capable of brief hovering (Iwaniuk and Wylie, 2007), implying a general evolutionary pathway to hummingbird specialisation, but this has not yet been established. The hippocampal formation is also enlarged (Ward et al., 2012), which may underlie spatial memory crucial for hummingbirds' breeding and feeding territoriality (Henderson et al., 2006). It would be interesting to test the role of the hippocampus among territorial and non-territorial species and sexes. As well, the hippocampus may have seasonal enlargement and changes in neurogenesis (Sherry and Hoshooley, 2010) coinciding with breeding.

Despite progress in understanding hummingbird form and function, the major question remains, what defines hummingbird maximum performance (i.e., the performance envelope), and do hummingbirds make use of the entire accessible performance space? In aircraft engineering the performance envelope is typically well-defined given what is known about the role of various factors in the intended design, such as load factor (maximum force/weight). Comparatively little is known about the crucial functional context of the hummingbirds body plan, because it has not yet been possible to link any important ecological measures to an aspect of flight performance, such as flight speed or turning rate. Recent approaches have laid the groundwork for Arnold's lab-to-field method (Segre et al., 2015; Segre et al., 2016). A critical

question will be to what extent measures of maximum performance are predictive of the normal range of flight behaviours, and which one is a better predictor of fitness components.

Early ecomorphological attempts to address the importance of different aspects of flight performance melded form and function in a calculation called the wing disc loading [body weight/ $(\pi \cdot \text{wing span}^2)$ , where  $\pi$  is the assumption of a 180° stroke amplitude, (Epting and Casey, 1973)]. Wing disc loading was proposed by analogy to helicopters: it was thought that wings flap through a stroke plane (Figure 1.2) in the same way that helicopter blades rotate through a disc. Low wing disc loading should correspond to cheaper flight because for the same lift production, a larger disc area can be swept out by a longer wing moving at lower velocity, corresponding to reduced velocity of air in the wake. The mechanical power initially supplied by the muscles and injected into the wake is therefore also reduced (Epting and Casey, 1973). This assessment was supported by measurements of reduced metabolic demands among individuals and species with lower wing disc loading (Epting, 1980). Conversely, it was proposed that high wing disc loading results from a short wing capable of higher stroke frequencies, which increases maneuverability (Feinsinger and Chaplin, 1975). The wing disc loading is also very similar to wing loading (weight/wing surface area), a variable underlying many aspects of fixed-wing aircraft performance.

High wing disc loadings are expected to confer greater flight agility but with a greater power cost, an appealing trade-off between energetics and performance in light of the high cost of hummingbird flight. Wing disc loading was subsequently found to be reduced in conditions where efficiency should be prioritised: among females and juveniles compared to territorial adult males; among species at higher elevations; and among less aggressive hummingbird guilds such as trapliners (Ewald and Rohwer, 1980; Feinsinger and Chaplin, 1975; Feinsinger and Colwell,

1978; Feinsinger et al., 1979; Kodric-Brown and Brown, 1978). The presumed functional differences due to wing loading lead to a potential morphological conflict among migratory Rufous hummingbird (*Selasphorus rufus*). On the one hand, Rufous hummingbirds have great energetic demands for long-distance migration to breeding sites, which should favour low wing disc loading. On the other hand, they must be aggressive and maneuverable enough to competitively displace resident hummingbirds from floral territories along their migration route, which should favour high wing disc loading (Kodric-Brown and Brown, 1978). The appearance of highly emaciated individuals on the migration route suggests that these tradeoffs result in life on a knife-edge, most prominently in drought years with reduced floral abundances (Kodric-Brown and Brown, 1978).

Wing disc loading is derived solely from measurements of form and so does not account for function. Incorporation of real stroke amplitudes into wing disc loading, and substituting the more relevant wing length for wing span, yields better estimates of induced power requirements according to Ellington's method [(Altshuler et al., 2004a; Ellington, 1984a), but Ellington's method is calculated from the same measurements, so is not an independent assessment of the accuracy of power estimation]. Importantly, only when form and function are integrated is it possible to predict competitive dominance among pairwise species interactions. Nonetheless, the calculations show exactly the opposite trend to that predicted by wing disc loading. Dominant species had lower wing disc loading than subordinate species, the condition which was hypothesised to correspond to energetic efficiency and not to competitiveness (Altshuler et al., 2004a). Foraging behaviour of hummingbirds throughout the day likewise contrasts with the wing disc loading predictions. Hummingbirds refrain from foraging during midday, which reduces body weight and is thought to increase agility (Hou and Welch, 2016), opposite to the

predictions of decreased wing disc loading. The behaviour is abandoned during premigration and hummingbirds feed constantly throughout the day to increase fat stores (Hou and Welch, 2016; Hou et al., 2015), which would increase wing disc loading. The physiological consequences and evolutionary origin of wing morphological divergence among species, sexes, and life history stages therefore remains unclear.

It seems likely that hummingbirds are capable of a broader range of behaviours than they routinely use. Examination of free flight behaviours, including competitive interactions and sexual displays, suggests that the performance envelope is determined by maximum muscle capacities (Altshuler et al., 2010; Segre et al., 2015; Sholtis et al., 2015). Most of the time, especially during solo flights, hummingbirds likely keep far from the bounds of the performance envelope (Segre et al., 2015; Sholtis et al., 2015).

In normal flight, it is expected that the optimal energetic strategy is to use the widest possible stroke amplitude and lowest possible stroke frequency (Ellington, 1984a). Like most animals though, hummingbirds fly with substantially lower stroke amplitudes than the energetic optimum [(Altshuler et al., 2004c; Tobalske et al., 2007a), and why wing disc loading is not predictive]. Usherwood suggested that hovering animals fly with suboptimal aerodynamic efficiency to minimise inertial (acceleration of the wing mass) costs, and therefore maximise overall efficiency (Usherwood, 2009). A more general reason for inefficiently-low stroke amplitudes is that hummingbirds rely extensively on stroke amplitude modulation for maneuvering flight, including burst forces and acrobatics such as flying backwards (Altshuler et al., 2012; Chai and Dudley, 1996; Read et al., 2016; Sapir and Dudley, 2012; Sapir and Dudley, 2013; Wells, 1993a). Aerodynamically, this makes sense because stroke amplitude is a principal determinant of aerodynamic forces on flapping wings (Lentink and Dickinson, 2009b). Flight

maneuvers and aerial agility are critical in hummingbird life history (Clark, 2009; Dearborn, 1998; Stiles, 1995; Stiles et al., 2005), and therefore the gain of energetic efficiency with larger stroke amplitude would sacrifice ecological opportunity. As well, the gain in energetic efficiency would be costly if it compromises the ability to escape by amplitude-mediated bursts of force. A recent behavioural study reported that hummingbirds adopt low stroke amplitudes and high stroke frequencies in alarming situations [such as the appearance of a dense vapour plume formed when hot water is poured over dry ice for flow visualisation (Pournazeri et al., 2013)]. The ability to choose between different kinematics even while doing similar work (hovering) is another example of the importance of the behavioural filter between performance and fitness (Garland and Losos, 1994).

### **1.2.3 Ecological context**

Hummingbird flight performance is strongly dependent on biotic ecological context, especially during aerial interactions when high maneuverability is thought to underlie competitive success. Hummingbirds visit a larger region of performance space during competitions than solo flights (Segre et al., 2015) and likely achieve the limits of their flight performance during courtship dives and, potentially, wing acoustic signalling (Clark, 2009; Hunter and Picman, 2005). Although studies are beginning to elucidate the morphological and physiological correlates of hummingbirds' aerial performance both individually and while competing, as yet even the biomechanical correlates of competitive dominance are poorly understood (Altshuler et al., 2004a). Linking form, function, and fitness remains a long-term goal. Some aspects of biotic context remain to be explored. The dramatic lifestyle of hummingbirds has afforded a great opportunity for a host-specific adaptive radiation of blood

parasites (Moens et al., 2016). With so much energy going into fueling their lifestyle, hummingbirds' immune function could be a critical contributor to physiology and flight performance.

Hummingbirds' ability to adapt their performance to abiotic ecological context is a major factor (and perhaps driver) in their success and diversification. As a vertebrate, thermoregulation is a key consideration. Like some insects (Harrison et al., 1996), hummingbirds can adopt energetically inefficient kinematics that generate excess heat to maintain stable body temperatures (Chai et al., 1997; Chai et al., 1998), presumably for biochemical and biomechanical efficiency (Reiser et al., 2013).

The major abiotic factor in hummingbird evolution was the Andean uplift and consequent diversification at high altitudes (Altshuler et al., 2004c; Feinsinger et al., 1979; McGuire et al., 2014). Altitudinal migrants are faced with dual challenges of reduced air density and oxygen availability, and compensate with increased stroke amplitudes and decreased stroke frequencies respectively (Altshuler and Dudley, 2003). The effect of the latter is slight, and the decrease in air density appears to principally limit high-altitude performance (Altshuler and Dudley, 2003; Segre et al., 2016). Adaptation to high altitude may restore most of the performance envelope (Altshuler et al., 2004c; Projecto-Garcia et al., 2013), and altitudinal natives outcompete transplants in their respective native habitats (Altshuler, 2006). Whether evolution of larger wings is the mechanism of adaptation to high altitudes is not yet clear [as in other animals, e.g., (Lack et al., 2016)], and Altshuler and colleagues suggested that changes in wing size with altitude are in proportion to increased body size (Altshuler and Dudley, 2002; Altshuler et al., 2004c). Like for biotic context, the fitness landscape of variation in performance with altitude is entirely unknown. Important advances will come from a better understanding of whether and

how altitudinal adaptation results in a shift in the performance envelope (Figure 1.1). For instance, if evolution at high elevation does come at a cost, hummingbirds might increasingly adopt less-aggressive and energetically-intensive display mechanisms, such as singing.

The hierarchical paradigm of form, function, and fitness is a convenient construct to guide studies of organismal evolution. In flying animals, there remains much that we do not even know about how morphology maps to performance and energetics. Unlike ground reaction forces or buoyancy, the mechanisms of weight support and thrust production in air are very difficult to even model theoretically because of the strong scale-dependence of fluid phenomena. As envisioned by Arnold's lab-to-field paradigm (Arnold, 1983), laboratory studies of flying animals have revealed many links between form and function (Ellington, 1984c; Ellington, 1984d) and a broadly comprehensive set of methods to study comparative limits of performance in the field (Altshuler and Dudley, 2002; Darveau et al., 2005b; Dudley, 1990; Dudley, 1991). Laboratory studies have been crucial for uncovering the functional (aerodynamic) features of flying animal morphology (Altshuler et al., 2015; Hedenström and Lindström, 2017; Hedrick et al., 2015; Socha et al., 2015; Warrick et al., 2012), but the range of laboratory-testable behaviours and animals is limited. The recent advent of field- and animal-portable techniques and equipment is resulting in rapid steps toward understanding performance in the field (Bishop et al., 2015; Bowlin and Wikelski, 2008; Hawkes et al., 2011; Rattenborg et al., 2016; Reynolds et al., 2014; Segre et al., 2016; Taylor et al., 2016; Theriault et al., 2014; Voelkl et al., 2015; Weimerskirch et al., 2016). This will be particularly important because the majority of field hummingbird flight performance has been evaluated based on models of hovering flight, rather than maneuvering forward flight.

### 1.3 Allometry and the origin of the hummingbird performance envelope

Fitness is difficult to assess directly, but comparative analyses among species can reflect the products of selection. The most common framework is to compare differences among species in the common reference frame of body mass (Günther et al., 1992). This approach is termed *allometry* when the comparison is made on the basis of ‘allometric’ power exponents of mass (Figure 1.3). This is a reasonable approach for many biomechanical traits, consistent with the central importance of size in mechanically linking form and function, but whether body mass is an appropriate basis for comparison in other cases is frequently disputed (Apol et al., 2008; Butler et al., 1987; Pélabon et al., 2014).

The elementary question of allometry is whether mathematical functions of body mass represent laws or opportunities (Gould, 1966; Hirt et al., 2017; Marden, 1994; Voje et al., 2014; West et al., 1997). To what extent can mechanisms be common to all living organisms (Brown et al., 2004; Fox Keller, 2007), and when does the inevitable exception (Sandell and Otto, 2016) prove or disprove the rule? How do we discriminate evolution of form and function *required* by size versus that *permitted* by size (Gould, 1966)? Ultimately, when and how do allometric relationships evolve (Pélabon et al., 2014; Uyeda et al., 2017; Voje et al., 2014)? It is critical to reevaluate how physically and mechanically analogous allometry truly is to formal dimensional analysis (Butler et al., 1987; Gould, 1966; Prothero, 2002), which is of greatest concern when dimensional analysis is used to derive the isometric null hypotheses of allometric analyses [e.g., (Günther et al., 1992; McMahon, 1973; Pennycuick, 1990; Platt and Silvert, 1981)].

Reevaluating existing methods can lead to new insights and analyses.

Interpreting allometric trends as constraints is often circular because the ‘laws’ are applied to explain the observations that inspired the laws. For instance, larger animals are not

observed to hover, and allometric laws can be derived that indicate adverse scaling of aerodynamics means hovering is only favourable for smaller animals (Ellington, 1991; Warrick et al., 2012). This method can neither support nor refute a given hypothesis. The pitfalls of the allometric approach are exemplified by a recent analysis of the extreme allometry of animal adhesive pads (Labonte et al., 2016). The authors extrapolated their results to prove that Spider-Man cannot exist because the body surface area required for adhesion (40%) would be unrealistic. The authors concluded that the absence of a human-sized gecko proves the impossibility of human-sized geckos, unaware that a Stanford research group was already adhering graduate students to walls (Hawkes et al., 2015). To do so, the Stanford group built upon principles of gecko surface adhesion to generate a novel and more efficient design able to bear human weight, a quintessentially evolutionary approach. So in the sense that the existing allometry could not be extended to humans, Labonte et al. (Labonte et al., 2016) were correct, but extrapolation of allometric correlations fails to account for evolutionary innovation. Extrapolation from exponents should therefore be done with the utmost caution.

In addition to conceptual difficulties, it is important to account for a number of statistical issues that can bias estimates of exponents. Chief among these is a need to account for phylogenetic relatedness (Felsenstein, 1985; Garland and Adolph, 1994). Apparent allometry in wing proportions may disappear when allowing for shared evolutionary history (Nudds, 2007). Accordingly, it is crucial to account for phylogenetic relatedness, but it is also necessary to recognize that branch support varies across most trees and in some cases may be weak, and so phylogenetic uncertainty should also be considered (de Villemeireuil et al., 2012; Mahler et al., 2013; Mahler et al., 2013; Rangel et al., 2015). Comparative studies must also assess the confidence in the estimated species measurements, which may be highly unreliable when species

are represented by few individual observations. Measurement error, comprising within-species variance due both to sampling and biological effects, may represent a source of bias as great as phylogenetic inertia (Garamszegi, 2014). Even a few repeated measurements may greatly increase statistical power (Blomberg et al., 2003; Harmon and Losos, 2005), which is critical when attempting to distinguish between close scaling exponents, or if confidence intervals appear to only weakly support or reject an hypothesis. Similarly, allometric exponents commonly diverge within and between species (Green et al., 2001; Higginson et al., 2015), which can bias the estimate of the interspecific relationship (Felsenstein, 2008). Finally, comparative studies are susceptible to interactions between all these problems, because measurement error inflates the apparent differences in species traits between closely related species (Felsenstein, 2008; Ives et al., 2007; Martins and Hansen, 1997; Ricklefs and Starck, 1996).

Within species, there may be substantial variation due to a variety of sources which collectively constitute measurement error (Hadfield and Nakagawa, 2010). The impact of measurement error on phylogenetic comparative studies, and methods for handling it, have received considerable recent attention (Cornwell and Nakagawa, 2017; Felsenstein, 2008; Garamszegi, 2014; Garamszegi and Møller, 2010; Hadfield and Nakagawa, 2010; Ives et al., 2007). Most strategies are specific cases of restricted maximum likelihood that are well developed in quantitative genetics (Hadfield and Nakagawa, 2010). An emerging alternative is Bayesian Markov chain Monte Carlo (MCMC) (Hadfield and Nakagawa, 2010). A major advantage of MCMC is its flexibility in integrating over all sources of variation in a study, such as phylogenetic uncertainty (de Villemereuil et al., 2012). With MCMC, posterior distributions are obtained for all parts of the model (Kruschke, 2013), allowing inferences on parameters, such as phylogenetic signal, for which it would generally be more difficult to draw conclusions.

Comparative studies can also be influenced by error in the form of sampling bias. Across species, samples may not be representative of the clade as a whole due to oversampling of common, convenient, and 'fluffy' species (Nakagawa and Freckleton, 2008).

The ability of allometric relationships to provide broad insight into commonalities among species is not always clear. One reason is that in the allometric perspective, essential aspects of trait variation are captured by static measurements of morphology and physiology, even though animals owe most of their success to adaptability and plasticity. Additionally, many assumptions of allometry, such as geometric similarity, 'vitiates analysis of size-independent diversity, and the fallacy underlies the problems of using scaling' (Rayner, 1988). Biomechanical analyses are uniquely equipped to probe the consequences of morphological and physiological diversity, and provide a mechanistic understanding of Newtonian and Darwinian forces. How does body size constrain locomotor modes (Borazjani and Sotiropoulos, 2010; Walker and Westneat, 2000)? How does shape variation affect performance (Borazjani and Daghooghi, 2013; Kruyt et al., 2014; Ray et al., 2016)? How do three-dimensional features of wing morphology compare to simple (e.g., planform) measurements of size and shape (Altshuler et al., 2004b; Bokhorst et al., 2015; Bowlin and Wikelski, 2008)? How does dynamic control of wing shape contribute to performance (Lentink et al., 2007; Riskin et al., 2010; Thomas, 1996; Young et al., 2009a; Zheng et al., 2013), and when is it advantageous to be morphologically and behaviourally flexible (Boller and Carrington, 2007; Elliott et al., 2013; Henningsson et al., 2014; Vogel, 1989)? These are questions that must be addressed by measurements in active organisms, and cannot be resolved by allometry alone.

Intraspecific variation is an underutilised resource (Bennett, 1987), but essential for evolutionary inference. This is particularly relevant when interindividual performances can differ

by an order of magnitude, such as running speed and endurance (Bennett, 1987). Variation in performance defined broadly through differences in morphology and physiology alone may be sufficient for comparisons among clades and species [e.g., (Norberg and Rayner, 1987; Rayner, 1988)], where function may be implied by form due to coevolution (Donley et al., 2004). However, fitness is defined at the level of populations and individuals, and covariation of form and function within and among individuals may be very different from that observed among species (Careau and Wilson, 2017; van de Pol and Wright, 2009). For instance, despite a very tight relationship between metabolic rate and body mass among bee species (Darveau et al., 2005a), idiosyncrasies among many covarying morphological and physiological factors result in over two-fold variation in metabolic rate at the same body mass within species (Skandalis and Darveau, 2012). Disentangling form from function within species is much more difficult than among species, perhaps why morphological variation is often difficult to link to fitness even when morphological patterns appear clear among species (Careau and Garland, 2012; Careau and Wilson, 2017; Houle et al., 2010; Irschick and Garland, 2001).

Analyses of variability are rare in flight biomechanics and physiology, where sample sizes tend to one or a few individuals. Insight from individuals can nevertheless inform, and perhaps question, the generality of many theories. For example, despite the common view that flight power depends on flight speed through relationships that resemble J- and U-shaped curves (Dial et al., 1997; Rayner, 1988; Tobalske et al., 2003), individuals actually display variable and sometimes even linear power curves (Busse et al., 2013; Clark and Dudley, 2010; Ellington et al., 1990). An important step will be to understand how interindividual variation in morphology and kinematics (Iriarte-Diaz et al., 2012) underlies variation in types of flight-speed power curves. In hummingbirds, lower wing loading results in flatter power curves at low airspeeds, but

similar power at intermediate airspeeds (Clark and Dudley, 2010). For highly active and maneuverable species that constantly adjust flight speed, selection might therefore act on functions (Bolstad et al., 2015) of performance rather than specific capacities.

Many insights have come from hummingbirds, which exhibit an order of magnitude variation in body size, and have seized an ecological and biomechanical opportunity at the insect-like limit of vertebrate performance (Ellington, 2006; Warrick et al., 2005). The morphological convergence necessary to execute insect-like flight has been thought to have been accompanied by relinquishing bird-like wing control (Chin et al., 2017; Ellington, 2006). This assumption has rarely been examined directly (Hedrick et al., 2012; Song et al., 2014; Tanaka et al., 2013; Tobalske et al., 2007a), and never completely, and so our knowledge of the tradeoffs involved in the evolution of even this well-studied group remains limited.

#### **1.4 Thesis objectives and outline**

The objective of this thesis is to explore the constraints and opportunities that collectively determine the performance envelope and flight energetics of hummingbirds. At the start of the research, I hypothesised that,

(1) Evolution of wing morphology inherently involves a trade-off between minimum flight power requirement and maneuverability. I predicted that known wing area allometry in hummingbirds would be consistent with minimising power, but result in reduction in a measure of burst flight performance.

(2) Adopting three-dimensional wing shapes broadens the flight performance envelope. I predicted that a) hummingbirds have maintained a major feature of avian flight, the ability to dynamically control wing size and shape throughout the stroke cycle, and b) hummingbirds increase twisting and cambering to fly in challenging conditions.

To address hypothesis (1), in Chapter 2, I investigate the integration of form, function, energetics, and ecological context (Figure 1.1) to develop a consistent biomechanical framework to integrate performance and energetics in an ecological context. I compare allometries within and among species to predict the likely selective factors that have contributed to hummingbirds' unusually large wing area allometry. Unexpectedly, and contrary to the hypothesis, I find that the same adaptation that minimises energetic costs also maximises one measure of flight performance; the predicted trade-off is absent. However, in Chapter 4 I expand this allometric analysis and show that there is indeed a cost to another measure of maneuverability, but only for increasing body size. I further explore how this could be related more generally to body size evolution in hummingbirds.

To address hypothesis (2), in Chapter 3, I develop experimental and analytical methods that allow a high-resolution reconstruction of the wing surface during a set of challenging flight conditions. I find that hummingbirds do modulate their three-dimensional wing shape throughout the stroke cycle, and utilise different shapes to accomplish diverse flight goals, which supports hypothesis (2). Unexpectedly though, hummingbirds do not use the predicted high-lift, three-dimensional wing shapes when pushed to the extremes of their abilities, but precisely the opposite: they appear to adopt flatter, plate-like models. Based on a blade-element analysis of the forces acting on the wing (Song et al., 2015b), I propose that hummingbirds typically modulate their wing shape to maximise energetic efficiency, but can sacrifice efficiency if it enables a desired goal. Hummingbirds have thus retained avian capacities for wing morphing despite convergence on insect-like flight, and this behavioural flexibility offers further flight control degrees of freedom that can be called upon as required.

In Chapter 4, I explore how the conceptual framework of Chapter 2 can be applied for new insights into standing allometric problems. I also explore whether and how the morphological flexibility described in Chapter 3 is a general feature that must be considered in the form-function-fitness paradigm. Finally, I present some perspectives on future directions of research on hummingbird form and function.

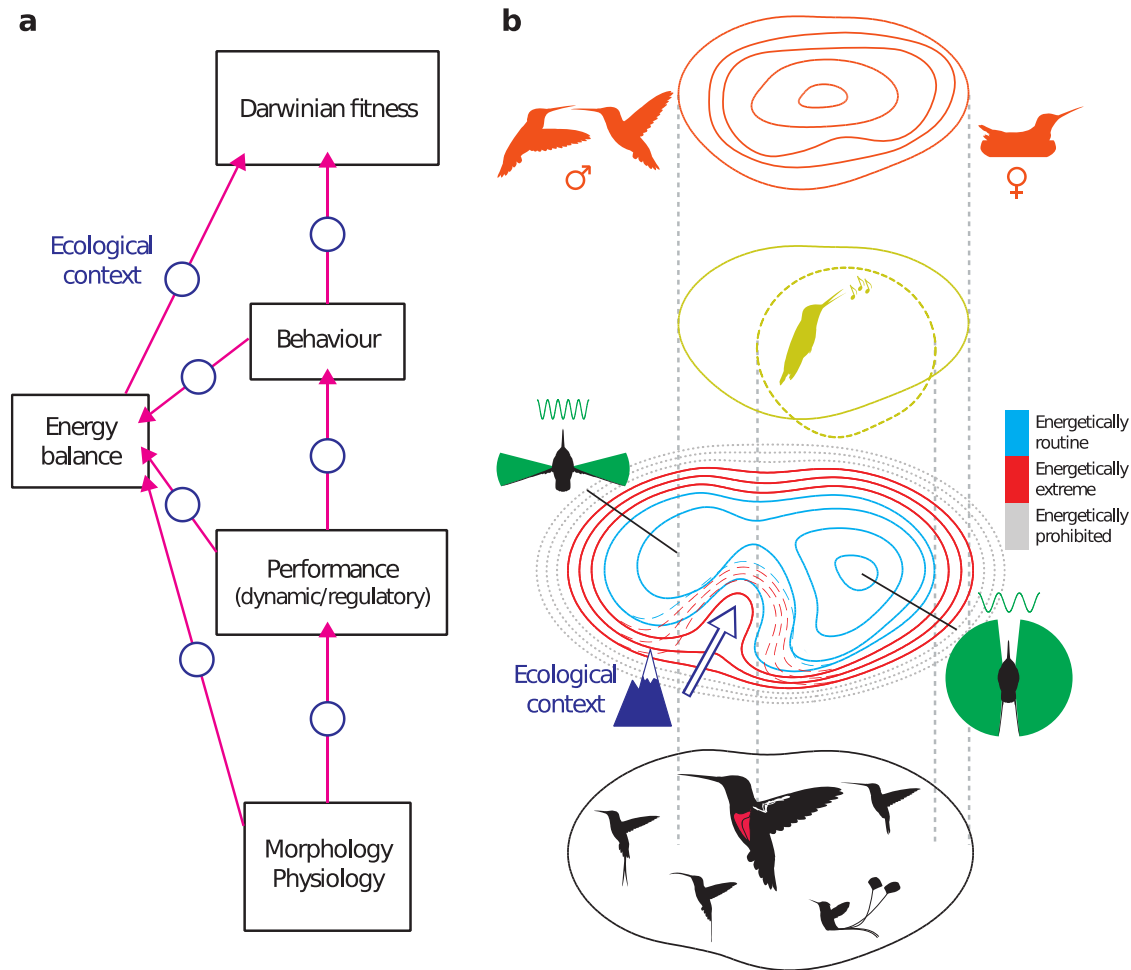


**Figure 1.1** Hierarchical paradigm of form, function, and fitness. **a** Morphology and physiology impact fitness insofar as they dictate the performance envelope, which itself forms only the bounds in which an animal can behave. Behaviour is directly tied to Darwinian fitness, for example through predation and predator avoidance, or social and sexual activities. Animal behaviour within the performance space dictates energy uptake and expenditure, and therefore net energy balance. Energy balance directly impacts fitness, for example through immediate impacts such as death by exhaustion, or insufficient resources to produce offspring or ensure offspring survival. Ecological context due to biotic (e.g., parasites, competition) and abiotic (e.g., temperature, air density) factors influence each of these arrows. **b** The elements of the hierarchical paradigm are visualised by a fictional performance, energetic, behavioural, and fitness landscapes based on knowledge of hummingbird biology. The stages are viewed as a set of overlapping functions, joined by the dashed lines. Morphology and physiology can directly contribute to energy balance through factors such as developmental costs, and collectively determine the whole-animal performance

envelope. Maintaining performance introduces regulatory costs, such as membrane polarisation, and the dynamic costs of behaving. Energy balance is therefore dictated by the range of behaviours an animal uses within its envelope, including behaviours that lead to energy gain and consumption. Energetic isoclines within the performance space dictate the energy balance, corresponding to the routine range of behaviours (blue), potential but rarely recruited and highly costly behaviours (red), and energetically and morphologically prohibited behaviours (dashed gray). Here, the cartoon represents an energetic basin corresponding to a hypothetical maximally efficient behaviour, but also a large range of behavioural states with broadly similar energy usage. An example in hummingbirds is the large range of stroke amplitudes and frequencies they can employ, with apparently minimal aerodynamic costs [exaggerated for effect, (Wells, 1993a)]. The space of possible performance states is larger than the range of behaviours routinely exhibited. This affects the energy balance, and provides a filter between animal performance and fitness. The fitness landscape does not need to coincide with the energetic cost of behaviours. Here, two separate peaks are drawn, emphasising that the behavioural and performance range of the two sexes may be very different. The optimum for males significantly overlaps with areas of the performance space that are energetically very costly, such as vibrant sexual signalling displays, whereas the optimum for females lies in an area favouring energetic efficiency. All relationships are contingent on ecological context. In this example, living at high altitude modifies the performance landscape, increasing the energetic cost (dashed isoclines) of many performance states. Animal behaviour may change to compensate, shown as a shift in the behavioural envelope. This could include greater use of energetically more economical behaviours, such as singing. The conflict with the fitness space may lead to morphological and physiological adaptation, or a shift in the fitness space itself.

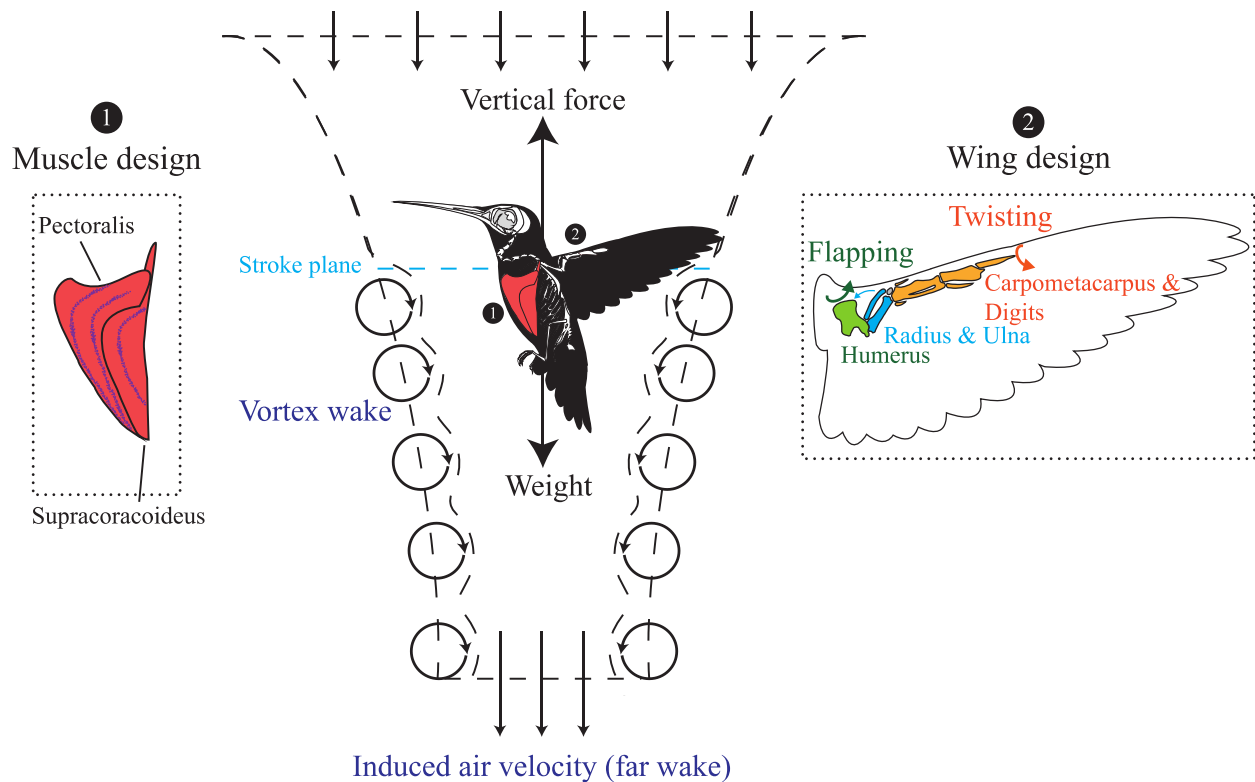


**Figure 1.2** Biomechanics of hummingbird hovering flight. Hummingbirds must generate sufficient vertical force (lift) to support their body weight. The animal performs work to accelerate a mass of air through the stroke plane (actuator disc). The induced power requirements are proportional to the induced air velocity at the actuator disc. An ideal rotor wake smoothly accelerates air (wake bounds dashed line), but the wake boundary of reciprocating wings involves shed vortices that introduce wobbliness and increase induced power costs. Hummingbirds have many adaptations to allow stable hovering, including greatly enlarged flight muscles and specialised wing anatomy. Muscles exhibit further specialisations, such as ordered motor endplate organisation and maximum enzyme packing. Hummingbird wing bones have evolved to maximise the transmission of muscle power into the stroke through shortening of the humerus. Additionally, twisting of the handwing (carpometacarpus and digits) allows hummingbirds to twist the wing into downstroke and upstroke configurations, allowing lift production throughout the stroke cycle. Hummingbird aerodynamic visualisation adapted from helicopter wake visualisation (Leishman, 2000). Skeleton and muscle silhouette by Benny Goller and Douglas L. Altshuler. Wing bones (right) by DAS.

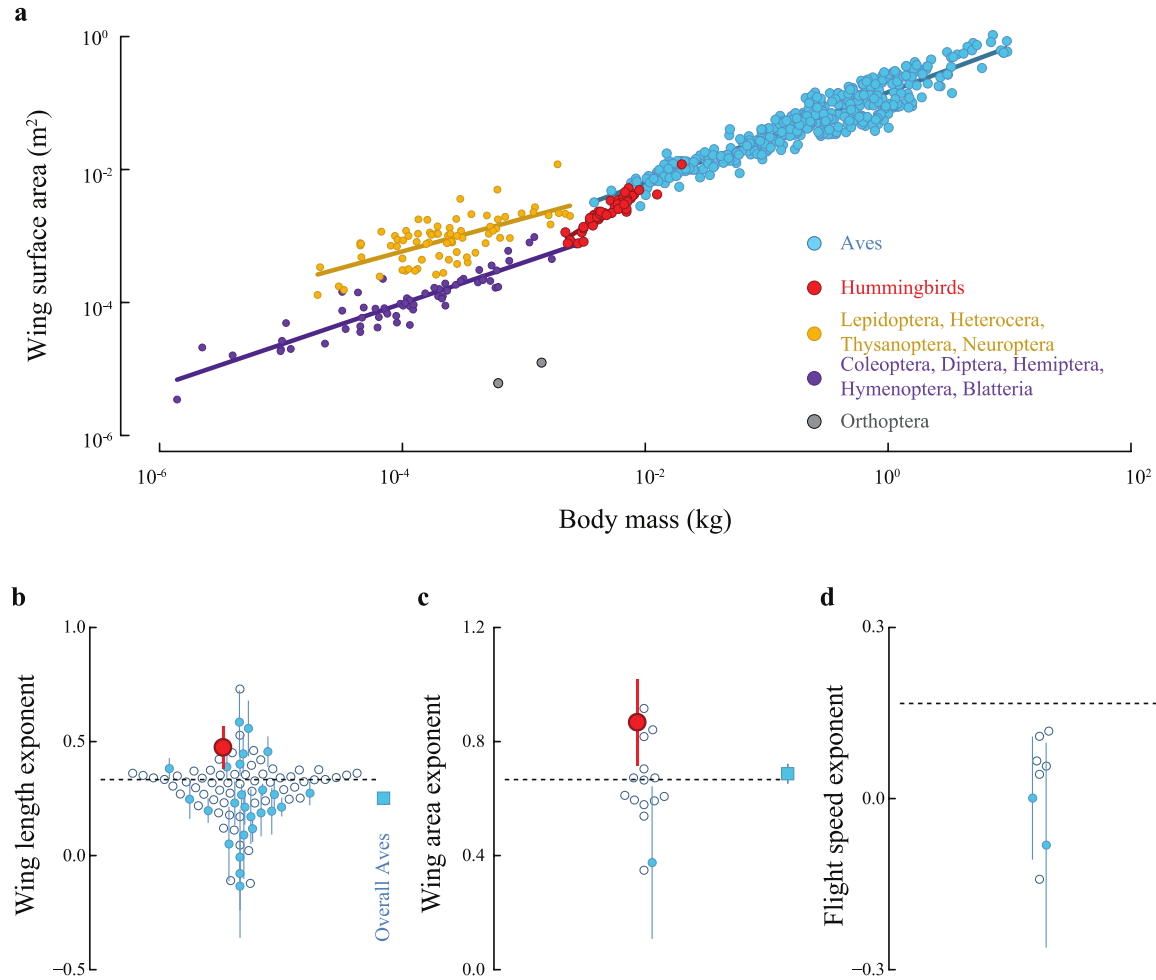


**Figure 1.3** Allometric relationships in flying animals. **a** Greenewalt (Greenewalt,1962) identified five major groups of flying animals, based on the relationship between wing area and body mass. Hummingbirds appear to have a distinctly great increase in wing area with body mass, compared to all other groups. However, this could be due to the different taxonomic levels represented here. Family-wise reanalysis of the avian allometries of wing length (**b**) and wing area (**c**) suggests that hummingbirds do lie at the upper end of the distribution of exponents, but so do other Families. Exponents are filled and shown with 95% confidence interval (CI) if the CI excludes the isometrically predicted exponent based on geometric similarity. The credible intervals suggest that wing lengths and area in hummingbirds increase with body mass to a greater extent than predicted by proportional growth alone. **d** On the whole, exponents of air speed are less than the isometric prediction, and generally closer to zero, indicating that air speed is independent of body size within a Family. In **b,c,d** right-side filled squares indicate the overall phylogenetic mean exponent.

## Chapter 2: The biomechanical origin of extreme wing allometry in hummingbirds

### 2.1 Introduction

Flight requires specialised morphology and physiology, and among the extant flying animals, hummingbirds exhibit some of the most extreme adaptations (Chai and Dudley, 1996; Clark, 2009; Hedrick et al., 2012; Suarez et al., 1991). Hummingbirds sustain hovering, a highly energetically costly behaviour supported by numerous morphological and kinematic innovations (Altshuler and Dudley, 2002; Hedrick et al., 2012; Tobalske et al., 2003). Perhaps as ecologically fundamental, hummingbirds are highly aggressive, with frequent aerial competitions determined by aerial agility (Segre et al., 2015; Sholtis et al., 2015) and possibly influenced by differences in body size (Dearborn, 1998). An often overlooked feature of hummingbird morphology is an unusually large increase in wing area with increasing body weight ( $W=M_{\text{Bg}}$ ) compared to other birds (Greenewalt, 1962). The exponent of the allometric relationship (equations of the form  $Y=aW^b$ ) of hummingbird wing area to body weight has been estimated between 1.1 and 1.3, compared to about 0.7 across all other birds (Greenewalt, 1962; Rayner, 1988). This large exponent indicates that larger species have very large wings for their body weight, even though larger wings are predicted to be negatively associated with many aspects of aerial agility (Rayner, 1988) and so could compromise flight performance.

Understanding the origin of this wing area allometry and how it influences flight performance has the potential to explain how hummingbirds have diversified into their specialised ecological niche, and explain the biomechanical evolution of flying animals more

generally. The challenges of studying allometric variation are to place calculated exponents into a functional context and to link patterns among species to variation within species (Bolstad et al., 2015; Pélabon et al., 2014). Addressing these challenges allows us to assess the possible significance and origin of proposed allometries.

Allometries linked to flight performance do not evolve in isolation. The coevolution of suites of biomechanical traits dictates organismal performance, resulting in patterns such as the dependence of flight performance allometry on species elevation (Altshuler et al., 2010). The functional evolution of any one trait, such as wing area, must therefore be considered alongside many correlated biomechanical traits. Previous work has focused to a great extent on the evolution of flight performance in response to changes in elevation (Altshuler and Dudley, 2002; Altshuler and Dudley, 2003; Altshuler et al., 2010), but a general theory linking this variation to the proximate determinants of flight performance has not yet been developed. Moreover, because allometries are evolving traits, a general understanding of the evolution of flight performance must start at the variation observed among individuals and populations. A barrier to such studies is the daunting number of traits that can potentially be related to flight performance, making it difficult to choose a suite on which to build a complete framework. Simultaneously, the large number of traits might suggest that there are many potential evolutionary paths resulting in similar flight performance. An integrative perspective on this problem must be able to explain not just the presence or absence of an allometry, but also explain its magnitude. We approach this general problem by considering the mechanisms that contribute to the generation and cost of aerodynamic force in flight, and thus develop a framework to unify many aspects of hummingbird flight physiology.

All animals that use powered flight must generate time-averaged forces to support their body weight, which therefore represents the minimum level of selection. Flight forces in excess of body weight can then contribute to other flight behaviours, such as aerial displays and aggressive encounters. The dependence of aerodynamic forces on kinematic and morphological parameters is encapsulated by well-known scaling relationships. According to the blade element model, the time-averaged equation for vertical, weight-supporting aerodynamic force during hummingbird hovering is,

$$\bar{F}_V = W = \frac{1}{2} \rho \bar{U}^2 S \bar{C}_V \quad (1)$$

following the Buckingham  $\pi$  theorem, where the mean force  $\bar{F}_V$  is the product of air density ( $\rho$ ), representing the association between body mass and the physical environment a hummingbird has selected; stroke-averaged wing velocity [ $\bar{U}=4f\Phi R_2$ , where  $f$  is stroke frequency,  $\Phi$  is stroke amplitude, and  $R_2$  is the wing length corrected for the spanwise chord width distribution (Ellington, 1984d)]; wing surface area ( $S$ ); and a dimensionless stroke-averaged force coefficient ( $\bar{C}_V$ ) that subsumes evolved differences in wing morphology such as wing twist and camber, and dimensionless postural changes such as angle of attack. The aerodynamic force equation has conventionally been used to derive isometric predictions of the right-hand side terms (Alerstam et al., 2007; Rayner, 1988; Riskin et al., 2010) against which empirical relationships are then compared. However, because in this approach only isometries are explained by theory, we lack functional context in the more common situation that animals violate the isometric model.

Here, we develop an integrative allometric framework from aerodynamics principles to resolve the functional consequences of allometric variation in hummingbirds. We consider the sum of the individual contributions to weight support of each component of equation (1), while

considering common sources of bias in phylogenetic comparative models, such as measurement error and phylogenetic uncertainty (Cornwell and Nakagawa, 2017). We then examine how this allometric variation affects the cost of flight behaviours and limits maximum performance. This framework applies equally among and within hummingbird species, providing an evolutionary pathway from intraspecific patterning to interspecific allometries.

## **2.2 Methods**

### **2.2.1 Data collection**

We use our allometric framework to analyse a data set obtained from individual hummingbirds sampled at different sites in Brazil, Canada, Costa Rica, Ecuador, Peru, and the United States (Figure 2.1). We do not explicitly distinguish sexes. Some kinematic and morphological data for these species have appeared elsewhere (Altshuler et al., 2004c; Altshuler et al., 2010; Chai and Millard, 1997; Groom et al., 2017; Mahalingam and Welch, 2013; Segre et al., 2015). Sample sizes in each bivariate regression in numbers of species and individuals are presented in Table 2.1. All data collection was performed in compliance with respective institutional guidelines. No randomisation or blinding was performed in this study. For the results reported here, we used all available samples, but investigated the impact of data subsets, as described below. Decisions on species naming and placement are listed in Appendix A.

Air density was calculated from elevation using standard pressure and temperature relationships with elevation. We emphasise that in the context of this analysis, the allometry of  $\rho$  is interpreted as evidence for an association between body mass and air density (or elevation), whether due to individuals or species selecting their environment or adapting to it, and not as hummingbirds effecting changes in local air density. Given a species' or individual's body mass,

this regression is a prediction of the environment in which it will be found. In preliminary analyses, we found that  $b_p$  was somewhat influenced by the inclusion of the unusually large and phylogenetically distinct species *Patagona gigas*, and by inclusion of species with a single observation (Figure 2.2). Removal of these progressively reduces the air density allometric exponent toward zero, and so the overall influence of elevation and air density on species body mass is uncertain. Nonetheless, it is notable that the exponent is similar among and within species, which could indicate a common underlying mechanism. We investigated whether independent data sets might show evidence of a correlation between body mass and elevation. We collected species mean body masses and elevational midpoints from the Handbook of the Birds of the World (HBW) (Schuchmann, 1999) and calculated mean species elevations from range maps provided by BirdLife International (BL) (BirdLife International and NatureServe, 2014). Mean elevations from the two sources are well correlated (Figure 2.3), though with somewhat more error for low elevation species. Predictions of species maximum elevation were uncorrelated, likely because the range maps coarsely include all elevations within a contour. Elevation and body mass were examined using a phylogenetic regression implemented in *MCMCglmm*. For all elevational parameters (minimum, mean, and maximum) in both data sets, the credible intervals of the slopes overlap 0 (Figure 2.3).

We examined whether capturing individuals at discrete sites influences results, because discrete sampling might not reflect continuous elevational distributions. We therefore sought to compare our results to independent estimations of species elevations, derived from species range maps (BirdLife International and NatureServe, 2014). Our observational data are reasonably well correlated with the derived species mean elevation and the distribution of species elevations (Figure 2.4).

Wing morphological variables were digitised from photographs of spread wings as described by Altshuler et al. (Altshuler et al., 2010) or from wings spread on graph paper and traced in Adobe Illustrator (CCW collection, see preface). We obtained the area of both wings,  $S$ , and length,  $R$ , and second and third moments of area,  $\hat{r}_2$  and  $\hat{r}_3$ , from these photos, and the aspect ratio was calculated as  $AR=4R^2/S$ .

Kinematics (mean stroke amplitude and frequency) were digitised as previously described (Altshuler et al., 2010; Groom et al., 2017; Mahalingam and Welch, 2013). The mean wing velocity at the second moment of area was calculated as the product of stroke frequency, stroke amplitude, wing length, and the second moment of area, ( $\bar{U}=4f\Phi\hat{r}_2R=4f\Phi R_2$ , see below). Our results do not differ depending on this definition of wing velocity, or the use of the wing tip velocity directly, because  $\hat{r}_2$  is not correlated with body mass (Table 2.1). We calculated the vertical force coefficients in flight while hummingbirds support weight ( $\bar{C}_{w,v}$ ) or during burst load lifting ( $\bar{C}_{b,v}$ ), by rearranging equation (1).

Comparisons among authors are shown in Figure 2.5. Although there is variation among authors (Figure 2.5a–d), the high degree of correlation in wing morphology and air density measurements among authors with overlapping species measurements (DLA, CCW, and PSS data sets, see preface; Figure 2.5e,f), suggests that differences between data sets are largely attributable to species sampling.

## 2.2.2 Phylogenetic uncertainty

We allow for uncertainty in the phylogenetic hypothesis by integrating over a large number of phylogenetic scenarios. Suitable species phylogenetic hypotheses were derived from the posterior distribution of trees previously generated by BEAST analysis (McGuire et al.,

2014). The tree posterior distribution comprised four chains run for one thousand generations each with a thinning rate of four, which we subsampled by half due to constraints on computer memory and run time. Inspection of the tree convergence suggested a burn-in period of 25 samples in the posterior was sufficient, yielding 450 trees ( $\Sigma$ ). We then replicated these trees four times each in a procedure to account for uncertainties in species relationships created by different choices of individuals as species representative (this 1:4 ratio qualitatively balanced uncertainty and tree redundancy). In each replicated tree, for species in the phylogeny in which more than one individual was sampled, we randomly chose one individual as the species representative for that tree. The phylogenetic signal in the independent and dependent variables was allowed to be weaker than strict Brownian motion through Pagel's  $\lambda$  implemented as  $\Sigma_\lambda = \lambda\Sigma + (1-\lambda)\mathbf{I}$ , where  $\mathbf{I}$  is the identity matrix (de Villemereuil et al., 2012; Pagel, 1999). Phylogenetic independence and dependence are implied by  $\lambda=0$  or 1, respectively, and as we have no expectation for the phylogenetic strength, we assume a uniform distribution in this range (de Villemereuil et al., 2012).

We examine differences among the hypotheses represented in the posterior tree distribution using the method of Kendall and Colijn (Jombart et al., 2017; Kendall and Colijn, 2016). Each tree is encoded by a score that reflects the extent to which the tree is completely described by the lengths or branching pattern of its edges. The set of scores then forms a Euclidean metric space, i.e., the difference between a pair of trees can be found by the difference in their scores. We visualise the broad uncertainty in the phylogenetic hypothesis by projecting the trees' pairwise distances into two principal coordinates (Jombart et al., 2017; Kendall and Colijn, 2016), clustering of which revealed four subgroups of trees. Assuming each subgroup encapsulates a distinct source of phylogenetic uncertainty, we can summarise this uncertainty by

finding the tree that lies at the geometric median of that subgroup, and then comparing this median tree to the Maximum Clade Credibility species phylogeny of McGuire et al. (McGuire et al., 2014). Major topological differences are highlighted in Figure 2.6. Because trees were pruned to the species available in this study, these results do not reflect overall sources of uncertainty in the phylogenetic hypothesis across all hummingbirds.

### 2.2.3 Regressions and hierarchical Bayesian modeling

We used Markov Chain Monte Carlo (MCMC) simulations to analyse log-linear relationships (de Villemereuil et al., 2012; Hadfield, 2010; Plummer, 2003). For analyses presented in Figures 2.7 and 2.8 and Table 2.1, we model relationships while allowing for uncertainty in both the true, unobserved species means and in the phylogenetic hypothesis. We assumed flat, uninformative priors for the regression intercepts and slopes,  $\alpha$  and  $\beta$  respectively, and for all standard deviations (Gelman, 2006),  $\sigma$ . Note that the modelling is typically done on the precision,  $\tau = \sigma^{-2}$ , the reciprocal of the variance. The regression relationship for species means  $Y$  and  $X$ , with phylogenetic variances  $\sigma_Y^2 \mathbf{\Sigma}$  and  $\sigma_X^2 \mathbf{\Sigma}$ ,

$$Y|X \sim \mathcal{N}(X\beta + \alpha, \sigma_Y^2 \mathbf{\Sigma})$$

$$X \sim \mathcal{N}(\mu_0, \sigma_X^2 \mathbf{\Sigma})$$

$$\alpha, \beta \sim \mathcal{N}(0, 10^3)$$

$$\sigma_Y, \sigma_X \sim \mathcal{U}(0, 10^3)$$

where  $\mathcal{N}$  and  $\mathcal{U}$  denote the normal and uniform distributions, respectively. This basic model states that  $Y$  and  $X$  are phylogenetically distributed in the same way, although the phylogenetic variance,  $\sigma^2$ , may differ. As discussed above, we relax this assumption through Pagel's  $\lambda$ , and introduce phylogenetic uncertainty by drawing on the set of posterior trees with some unknown

distribution,  $\Pi(\xi)$ .

$$\Sigma \sim \Pi(\xi)$$

$$\lambda_Y, \lambda_X \sim \mathcal{U}(0,1)$$

$$\Sigma_\lambda \sim \lambda \Sigma + (1 - \lambda) \mathbf{I}$$

and the last equation can be applied to each variable independently.

The joint distribution of individual observations  $x,y$  is the covariance matrix  $\Sigma_w$ , with species means  $X,Y$ . One approach to modelling within-species covariance in bivariate relationships is to place priors directly on the elements of the correlation matrix, but we found this led to poor mixing and a tendency to fixate on a correlation coefficient of  $r=\pm 1$ . We instead model the within-species covariances by a minimally informative inverse-Wishart prior,  $\mathcal{W}^{-1}(\Psi/k_\psi, 2)$ , with an introduced scale factor  $k_\psi$ . The sampling standard deviations,  $\sigma_x, \sigma_y$ , and correlation coefficient  $r_{xy}$ , are then obtained from the posterior distribution of  $\Sigma_w$ . From these, the least-squares intraspecific slope is simply obtained by,  $\beta_{xy} = r_{xy} \cdot \sigma_y / \sigma_x$ . With this modelling procedure, we can assess an average intraspecific pattern, but cannot discriminate if this varies among species. In general, because intraspecific observations are randomly distributed around an unknown relationship, it is not possible to discriminate sampling effects from true species patterns. A related technique is to center observations on the empirical species means, and then treat the slopes as random effects (van de Pol and Wright, 2009). The effect is similar to the current procedure. The measurement error model for the  $i$ th individual of species  $n$  is, finally,

$$x_{ni}, y_{ni} \sim \mathcal{N}(X_n, Y_n; \Sigma_w)$$

$$\Sigma_w \sim \mathcal{W}^{-1}(\Psi/k_\psi, 2)$$

$$k_\psi \sim \mathcal{U}(0, 10^3)$$

We additionally examined whether there is any evidence that specific clades depart from

the overall trends across all hummingbirds. The previous models, allowing for measurement error but not phylogenetic uncertainty, and with the previous uninformative priors, resulted in very wide credible intervals in some clades due to the reduced sample sizes. Because our objective was to find evidence for departures from the overall trend, we therefore used more reasonably informative priors. Following the overall trends, we employed a normal distribution with  $\tau=1$  and either a mean of 1, for wing area, or 0, for other variables. Other precisions were modelled directly through a weakly informative conjugate gamma prior with shape and scale equal to  $10^{-3}$ .

For each regression, we ran four parallel MCMC chains for ten thousand iterations each. The first five thousand samples of each chain were discarded as burn-in, yielding twenty thousand samples from the posterior. Whether a given slope credibly excluded a relevant value, such as zero, was assessed by comparing the overlap of the 95% equal-tailed credible intervals of the regression parameters to the reference value. We verified the trends reported here using the R package MCMCglmm (Hadfield, 2010) (uniform prior:  $V=0$ ,  $\nu=0$ ; 25,000 iterations, 15,000 burn-in samples, three chains), including testing the effect of data subsets on the resulting exponents, notably the air density exponent (Figure 2.2). MCMCglmm did not support estimation of the unobserved species means, so intraspecific trends were calculated using the within-species centering method (Garamszegi, 2014; van de Pol and Wright, 2009).

#### **2.2.4 Force equation for flapping flight**

Dimensional analysis yields the familiar expression for steady aerodynamic force,  $F = \frac{1}{2} \rho U^2 SC_F$  (noting that the force coefficient for hovering flight additionally absorbs differences in

angle of attack). Because flapping wings generate unsteady forces, any allometric relationship for flight must consider a more general time-averaged approach to the vertical force,

$$\overline{F_V} = \overline{\frac{1}{2} \rho U^2 S C_V}$$

where the velocity is calculated at the radius of gyration [second moment of area, (Ellington, 1984d)]. From this departure point, we can tailor the force equation to a form appropriate for the organisms of interest, by considering how the parameters vary over a stroke. In hovering hummingbirds, it is reasonable to assume that (i) wing area is constant through the stroke (Tobalske et al., 2007b), (ii) air density is constant through the stroke, and (iii)  $\overline{U^2 C_V} = \overline{U^2} \cdot \overline{C_V}$ , because by definition,

$$\overline{C_V} = \frac{\overline{\frac{1}{2} \rho U^2 S}}{\overline{F_V}}$$

Assumption (i) of constant wing area is not true for all flying animals, and we therefore derive the following equation specifically for hummingbirds,

$$\overline{F_V} = \frac{1}{2} \rho \overline{U^2} S \overline{C_V}$$

For convenience, we calculate the square of the average wing velocity, but for sinusoidal flapping motions, this differs from the average squared velocity only by a constant. We consider the instantaneous velocity of a flapping wing in hovering flight (body velocity=0) (Lentink and Dickinson, 2009b) which is to within a good approximation a cosine function (zero velocity at tip reversal and maximal at midstroke) (Ellington, 1984b; Tobalske et al., 2007b),

$$U(t) = R_2 \dot{\phi}(t) = R_2 \Phi 2\pi f \cos(2\pi f t)$$

where  $\Phi$  and  $f$  are the mean stroke amplitude and frequency. Because the radius of gyration ( $R_2$ ) can be assumed constant in hovering hummingbirds (but not for birds in general, for bats, or hummingbirds in forward flight), it is sufficient to calculate the average angular velocity (which is always positive),

$$\bar{\Omega} = \frac{1}{T} \int_0^T |\dot{\phi}| dt = \frac{1}{T} \int_0^T (\Phi 2\pi f) \cdot |\cos(2\pi f t)| dt = 4\Phi f$$

and therefore,

$$\bar{U} = 4\Phi f R_2$$

Note that  $\Phi$  here refers to the amplitude of the cosine function, one-half of the pronation-to-supination amplitude used elsewhere. Substituting this difference in definition,

$$\bar{U} = 4(\Phi/2) f R_2 = 2\Phi f R_2 \text{ as in Ellington (Ellington, 1984b).}$$

### 2.2.5 Allometry of aerodynamic force

Allometric equations relate some measurement to (most often) body weight, in the form  $Y = aW^b$ . We assume that the intraspecific variation we observe is primarily biological, such that we can make meaningful inferences. This implies stable variances on the logarithmic scale, so it is appropriate to log-transform the allometric equation,  $\log Y/Y_0 = \log a/a_0 + b \log W/W_0$ . Here, we have preserved the requirement of dimensionless arguments by introducing the characteristic scales  $Y_0$ ,  $a_0$ , and  $W_0$ , to obtain reduced dimensions  $Y'$ ,  $a'$ , and  $W'$ . The intercept,  $\log a/a_0$ , is dependent on the choice of characteristic scales. A usual approach is to choose 1 unit of measurement, e.g., 1 gram. An alternative reasonable choice is the clade-wide mean of each variable as the characteristic scale for interspecific analyses, and the intraspecific mean for

intraspecific analyses. With this choice, the intercept of the linear regression ( $\log a'$ ) must pass through the origin, because the expected values of  $\log Y'$  and  $\log W'$  are both zero.

The allometric version of the aerodynamic force equation [equation (1)] can thus be obtained by equating each term with body weight (omitting the constant of  $\log 1/2$ ). The slopes  $b$  are subscripted with the relevant term from the force equation (equation (1)), and for simplicity we drop the prime notation.

$$\log_{10} \overline{F}_V = b_F \cdot \log_{10} W = b_\rho \cdot \log_{10} W + 2b_{\overline{U}} \cdot \log_{10} W + b_S \cdot \log_{10} W + b_{\overline{C}_V} \cdot \log_{10} W$$

$$b_F \cdot \log_{10} W = (b_\rho + 2b_{\overline{U}} + b_S + b_{\overline{C}_V}) \cdot \log_{10} W$$

Allometric exponents are determined individually, allowing us to take advantage of partly overlapping data sets which may include observations of only some variables. In principle, separation of the problem into components could allow different statistical methods to be applied to each exponent, if warranted (Xiao et al., 2011).

We can infer the statistical validity of the exponents as a group based on whether they correctly predict the relationship of force and body weight,  $b_F$  (Figures 2.9, 2.10). When the exponents do not sum to  $b_F$ , some or all of them are likely biased. We cannot provide a hard ‘rule’ for violation of this constraint, but the magnitude of the difference can help place a minimum bound on the difference from a prediction (e.g., isometry) that can reasonably be considered an allometry. For instance, consider a scenario in which we find that the allometric exponent of wing area versus body mass is 0.57, and that the confidence (or credible) intervals exclude isometry (exponent 0.67). If, however, we also find that the sum of the exponents across the full model of force allometry ( $\Sigma b$ ) equals 0.90, then at least one exponent, possibly wing area, is underestimated by a margin that could explain the discrepancy from isometry.

Caution is necessary interpreting the slope of  $\overline{C}_V$ . From dimensional analysis,  $\overline{C}_V$  is a

scale-free factor, and so cannot depend on body mass over orders of magnitude in size. Within an order of magnitude or less, some progressive changes in  $\bar{C}_v$  might contribute to weight support. However, because  $\bar{C}_v$  is calculated from other variables, it cannot be distinguished from variable errors on its own, and so if such an effect is present, it must be properly attributed to a cause (Riskin et al., 2010). Incorporating  $\bar{C}_v$  can therefore be viewed, at a minimum, as a check on whether there is a correlation between measurement bias and body weight. However, further detailed studies on the nature of the  $\bar{C}_v$  allometry can reveal aspects of the evolution of both wing form and function that are not easily described by the mean dynamic pressure and wing area alone, such as camber or stroke kinematics. Incorporating this term thus serves as a link between readily studied dimensional components and pervasive but less easily quantified functional variation.

Given the computational dependence of  $\bar{C}_v$  on the other variables and their errors, it could be argued that the sum-to-one constraint is trivial. This is not the case for this analysis for two reasons. The first is that our exponents are derived from overlapping but not identical data sets. A more general reason is demonstrated through simulations in which we introduce random errors (Gaussian-distributed error with standard deviation equal to 0.1 of the mean) into fixed species means of one or more variables. We then recalculate  $\bar{C}_v$  and all exponents, and examine the resulting sum. We do not distinguish between technical and biological error or phylogenetic relatedness, as the emphasis is on any deviation from perfectly predicted exponents. This analysis demonstrates that when only a single variable contains errors, e.g., wing area, the sum-to-one constraint is indeed trivially obeyed (Figure 2.11, row 1; sum of exponents slightly differs from 1 due to use of empirical data). In this case, the error in  $\bar{C}_v$  is simply the error in wing area and so always compensates. When  $\bar{C}_v$  absorbs multiple errors, the sum of exponents in any given

data set may differ substantially from the true sum, and we find a distribution of possible values (Figure 2.11, rows 2-3).

### 2.2.6 Induced power calculation

The mechanical power requirements of flapping flight can be derived using a vortex theory (Ellington, 1984a) or from a blade element model (Kruyt et al., 2014) and are grouped as the aerodynamic (comprising induced and profile power) and inertial components. Profile and inertial powers are strongly dependent on modelling assumptions, and we have therefore focused on induced power, the energy imparted by the bird into its wake.

The induced power can be derived by considering mass flux through the disc area swept out by the wings ( $A=\phi R^2$ ). Induced power is critical because it is the minimum power required for flight: the muscle must perform work on the wing to add kinetic energy into the slipstream (Leishman, 2000). From conservation of momentum, the induced velocity of the fluid is  $\bar{v}_{ind}=\sqrt{(F/2\rho A)}=P_{RF}^*$ , the Rankine-Froude specific power estimate (here and elsewhere,  $P^*=P/W$ ). We can express the induced velocity directly as a function of the wing velocity  $\bar{U}_{wing}$  through the inflow ratio (Leishman, 2000),  $\lambda=\bar{v}_{ind}/\bar{U}_{wing}$  which yields the induced power  $P_{\lambda,ind}^*=\bar{v}_{ind}=\lambda\bar{U}_{wing}$ . Assuming constant inflow ratio for hovering flight and like in helicopters and actuator disks in general (Leishman, 2000) then  $P_{\lambda,ind}^*\propto\bar{v}_{wing}$ . This expression for induced power depends only on the wing velocity, but we can apply Ellington's model to study the possible influence of biologically-relevant morphological and kinematic parameters (Ellington, 1984a). Ellington derives temporal ( $\tau$ ) and spatial ( $\sigma$ ) correction factors to the Rankine-Froude induced power, so that  $P_{ind}^*=P_{RF}^*(1+\tau+\sigma)$ . The spatial correction factor models how wing morphological variation and kinematics (we assume harmonic motion of the wing) impact the induced wake, and the

temporal correction factor models unsteadiness in the wake due to kinematic parameters such as the stroke frequency. Although the correction factors typically alter the induced power estimate by only 10-15% (Ellington, 1984e) this difference ostensibly could depend on species' and individuals' body masses (perhaps through indirect correlations with morphological variation). The induced power relationships might therefore change in ways that are not expected from the Rankine-Froude estimate alone. Use of any of  $P_{\lambda,ind}^*$ ,  $P_{RF}^*$ , and  $P_{ind}^*$  support our conclusions, though only  $P_{ind}^*$  is reported here.

Detailed experimental measurements of the drag on the wing are needed to estimate profile power, which was not possible in these field studies. Absent such studies, we must adopt the quasi-steady assumption of a nearly flat plate at low angles of attack, as in Ellington (Ellington, 1984a) in which case profile power is dominated by surface friction. This results in a dependence on the stroke-averaged Reynolds number [mean  $Re=4\Phi R^2f/\mu AR$ , where  $\mu$  is the kinematic viscosity calculated with Sutherland's formula (Kruyt et al., 2014) and AR is the aspect ratio], giving a profile drag coefficient of  $\bar{C}_{D,pro} \approx 7/\sqrt{Re}$  (Ellington, 1984a). From the exponents in Table 2.1,  $Re$  approximately scales as  $W^{0.5}$  among and within species, and the profile drag coefficient constructed this way would decline as  $W^{-0.25}$ . Summing allometric exponents of the profile power,  $P_{pro}=F_{pro} \cdot \bar{U} = \frac{1}{2}\rho S \bar{U}_3^3 \bar{C}_{D,pro}$ , we would therefore predict that the specific profile power during hovering declines among, but not within, species (using allometric slopes in Table 2.1).

The previous calculation of profile power is limited in two respects. First, Reynolds number variation does not significantly explain aerodynamic performance of spinning, prepared hummingbird wings (Kruyt et al., 2014; Kruyt et al., 2015) and so it is doubtful that Reynolds number is an appropriate predictor of profile drag coefficient variation among and within

species. Aerodynamic performance is instead dominated by the Rossby number (Lentink and Dickinson, 2009b; Phillips et al., 2015) the aspect ratio with respect to the center of rotation. Because aspect ratio does not vary with species body mass among species (Table 2.1), it is similarly unlikely that the profile power drag coefficient varies among species. It may, though, increase somewhat within species due to small changes in aspect ratio. Reexamining the scaling of profile power with a constant  $\bar{C}_{D,pro}$ , we predict that among species,  $P_{pro}^* \propto W^0$  because  $S \propto W^1$  and  $\bar{U}^3 \propto W^0$ . Conversely, within species  $S \propto W^{0.41}$  and  $\bar{U}^3 \propto W^{0.75}$  which predicts  $P_{pro}^* \propto W^{0.16}$ , and we would conclude that profile power increases within species more rapidly than among species (possibly compounded by increasing aspect ratio within species, Table 2.1). We nonetheless emphasise that this method and Ellington's method (Table 2.1) both predict that the scaling exponent of profile power is greater within species than among species. Because this is due to differences in the allometry of wing area and wing velocity, the general predictions of equation (4) are supported in both cases.

The cost of flight might also be influenced by the inertial power required to accelerate the wing at each stroke, which might increase with larger wing sizes. The contribution of inertial power to total power is unclear because of uncertainty in the magnitude of elastic energy storage. To estimate inertial power, we require knowledge of the total wing mass,  $m_w$ , and the wing mass moment of inertia,  $\hat{r}_2(m)$ . For ethical reasons, the wing mass and moment were not collected for every individual but only obtained after incidental deaths during field experiments. Twenty-six measurements of the wing mass moments paired with wing areas were obtained from 10 species (Altshuler et al., 2010; Wells, 1993b) and a further 10 mass moment measurements unpaired with wing area from one species (Chai and Dudley, 1996). Total wing mass,  $m_w$ , was very strongly correlated with wing area, body mass, and wing length across all individuals

(correlation with wing area,  $r=0.968$ ;  $m_w=-0.16 S^{1.25}$ , see also Table 2.1). The wing mass was therefore imputed for all missing individuals from the predicted values of (non-phylogenetic) linear regression on wing area, body mass, and wing length, implemented in the R package *mice* (van Buuren and Groothuis-Oudshoorn, 2011). The wing mass moment was not obviously correlated with any other parameter, suggesting it may be generally invariant among hummingbirds, and was therefore imputed from the second moment of wing area,  $\hat{r}_2(S)$ , the wing length, and the wing area. Each reported imputed value is the mean of five multiple imputation chains.

Inertial power was then calculated according to the method of Ellington (Ellington, 1984a). Specific inertial power requirements are constant among species (Table 2.1), indicating that the increasing weight of the wing is offset by the decreasing frequency of accelerations (decrease in stroke frequency). Conversely, specific inertial power increases within species. Total power, assuming no elastic energy storage ( $P_{zero}^*$ ), is independent of body mass among species, but increases with weight within species. We do not include inertial power in the main text because of the uncertainty in elastic energy storage, and because we have not been able to study the possibility that the relationship of wing mass and wing area differs among and within species. Assuming this relationship is equivalent, then the total power with no elastic energy storage ( $P_{zero}^*$ ) is independent of body weight among species, but increases with weight within species (Table 2.1). With the preceding caveats, the scaling of inertial power thus supports our arguments as well.

### **2.2.7 Data analysis**

All analyses were performed with R 3.2.0 to organise data and interface with JAGS 4.2<sup>2</sup>).

We also used the R package *dplyr* for data manipulation (Wickham and Francois, 2015); *ape*, *nlme*, and *treemap* for phylogeny manipulation, visualisation of phylogenetic uncertainty, and comparison of our parameter estimates to those obtained by maximum likelihood (Jombart et al., 2017; Paradis et al., 2004; Pinheiro et al., 2016); and *rjags* and *R2jags* for interfacing with JAGS (Plummer, 2016; Su and Yajima, 2014).

The map in Figure 2.1a was generated in R using the packages *mapplots*, *raster*, *rworldmap*, and *sp* (Gerritsen, 2014; Hijmans, 2015; Pebesma and Bivand, 2005; South, 2011). The map of the Americas, and the latitudes and longitudes of the collections sites, were transformed to a Mollweide projection centered on (Lat 0, Lon -90). For clarity, we omitted collection sites with a single record, and grouped nearby sites (usually transects) in 0.5x0.5 degree cells. The map is shaded to provide elevational context for hummingbird ranges, and the elevation of individual collection sites, relative to 5000m, is depicted in a cartoon. The phylogeny in Figure 2.1b was drawn with the aid of the package *phytools* (Revell, 2012). The sample size for partial kinematics was the number of individuals with a calculated force coefficient in hovering, and the sample size for full kinematics was determined as the number of individuals with both a hovering and burst load lifting force coefficient. The sample size for morphology alone was determined as the number of individuals with weight, elevation, and wing area data.

### 2.3 Results

A general allometric version of equation (1) can be written as (omitting constants),

$$\log_{10} \bar{F}_V = b_F \cdot \log_{10} W = (b_p + 2b_{\bar{U}} + b_S + b_{\bar{C}_V}) \cdot \log_{10} W \quad (2)$$

where each slope  $b$  refers to a variable in equation (1), according to its subscript. This model, which we term force allometry, offers two useful insights. First, the allometric exponents of the right-hand side variables must sum to the allometric relationship of force and body weight,  $b_F$ . For a weight-supporting force,  $b_F \equiv 1$  as required by equation (1), and the right-hand side exponents must sum to unity. We consider below the alternative case that other slopes are possible when considering forces generated during flight behaviours that require greater than body weight support, such as burst maximum performance. This summation requirement is a fundamental check of the derived exponents that applies to all flying animals, because if it is not met, then some relevant parameters could be missing or badly estimated, and we may not confidently make predictions about the biological relevance of the allometries. A second essential result from this model is that because only the sum of the exponents in equation (2) is constrained, we predict a continuum of physical, morphological, and kinematic strategies that can conceivably support weight, and the allometric exponents reveal which strategies are actually employed.

We have assembled a large data set that includes measurements of all components of equation (2) in birds generating weight-supporting (hovering,  $W$ ) and burst maximal (asymptotic load lifting,  $\bar{F}_{burst}$ ) forces. These data collect up to 1500 individual records over 25 years (Table 2.1), encompassing most of the biogeographic (Figure 2.1a) and phylogenetic (Figure 2.1b) distribution of the hummingbirds. Broad sources of uncertainty in the phylogenetic relationships among species in this study were visualised by ordination (principal coordinates, PC) and comparison to the species phylogeny published with McGuire et al. (Figure 2.6) (McGuire et al., 2014). The majority of variation among trees reflects uncertainty within the Hermit and Brilliant clades (PC 1, 33%), and further ambiguities within the Hermit clade alone (PC 2, 22%). All

phylogenetic scenarios were sampled with equal probability, but the majority of trees fall into group i along with McGuire et al. (52% of trees), and only 6% of trees correspond to the largest topological differences from McGuire et al., group iv.

Our modelling procedures produce reliable inter- and intra-specific estimates of each allometry in equation (2), as judged by close agreement with the sum-to-one condition (weight support:  $\Sigma b_{\text{among}}=0.98$ ,  $\Sigma b_{\text{within}}=0.98$ ; Figure 2.9). Measurement error and phylogenetic relatedness impacted each variable differently even while maintaining the summation constraint (Figure 2.10). Phylogenetic uncertainty, as we model it here, altered mean exponents and credible interval widths by <1%. Simulations in which we recalculate  $\bar{C}_V$  under different conditions show that as long as measurement error is present in all variables, the summation condition is neither a trivial nor circular consequence of the calculation of  $\bar{C}_V$  from the other components of equation (2) (Figure 2.11, Methods). Clade-wise examination of allometric exponents broadly confirms that the allometries we report are neither dominated by a single clade nor the result of averaging over many different clade-specific force-generating strategies (Figure 2.12).

Among hummingbird species, wing surface area scales almost exactly as one,  $S \propto W^{1.01}$  [Bayesian credible interval (CI): 0.908,1.113; Figs. 2,3, Table 2.1]. In the context of the force equation, the sum-to-one rule predicts the other components are constrained to sum to zero, which is what we observe. Although it is possible that large hummingbirds could move to lower elevation, thus leading to a positive allometry with air density, there is no evidence that this occurs. Instead, we find a slight negative allometric exponent of air density ( $\rho \propto W^{-0.06}$ , CI: -0.112, -0.003) but this may depend on inclusion of outlier and poorly sampled species (Figure 2.2). Wing velocity among species is independent of body weight ( $\bar{U} \propto W^{0.01}$ , CI: -0.054,0.074),

in contrast to the isometric prediction that these should be positively correlated (Alerstam et al., 2007; Rayner, 1988) and derives from a constant stroke amplitude, coupled to a decline in stroke frequency proportional to the increase in wing length (Figure 2.8). The force coefficient during weight support,  $\bar{C}_{w,v}$ , does not vary substantially ( $\bar{C}_{w,v} \propto W^{0.01}$ , CI: -0.122,0.137), indicating that hummingbirds are dynamically similar in flight, unlike bats (Riskin et al., 2010). Among species, increasing weight support is therefore provided entirely by increasing wing area.

The reliance on increasing wing area to support body weight among species is not observed within hummingbird species (Figure 2.7). Indeed, the average intraspecific pattern more closely resembles biomechanical strategies suggested to occur among other bird species (Alerstam et al., 2007; Rayner, 1988): weight support is provided by a combination of increasing wing area ( $S \propto W^{0.42}$ , CI: 0.366,0.468) and wing velocity ( $\bar{U} \propto W^{0.27}$ , CI: 0.182,0.354; Figures 2.7, 2.8). Intraspecific wing tip velocity increases with body weight due to constant stroke amplitude but unequal changes in stroke frequency and wing length (Figure 2.8). Larger individuals tend to be associated with lower air densities at higher elevations, with an exponent similar to that found among species ( $\rho \propto W^{-0.07}$ , CI: -0.085,-0.045; Figure 2.8). A positive but uncertain change in  $\bar{C}_{w,v}$  with body weight within species ( $\bar{C}_{w,v} \propto W^{0.10}$ , CI: -0.094,0.289) must be interpreted cautiously until assigned to a specific cause, such as a systematic change in angle of attack.

We next examine the allometry of burst flight capacities through asymptotic load lifting, an unequivocal measure of maximum muscle capacity and performance that is predictive of maneuverability, foraging strategies, and competitive ability (Altshuler, 2006; Segre et al., 2015; Sholtis et al., 2015). This capacity can be expressed as the load factor, the maximum burst force as a proportion of body weight ( $n = \bar{F}_{burst}/W$ ). Among species, load factor is size-invariant ( $n \propto W^{-0.01}$ , CI: -0.112,0.082; Figures 2.7, 2.8), indicating that maneuverability and competitive

ability are independent of body weight. Conversely, within species load factor declines with body weight ( $n \propto W^{-0.24}$ ,  $-0.364, -0.107$ ), meaning that, on average, aerial performance is compromised in larger individuals. As for body weight support, we check the summation condition of equation (2) for burst performance, and find close agreement between the exponent of load factor and the sum of individual allometric exponents obtained during load lifting (Figure 2.9).

A key difference among and within hummingbird species is the extent of dependence on increasing wing velocity for increasing weight support, which can influence the energetic demands of flight. Wing velocity is a key determinant of specific induced power ( $P_{ind}^* = P_{ind}/W$ ), which is the minimum power required to support weight (Ellington, 1984a; Leishman, 2000). The overall scaling trends presented here are not affected by the including of profile and inertial powers.

Induced power is a function of the induced velocity,  $\bar{v}_{ind}$ , of the wake and of the wing velocity such that (Leishman, 2000),

$$P_{ind} = nW \cdot \bar{v}_{ind} = nW \cdot \lambda \bar{U}_{wing} \quad (3)$$

where  $\lambda \equiv \bar{v}_{ind}/\bar{U}_{wing}$  is the dimensionless inflow ratio from actuator disk theory relating the mean wing velocity to the induced flow (Leishman, 2000) and, like the force coefficient, depends on both wing morphology and kinematics. We again equate terms with body weight to develop an allometric expression for the scaling of specific induced power,

$$\log_{10} P_{ind}^* = b_{P^*} \cdot \log_{10} W = (b_n + b_\lambda + b_{\bar{U}}) \cdot \log_{10} W \quad (4)$$

Equation (4) principally relates changes in specific induced power, load factor, and wing velocity. We cannot directly assess the contribution of inflow ratio,  $b_\lambda$ , because we have not measured the induced velocity,  $\bar{v}_{ind}$ , but we do not expect large differences among individuals

and species with similar morphology and kinematics. Unlike the allometry of force in equation (2), the allometry of specific induced power,  $b_{P^*}$ , will vary depending on flight behaviour. For example, during hovering, the allometry of load factor is 0, and the allometry of specific induced power varies as a positive function of the allometry of wing velocity. In contrast, during maximum performance, the allometry of specific induced power is fixed at the maximum muscle capacity, and thus the allometry of load factor is a negative function of the allometry of wing velocity.

Specific induced power for hovering is constant among species (Figures 2.7, 2.8;  $P_{w,ind}^* \propto W^{0.02}$ , CI: -0.033,0.063), but increases within species ( $P_{w,ind}^* \propto W^{0.25}$ ; 0.193,0.315). Burst specific induced power expended during load lifting, reflective of maximum muscle capacities, is independent of body weight both among ( $P_{b,ind}^* \propto W^{0.07}$ , CI: -0.21,0.15) and within ( $P_{b,ind}^* \propto W^{-0.03}$ , CI: -0.212,0.147) species. Reserve power, the difference in the allometries of maximum and hovering power, therefore declines in large individuals, but not large species. Overall, there is a decline in the production of burst vertical force relative to expended power in larger individuals, and although larger individuals proportionately expend the same maximum power during burst performance, they produce less relative force.

## 2.4 Discussion

In principle, hummingbird species could adopt any one of multiple strategies to support difference in body weight during flight (equation 2), expressed as movement to lower elevations with higher air density ( $\rho$ ), increase in wing area ( $S$ ), increase in wing velocity ( $\bar{U}$ ), or adaptation of wing morphology and kinematics ( $\bar{C}_v$ ). The potential contribution of each strategy differs; for instance, an order of magnitude in air density to support an order of magnitude in body weight is

not possible. Each strategy may also entail tradeoffs, such as sacrificing potential habitats (air density allometry) or reconfiguring the wing (force coefficient allometry). We find that the allometry of force production among and within hummingbird species is solely a function of changes in the allometries of wing area and wing velocity. Among species, increasing weight support is provided exclusively by increasing wing area and maintaining constant wing velocity, whereas within species, weight support is provided both by increasing wing area and velocity. The advantage of maintaining constant wing velocity is apparent from equation (4), which shows that when  $b_U=0$ , expended power is only a function of the load factor, or reciprocally, the maximum load factor is only a function of the maximum available muscle power. The dependence on positive wing velocity allometry within species thus results in degrading burst force capabilities and escalating cost of flight in larger individuals. The extreme wing area allometry among hummingbird species appears to be an evolutionary strategy to mitigate the performance and energetic disadvantages that would arise if the body plan of large species was extrapolated from intraspecific patterns.

The emergence of this extreme allometry among hummingbirds is likely due to pressures of their energetically demanding hovering flight and territoriality, frequently engaging conspecifics and confamilials in aerial bouts (Altshuler, 2006; Dearborn, 1998). Selection can therefore be expected to favor constant or minimally-increasing routine flight costs and burst aerial performance, which is supported by the weight independence of specific daily energy expenditure among hummingbird species,  $DEE^* \propto W^{-0.03}$  (Fernández et al., 2011). As observed, the force allometric pattern within species cannot be scaled up across the size range of hummingbirds without incurring severe penalties to both flight costs and burst forces. Maintaining burst performance margins could entail adaptation of the flight musculature, as may

occur in other flying animals (Ellington, 1991; Marden, 1994) but the invariance of maximum available power among and within species suggests that hummingbirds' specialised muscles (Fernández et al., 2011; Suarez et al., 1991) have reached the physiological limits of performance. Hummingbirds must therefore reduce energetic demand rather than supply, and increasing relative wing area is the simplest solution that both minimises flight costs and maximises performance.

Force allometry is a flexible method for examining the functional context of allometric variation in wing area. The approach can be applied among and within species to gain insight into the energetic and performance consequences of divergent force generation strategies. Separating the problem into its constituent components [equations (2) and (4)] and then comparing the resulting exponents provides a framework for evaluating both the functional and statistical relevance of hypothesised allometries. This linear separation allows disparate data sets to be merged to provide consistent inference. Perhaps the most important insight from our framework is a shift in emphasis from single exponents intended to explain variation across all clades, to a nuanced view of possibly clade-specific balancing of weight-supporting strategies, including the possible contributions of the force coefficient (Riskin et al., 2010). We therefore applied our method to probe whether there is any evidence of variation in strategies among hummingbird clades. We find that the Bee clade has a uniquely low wing area exponent, comparable to that observed within species (Figure 2.12). This is particularly striking in light of the fact that the Bee clade is the most recently derived and most rapidly diversifying group of hummingbirds (McGuire et al., 2014). Combined with the observation that they also have uniquely low variation in body mass, this suggests a hypothesis that physiological diversification in the Bee clade is lagging behind species diversification. We have derived the equations here

specifically for hummingbirds, but the force allometry approach can be applied to other flying animals with adjustments to account for the complexities of different wing strokes. This method could prove especially useful for quantifying subtle allometries in other families of flying animals, which likely operate in distinct selective regimes.

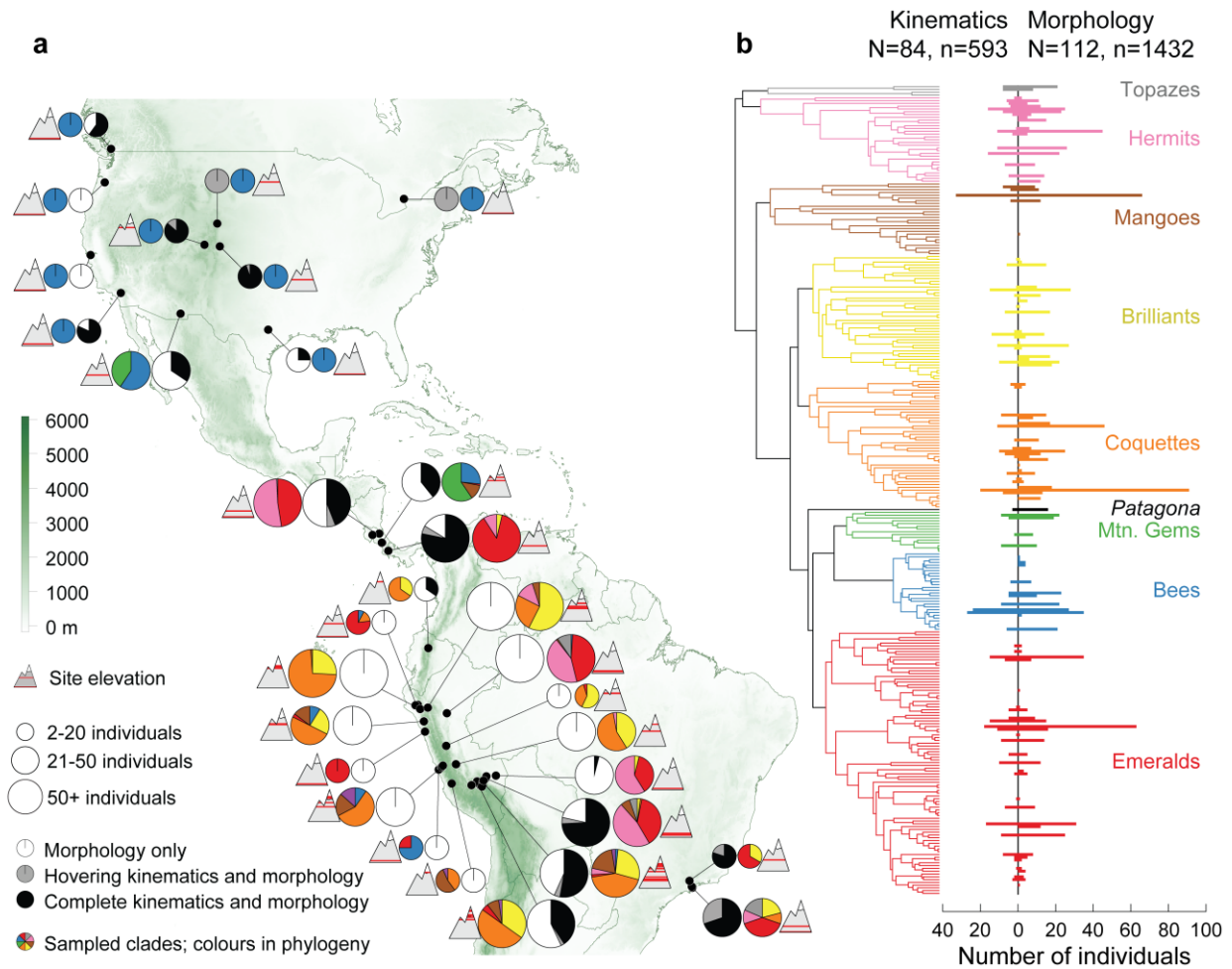


**Figure 2.1** Biogeographic and phylogenetic sampling of hummingbirds. **a** Individual collection sites, grouping nearby sites in  $5^{\circ} \times 5^{\circ}$  cells, along with the relative collection site elevation, biodiversity, and type of collected data (morphology, hovering kinematics, or hovering and load lifting kinematics). Colours in pie charts correspond to the colour scheme denoting humming bird clades in **b**. **b** All major clades of hummingbirds defined by McGuire et al. (McGuire et al., 2014) were sampled both for kinematic and morphological parameters, though sampling effort varied widely across species and data type.

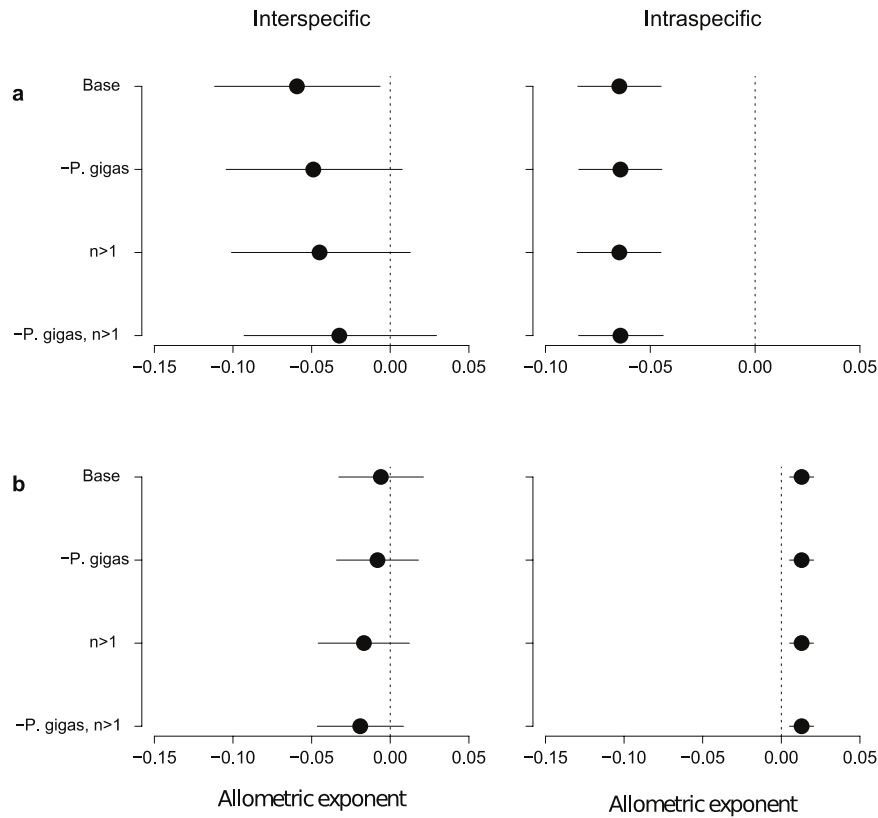


**Figure 2.2** Impact of data subsets on the estimated slope of air density on body weight. **a** Effect of removing *Patagona gigas* and poorly sampled species on estimated air density regression exponents. Regression on the complete data set suggests a small but significant contribution of air density to force allometry across hummingbirds. However, performing regressions after filtering out *P. gigas* (-P. gigas) or species with a single observation ( $n>1$ ), or both, results in progressive diminution of the exponent toward zero, suggesting either that this is not a robust biological observation or that we do have sufficient evidence to resolve such a relationship. Subsetting did not alter the trend within species. **b** To compare with previous work (Altshuler et al., 2004c; Altshuler et al., 2010) we also examine the regression exponent of body mass as a function of elevation directly. All slopes among species overlap zero, whereas all slopes within species do not. Exponents were estimated with *MCMCglmm*, and may therefore differ from models implemented in JAGS (see Methods).

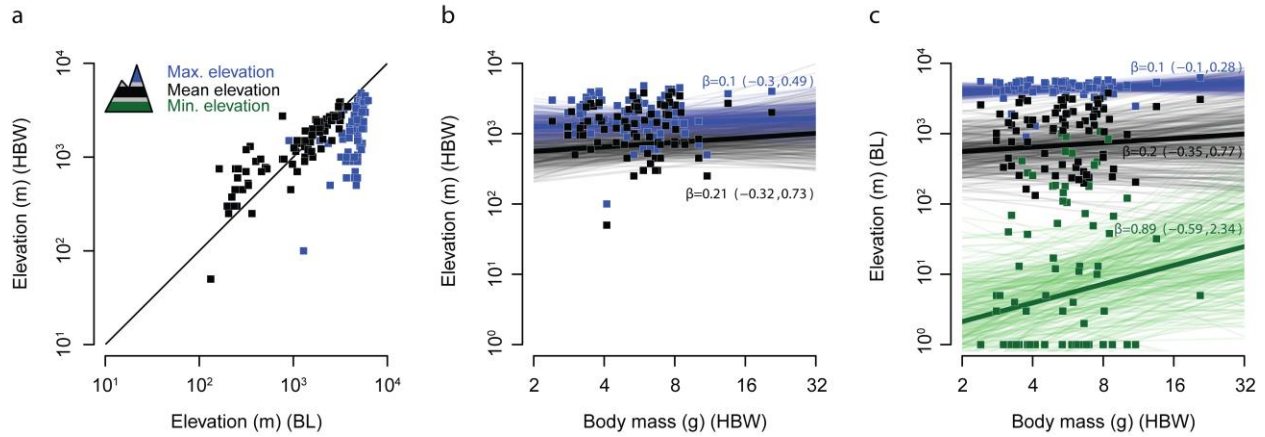


**Figure 2.3** No association between literature-derived species mean body mass and elevation. The robustness of the relationship between body mass and elevation was examined through an independent data set of species mean body masses and elevations. Mean species mass and mean and maximum elevation were obtained from the literature (HBW), and minimum, mean, and maximum elevations were also estimated from species range maps (BL). Mean elevations obtained from both methods were reasonably well correlated, but maximum elevations diverged substantially (a). HBW body masses and elevations are uncorrelated (b), as are HBW body masses and BL elevation parameters (c).

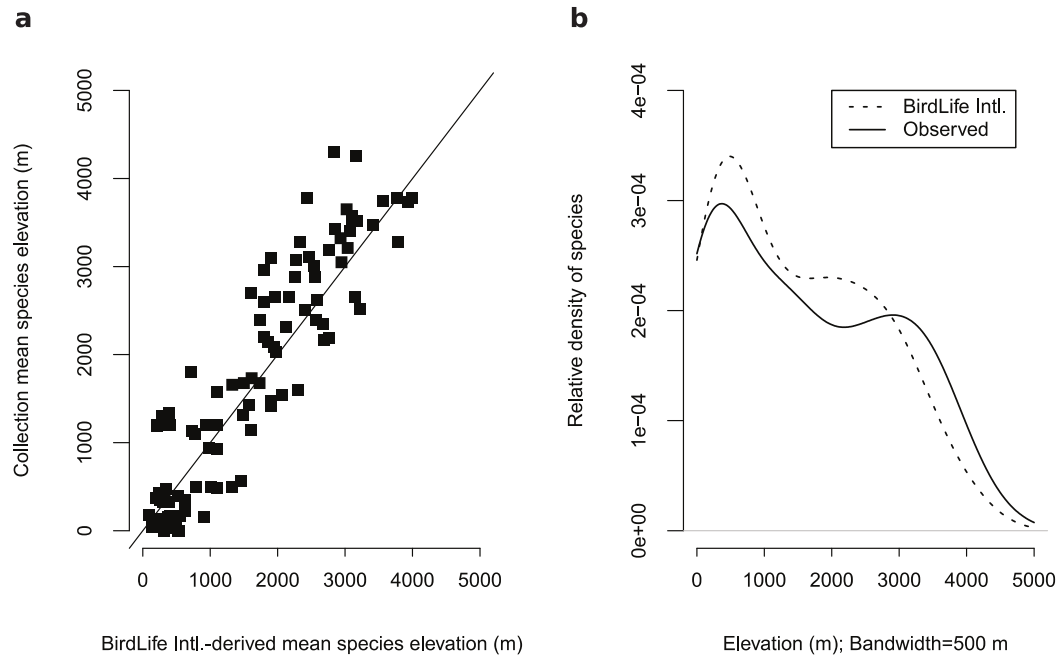


**Figure 2.4** Concordance between sampled and theoretical species mean elevations. The species mean elevations calculated from our sampling and those derived from digital range maps (a) were strongly correlated. Our elevational sampling also broadly conforms to the overall distribution of species mean elevations (b).

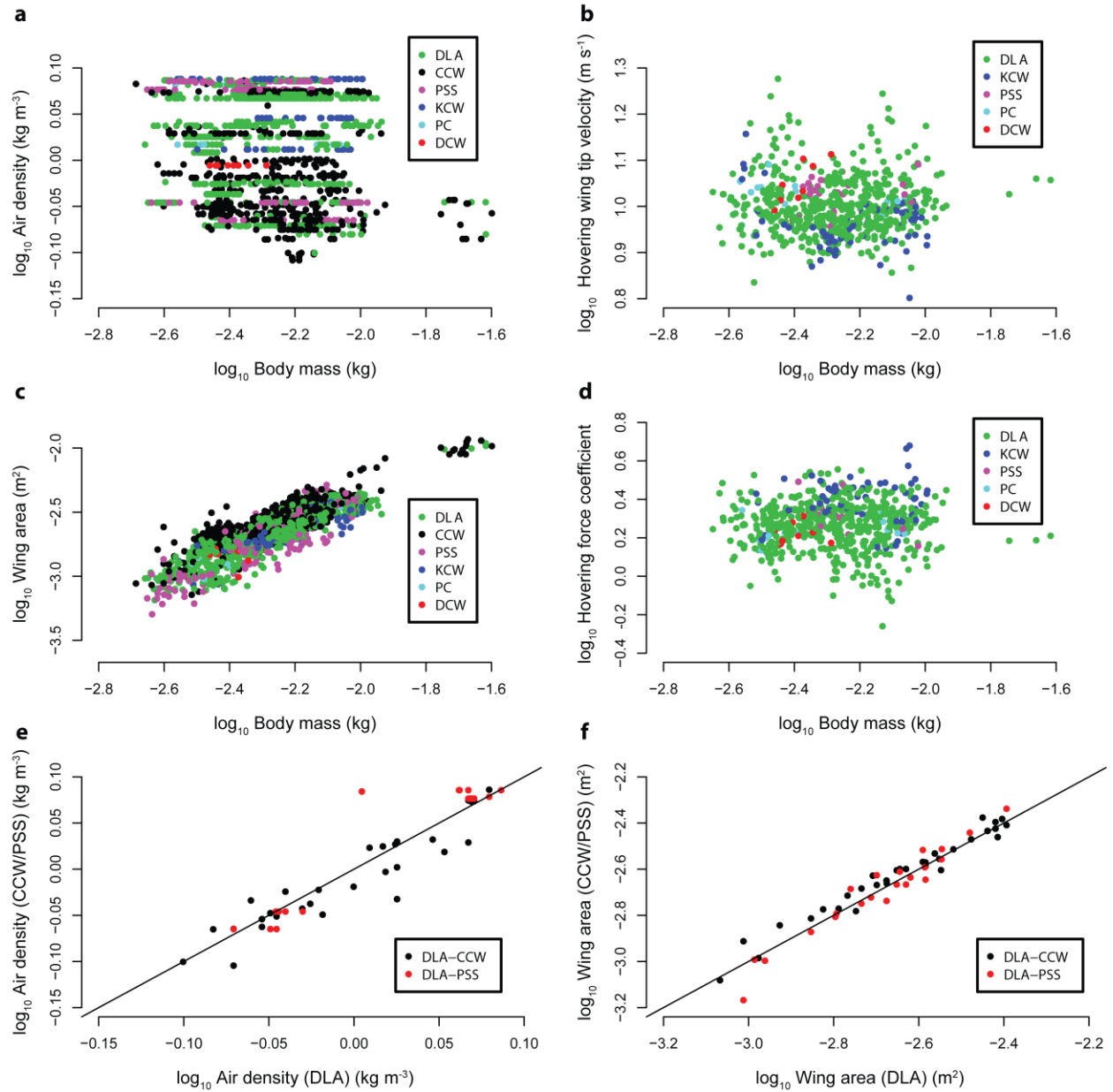


**Figure 2.5** Comparison of collector data sets for systematic bias. The overall similarity of measurements is compared (a–d) was examined for systematic biases. Where species observations overlapped, we compared the estimated trait mean (e,f). Species means among authors were in good concordance, suggesting that apparent differences among authors are most likely due to species sampling.

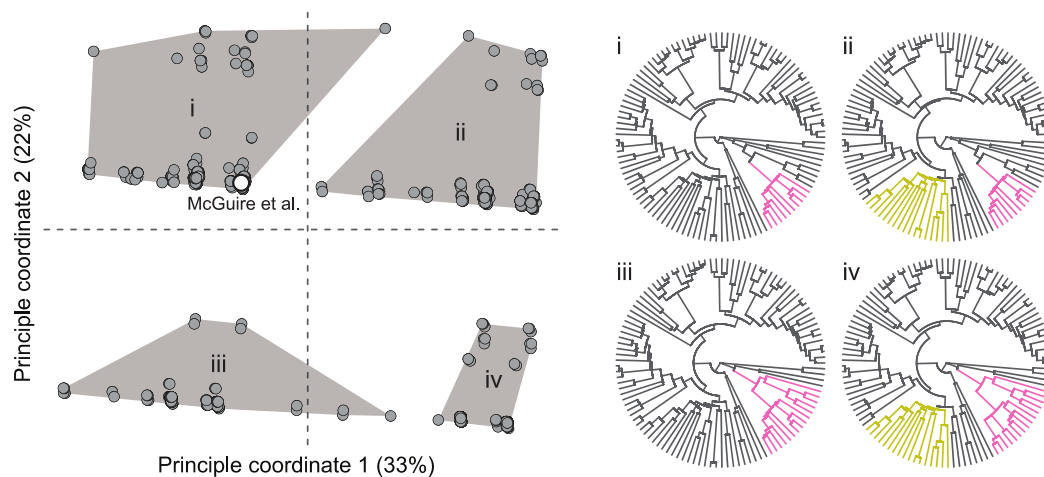


**Figure 2.6** Uncertainty in phylogenetic relationships among species in this study. The variability in tree topology and branch length is mapped to a reduced-dimensional Euclidean space (Jombart et al., 2017; Kendall and Colijn, 2016). The majority (55%) of uncertainty in species relationships is presented by two principal coordinates (PCs). Individual trees are shown by filled circles and clustered by similarity. To interpret the variability represented by the two PCs, we compare the median tree corresponding to each cluster (i–iv) to the Maximum Clade Credibility (MCC) tree of McGuire et al. (McGuire et al., 2014). The principal clade differences between the cluster median trees and the MCC are coloured in i–iv according to the scheme in Figure 2.1. This method reveals that among species in this study (not hummingbirds overall), phylogenetic uncertainty primarily represents ambiguities in the Hermit and Brilliant clades. We allow for this uncertainty by integrating over many phylogenetic hypotheses.

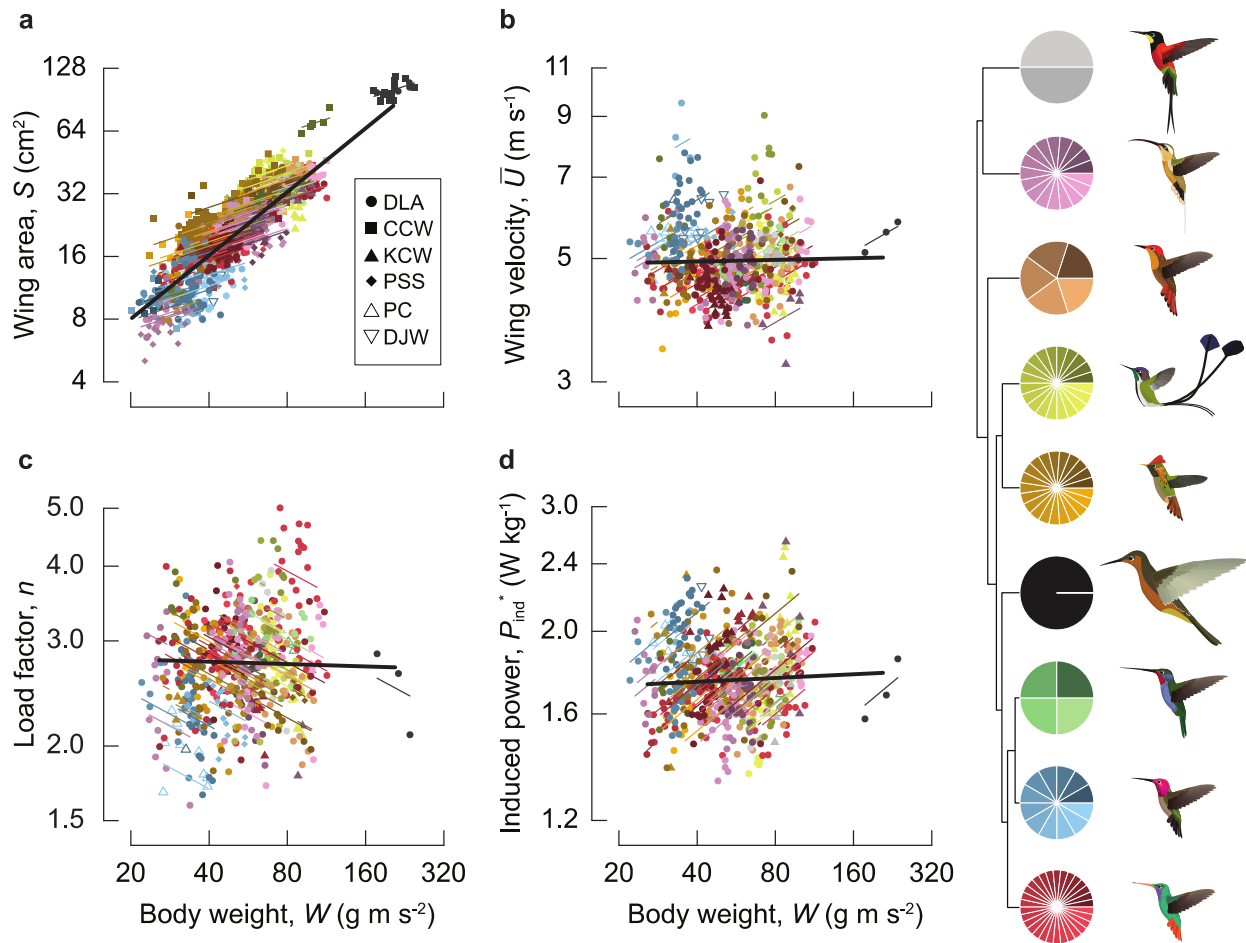


**Figure 2.7** Allometric divergence among and within species. We contrast the slopes of wing area (a), wing velocity (b), load factor (c) and induced power requirements (d). The slope of each variable on body weight among species is shown in black, and each was calculated allowing for phylogenetic nonindependence and measurement error. Individual records are shown along with the mean within-species slope fit through the respective empirical species means. Symbols denote collector. Individual observations and within-species slopes are coloured and shaded by species within clade, according to the cartoon phylogeny at right (colours as in Figure 2.1).

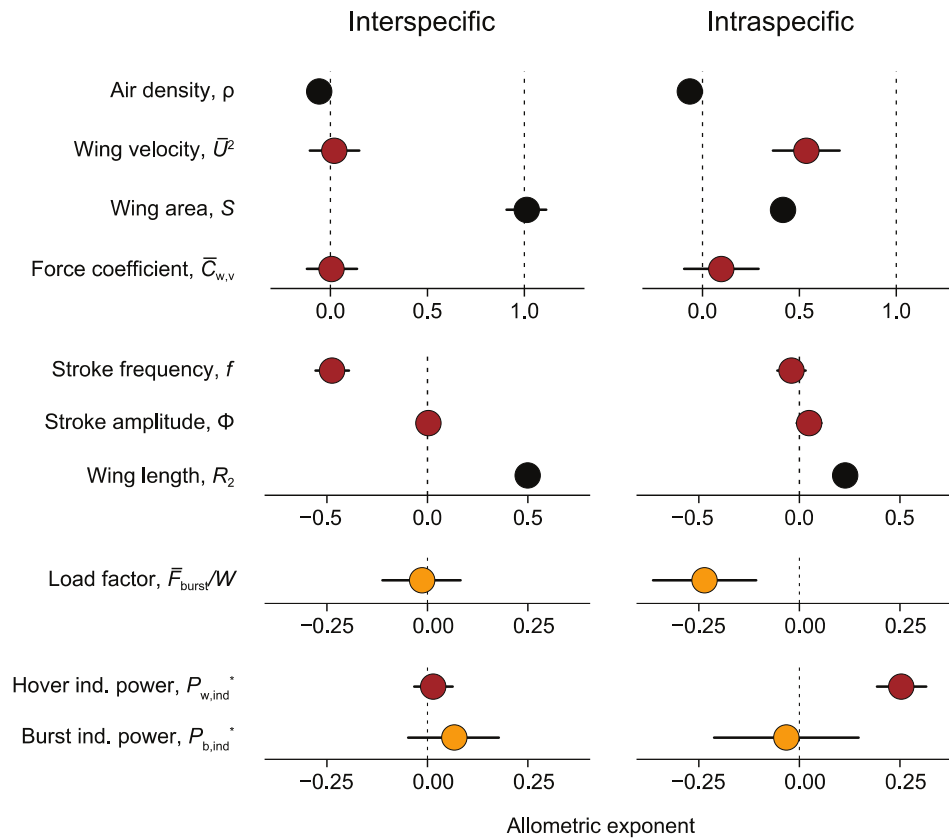


**Figure 2.8** Comparison of allometric variation among and within species. Constant allometry of wing velocity among species coincides with constant burst force generation (load factor) and induced power. Positive allometry of wing velocity within species coincides with reduced load factor and escalating power requirements. The mean and 95% equal-tailed credible intervals of the posterior distribution of the allometric exponents are shown for each variable. Black circles are static morphological and environmental measurements, red circles were measured during hovering, and gold circles were measured during burst performance.

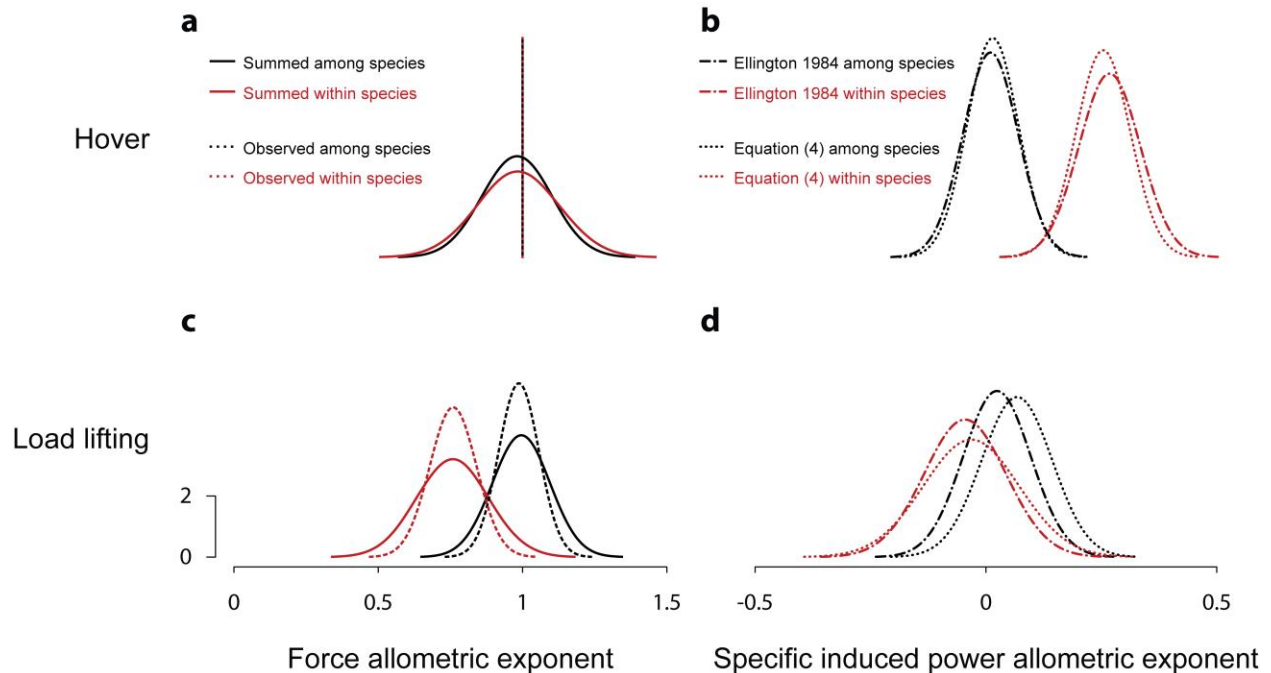


**Figure 2.9** Comparison of different methods of reconstructing the allometry of force and specific induced power. **a** In hovering, the force produced is exactly equal to body weight, which we therefore ‘observe’ to be exactly equal to 1 (vertical dashed lines) both among and within species. For predictions derived from force allometry to be valid for hovering flight, it is necessary that the sum of the posterior distributions of each term (solid lines) match the observed force generation, and must therefore be centered on 1. This condition is met both among (black) and within (red) species. **b** During burst performance, the allometry of force generation may differ from unity. The exponent of the empirically measured burst force (dashed lines) is compared to the reconstructed burst force obtained by summing the exponents of each term as measured during the assay (solid lines). Among and within species, the two methods again substantially agree with each other. **c,d** In this study, the allometry of specific induced power cannot be observed directly, but must be computed either as described by Ellington (Ellington, 1984a) and in the Methods (long-dashed lines), or by summing the contributions of the power allometry (dotted lines). Specific induced power exhibits significant positive allometry in hovering (**c**) within species, but neither among nor within species during load lifting (**d**). Distributions are smoothed with bandwidth=0.05.

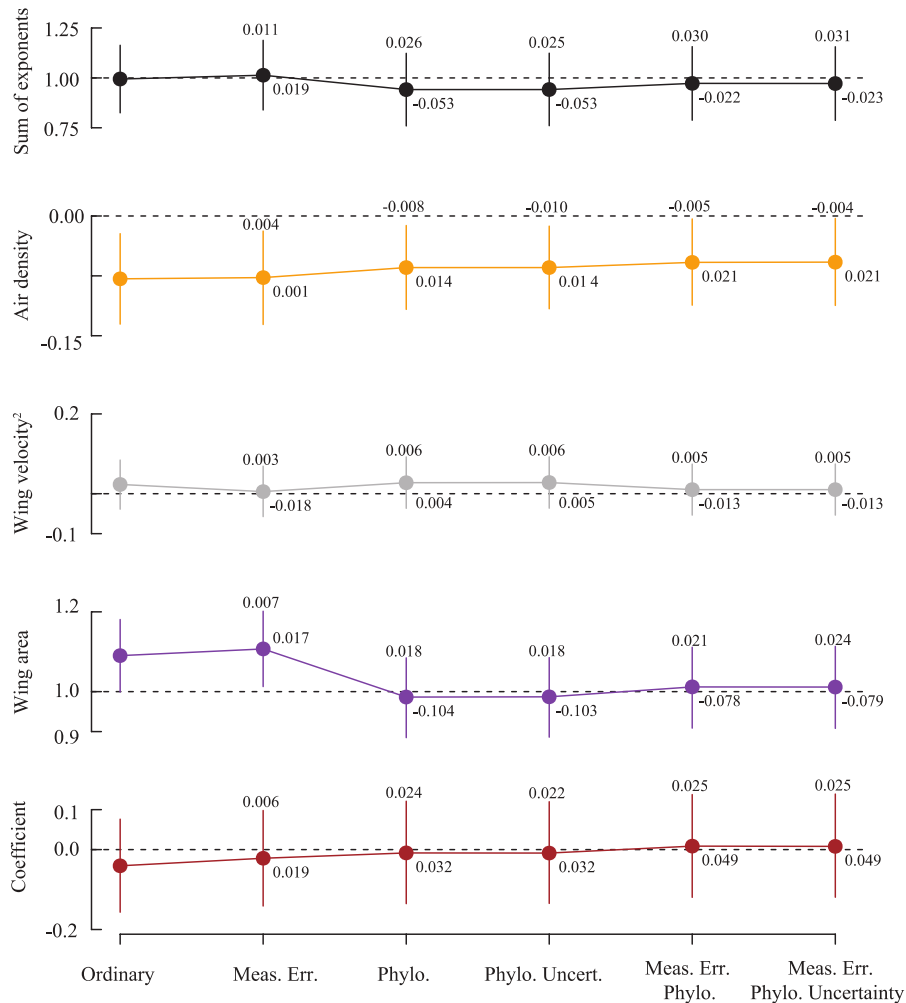


**Figure 2.10** Effect of modelling assumptions on estimated allometric exponents and sum of exponents. We performed regressions using ordinary least squares (Ordinary), and for combinations of accounting for intraspecific variation (Meas. Err.), including a phylogenetic hypothesis (Phylo.), and accounting for uncertainty in the phylogenetic hypothesis (Phylo. Uncert.). The difference in the mean and width of credible intervals are printed next to the circle (mean) or upper range of credible intervals. Effects were unpredictable and variable-specific, but in no case did we find that accounting for phylogenetic uncertainty contributed any more than accounting for the maximum clade credibility phylogenetic hypothesis alone. Air density was influenced by phylogenetic relatedness and its interaction with measurement errors; wing tip velocity was primarily influenced by measurement errors; wing area was greatly influenced by phylogenetic relatedness, but there were interactions between the phylogenetic hypothesis and measurement error; the force coefficient was influenced by both measurement error and phylogenetic relatedness.

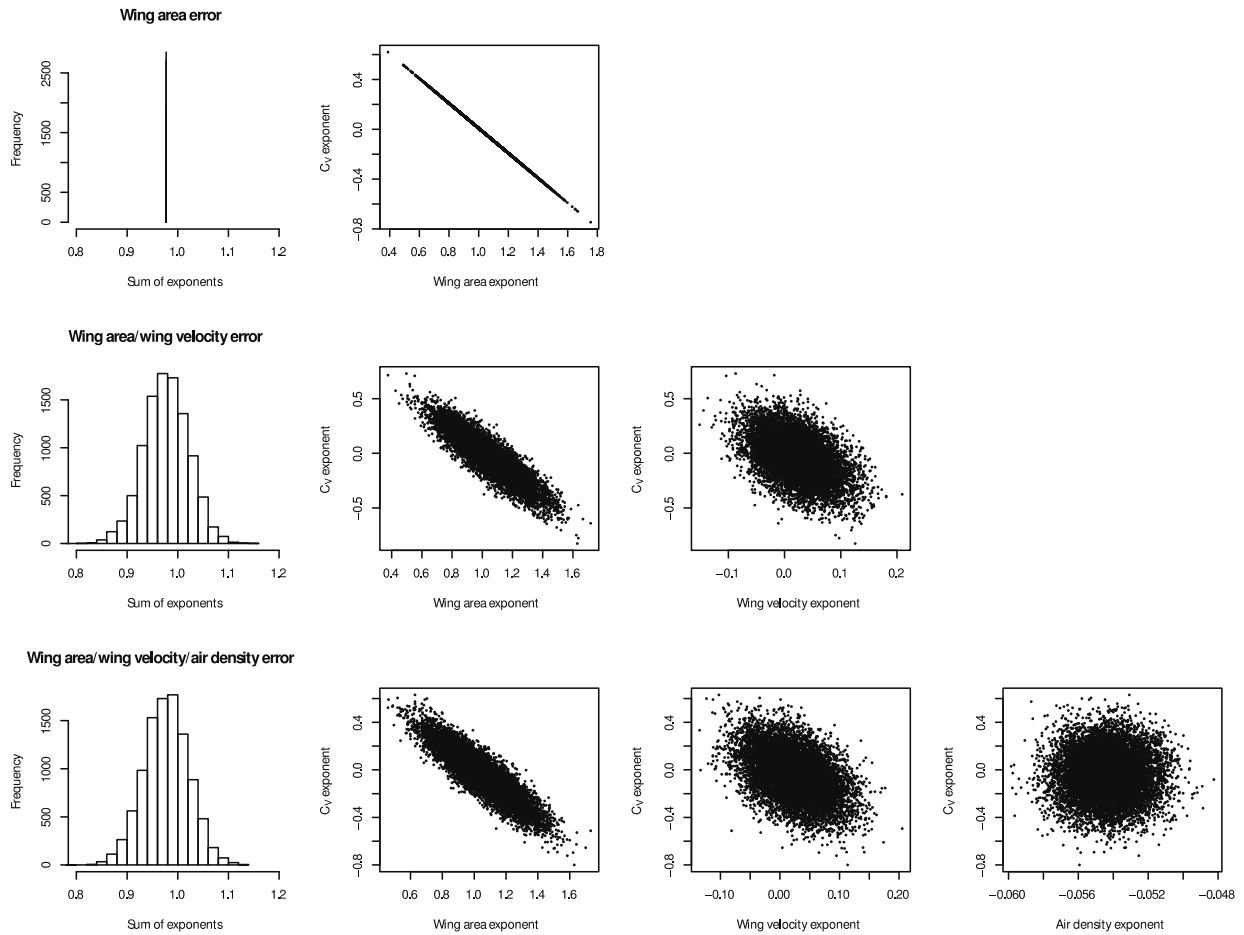


**Figure 2.11** Effect of force coefficient calculation on sum-to-one constraint. We simulate how the calculation of the force coefficient,  $C_v$ , from the empirical observations affects the sum-to-one constraint, and whether the constraint is trivially true. We use the empirical species mean of body mass, wing area, wing velocity, and air density. For each simulation, we add random error to the species mean of one or more variables (Gaussian error with standard deviation equal to 0.1 of each variable's mean), recalculate  $C_v$  for each species with these new values, and then repeat our scaling analysis. In row 1, we show that when only a single variable, wing surface area, contains error, the error in  $C_v$  is simply equal to the error in surface area. In this case, the sum of exponents is always equal to the true (empirical) sum, as shown in the histogram, showing that indeed, the constraint is trivial. When more than one variable has error (rows 2-3), as in any real system, the sum of exponents in any given experiment is not equal to the empirical sum. The width of the resulting distribution, i.e., the range of possible apparent force allometries that can be obtained, depends on the magnitude of errors in each variable (simulations not shown).

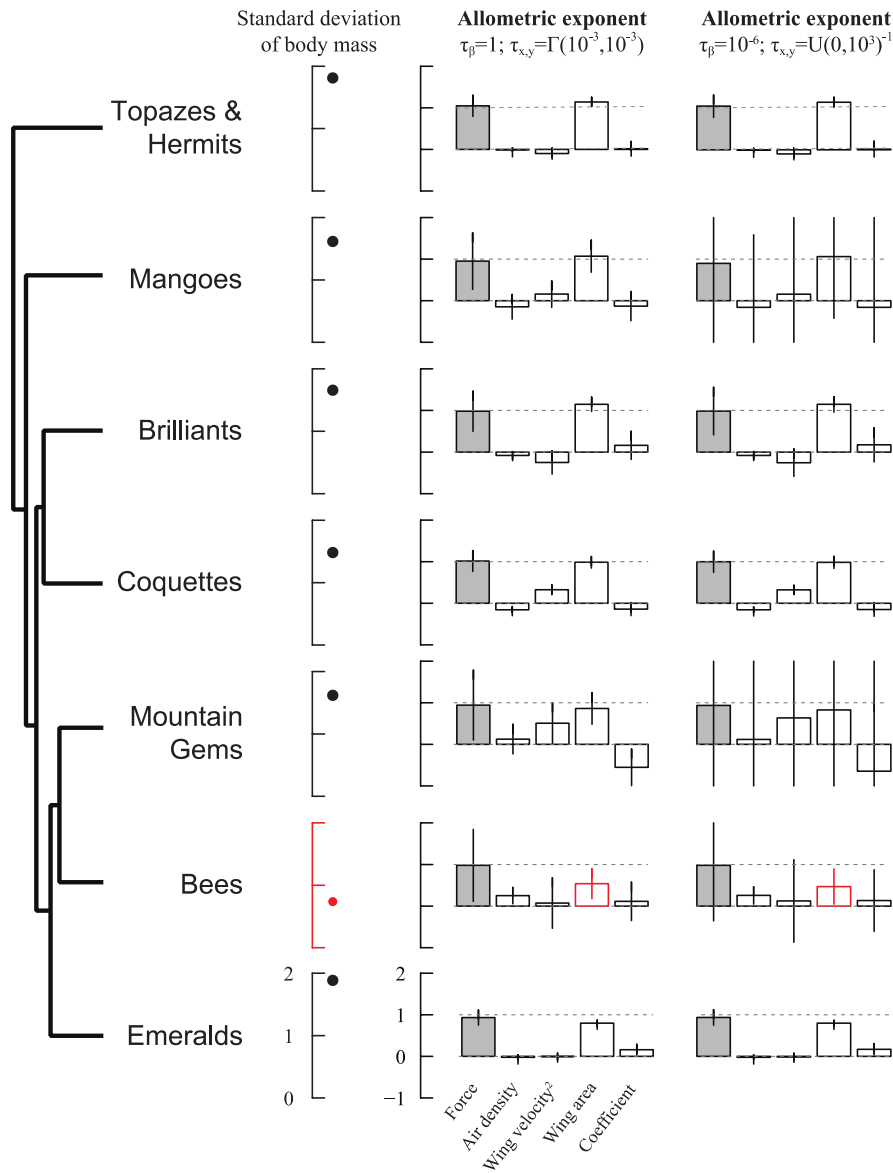


**Figure 2.12** Force allometry and mass variation in individual hummingbird clades. Comparisons within clades were made using the flat priors for precision ( $\tau=\sigma^{-2}$ ) used for the general modelling, which resulted in very large posterior variances (error bars, clipped at borders). Prior distributions are discussed in Methods. We also examined trends using informative priors focused on  $\beta=1$  for wing area, and  $\beta=0$  for all other parameters. The general among and within-species patterns are visible in most clades: weight support among species is derived primarily from large wing area exponents. A possible exception is the Bee clade, which has exceptionally low wing area scaling, and also comparatively low intraclade variation in body mass. Topazes were combined with hermits due to insufficient sample size.

**Table 2.1** Sample sizes, exponents, and 95% credible intervals for variables studied in Chapter 2.  $N$  species,  $n$  individuals. † calculated using MCMCglmm.

Variable	Symbol	$N$	$n$	Interspecific (2.5%,97.5%)	Intraspecific (2.5%,97.5%)
Air density	$\rho$	112	1446	-0.058 (-0.112,-0.003)	-0.065 (-0.085,-0.045)
Wing length	$R$	112	1433	0.498 (0.455,0.539)	0.228 (0.201,0.256)
Wing length corrected for $\hat{r}_2$	$R_2$	89	901	0.491 (0.441,0.539)	0.223 (0.185,0.261)
Non-dimensional second moment of area	$\hat{r}_2$	89	900	-0.008 (-0.016,0.001)	0.006 (-0.003,0.014)
Non-dimensional third moment of area	$\hat{r}_3$	89	893	-0.011 (-0.021,0.000)	0.010 (-0.002,0.021)
Wing surface area	$S$	112	1432	1.012 (0.908,1.113)	0.417 (0.366,0.468)
Wing aspect ratio	$AR$	112	1431	-0.023 (-0.062,0.017)	0.039 (0.006,0.073)
Wing velocity	$\bar{U}$	84	593	0.010 (-0.054,0.074)	0.268 (0.182,0.354)
Wing velocity (burst)	$\bar{U}_b$	81	571	0.037 (-0.006,0.081)	0.190 (0.121,0.258)
Wing tip velocity	$\bar{v}_{tip}$	84	607	0.018 (-0.046,0.082)	0.249 (0.165,0.333)
Wing tip velocity (burst)	$\bar{v}_{b,tip}$	81	585	0.053 (0.010,0.096)	0.180 (0.113,0.248)
Force coefficient	$\bar{C}_{w,v}$	84	593	0.007 (-0.122,0.137)	0.097 (-0.094,0.289)
Force coefficient (burst)	$\bar{C}_{b,v}$	81	581	-0.059 (-0.147,0.029)	0.057 (-0.111,0.223)
Stroke frequency	$f$	84	610	-0.474 (-0.557,-0.39)	-0.039 (-0.110,0.031)
Stroke frequency (burst)	$f_b$	81	604	-0.428 (-0.496,-0.358)	-0.050 (-0.103,0.002)
Stroke amplitude	$\Phi$	84	607	0.005 (-0.038,0.046)	0.049 (-0.013,0.110)
Stroke amplitude (burst)	$\Phi_b$	81	585	0.001 (-0.023,0.024)	-0.003 (-0.033,0.033)
Total lifted mass	$M_T$	81	623	0.987 (0.889,1.084)	0.759 (0.632,0.887)
Load factor	$n$	81	623	-0.013 (-0.112,0.082)	-0.235 (-0.364,-0.107)
Wing mass†	$w_m$	15	33	1.375 (0.996,1.705)	-
Induced power	$P_{w,ind}^*$	84	607	0.015 (-0.033,0.063)	0.254 (0.193,0.315)
Induced power (burst)	$P_{b,ind}^*$	81	581	0.067 (-0.21,0.15)	-0.032 (-0.212,0.147)
Profile power	$P_{w,pro}^*$	84	593	-0.269 (-0.413,-0.123)	-0.059 (-0.283,0.166)
Profile power (burst)	$P_{b,pro}^*$	81	571	-0.182 (-0.307,-0.057)	-0.254 (-0.460,-0.048)
Inertial power	$P_{w,acc}^*$	76	535	0.063 (-0.104,0.237)	0.408 (0.16,0.655)
Inertial power (burst)	$P_{b,acc}^*$	76	529	0.150 (0.034,0.268)	0.233 (0.023,0.443)
Total power (Ellington) – perfect	$P_{w,per}^*$	84	587	-0.033 (-0.074,0.009)	0.19 (0.145,0.235)
Total power (Ellington) (burst) – perfect	$P_{b,per}^*$	81	565	0.036 (-0.069,0.137)	-0.058 (-0.220,0.107)
Total power (Ellington) – zero	$P_{w,zero}^*$	76	529	0.05 (-0.086,0.188)	0.352 (0.153,0.550)
Total power (Ellington) (burst) – zero	$P_{b,zero}^*$	76	523	0.119 (0.025,0.212)	0.138 (-0.037,0.313)

## **Chapter 3: Hummingbirds dynamically control wing shape to tune flight efficiency and modulate aerodynamic force**

### **3.1 Introduction**

Understanding the link between wing morphology and function is fundamentally challenging because of the complexity of aerodynamic force generation. Selection on diverse aspects of flight performance has resulted in enormous morphological diversity to harness many possible mechanisms of force production (Bachmann et al., 2012; Johansson et al., 2013; KleinHeerenbrink et al., 2017; Kruyt et al., 2014; Norberg and Rayner, 1987; Rayner, 1988; Tucker and Parrott, 1970). Even with similar wing morphology, species and individuals can modulate an immense array of kinematics to harness steady and unsteady aerodynamic forces and further expand their flight envelope (Altshuler et al., 2005; Bomphrey et al., 2017; Cheney et al., 2014; Iriarte-Diaz et al., 2012; Konow et al., 2017; Lentink and Dickinson, 2009b; Muijres et al., 2012b; Sane and Dickinson, 2002). Dynamic changes in wing size and shape adds a further layer of complexity. Wing shapes are not static, but exhibit time-varying three-dimensional shapes throughout the stroke cycle that are not readily predicted from conventional planform measurements of prepared specimens [e.g., (Bachmann et al., 2012; Riskin et al., 2010; Zheng et al., 2013)]. Wing size and shape changes on the fly in response to passive aerodynamic and inertial forces and to active morphing and reconfiguration, which in turn alters aerodynamic function. Passive forces are tightly coupled to the velocity of the wing, whereas active control allows the animal to modulate wing velocity and morphology independently. A major question is the extent to which animals use this active and passive wing reconfiguration to enable flight in diverse conditions.

Insect wings are the simplest system to examine dynamic morphology. Because they are actuated only at their base, shape changes are a product of aeroelastic and inertial loads (Du and Sun, 2010; Koehler et al., 2012; Le et al., 2013; Ma et al., 2015; Walker et al., 2009; Wang et al., 2002; Zheng et al., 2013). Passive deformation can result in changes in local angle of attack across the wing span, called twisting, and changes in wing curvature, called chordwise and spanwise cambering. The deformation characteristics of the wing are supported by evolution of the wing mechanical design (Combes and Daniel, 2001a; Ennos, 1988; Lehmann et al., 2011; Ma et al., 2015), presumably because flexibility confers enhanced aerodynamic performance through proximate mechanisms like wing twisting (Du and Sun, 2010; Le et al., 2013; Lehmann, 2012; Phan et al., 2017; Young et al., 2009b; Zheng et al., 2013). In a clever study, splinting bumblebees' wings was found to reduce flexibility and diminish burst flight performance (Mountcastle and Combes, 2013), showing that dynamic wings are important in natural behaviours, not only for efficient weight support. Considerably less is known about the role of passive cambering and twisting in bird wings, where the stiff feather veins and musculoskeletal system prevent many aspects of passive deformation, even in the insect-like flight of hummingbirds (Warrick et al., 2005). However, some birds can rely on automatic extension of the alula and covert feathers to control aerodynamics at the leading edge and dorsal surface, respectively (Àlvarez et al., 2001; Chin et al., 2017; Lee et al., 2015). Aero- and inertial-elastic flexibility of the flight feathers may also contribute to some birds' flight abilities by creating favourable wing twist that stops the leading edge vortex from bursting (Muijres et al., 2012b).

In addition to passive deformation, flying and gliding vertebrates actively morph their wings and tails to control features such as surface area and active cambering, greatly expanding the flight performance envelope (Altshuler et al., 2015; Thomas, 1996). Morphing is a general

feature of vertebrate aerial performance, and likely even enables proficient gliding and maneuvering in diverse taxa including frogs, snakes, and flying squirrels (Socha et al., 2015). Animals with the capacity for wing morphing can modulate useful and counterproductive aerodynamic forces, and control the aerodynamic and inertial energetic costs of flight (Bahlman et al., 2013; Bergou et al., 2015; Hedrick et al., 2002; Lentink et al., 2007; Riskin et al., 2012; Tobalske et al., 2009; Tucker and Parrott, 1970). Wing morphing has been observed in relation to flight speed (Hedrick et al., 2002; Iriarte-Diaz et al., 2012; Konow et al., 2017; Tobalske et al., 2007b; Tucker and Parrott, 1970), during maneuvering flight (Bergou et al., 2015; Lentink et al., 2007), and to maintain stability in response to turbulence (Reynolds et al., 2014). Like insects, vertebrates employ wing twisting and cambering to generate flight forces (Bachmann et al., 2012; Konow et al., 2017) but unlike insects, these are behaviourally labile traits that may differ between even morphologically similar species (Konow et al., 2017). As yet, there is no consensus on the use or limits of wing morphing and deformation in animal flight, in large part because it is difficult to introduce controlled flight challenges. For this reason, we examined the wing morphing capacities of hover-feeding hummingbirds, in which the stationary flight enables a detailed analysis of the wing surface. Hummingbirds are an excellent candidate model for this problem because they are thought to balance convergent evolution on insect-like flight with an avian phylogenetic ancestry.

Despite their impressive aerial abilities, hummingbirds appear to have the least dynamic wings among vertebrates (Chin et al., 2017), exhibiting a generally symmetric stroke cycle with only small variation in wrist flexion compared to other birds (Song et al., 2014; Tobalske et al., 2007b; Warrick et al., 2005). The lack of folding enables sustained production of force throughout the stroke cycle (Hedrick et al., 2012; Song et al., 2014; Warrick et al., 2005), and it

is possible that the reliance on upstroke lift limits the ability to recruit wing morphing to adjust force generation, such as with increasing flight speed (Tobalske et al., 2007b). Alternatively, some authors have questioned whether the magnitude of upstroke weight support [ $\sim 30\%$ , see for instance, (Song et al., 2014; Warrick et al., 2005; Wolf et al., 2013)] is less important than the details of stroke cycle aerodynamics, such as how the wing is flipped during stroke transitions (Warrick et al., 2012). In that case, hummingbirds might have substantial ability to control and modify the aerodynamics around their wings, perhaps most substantially during the upstroke.

We test two hypotheses related to morphological flexibility in hummingbirds. First, we test the hypothesis that hummingbirds have lost morphological flexibility through convergence on insect-like flight. Second, we test the hypothesis that increased twisting and cambering enhance flight performance. Contrary to the first hypothesis, we predict that (1) hummingbirds retain the avian morphologically-active stroke cycle and consequently exhibit great variation in shape throughout, and (2) hummingbirds employ these changes in posture and wing shape, including aerodynamically-important variables such as wing cambering, to precisely control aerodynamic mechanisms of weight support. Following from third hypothesis, we therefore predict that (3) hummingbirds adopt greater cambering and twisting to support hovering in challenging flight conditions (Iriarte-Diaz et al., 2012; Muijres et al., 2008; Young et al., 2009a). We develop a weightless marker tracking technique and analytical tools to track and describe wing configurations with high resolution. We probe the extent of hummingbirds' wing morphing through flight challenges known to elicit both shorter and wider stroke amplitudes than observed during normal hovering. Finally, we apply a blade element force analysis to real wings and flat plates with the observed kinematics to suggest the possible aerodynamic function of wing morphing in hummingbird flight.

## **3.2 Methods**

### **3.2.1 Wing anatomy**

We dissected the left wing of a male Anna's hummingbird (*Calypte anna*) sacrificed in an unrelated experiment. The musculoskeletal system and feather insertions were exposed and photographed in a spread posture on a custom light table. Positions of the bones, feathers, and connective tissue between the feathers were traced in Adobe Illustrator. The anatomy was verified in two additional dissections.

### **3.2.2 Hovering flight challenges**

Five male *C. anna* were wild caught on the campus of the University of British Columbia, and housed in an animal care facility. The experimental flight chamber was made of clear acrylic measuring 52 cm on each side, with an opening in the bottom panel covered by a 1 cm<sup>2</sup> mesh to prevent the downwash from recirculating within the chamber. The tip of the feeder was centrally placed 18 cm from the wall, >3 wing lengths away (*Calypte anna* wing length ~5.5 cm). The mouth of the feeder was extended about ~1.5 cm to force the bird to adopt a similar head position at each entry, although some twisting of the body still occurred. Each bird was provided with a perch on a mass balance (Ohaus Scout Pro), and allowed to acclimate to the chamber for at least one day before experimentation. We used operant conditioning to train the bird to associate activation of filming lights and the experimenter placing the feeder in the chamber with the start of feeding bouts. To minimise the on duration of the four 500W halogen bulbs, we required feeding to begin within 30 s, or the session was skipped (rare among well-trained birds). In general, filming time was <30 s, and the feeder was immediately removed. The

weight,  $W$ , during the bout was recorded as the average of pre- and post-feeding measurements. This filming period is shorter than the length of time for a hummingbird feeding to satiation, so we immediately inspected the filming, repeating the session if required; if not, the films were immediately saved to hard disk, and the bird allowed to feed until he returned to his perch, when the feeder was removed again. In addition, after every three trials the bird was allowed to feed *ad libitum* for 15 minutes, resulting in a half-hour break.

We examined birds' kinematics and wing morphology during regular hovering feeding ('control') and during two flight challenges: 1) mask; 2) load lifting. When hover-feeding near a visual obstacle, such as a large flower, hummingbirds avoid wing collisions with the obstacle by reducing stroke amplitude and increasing stroke frequency and stroke plane angle (Wells, 1993a). We constructed a thin plastic mask with the majority of the interior cut out, and placed this over the feeder. The side length of the mask was 5.75 cm, about 55% of the wing length. The remaining thin border was nearly parallel with the direction of motion of the wing, so aerodynamic interference is expected to be minimal, in contrast to, for instance, hovering at a large flower. We did not observe any collision between the wing and the mask. During pilot experiments, we found that birds could only hover transiently at very large masks, briefly darting in to the feeder with their necks extended. This could be the upper bound of hovering capacity, but was too unsteady to be comparable. We therefore reduced the mask size to challenge birds but maintain a hover-feeding bout of several seconds. Nonetheless, feeding duration was reduced compared to hovering at the unmasked feeder.

Aerial agility in hummingbirds is strongly correlated with the capacity to generate large burst forces (Altshuler et al., 2010; Segre et al., 2015; Sholtis et al., 2015). Maximum burst capacities assayed by asymptotic load lifting (Altshuler et al., 2010) are not sustainable for more

than about a second (Chai et al., 1997). We instead challenge birds' submaximum load lifting (Mahalingam and Welch, 2013; Wells, 1993a). Birds were fitted with beads on an elastic band looped around the neck, equal to 20-25% of body weight. In initial experiments, we found this was the highest ratio for which we could expect the bird's cooperation, and which did not result in flight distress. One individual refused to fly with weights, and was excluded from this part of the analysis.

### **3.2.3 Wing and body marking**

Three-dimensional reconstruction of the dynamic wing shape through marker tracking requires a large number of markers distributed across the wing, which precludes the use of weighted markers (Song et al., 2014; Song et al., 2016; Tobalske et al., 2007b). The hummingbird wing is generally featureless and has few landmarks, unlike the veins and patterns on insect wings (Koehler et al., 2012; Le et al., 2013; Phan et al., 2017; Young et al., 2009b). The rachis of the feather can be tracked with sufficient lighting (Tanaka et al., 2013), and it may also be possible to automate surface reconstruction through structured light (Deetjen et al., 2017), photogrammetry (Bachmann et al., 2012; Gillies et al., 2011; Heinold and Kähler, 2015; Walker et al., 2009), or optic flow (Martínez et al., 2015). However, we found these techniques to be difficult to apply to the highly twisted hummingbird wing with the available equipment. We therefore developed a weightless marker technique (the 'hummingbird salon') by bleaching spots on the surface of the wing with a commercially available hair bleach foaming agent, L'Oréal Paris® Perfect Blondissima Crème™.

Birds were restrained in a tensor bandage with a slot for one wing, and laid in a foam cradle. The wing was held extended through gentle pressure on the outer primaries, and the bird gently restrained by holding the beak between thumb and forefinger. We applied at least three

dots of bleaching foam to each feather, from root to tip, generally along the rachis of the feather. We also applied markers to the dorsal surface and leading edge of the handwing. After filming, we found that the sixth secondary flight feather (S6) was too small and inconsistently visible to be trackable, and was therefore excluded. The bleaching agent was allowed to dry for at least five minutes, and then thoroughly soaked and rinsed with multiple washes of tap water. Because residues of the bleaching agent could be ingested by a preening bird, special care was taken during the cleaning step, and we observed no difference in health or flight capacity between marked and unmarked birds in our population. Due to the small size of the wing, and to limit handling stress to the bird, we applied the entire marker set over multiple sessions of about 30 minutes each. Both marking experience and the small size of the animal relative to the restraining hands led to some differences in the number and placement of markers, resulting in 58-64 markers over the whole wing.

Although this marking technique can be applied to the body contour feathers, this results in low contrast and inconsistent placement due to feather displacement over the days after marking. We therefore applied five white paint spots (Bic® Wite-Out or Paper Mate® Liquid Paper) to the bird's back on the day of experimentation. The mass of these spots is about 0.07 mg, and so minor compared to the body inertia.

### **3.2.4 Marker tracking**

Markers were manually tracked from at least four colour high-speed camera views (one Miro4 and three Miro120s, Vision Research, Inc.), at 2200 Hz. Depending on availability, we also used a greyscale Phantom v12.1 and Phantom v311 (Vision Research, Inc.). Each camera filmed with 512x512 pixel resolution. Camera frame synchronisation was controlled by a

function generator (Tektronix AFG3021B), and shutter time was a maximum of 150  $\mu$ s, depending on the camera's capabilities and lens aperture. We used 24, 32, and 50 mm lenses, and due to the sensor crop factor and small image size in the center of the lens, nonlinear distortions in the images were negligible. Cameras were calibrated using direct linear transform coefficients (Hedrick, 2008), determined by a physical calibration object or through sparse bundle adjustment (Theriault et al., 2014). In the former case, the physical calibration object was suspended through its center of mass, so the gravitational vector was assumed to point along the object's +Z axis. In the latter case, the gravitational vector was found directly by dropping a bead through the cameras' fields of view.

Feather movements, variation in lighting through the stroke cycle, and parallax in each camera view contributed to ambiguity in the position of the marker centre. In extreme cases, the wing morphing results in partially or completely obscured markers. Where possible, the marker position was estimated based on nearby markers, or for short gaps of a few frames, the position was interpolated by a smoothing spline as described below. Otherwise, the marker for that individual was deleted from the dataset. Markers at the wing base (secondary flight feathers) were most affected, but are densely placed, and therefore the reconstruction is not greatly affected. The position of each marker was smoothed by applying a 2D smoothing spline to each dimension of each marker. The digitisation precision of each marker in each frame is estimated by the reprojection error of the reconstructed 3D position. We enforce a minimum digitising root mean square error (RMSE) of 1, and the marker standard deviation was calculated by bootstrapping (100 iterations) the residual error in each camera view and recalculating the 3D reconstructed position. The smoothed marker positions were then found by a cubic spline weighted by the relative standard deviations of all points in the time series. This fitting procedure

results in the smoothest function consistent with the marker positions and the digitising error. Enforcing a minimum digitising error amounts to a low-pass filter dependent on the magnification of the marker in each camera view. Overall, the appearance of features in the time series depends on the quality of evidence (e.g., number of camera views on marker, precision of calibration, precision of digitisation), and high-frequency features require more evidence and denser time sampling. This method is generally conservative (type I error), and may miss some real features (type II error), which could be improved by incorporating each marker's periodicity (i.e., incorporating its expected motion path). The smoothing method is implemented in a custom Matlab package (Hedrick, 2008).

### **3.2.5 Mesh reconstruction**

We initially computed a 2D mesh dependent only on markers around the wing perimeter. We selected the mid-downstroke as a representative time step in which the wing is flattest, and project the wing points into the plane. The wing perimeter was then upsampled by a cubic spline, and forty chord strips interpolated by joining paired points along the leading and trailing edges, with a target interior density of 0.5 mm. This resulted in >1000 interior points. The mesh was computed by 2D Delaunay triangulation of the interpolated points, and pruned to exclude faces with centroids falling outside the wing perimeter. The interior interpolation could then be applied to all other frames in all treatments, resulting in a single, consistent mesh for each individual.

To compute the full wing reconstruction, at each time step we rotate the digitised 3D points into the plane, using the singular vectors of the digitised point set. The surface is then found using the custom *gridfit* Matlab function (John D'Errico, <https://www.mathworks.com/matlabcentral/fileexchange/8998-surface-fitting-using-gridfit>,

accessed 13 July 2017), attempting to find a scheme in which the gradient is as smooth as possible in all directions. However, the fitted mesh was heavily distorted by very high curvatures along the secondary feathers during the upstroke, and overfit spanwise features along marker lines, leading to irregularities along feathers. Better results were obtained by applying a cubic spline to initially interpolate ten points along selected secondary flight feathers, and stiffening the fitted mesh to weaken the contribution of individual markers. This process incorporates spatial information into the mesh fitting, because the local fitted surface becomes a function of multiple nearby markers. The resulting meshes generally fit the data well, but oversmoothed real, high-curvature topologies in the secondary flight feathers during the upstroke. However, this does not form part of our analysis. The 2D interpolated points were finally projected onto the fitted surface, using the *iso2mesh* Matlab toolbox (Qianqian Fang, <http://iso2mesh.sf.net>, accessed 2 June 2017), yielding a camber profile along predetermined lines, and the same triangulation as the 2D mesh.

### 3.2.6 Kinematics and morphology in flight

We digitised three consecutive strokes, and a quarter stroke before and after. All digitised points were rotated to align the body markers with the global +X vector. The wing frame is described with respect to a reference frame  $xyz$  aligned with gravity, but with  $x$  perpendicular to the body (Figure 3.1). The wing-fixed reference frame is described by the least squares plane with normal  $z''$ , which passes through the geometric centroid of the wing. The wing is first rotated around  $z$  by an angle  $\varphi$  (excursion), so that  $x''$  lies in the  $xz$  plane, then rotated by an angle  $\theta$  (elevation), so that  $x'$  and  $x$  are parallel. In the  $x',y',z'$  frame, the geometric angle of attack,  $\beta$ , is the angle between  $y'$  and  $y$ , and is found for each chord. The transformations are depicted in

Figure 3.1. The peaks of  $|\varphi|$  were used to define the stroke reversal periods, from which we obtained the mean stroke frequency. Comparisons are made on the basis of the normalised stroke period  $T$ .

Along with its chord vector, each chord strip is described by its unit normal vector  $\hat{n}$  and velocity vector  $\mathbf{v}$ . To calculate the chord normal, we find the unit vector  $\hat{s}$  pointing from the center of chord  $i$  to the center of chord  $i+1$ , and then  $\hat{n} = \hat{c} \times \hat{s}$ , where  $\times$  is the vector cross product. Surface normals are very sensitive to noise, so we smooth the normal of chord  $i$  by central differences. The aerodynamic angle of attack was calculated by  $\text{acos}(\hat{c} \cdot \hat{v})$ . The time derivatives (expressed with a dot) of the three angular components comprise the angular velocity,  $\boldsymbol{\omega} = (\dot{\varphi}, \dot{\theta}, \dot{\beta})$ , and angular acceleration,  $\dot{\boldsymbol{\omega}} = (\ddot{\varphi}, \ddot{\theta}, \ddot{\beta})$ .

The wing area,  $S$ , is calculated by summing the areas of each face in the 2D mesh. The location of the rotational axis was found for each blade in the  $x',y',z'$  frame. For each strip, we find the closest point between the strips at time steps  $t_0$  and  $t_1$  (Lehmann et al., 2011). The rotation axis was calculated throughout the stroke and then averaged for each strip, and lies ~50% of the chord length behind the leading edge, although this moves somewhat forward at both ends of the wing.

Section camber and twist were computed for each strip. Wing twist,  $\Theta$ , is expressed as the total change in geometric angle of attack from tip to root (Leishman, 2000). For a thin aerofoil, chordwise camber is given by  $h_{\text{max}}/c$ , where  $h_{\text{max}}$  is the maximum height of the 3D strip above the chord vector (Ennos, 1988). To compute spanwise features, we find the line,  $s$ , connecting a point at 95% of wing base chord length, to the wing tip. Projecting this path onto the 3D wing, we obtain the instantaneous wing length,  $R$ , and the height of  $s_{\text{max}}/R$  is the spanwise camber.

### 3.2.7 Aerodynamic forces

Blade element modelling (BEM) of forces acting on a wing assume that aerodynamic performance is a function only of instantaneous position and kinematic parameters, and not a function of time evolution (with some exceptions, e.g., (Truong et al., 2011; Walker and Westneat, 2000)). Spanwise flow is considered implicitly through the use of empirical force coefficients measured on real wings, where 3D effects are inescapable (Ellington et al., 1996; Kruyt et al., 2014; Usherwood and Ellington, 2002). The total force acting on a wing is a superposition of separate forces with distinct time histories, including interactions between the wing and its own wake, or between opposing wings. In hummingbirds hovering with moderate ( $\sim 140^\circ$ ) stroke amplitudes, computational fluid dynamics (CFD) simulation suggests wing-wing interactions are minimal (Song et al., 2014). Similarly, while wake interactions may be important, they are not necessary to achieve similar weight support to CFD (90%) (Song et al., 2015b). Therefore, we consider the following typical force contributions (Song et al., 2015b) to the aerodynamic force,

$$\mathbf{F}_{aero} = \mathbf{F}_{trans} + \mathbf{F}_{rot} + \mathbf{F}_{acc}$$

The wing rotates around the shoulder (which is possibly not a fixed point), and so the velocity of a blade includes translational and rotational components, linearly separable as translational ( $\mathbf{F}_{trans}$ ) and rotational ( $\mathbf{F}_{rot}$ ) forces (Lentink and Dickinson, 2009a; Lentink and Dickinson, 2009b; Sane and Dickinson, 2001; Sane and Dickinson, 2002; Walker, 2002). The accelerating wing displaces a volume of fluid, generating a reactive added-mass force,  $\mathbf{F}_{acc}$ , that opposes wing motion and acts normal to the wing chord (Daniel, 1984; Truong et al., 2011).

The translational force acting on a wing at time  $t$  is analogous to a propeller rotating with constant angular velocity,  $\dot{\phi}$ , and angle of attack-dependent lift and drag coefficients  $C_T = \sqrt{C_L^2 + C_D^2}$  (Kruyt et al., 2014; Usherwood and Ellington, 2002; Weis-Fogh, 1972). The force coefficients for prepared *Calypste anna* wings were previously determined empirically (Kruyt et al., 2014). The rotational force is dependent on the product of the wing angular velocity and rotational velocity around the rotational axis, with some coefficient  $C_{rot}=\pi(0.75-d)$ , where  $d$  is the mean distance to the rotational axis behind the leading edge (Sane and Dickinson, 2002). The coefficient was found to be about 0.93 in Rufous hummingbirds (*Selasphorus rufous*) (Song et al., 2015b) and  $\sim 0.7$  here. To calculate the added mass force, we assume the wing entrains a volume of fluid with an elliptical cross-section. The first term of  $\mathbf{F}_{acc}$  represents the angular acceleration of the blade element, and dominates as  $\alpha \rightarrow \pi/2$  (strip perpendicular to the flow), while the second is the product of the section angular and rotational velocities, and dominates as  $\alpha \rightarrow 0$  (strip parallel to the flow). The third term represents the displacement of fluid by the wing pitching motion, and is independent of the wing velocity. It is rescaled to reflect the pitching axis of a hummingbird wing (Song et al., 2015b). The aerodynamic forces acting on the wing at time  $t$  are thus,

$$\mathbf{F}_{trans}(t) = \int_0^{r=R} \frac{1}{2} \rho \|\mathbf{v}\|^2 r c(r) C_T(\alpha) dr$$

$$\mathbf{F}_{rot}(t) = \int_0^{r=R} \frac{1}{2} \rho \dot{\phi} \dot{\alpha} r^2 c(r)^2 C_{rot} \hat{\mathbf{n}} dr$$

$$\mathbf{F}_{acc}(t) = \frac{1}{4} \rho \pi \int_0^{r=R} r^2 c(r)^2 (\ddot{\phi} \sin \alpha + \dot{\phi} \dot{\beta} \cos \alpha) \hat{\mathbf{n}} dr + \frac{1}{53} \rho \pi \int_0^{r=R} r c(r)^3 \ddot{\beta} \hat{\mathbf{n}} dr$$

where the instantaneous translational velocity,  $\mathbf{v}$ , is the vector pointing from the midpoint of the chord from  $t_0$  to  $t_1$  (i.e., angular velocity minus the chord rotational component). The total force vector is decomposed into vertical ( $\mathbf{F}_v$ ) and horizontal ( $\mathbf{F}_h$ ) components, which directly informs the weight support,  $2\mathbf{F}_v/W$  (the factor of two compensates for the single wing). We normalise force components by  $C_F = \mathbf{F}/\frac{1}{2}\rho\bar{U}_2^2\bar{S}$ , where  $\bar{U}_2 = \bar{U}\hat{r}_2$  is the mean wing velocity through the stroke corrected for the second moment of area (Ellington, 1984d; Kruyt et al., 2014; Usherwood and Ellington, 2002), and  $\bar{S}$  is the mean wing area through the stroke. The forces are therefore normalised to the average dynamic pressure applied over the average actuator disc.

The instantaneous aerodynamic cost of moving the wing is the aerodynamic torque.

$$P_{aero}(t) = -\boldsymbol{\tau}_{aero}(t) \cdot \boldsymbol{\omega}(t) = - \int_0^{r=R} \mathbf{F}_{aero}(t) \cdot \mathbf{v}(t) dr$$

### 3.2.8 Function of the dynamic wing

We adopt an analytical approach to investigate the aerodynamic performance of morphing wings. Aerodynamic performance can be characterised by the force produced and the power consumed. Hummingbird wings compare favourably with helicopter rotors (Altshuler et al., 2004a; Kruyt et al., 2014), and we therefore use basic measures of helicopter performance to characterise the performance of the wing models. A basic metric is the ratio of vertical to horizontal forces,  $C_v/C_h$ , which is the extent to which aerodynamic force is helping support body weight during hovering [proportional to the glide ratio, (Kruyt et al., 2015)]. A nondimensional measure of the ratio of useful force to power expended is derived by considering the ideal power consumption at the actuator disk (induced power), which is proportional to  $C_v^{3/2}$  (Leishman,

2000). Comparing ideal and measured power factors, we obtain (Berman and Wang, 2007; Kruyt et al., 2014; Leishman, 2000; Usherwood, 2009),

$$PF = \frac{C_V^{3/2}}{C_P}$$

We explore the functional significance of wing morphing (area changes) and wing twisting by examining the aerodynamic performance of simplified wing models (Le et al., 2013; Phan et al., 2017; Zheng et al., 2013). The first wing model is obtained by untwisting the instantaneous configuration of the wing by rotating each blade into  $x''', y''', z'''$ . This procedure preserves area changes, which we term the ‘morphing 2D plate’. The second wing model is a rigid plate in mid-downstroke configuration rotated to the orientation of the morphing rigid plate model, and aligned at the shoulder. The ‘downstroke 2D plate’ is effectively the conventional quasisteady model of hummingbird flight, including that of Chapter 2.

### **3.2.9 Statistical analysis of flight performance**

We statistically evaluated the major features of wing morphing through the stroke cycle by geometric morphometric analysis of the digitised marker positions. Each marker was treated as a landmark and each frame as an instantaneous wing configuration. The configurations were aligned through Procrustes superimposition, and because changes in wing area are of interest, differences in size are preserved by not scaling the markers to the centroid size (size-and-shape analysis). Major differences in shape are summarised by principal components analysis.

Kinematic and morphological variables were computed and aggregated over all birds through custom Matlab scripts. Some variables, usually 3D parameters, were not calculable in all individuals, resulting in 4-5 individuals in the mask treatment, and 3-4 individuals in the load

lifting treatment. Because of the low number of individuals and large number of possible tests, we pruned analyses to selected planned comparisons. Statistical significance among treatments was examined by mixed-effects modelling, incorporating individual as a random effect. We examined only the overall difference among wing model types (rather than interactions between wing model and flight challenge). In those models, individual and flight challenge were included as random effects. Statistical analyses were performed in R 3.4.0 (R Core Team, 2017), with the packages *Morpho* for geometric morphometric analysis (Schlager, 2017), and *lsmeans* (Lenth, 2016) and *lmerTest* (Kuznetsova et al., 2016) for mixed-effect modelling and identification of differences among group means.

### **3.3 Results**

#### **3.3.1 Anatomy of the wing**

We first examined the anatomy and insertion points of the primary and secondary flight feathers in the handwing (Figure 3.2, drawn from photographs of the spread wing). Primary (P) feathers insert on the carpometacarpus, and phalanges 1 and 2 of digit II (handwing), whereas secondary (S) feathers insert on the ulna. All the flight feathers are mechanically linked through connective tissue. Primary feathers have greater flexural stiffness compared to secondaries, due to a much larger rachis, such as primary flight feather 10 (P10), which forms the leading edge. The pattern of insertion points on the handwing suggests that the largest torsion will be experienced in the distal-most primaries, and the separate insertion points of P10 from P7–9 suggests that wing camber could be controlled by twisting phalanx 2. Moreover, the actuation of primaries by the handwing and secondaries by the ulna suggests that the wing may act as two mechanically coupled plates during the stroke cycle.

### 3.3.2 Geometric morphometric analysis of dynamic morphology

As an initial step toward describing the complexity of wing motions in flight, we plot the motion paths of selected markers throughout the wing in a handwing-fixed reference frame (Figure 3.3; anchoring markers denoted with asterisk, and alternating secondaries omitted for clarity). In the handwing frame, the distal primary flight feathers (wing tip), secondary flight feathers, and shoulder show the maximum relative activity, according to the size of the path. The wing tip charts a nearly figure eight path, with the largest deviations occurring in the downstroke. Motion in the chordwise direction is due to wing flexion, whereas motion normal to the handwing occurs because of tip bending during the downstroke and ‘cupping’ from negative curvature during the upstroke. The secondaries move in a direction in opposition to the primaries, because they are folded against the body during the upstroke, and expanded for maximum area during the downstroke. The shoulder marker is highly dynamic due to the twisting of the joints which control the wing movements and surface (Hedrick et al., 2012). Additionally, during supination, the wing twist is so extreme that a discontinuity appears between P1 and S1, as predicted by separate actuation of the groups of feathers by the handwing and ulna, respectively (Hedrick et al., 2012) (Figure 3.2). Consequently, the supination torsional wave does not travel the full length of the wing. The discontinuity persists for approximately the first half of the upstroke while the wing is accelerating, and no gap is visible in the travelling direction.

The marker paths through the stroke, and thus the change in wing configuration, is not easily described. We therefore find a reduced dimensional representation of the instantaneous wing configuration for a representative individual, by projecting the wing into the size-and-shape

tangent space (Dryden and Mardia, 2016; Schlager, 2017). Because this space is linear, the configuration in any frame is summarised by its principal components score. Two principal components (PCs) explain >90% of the variation over the stroke cycle and among treatments (PC 1: 79.2%, PC 2:11.7%; single individual). The variation explained by these two components is visualised by warping a mesh from the stroke-averaged configuration to the minima and maxima of the two PCs (Figure 3.3). The first PC primarily explains changes in the wing area (as expected from the size-and-shape space), driven by compaction of the secondaries and rotation of the shoulder, and potentially activity in the patagial muscles and flexion at the elbow (Figure 3.3). The second PC almost entirely derives from the twisting of the wing, and the flexion and extension of the outer primary flight feathers are particularly evident. Some changes in projected area are additionally encoded by negative second PC values.

We interpret shape changes at key points of the stroke cycle in the same manner. During pronation (stations i to ii in Figure 3.3d), the secondaries are initially compacted against the body and the tip is flexed. The secondaries rapidly splay and the tip is extended as the wing twists and begins to translate. At mid-downstroke, the wing has reached maximum area, and reverts its shape almost entirely along PC1. The opposite signs of PC1 and PC2 reflects stationary secondaries while the primaries flex, twist, and reverse direction. The time course of the PC scores is not symmetric, reflecting different wing shapes in the down- and up-strokes caused by the limitations of hummingbird anatomy (Hedrick et al., 2012; Welch and Altshuler, 2009). The previously noted behaviour of the wing during the first half of the upstroke may explain the time course of the PCs from stations iii to iv, after which the wing progresses with a nearly constant rate of shape change until pronation. Notably, the trajectories of the wing through shape space

are very similar in each stroke, reflective of hummingbirds' highly stereotyped muscle activation patterns and flapping behaviour (Altshuler et al., 2012).

### **3.3.3 Aerodynamic analysis of dynamic morphology**

We next describe the wing morphology using aerodynamic measures of wing area, twisting, and cambering. The patterns in the principal components are broadly confirmed by examining the time course of wing area. Wing area increases through the stroke, reaching a maximum approximately mid downstroke, then decreases as the wing approaches supination (Figure 3.4a wing area time profile for the same individual as Figure 3.3). Variation in wing area during the stroke cycle is mostly due to activity of the secondary feathers. Due to the compaction of the secondaries, the wing area is reduced in the upstroke even though the wing length does not greatly vary (the extension and flexion occur over very small angles, as evident from PC2 in Figure 3.3c). As the upstroke continues, the secondaries continue to be pressed against the body, until immediately prior to pronation, when they fan out.

We next characterise the dynamic behaviour of the wing with respect to the aerodynamic variables twist and camber. The reconstructed chord and camber lines in mid-downstroke and upstroke, along with their time profiles in one representative wing stroke, are shown in Figure 3.5. The wing is minimally twisted near the stroke reversals [corresponding to the method of determining stroke reversal points in, e.g., (Altshuler et al., 2012)]. In accordance with aerodynamic theory (Leishman, 2000), the wing exhibits approximately linear twisting over its span during both mid-downstroke and mid-upstroke (not shown). Twisting is negative from tip to root (Figures 3.5, 3.6), and the tip angle can even become negative. However, the downstroke aerodynamic angle of attack,  $\alpha$ , is positive and greater than  $\beta$  across the span. The wing is much

more twisted during the upstroke, leading to higher morphological angles of attack, but here, the aerodynamic angle of attack is actually lower.

Wing camber is typically 10-15% during the downstroke (Figures 3.5, 3.6). Inspection of the reconstructed wing meshes shows that the cambering mostly arises in the distal primaries, suggesting that the majority of camber is caused by finger twisting. Accordingly, during the upstroke the design of the slotted wing prevents the same amount of twisting, and camber is substantially reduced (Figures 3.5, 3.6). We note that the cambering at the wing base is substantially overestimated here because the extreme twisting of the handwing (Hedrick et al., 2012) is visible as deformation of the wing surface, and we cannot presently reconstruct the ventral surface of the wing.

The wing exhibits substantial spanwise cambering during both strokes (Figure 3.6). During the downstroke, spanwise camber develops due to tip drag (Lehmann et al., 2011). During the upstroke, spanwise camber is greater as the wing is cupped in the direction opposite its travel. At present, it is unclear how this is achieved, but could be related to coupling of joint motions in the wrist. Although hummingbirds generate force through the stroke, the highly twisted, compacted, and nonplanar wing shape contributes to reduced upstroke force generation (Song et al., 2014; Warrick et al., 2005). Upstroke kinematics may therefore serve to contribute some weight support while minimising drag and excess power expenditure (Bahlman et al., 2013).

### **3.3.4 Dynamic morphology during flight challenges**

We predicted that hummingbirds would recruit lift-enhancing mechanisms like greater chordwise wing camber to supplement kinematic modulation. When flying with a feeder mask,

hummingbirds greatly reduced their amplitude,  $\Phi$ , and when flying with weights, increased  $\Phi$  (Mahalingam and Welch, 2013; Wells, 1993a). Stroke frequency,  $f$ , was increased in compensation at the feeder mask, but actually decreased during load lifting. Mean kinematic and morphological parameters during the flight challenges are listed in Table 3.1.

Wing configurations identified by geometric morphometrics differed among the flight challenges, throughout the stroke cycle but most prominent during the upstroke (Figure 3.3b). Qualitatively, the three treatments differ subtly during pronation (i in Figure 3.3), but are indistinguishable through the first half of the downstroke. Wing configuration begins to diverge following mid-downstroke (ii) in preparation for supination. At the mask, the wing sharply and suddenly exhibits very high values on PC2. Comparison to the wing area time course (Figure 3.4), suggests this is due to expansion of wing area from the distal primaries or secondaries, as the wing area is briefly greater than in normal hovering. This interpretation is supported by a similar PC2 profile during load lifting, along with similarly increased wing area compared to control hovering. The sharp change in the configuration could be related to the visual observation that at the mask, the wing does not complete a normal shape cycle, but instead reverses direction without fully flexing. As a result, the wing area is generally greater throughout the stroke (Figure 3.3). The wing configuration during load lifting is more similar to that in the control condition, but the wing is also more extended at mid-upstroke (PC2, Figure 3.3b), leading to a slightly larger wing surface area (Figure 3.3). Overall, this analysis of wing shape suggested to us that control of wing configuration during the upstroke is of principal importance.

We next examined how wing reconfiguration affects aerodynamic parameters. In four of five birds at the feeder mask, wing area was increased during the downstroke (Figure 3.3), though this was not overall statistically significant. Midspan angle of attack was sharply

increased at the mask (Table 3.1), which increases both lift and drag (Kruyt et al., 2014). The midspan angle of attack (immediately distal to the fingers) can be controlled by twisting the wing. When feeding at the mask, hummingbirds greatly decrease their wing twisting both during downstroke and upstroke (Figure 3.6, significant differences in group means denoted by letters). Accompanying the decrease in wing twisting at the feeder mask was decrease downstroke chord camber (Figure 3.6). During load lifting, there is an overall consistent trend toward smaller values of aerodynamic parameters (Table 3.1), such as angles of attack and stroke plane angle. We lack statistical power to discriminate these changes, but it is clear that even so, kinematic and morphological adjustments for load lifting are slight. Finally, we found that spanwise camber greatly increased during the downstroke in both conditions, and during the upstroke at the feeder mask. During the downstroke, increased spanwise camber likely coincides with increased tip drag, resulting in tip bending. In sum, the wing is highly dynamic both during the stroke and selectively modulated during flight challenges, showing that hummingbirds actively control their wing configuration.

### **3.3.5 Performance of morphing wings**

We studied the functional implications of wing adjustments through quasisteady analysis of aerodynamic force and power. Weight support predicted by the blade element model (BEM) was 74%, in contrast to the 91% predicted earlier (Song et al., 2015b), due to our use of empirical (Kruyt et al., 2014) rather than simulated (Song et al., 2015b) force coefficients (near-complete weight support is predicted by substituting the latter). Our value is more similar to the typical values of weight support predicted by BEM (Kruyt et al., 2014). Weight support at the mask feeder and during load lifting was significantly less than in control by 10-15% of the

control value (Table 3.1). This could point to recruitment of unsteady lift-enhancing mechanisms to cope with flight challenges, such as a strengthening of the downstroke leading-edge vortex, or alterations to the vortex-shedding and wake capture patterns (Altshuler et al., 2009; Warrick et al., 2005; Wolf et al., 2013).

By considering force produced through the stroke, we can observe the functional significance of many small adjustments even when different individuals use slightly different mechanisms. We first examine the decomposition of the BEM-modelled total force into translational, rotational, and added mass reactive forces (Figure 3.7a,b,c). The force profiles mirror those observed previously [(Song et al., 2015b), on which the analysis is based]. Among treatments, the principal difference is at the feeder mask, which exhibits shifts in the location, magnitude, and width of each force peak during the downstroke, and a reduced translational force peak during the upstroke. Comparing force coefficients, the peak vertical force coefficient,  $\bar{C}_V$ , at the feeder mask is much higher than in the control condition, whereas  $\bar{C}_V$  is reduced during load lifting (Figures 3.7d, 3.8a). The change in force coefficient comes at the expense of the power coefficient,  $\bar{C}_P$ , which is greatly increased at the feeder mask, and slightly decreased with weights (Figures 3.7f, 3.8b). Due to the wing posture and kinematics, hummingbirds at the mask generated much larger horizontal forces, resulting in reduced force ratio,  $\overline{C_V/C_H}$  (Figure 3.8c). The vertical force is constant (hovering), meaning that more of the aerodynamic force production is wasted, explaining the large increase in power coefficient. Direct comparison of the vertical force and power coefficients factor shows a substantial reduction in power factor,  $PF$ , when feeding at the mask (Figure 3.8d). There is no significant change in  $\overline{C_V/C_H}$  during load lifting, and the increase in power factor is significant but insubstantial. The decline in vertical force coefficient thus results in an isometric decline in power coefficient.

The more plate-like and two-dimensional profile of the wing at the feeder mask is counter to our prediction that hummingbirds would recruit more three-dimensional shapes like increased curvature (chordwise camber). We therefore compared the aerodynamic performance of an untwisted model of the wing which retains morphing (area changes). Comparing force profiles, the flat plate wings generate greater force through the stroke cycle, primarily from translational forces (Figure 3.7a). The greater force results in increased vertical and horizontal forces, and therefore greater power expenditure (Figures 3.7d-f, 3.8). To assess the impact of the wing morphing alone, we actuated a flat model of the downstroke with the observed real kinematics. Vertical force and power coefficients increase proportionately in the non-morphing model, indicated by little to no change in  $\overline{C_V/C_H}$  and  $PF$  (Figure 3.8). In accordance with aerodynamic theory, the overall effect of wing twisting on aerodynamic efficiency is nonlinear, and the effect of morphing is linear (Leishman, 2000). However, the non-morphing wing also exhibits behavior specific to flapping wings, and produces larger negative rotational and added mass forces near supination and pronation respectively (Figure 3.7b,c). The effect of the morphing on rotation is exemplified by the force coefficients, which show a stark increase in horizontal force coefficient and power consumption during pronation (Figure 3.7e,f).

### 3.4 Discussion

Flexibility is a major feature of insect and vertebrate propulsor design, and results in increased force production (Mountcastle and Combes, 2013; Young et al., 2009b) and flight efficiency (Young et al., 2009b; Zheng et al., 2013), and wider safety margins for structural damage (Corning and Biewener, 1998; Lentink et al., 2007; Mountcastle and Combes, 2014). In vertebrates, the added ability to actively morph propulsor appendages greatly expands the

performance envelope (Alben et al., 2007; Bergou et al., 2015; Combes and Daniel, 2001b; Dial, 1992; Iriarte-Diaz et al., 2012; Lentink et al., 2007; Reynolds et al., 2014; Thomas, 1996; Walker and Westneat, 2000). Bats especially are known to rely on a variety of wing shapes to accomplish different kinds of flight (e.g., slow and fast flight). Hummingbirds combine features of all groups of flapping fliers, including insect-like kinematics and avian wing design and control (Hedrick et al., 2012). We hypothesised that hummingbirds exhibit a capacity to control wing cambering hitherto found only in bats.

We first tested the hypothesis that hummingbird dynamic wing morphology is a major mechanism explaining body weight support during hovering. A key difference between hummingbirds and insects is that hummingbirds still generate the majority of weight support during the downstroke, like vertebrates (Tobalske et al., 2007b). It is possible that this is due to basic anatomical limitations of vertebrate flight (Hedrick et al., 2012), which precludes a symmetrical wing geometry in both strokes. Our own results suggest that the wing cannot be as effectively cambered during the upstroke, and therefore that the mechanisms of force production will also differ (Figure 3.6c). We instead hypothesised that hummingbirds do have the capacity to generate greater forces during the upstroke, but avoid doing so to balance force production and energy expenditure. We find that hummingbird wing geometry varies constantly through the stroke cycle due to aerodynamic deformations and active morphing and twisting (Figure 3.3). Comparing real wings and simulated flat plates, real wings have reduced vertical force coefficients, but also expend considerably less aerodynamic power (Figures 3.6, 3.8). Moreover, compared to the real wing, the flat plate models generate relatively more horizontal forces than vertical forces (Figure 3.8c). We find that wing morphing (area changes) during the stroke cycle minimises adverse force production compared to a constant-area model (Figures 3.6, 3.8).

Although this largely follows from the linear dependence of the force coefficient on wing area (see Methods), we found that morphing also minimises production of adverse rotational and added mass forces (Figure 3.6) during reciprocating wing motions unique to animals. Together, these suggest that even given anatomical limitations, hummingbirds may indeed prioritise minimum upstroke drag and power over maximum weight support. This is similar to bats, which ostensibly have the capacity to generate greater upstroke weight support with much greater inertial and aerodynamic power cost (Bahlman et al., 2013; Riskin et al., 2012).

A potential criticism is that the flat plate wing model is not a strictly fair comparison, because the flat wing was actuated with real upstroke kinematics. If hummingbirds could execute symmetrical strokes, the kinematics of both the downstroke and upstroke would be different, to reflect the increased contribution of the upstroke to weight support. The true what-if scenario would require detailed optimisation studies (Berman and Wang, 2007; Hedrick and Daniel, 2006). Our approach is useful for the conclusions presented here and for consideration of quasisteady analyses (Chapter 2) (Kruyt et al., 2014; Read et al., 2016), because the hummingbird anatomy prohibits symmetrical strokes. Hummingbirds apparently lack the ability to twist the entire wing further during the upstroke, which means that the secondary flight feathers are constrained to have very high angles of attack during the upstroke. Unlike in insects, hummingbird wing camber is morphological (feathers) and anatomical (wrist twist), not aerodynamic or inertial (autocamber), and thus cannot be symmetrical between strokes (Warrick et al., 2005). Comparing our analyses to these fundamental morphological constraints predicts that hummingbirds are balancing the cost of less efficient upstroke weight support.

We next tested the hypothesis that hummingbirds reconfigure their wing shape to cope with distinct flight challenges by modulating force and power output. Hummingbirds hold a bag

of kinematic tricks to accomplish diverse aerial feats (Altshuler et al., 2012; Ortega-Jimenez et al., 2016; Read et al., 2016; Sapir and Dudley, 2012), but their ability to morph their wings is considered to be limited (Chin et al., 2017; Tobalske et al., 2007b). Nonetheless, this has only been tested with very limited resolution of the reconstructed hummingbird wing surface in flight (Song et al., 2014; Song et al., 2016; Tobalske et al., 2007b). We developed a weightless marker tracking and wing surface reconstruction protocol, and found that hummingbirds can indeed control their twisting and camber (Figures 3.5, 3.6). Kinematic and morphological adjustments during load lifting are too subtle or underpowered to detect statistically (Table 3.1, Figure 3.4), but are consistent with previous studies of the same challenge, such as reduced stroke frequency and stroke plane angle (Mahalingam and Welch, 2013; Wells, 1993a). Despite these shortcomings, the sum of kinematic and morphological adjustments is a decrease in force and power coefficients (Figure 3.8). The largest changes were observed while hovering with the feeder mask, in which hummingbirds appear to be flattening the wing to increase force coefficients at the cost of greatly reducing flight efficiency (Figures 3.6, 3.8).

The observed wing morphing and sacrifice of flight efficiency could be recruited during maximum burst performance, as tested by asymptotic load lifting. In these tests, hummingbirds are thought to be motivated by an escape reflex, and so flight efficiency will not be important. Less than 25% of the observed burst load lifting capacity among individuals can be explained by the proximate quasisteady mechanisms of wing loading or factorial increase in wing velocity [species-centered individual measurements (Chapter 2), considering the fixed-effect  $R^2$  with species as random effect (Nakagawa and Schielzeth, 2013)]. This suggests there is a substantial possibility for recruitment of wing morphing during these burst maneuvers particularly, and maneuvering flight generally.

We propose stroke amplitude modulation and tuning flight efficiency are the central features of hummingbird hovering flight. Purely aerodynamically, when the majority of weight support is generated by translational forces (i.e., not rotational or added mass forces), efficiency is largely a function of maximising the area of the actuator disc over which the pressure pulse is applied (Ellington, 1984a). In virtually all cases, animals hover with energetically suboptimal kinematics, including stroke amplitudes much lower than the maximum (Altshuler et al., 2010; Usherwood, 2009). A major reason is that nearly all animals rely on stroke amplitude modulation for maneuvering flight. A hummingbird with  $180^\circ$  stroke amplitude could be aerodynamically efficient, but unable to respond to aerial attacks by a conspecific (Segre et al., 2015). Consequently, a sacrifice of energetic efficiency is unavoidable. Despite the very small difference in stroke amplitude between normal hovering and load lifting, we nonetheless find a slightly increased power factor, consistent with this explanation. Modulation of energetic efficiency similarly underlies hummingbirds' responses when forced to use short stroke amplitudes. In that treatment, we observed extensive dynamic reconfiguration of the wing to be more plate-like, corresponding large increases in force coefficient and power coefficient, and a drop in power factor. Overall, it appears that hummingbirds dynamically tune their kinematics and wing morphology to maximise the flight envelope. This may suggest stabilising selection on intermediate values of stroke amplitude, explaining why amplitude is size invariant among and within species (Chapter 2).

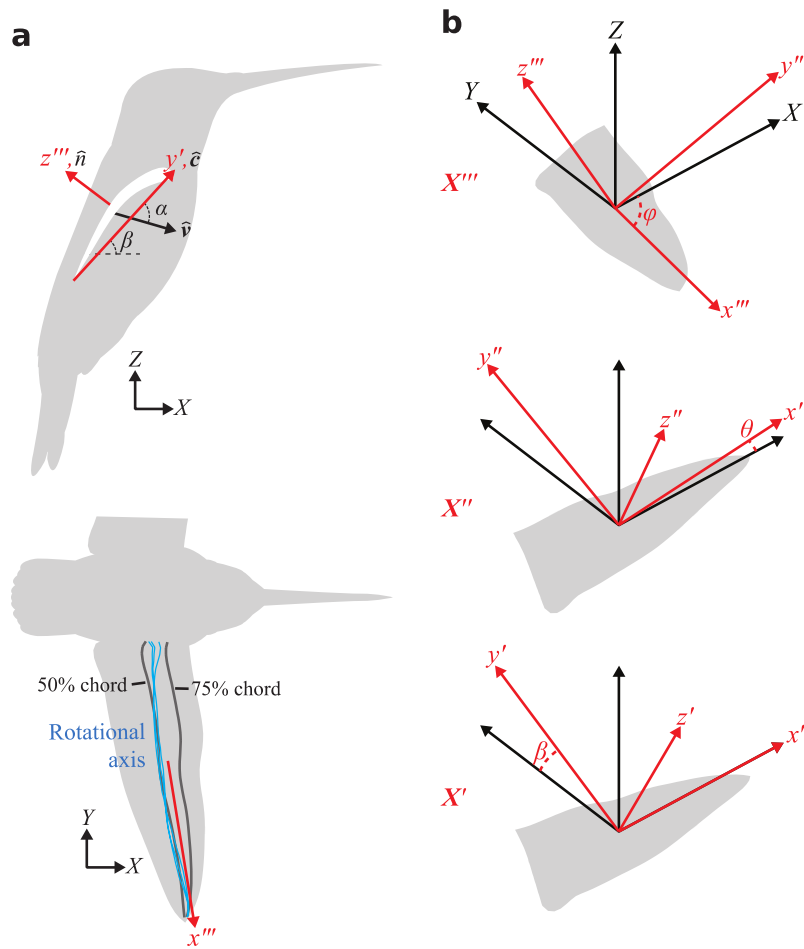


**Figure 3.1** Coordinate system in this study. **a** Side and top views of a hovering hummingbird. We show the chord, normal, and velocity vectors of the wing, and reference frame vectors according to the coloring and labelling scheme of the reference frame system in **b**. The average chord-wise rotational axis of the wing is shown in **a** and compared to the 50% and 75% chord lines. **b** Wing-centered reference frame ( $\mathbf{X}'''$ ) and global reference frame ( $\mathbf{X}$ ). The  $\mathbf{X}'''$  frame is determined by the least-squares plane passing through the centroid of the wing. The wing excursion  $\varphi$  is determined by the angle between  $\mathbf{x}'''$  and global  $X$ . The  $\mathbf{X}''$  frame is formed by rotating the wing around global  $Z$  by  $\varphi$  to find the elevation angle  $\theta$  between  $\mathbf{x}''$  and global  $X$ . Rotating the  $\mathbf{X}''$  frame by  $\theta$  yields the  $\mathbf{X}'$ , from which the wing pitch  $\beta$  is determined by the angle between  $\mathbf{y}'$  and global  $Y$ .

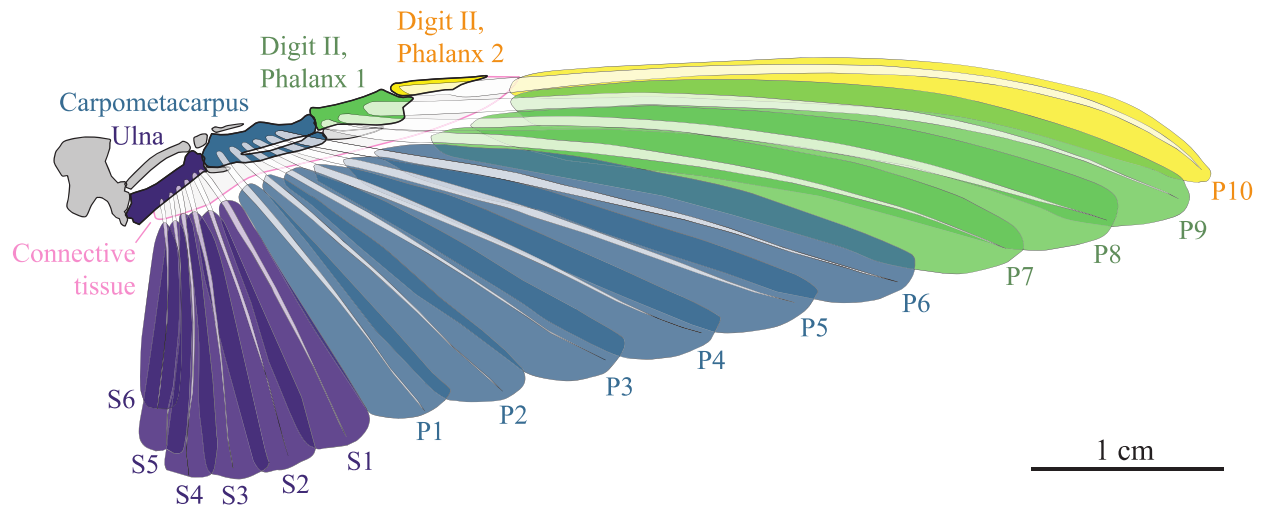


**Figure 3.2** Feather and bone anatomy of the hummingbird wing (dorsal view). Primary (P) and Secondary (S) flight feathers are colour-coded according to the bone on which they insert. The four bones with insertions are outlined for clarity, but the feather veins lie dorsally on the bones. The wing was posed in a mid-downstroke configuration, which frequently includes significant overlap of S6 on S5.

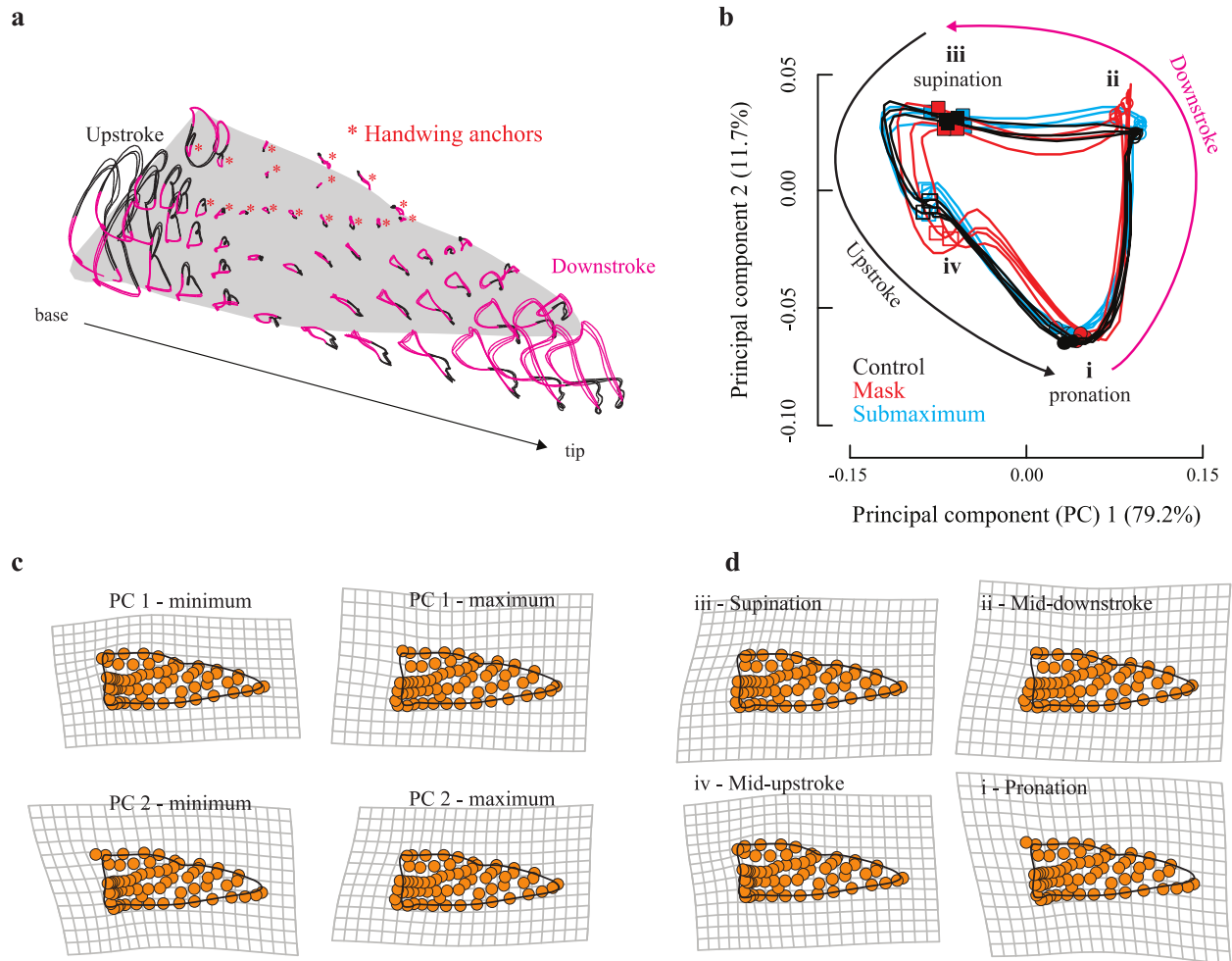


**Figure 3.3** Marker paths through the stroke cycle. **a** The paths of selected wing markers are plotted with respect to handwing markers denoted with a red asterisk. The position of the marker is shown during the downstroke (pink) and during the upstroke (black). Wing tip markers are deflected dorsally during the downstroke, whereas wing base markers are compacted against the body during the upstroke. **b** The complex motions of the markers, and therefore the wing shape, are summarised by geometric morphometric analysis. Instantaneous marker positions are superimposed and differences in shape encapsulated by principal components (PC) analysis. **c** Grid warping that accompanies reconfiguration of the wing from the mean marker positions (black outline) to the marker positions corresponding to the minima and maxima of the PCs (orange filled circles). **d** Grid warping and instantaneous wing configurations at selected times (i-iv) during the stroke cycle (control marker positions shown).

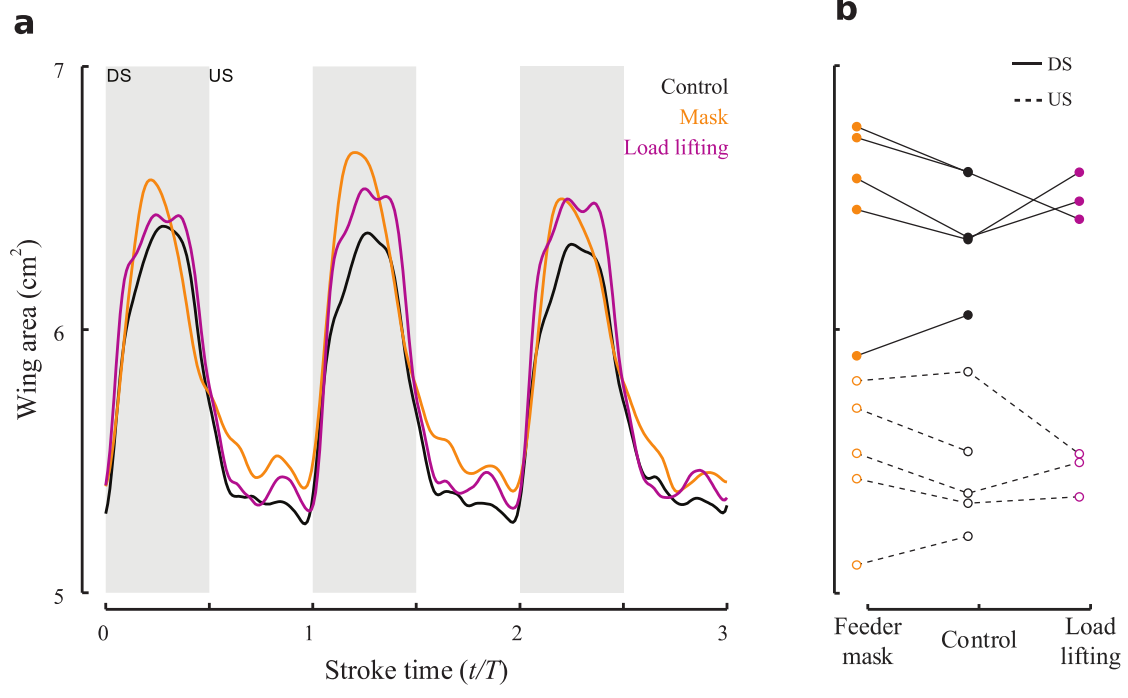


**Figure 3.4** Changes in wing surface area through the stroke cycle and among treatments. **a** Wing surface area was calculated from the 2D wing mesh. Peak downstroke area was in most cases higher while hovering at the mask (**b**).

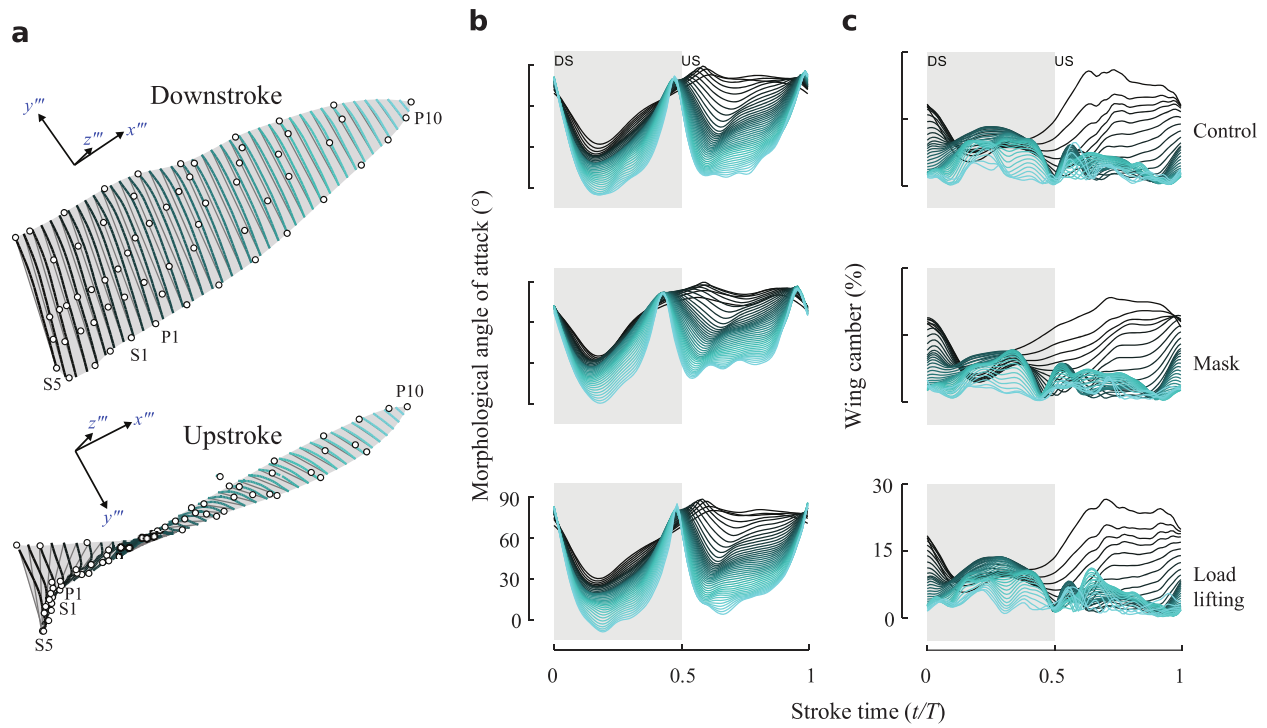


**Figure 3.5** Twist and camber profiles of the wing throughout the stroke cycle. **a** Reconstruction of twist and camber profiles from digitised data (white filled circles). Lines are shaded black to cyan corresponding to wing base to wing tip position (camber lines shaded, twist lines in gray). Representative downstroke and upstroke wing configurations are presented, along with the wing-fixed axes (see Figure 3.1) and the locations of selected primary (P) and secondary (S) feathers. **b,c** Instantaneous morphological angle of attack and camber for each chord line in a. DS, US: downstroke, upstroke.

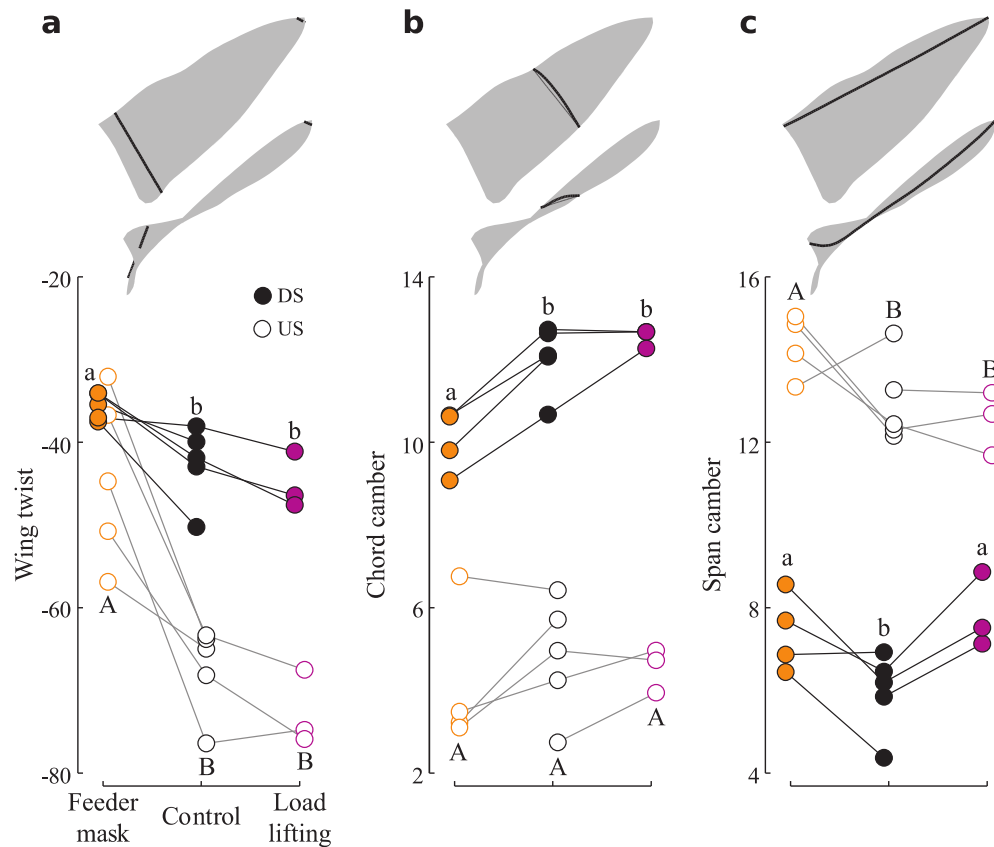


**Figure 3.6** Twisting and cambering of the wing during the downstroke and upstroke. **a** Wing twist is measured by the difference in morphological angle of attack the wing tip to the base (purple lines on wing schematic at left). More negative values indicate more twisting with a lower angle of attack at the base. Moderate twisting is observed during the downstroke, but is very high during the upstroke. Downstroke (dark line, filled circle) and upstroke (light line, open circle) wing twist are greatly reduced while flying with a feeder mask. **b** Hummingbird wings exhibit 10-15% camber along the midspan chord line during the normal downstroke, and substantially less (<7%) during the upstroke. Downstroke camber is significantly reduced with a feeder mask. **c** Spanwise camber (orange line in wing schematic) was measured along a line starting at a point lying at 95% of the base chord length and extending to the wing tip. Spanwise camber occurs throughout the stroke, and is greater in the upstroke than downstroke, but significant increases are observed only during the downstroke.

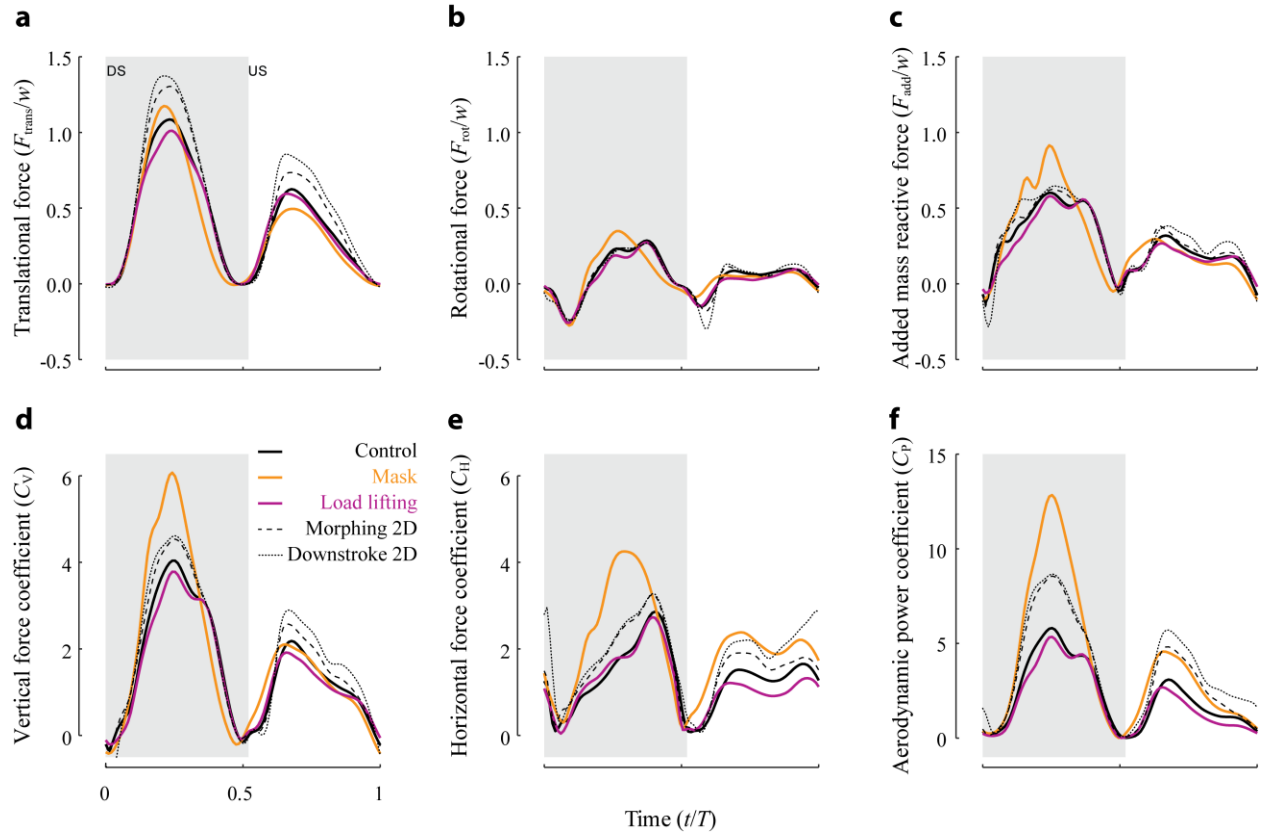


**Figure 3.7** Force and power profiles of real and simulated wings. The total force predicted by blade element modelling normalised to body weight was decomposed into translational (a), rotational (b), and added mass reactive (c) components. In each case, we examine the force profiles during the three flight conditions and compare these to simulated flat wings actuated with kinematics recorded in the control condition. Total force was used to calculate the force coefficients in the vertical (d) and horizontal (e) directions, and the aerodynamic power coefficient (f).

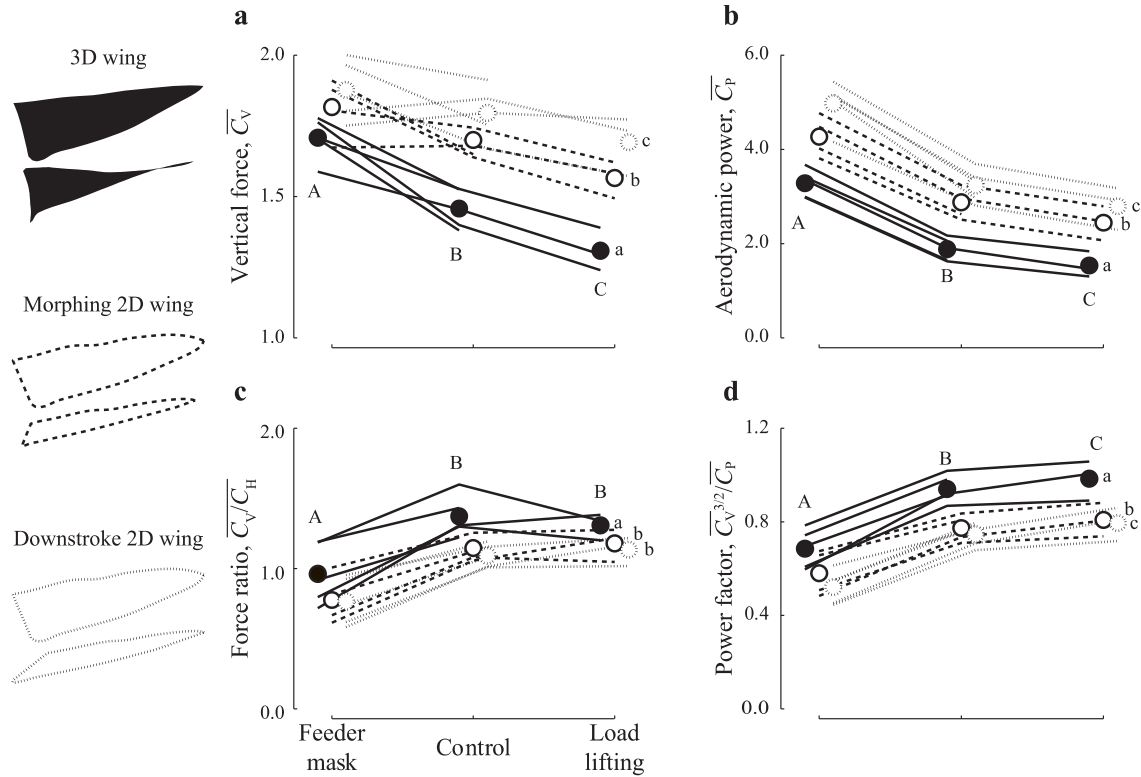


**Figure 3.8** Aerodynamic performance of real and flat plate model wings. **a** Vertical force coefficient of real 3D (black), morphing 2D (orange), and downstroke 2D (pink) wings. Real wings were reconstructed during normal (control) hovering flight, in front of a feeder mask, or while load lifting. Force coefficients decline across treatments, coinciding with reduced stroke amplitude. In all treatments, morphing (changing area) 2D wings exhibit higher force coefficients than real wings, and downstroke-modelled wings exhibit higher force coefficients than morphing 2D wings. **b** Power coefficients are highest at the feeder mask and lowest during load lifting, but lowest in real wings and highest in downstroke-modelled wings. **c** Flight at the mask or with flat wings results in a large increase in horizontal forces and a reduction in the ratio of vertical to horizontal force coefficients. **d** Flight at the mask or with flat wings results in reduced flight efficiency, as measured by reduced power factor.

**Table 3.1** Mean and standard deviation for selected kinematic parameters in Chapter 3. Each measurement is given with its units. Statistical significance is denoted by †:  $0.05 < p < 0.10$ , \*:  $0.01 < p < 0.05$ , \*\*  $0.001 < p < 0.01$ , \*\*\*  $p < 0.001$ . Morph. AoA = morphological angle of attack. Aero. AoA = aerodynamic angle of attack.

	<b>Mask (SD)</b>	<b>Control (SD)</b>	<b>Submax (SD)</b>
<b>Stroke amplitude (°)</b>	83.42 (4.15) ***	129.38 (9.40)	149.97 (10.93) **
<b>Stroke frequency (Hz)</b>	54.26 (3.96) ***	41.37 (1.71)	39.80 (2.21)
<b>Stroke plane angle (°)</b>	12.29 (3.96) ***	6.13 (2.03)	2.63 (2.32)
<b>Morph. AoA (°) (downstroke)</b>	27.44 (6.65) *	20.72 (4.69)	19.87 (6.67)
<b>Morph. AoA (°) (upstroke)</b>	56.12 (5.36) ***	40.52(4.58)	33.77(3.85)†
<b>Aero. AoA (°) (downstroke)</b>	49.80 (3.14) ***	36.79 (3.08)	33.86 (4.54) *
<b>Aero. AoA (°) (upstroke)</b>	41.00 (5.29) **	32.339 (2.34)	29.17 (1.77)
<b>Duty cycle</b>	0.52 (0.02) †	0.51 (0.01)	0.50 (0.01)
<b>Weight support (<math>F_v/W</math>)</b>	0.66 (0.06) **	0.74 (0.04)	0.64 (0.02) **

## Chapter 4: Conclusion

The objective of this thesis was to explore interspecific, intraspecific, and intraindividual contributors to the performance envelope in hummingbirds. I first examined the evolution of the hummingbird flight performance envelope (Chapter 1) through a robust allometric framework to integrate form, function, and ecological context (Chapter 2). I found evidence supporting the hypothesis that hummingbirds evolve toward constant wing loading (constant wing area/body weight), which minimises hovering costs and maximises burst flight capacity. I next examined how the bounds of the flight performance envelope are determined at an individual level by dynamic control of wing geometry (Chapter 3). I developed experimental and analytical methods to reconstruct the wing surface during flight challenges, and found that hummingbirds prioritise efficiency over upstroke weight support, but can sacrifice flight efficiency if it helps accomplish a goal. A persistent question in biomechanical evolution has been why differences in propulsor shape (wings, fins) evolve when even small variations in kinematics have a larger effect than large changes in shape [such as aspect ratio: JW Bahlman in (Middleton and English, 2015), see also (Borazjani and Daghooghi, 2013)]. Taking the results of this thesis together, I propose that this apparent paradox can be resolved if even subtle evolution of wing size and shape shifts the center of the performance envelope to coincide with species behaviours (Figure 1.1). Even where the performance envelope among species greatly overlaps, evolution of wing size and shape simultaneously maximises flight performance at the mean species body size and maximises the individual potential for kinematic variation within the envelope.

In the following, I will discuss four major questions arising from these analyses: (1) What drives body size evolution in hummingbirds? (2) How do hummingbirds adapt to montane

habitats? (3) Is there an allometry of biomechanical innovation? (4) Can the force allometry approach guide other allometric studies?

#### 4.1 What drives body size evolution in hummingbirds?

Allometry is classically interpreted as a systematic trait change accompanying evolution or development from a small to large body size, i.e., *scaling up*. This is the argument of Chapter 2, and explicated in Figure 4.1: if the smallest species is scaled to the size of largest species by extrapolating from the intraspecific exponents, the larger species winds up with undersized wings, excessively high wing velocity, and little or no burst force capacity. Implicit to this explanation is that selection acts to increase body sizes (Heim et al., 2015; Kingsolver et al., 2004), and so hummingbirds are evolving from a smaller ancestor. Conversely, what if we *scale down* from the largest species to the smallest? Then, the intraspecific scaling exponents yield relatively large wings, lower wing velocities and, by the logic of Chapter 2, much greater burst capacities than actually observed (Figure 4.1). One possibility is that such large wings would increase body weight and be costly to accelerate, so selection would favour reducing wing size back to an aerodynamic optimum, and this gradient could result in the observed allometry. The selective forces that apply to wing shape thus are dependent on the direction of body size selection, but force allometry predicts the consequences, not drivers, of changes in body weight. I will next present evidence that hummingbirds are generally shrinking, and explore the contribution of a more nuanced hypothesis of maneuverability than presented in Chapter 2.

Does evolution favour large individuals, or small? It has been proposed that larger individuals and larger species are typically favoured, called Cope's rule (Heim et al., 2015; Kingsolver et al., 2004; Morgado and Günther, 1998). In nearly 80% of documented cases of

selection related to morphology, linear selection gradients for survival, fecundity, and mating success favour larger body sizes, but are neutral for other morphological traits (Kingsolver et al., 2004). However, the influence of individual-level selection on macroevolutionary patterns like Cope's rule is unclear. For instance, in dragonflies, size and fitness are positively correlated, but there is no trend of body size evolution over 60 million years (Waller and Svensson, 2017). Selection for increased body size might not be the case in hummingbirds. Although specific power costs (Chapter 2) and specific daily energy expenditure (Fernández et al., 2011) are independent of body mass, they nonetheless increase in absolute terms. Consequently, a given flower patch has less of the dietary energy required for larger body sizes. This creates a behavioural and physiological conflict between feeding and breeding territory holding, and energetic requirements, which is then exacerbated when large groups of birds create wide denectarisation zones (Stiles and Wolf, 1979). Smaller body sizes can therefore be advantageous due to the greater availability of floral resources, which enables a wider variety of highly energetic behaviours.

Size reduction in the hummingbird lineage may have already begun well prior to the hummingbird split from the swifts (Ksepka et al., 2013), and then continued in the stem hummingbirds (Mayr, 2004). *Jungornis* and *Eurotrochilus*, the European ancestors of hummingbirds, were estimated to be larger than the current hummingbird average [(Bochenski and Bochenski, 2008; Mayr, 2003; Mayr, 2004), *Jungornis* > *Eurotrochilus*]. To examine evolutionary trends in body weight among hummingbirds, I performed an ancestral state reconstruction of body weight, shown by a phenogram (traitgram) in Figure 4.2. Body weights at internal phylogenetic nodes were reconstructed with measurement errors assuming a multivariate Ornstein-Uhlenbeck process with body weight, wing area, and lifted mass, where the last

variable is included to model correlated evolution of form and function [*Rphylopars*: (Goolsby et al., 2017)].

Remarkably, the reconstructed body weight at the root of crown Trochilids (a hypothetical ancestor) corresponds very closely to the estimated size of the oldest known stem hummingbird, *Eurotrochilus* [‘about the size of the extant rufous-breasted hermit *Glaucis hirsuta*’ (Mayr, 2004), ~6.9 g]. Subsequent splits among the major hummingbird clades are estimated to have occurred before any substantial divergence in body weight, as represented by selected nodes on the tree. Depending on the statistical model, hummingbird shrinkage appears to have accelerated 10-15 million years ago [additive model of internal node reconstructed weights versus age, *mgcv*: (Wood, 2004)], particularly with the rapid radiation of the Bee clade (blue branches, Figure 4.2). The median weight of all extant measured hummingbirds (5.4 g) is less than the estimated mass of the ancestor, and the median weights of the major clades are less than or about equal to the estimate of *Eurotrochilus* (Figure 4.2). This suggests that there has indeed been shrinkage in the hummingbirds, potentially accelerated by diversification into an unexploited vertebrate niche. The large ancestor does not support the implied mechanism of Chapter 2 that wing allometry is driven by hummingbirds’ having scaled up, but instead suggests they have scaled down. Although this analysis is suggestive, estimation of ancestral states may be biased by factors such as higher extinction risk among larger taxa (Bennett and Owens, 1997; Gaston and Blackburn, 1995), to which hummingbirds might be at risk due to low fecundity and dependence on specific habitats.

If acrobatic flight performance underlies selection in hummingbirds, then the trend toward smaller species size in Figure 4.1 would be consistent with processes in other volant taxa. Among species of shorebirds, gulls, and alcids (Charadriiformes) acrobatic sexual displays are

correlated with reduced body size in males (Székely et al., 2000). Similarly, among some bats, smaller male body size is correlated with greater reproductive success (Voigt, 2000), possibly due to increased energetic efficiency and maneuverability [(Stockwell, 2001; Voigt et al., 2005), although bat ecomorphological relationships are often unclear due indirect aerodynamic and morphological measures, and reliance on aircraft theory, (Swartz et al., 2006)]. Polygyny is also associated with larger males in Charadriiformes (Székely et al., 2000), but male hummingbirds generally do not provide parental care (Chapter 1), so this is unlikely to be a large force in hummingbird evolution.

Sexual selection also impacts the extent of morphological dimorphism within species. Evolution of body size follows from the intensity of sexual displays or combat. When sexual competition is intense but males are not very agile, males evolve to be proportionately much larger than females (Székely et al., 2004), suggesting an inherent advantage of large body size in physical confrontation. Conversely, when competitions are fierce but males are highly agile, males tend to evolve smaller body sizes, which is proposed to be advantageous for maneuvering flight. This pattern is suspected to explain why Charadriiformes adhere to Rensch's rule, the macroevolutionary trend that in clades exhibiting male-biased sexual dimorphism, the relative difference in body size between the sexes increases with male body size. The divergence in sexual size dimorphism is proposed to derive from strong selection on male body size, and weak, correlated selection on female size (Székely et al., 2004). Like Charadriiformes, hummingbirds exhibit the full range of Rensch's rule, suggesting that sexual displays and behaviours may similarly underlie selection on hummingbird body size (Colwell, 2000).

The prediction based on evolutionary patterns in other flying taxa is that acrobatic displays should be favoured in small hummingbird species, whereas larger species should be less

agile. [Some authors distinguish maneuverability (space for turning) and agility (time for turning), but these do not appear to be widespread definitions, and I use the terms synonymously; contrast e.g., (Hedrick et al., 2009; Norberg and Rayner, 1987).] This hypothesis appears to be at odds with the proposal of Chapter 2 that maneuverability is conserved by wing area evolution, which was developed by drawing on free-flight studies suggesting that burst forces best predict flight performance (Segre et al., 2015; Sholtis et al., 2015). However, there is no conflict because two forces are acting on agility: burst forces from the muscle, and frictional damping. The frictional damping arises from the wing motions, which in the case of *Drosophila* is 100× larger than friction on the body alone (Hesselberg and Lehmann, 2007). Thus, wing evolution may enable one aspect of maneuverability, but constrain another.

I investigated the possibility that agility is negatively correlated with body size by examining the scaling of frictional damping in hummingbirds. Frictional damping is a form of stability, acting to force a body back to a constant position (e.g., a heavily-damped oscillator). Flight stability is a function of wing dimensions, and although stability can be desirable, such as pendulum stability of the body conferred by a center of mass below the stroke plane, stability is inherently in opposition to maneuverability. Flapping counter torque,  $\dot{\omega}_{FCT}$ , is a rotational moment that arises passively from flapping motion,  $\Phi f$ , and resists turning capacity in all planes [here we consider yaw rate,  $\omega$ : (Cheng et al., 2010; Hedrick, 2011; Hedrick et al., 2009)],

$$\dot{\omega}_{FCT} \propto \frac{-\rho\omega R^3 S \Phi f}{I}$$

The expression is simplified by dropping nondimensionalised terms, and assuming the mean chord width is equal to wing area/wing length. Among widely varying taxa, Hedrick et al. assumed isometry of wing length  $R \propto W^{1/3}$ , surface area  $S \propto W^{2/3}$ , and moment of inertia  $I \propto$

$W^{5/3}$  (Greenewalt, 1962; Pennycuick, 1990). Among hummingbirds, though,  $R \propto W^{1/2}$ ,  $S \propto W^1$ ,  $I \propto W^{7/3}$  [estimated here for wing inertia imputed for all individuals in Chapter 2].

Substituting these exponents and those of Chapter 2, we observe that among species,

$$\dot{\omega}_{FCT} \propto -\omega W^{\frac{3}{2}} W^1 W^0 W^{-\frac{1}{2}} W^{-\frac{7}{3}} = -\omega W^{-\frac{1}{3}}$$

In a similar manner, the magnitude of active torque an animal must deliver to counter a body rotation is,

$$\dot{\omega}_a \propto (\gamma - 1) \frac{\rho R^3 S (\Phi f)^2}{I} = (\gamma - 1) W^{\frac{3}{2}} W^1 W^0 W^{-1} W^{-\frac{7}{3}} = (\gamma - 1) W^{-\frac{5}{6}}$$

where  $\gamma \in [0,1]$  is the flapping amplitude asymmetry between the wings during the maneuver [ $\gamma=0.944$  and assumed constant among species in (Hedrick et al., 2009), although stroke amplitude is not the sole mechanism for active torque generation in flapping flight: (Read et al., 2016; Ristroph et al., 2010)].

The respective allometric predictions suggest that active and passive torque mechanisms decrease with increasing species body weight, but not proportionately. The ratio of the torques reflects the capacity for active maneuvering (Hedrick et al., 2009),

$$\frac{\dot{\omega}_a}{\dot{\omega}_{FCT}} = \frac{-(\gamma - 1)}{\omega} W^{-\frac{1}{2}}$$

Based purely on scaling relationships, we therefore predict that the evolution of large wings comes at an increasing cost to aerial maneuverability even greater than that predicted by isometry, which is only  $W^{-1/3}$ . A decline in this measure of flight performance contradicts the hypothesised constant performance based on constant load factors among species Chapter 2. This suggests there are allometric trade-offs between minimising induced power costs, maximising maneuvers based on burst forces (Segre et al., 2015; Sholtis et al., 2015), and maximising

maneuvers based on torque modulation. How this has impacted the evolution of hummingbird flight remains to be determined, especially the influence of maneuvers dependent on  $\gamma$ , the flapping asymmetry. Amazingly though, because the intraspecific increases in wing lengths and areas are actually less than isometry and  $I \propto W^{4/3}$ , the same calculation within species predicts that  $\frac{\dot{\omega}_a}{\dot{\omega}_{FCT}} = W^0$ . This scaling method therefore predicts torque maneuvers are independent of size within species, whereas force-based maneuvers were found to be independent of size among species. The range and type of maneuvers exhibited within and among species may thus diverge, leading to evolution of the performance envelope (Chapter 1).

The predicted allometry of maneuverability bears on size evolution of hummingbirds and the paradoxical implications of Figure 4.1. To understand the predicted performance consequences of intra- and interspecific allometries, I plot the predicted impact on maneuverability of selection on body weight (Figure 4.3). In both allometric models, larger body size always leads to declining overall flight performance. Along the static (intraspecific) allometric trajectory, load factor declines but torque ratio is constant, and along the evolutionary (interspecific) allometric trajectory, load factor is constant but torque ratio declines. Conversely, smaller body sizes always lead to increased overall flight performance. Along the static allometric trajectory, load factor increases but torque ratio is constant, whereas along the evolutionary allometric trajectory, load factor is constant and torque ratio increases. A startling result is that according to the isometric model, flight performance measured by either criterion always declines with increasing body size. It is always better to follow one of the two allometric models than to grow or evolve isometrically, which may explain the prevalence of allometry in other groups of birds (Nudds, 2007; Rayner, 1988) (Chapter 1).

According to Figure 4.3, if there is any selection on flight performance in hummingbirds, then we should expect correlated reduction in body size (Hedrick et al., 2009; Székely et al., 2000). Both the static and evolutionary allometries predict constant or increasing performance with decreasing size. The evolutionary allometric strategy predicts larger overall gains in performance, but the static allometric strategy has a second benefit of predicting reduced power costs. Induced, profile, and inertial powers are all predicted to be greater under evolutionary allometry than static allometry (exponents in Chapter 2). It may be that the fitness benefits of maneuverability compensate for increased power, combined with a longer time to denectarise a flower patch in smaller birds. Resolving this will require better models of power, including the influence of wing inertia on hummingbird flight (Song et al., 2015a; Wells, 1993a), and the contribution of factors such as surface roughness in minimising profile power (Bokhorst et al., 2015; Kruyt et al., 2014). However, these are only the contributions to hovering power, and accounting for the contribution of power will need to take into account factors such as the dissipative loss that will accompany higher frictional damping. The latter suggests a way in which the power costs across all behaviours can still be less under the evolutionary allometry trajectory.

Overall, I propose that the combination of energetics and territoriality creates a downward pressure on hummingbird body size, as predicted by the ancestral character reconstruction (Figure 4.2). A model of hummingbird evolution giving rise to the observed interspecific allometry is shown in Figure 4.4. Different factors contribute to the direction of selection for larger or smaller body sizes (Kingsolver et al., 2004; Székely et al., 2000; Székely et al., 2004). Because evolution along the intraspecific regime results in wings that are too small or too large, selection is proposed to act through different proximate mechanisms (e.g.,

efficiency or turning ability) to restore wing areas to a constant wing loading (body weight/wing area). This hypothesis explains a gap in Chapter 2: energetic efficiency could explain the allometry of wing area, but not why hummingbird wings are overall smaller than expected for a similarly-sized non-hummingbird (Chapter 1). Selection for smaller body sizes and correlated selection for constant wing loading is expected to result in the observed allometric exponent and in a steep decrease in wing area of hummingbirds relative to non-hummingbirds of the same size.

The hypothesis is contingent on behaviour as the agent mediating the relationship between body and wing size, so different behavioural strategies that influence energy balance should result in different patterns (Feinsinger and Colwell, 1978; Feinsinger et al., 1979; Stiles, 2008). A natural experiment was proposed in Chapter 2, in which the Bee hummingbird clade may not be exhibiting the extreme wing allometry of the other hummingbird clades, so it may be diversifying under a different set of constraints. Deviation from the allometric strategy presented in Chapter 2 would suggest that Bee flight performance should be compromised, surprising given their intense territoriality [e.g., (Kodric-Brown and Brown, 1978; Stiles, 1971)]. On the other hand, the Bees are small and diversifying through the reinvasion of North America, essentially in the absence of the intense interspecific resource conflict that defines the South American, Caribbean, and Central American clades (Feinsinger and Colwell, 1978). The scaling of flight performance (Figure 4.3) suggests that the Bee allometric strategy is still favourable for smaller species, and can take advantage of the power benefits noted above. Further work in the Bee clade, which must emphasise members outside North America, should be highly revealing. More generally, the processes discussed here rely on extrapolation to species and individuals that do not exist (as critiqued in Chapter 1), and so direct comparisons of maneuverability among and within species are imperative.

A final observation is that the scaling of maneuverability could help explain a long-standing puzzle in hummingbird biology: why is *Patagona gigas* not only ten times the size of the smallest species, but nearly double the size of some of the next largest species? An energetic limitation on hummingbird body size is unlikely (Chapter 2) (Fernández et al., 2011), and I suggest that maximum body size is instead behaviourally limited. The combined constraints of hummingbird behaviour (Chapter 1), energetic efficiency (Chapter 2), and adverse allometry of flight performance (Figure 3) means there simply is not a favourable selective gradient toward larger body size generally (Figure 4.2) and such an extreme body size specifically. *Patagona*'s maneuverability is predicted to be compromised by the adverse scaling of passive frictional forces, and as agility decreases while conflict intensity is high, larger body sizes are favoured (Székely et al., 2004). *Patagona* should therefore be driven to larger body size as well, and its territorial chases (Altshuler, 2006) may rely less on maneuverability than pure intimidation. For this to be effective, absolute differences in body size are vital, because only large relative differences among species predict the winners of territorial interactions (Stiles and Wolf, 1979). This seems to be due, at least in part, to smaller species' reticence to engage a visibly bigger opponent (Dearborn, 1998). *Patagona* is therefore highly behaviourally and biomechanically specialised, which I suggest explains its uniqueness. This explanation relies on interspecific conflict as a major driver of body size evolution, which may be reasonable in hummingbirds that compete over floral resources regardless of species. Intraspecific drivers of body size evolution may be present as well.

## 4.2 How do hummingbirds adapt to montane habitats?

Abiotic ecological context is a critical factor in hummingbird evolution (Chapter 1). It has been suggested that colonisation of high altitudes did not come without a cost: as more energy is expended on weight support, less is available for burst performance (Altshuler et al., 2004c). Decreased air density is clearly detrimental to individual performance (Altshuler and Dudley, 2002; Segre et al., 2016), so the lack of compensatory evolution to restore performance is surprising. Altshuler et al. (Altshuler et al., 2004c) proposed that the decreased air density favoured evolution of larger body sizes and isometrically larger wing areas. This mechanism could be consistent with a selective benefit for larger males when there are intense but low-agility competitions (Székely et al., 2004). Conversely, I found that the association between species body weight and air density (elevation) is not robustly supported (Chapter 2). An older study also reported hummingbird morphological evolution consistent with longer wings at higher altitudes, but with a much smaller sample size and less robust analytical techniques [(Feinsinger et al., 1979), no phylogenetic control and conclusions based on wing disc loading, see critiques in (Altshuler et al., 2004a)].

To probe hummingbird adaptations to high altitudes, I develop an exploratory statistical method based on network analysis to address correlated biomechanical evolution of many parameters, including the role of air density (de la Fuente et al., 2004; Nagarajan et al., 2013; Scutari and Nagarajan, 2013; Shipley, 2000). This method fills a gap in the force allometry technique, which can only consider a convex (sum to 1) combination of variables that depend on body weight. The method therefore does not address coevolution and correlation among parameters. The basis of the analysis is that if there is a path diagram that intuitively relates parameters, we can find a statistical approximation of this diagram based on quantitative

relationships among parameters (Dale et al., 2015; Shipley, 2000; Shipley, 2004). The end result of the analysis is a set of edges (links) between pairs of variables that are more direct than can be explained by covariation with any other variable in the study.

In a basic example, we first test the significance of the zeroth-order relationship between wing area and air density; the set of all zero-order relationships is a correlation matrix (de la Fuente et al., 2004). We then test significant zero-order associations to first-order, such as whether the association is robust to covariance with either body weight or wing length; a common first-order analysis is the method of correlating body mass residuals, though the current method both generalises this approach to all residuals, and is more visual [e.g., compare to matrices in (Clark and Keith, 1989; Rezende et al., 2009)]. We can then test second-order and higher relationships (up to the number of variables minus two), such as whether the association of wing area and air density is robust to covariance with both weight *and* wing length. Where an edge in the final network is missing, any apparent correlation is either explained by an intermediate variable, or arose by random chance (5% of all correlations) and was not robust to multiple regression. Testing all orders of correlations in sequence has theoretical merit (de la Fuente et al., 2004; Shipley, 2000), but also a practical advantage of minimising statistical power loss for every increase in order [not all possible regressions must necessarily be performed because second-order can be sufficient even for bioinformatic applications, (de la Fuente et al., 2004)]. However, the method is conservative: as the number of variables is increased, the probability of rejecting true associations increases, specifically if the correlations are weak and the study design is unbalanced [type II error, (de la Fuente et al., 2004)]. I do not attempt to direct any of the resulting edges, and rely on biomechanical inference instead. Second-order links among- and within-species were examined through a modified version of the phylogenetic

comparative method of Chapter 2 [uninformative priors, each edge tested with three chains of 75,000 posterior samples and a 25,000 sample burn-in period; *MCMCglmm* (Hadfield, 2010), *pcalg* (Kalisch et al., 2012)].

The graphical approach to hummingbird integrative physiology supports the finding of Chapter 2 that the correlation between body weight and air density (elevation) is not robust (Figure 4.5). Among species, there is no direct link between body weight and density: air density is instead positively associated only with increased wing area. A second important result is that among-species variation in air density is correlated with burst force only when we control for the intermediate effects of wing area and length. Thus, evolution of larger wings at high altitudes supports body weight and maximises burst performance by maintaining constant wing loading, as predicted from the processes predicted from Chapter 2. Wing evolution explains why species perform best in their adapted altitudes (Altshuler, 2006). As in Chapter 2, stroke amplitude is independent of any other parameter among species, contrary to a previous analysis that found stroke amplitude increases at higher elevations (Altshuler and Dudley, 2003). However, the finding is consistent with a hypothesis of stabilising selection on intermediate stroke amplitudes which are high enough to avoid significant unsteady effects (Altshuler et al., 2005; Song et al., 2014), but low enough to enable maneuvering through stroke amplitude modulation. Together, this analysis predicts that there is no direct effect of reduced air density on among-species flight performance (as indicated by load factors).

The network of associations within species is very different from that among species (Figure 4.5). Crucially, and in contrast to the picture among species, body weight is positively associated with elevation (negatively with air density), and hovering stroke amplitude must increase to compensate, resulting in reduced capacity to modulate amplitude for performance

(Altshuler and Dudley, 2003; Chai and Dudley, 1995). Independently of any measured parameter, body weight is positively correlated with burst force, which likely coincides with a direct influence of relative muscle mass (Marden, 1994; Segre et al., 2015). However, numerous competing paths contribute to individual burst capacity, and the complicated web may explain why previous studies using conventional statistical models had difficulty disentangling the effects of morphology and muscle power (Segre et al., 2015). Body weight is positively associated with wing area, but larger wings have positive and negative influences on burst force through greater wing lengths and lower stroke frequencies, respectively [equal and opposite trends mask apparent relationships, (Skandalis and Darveau, 2012)]. In sum, comparing the among- and within-species networks supports the hypothesis that decreased air density is detrimental to individual performance and results in compensatory evolution among species (Figure 4.5).

A noteworthy feature of the hummingbird networks from a graph-theoretic perspective is the simplification that accompanies the transition from within- to among-species graphs. Many of the relationships revealed within species must be considered constraints, such as the need to increase stroke amplitude to support body weight in lower air densities, reducing performance. Among species, this constraint is alleviated by compensatory evolution of wing area, and restoration of mean species performance. I suggest that a graphical hypothesis of functional evolution is therefore the unblocking of biomechanical constraints and opening of ecological opportunities (Chapter 1). Many factors are missing from Figure 4.5, such as the motivating variables of energetics, force coefficients, and passive damping. This is because, like multiple regression generally, the graphical method strictly admits independent variables, which is violated by inclusion of variables that are composite functions of other variables.

### **4.3 Is there an allometry of biomechanical innovation?**

How much greater understanding into hummingbird evolution is gained by a comparative knowledge of complex biomechanical parameters such as wing morphing capacity, compared to an easily-measured factor like wing loading? A general problem in biomechanics is describing biomechanical complexity and integrating it into a comparative framework. A catch-all variable of biomechanical innovation was incorporated into the force allometry framework through the force coefficient. Formally, a dimensionless variable cannot scale because it is itself a determinant of dynamic scaling (Buckingham, 1914). In the allometric framework, scaling is a descriptive measurement of trait modifications that accompany changing body size, and so dimensionless variables can take on a broader meaning. Whereas dimensional variables indicate changing form, dimensionless variables can indicate changing function. Change in aerodynamic dimensionless coefficients with body size has been suggested in other cases. For example, allometry of the lift coefficient in bats (below), or allometry of the yaw stability coefficient to ensure fast responses to perturbations (Sachs, 2005). In this section, I explore the extent to which it is known that function, not just form, can evolve with increasing body size.

#### **4.3.1 Functional evolution in bats**

Evolution of function is proposed to be a substantial contributor to the demands of weight support and flight performance in bats (Riskin et al., 2010). Riskin et al. performed a comparative analysis of parameters contributing to weight support (Chapter 2), but also dynamic morphological and postural parameters such as wing camber and angle of attack (Chapter 3). The analysis was focused on accepting or rejecting isometric predictions (i.e., null hypothesis tests)

based on tests through phylogenetic generalised least squares (PGLS) or reduced major axis [RMA, critiqued in, e.g., (Smith, 2009)]. The tests give very different predictions as to the factors that are crucial in bat flight evolution.

The first important isometric prediction is that forward flight speed depends on body weight. On the basis of the force equation (Chapter 2), it has been proposed, and tested numerous times, that flight speed should increase among species according to the isometric prediction  $W^{1/6}$  (Alerstam et al., 2007; Rayner, 1988; Riskin et al., 2010). This prediction results from treating flapping flight as equivalent to fixed-wing aircraft aerodynamics so that the velocity,  $U$ , in the force equation represents flight speed. This is not the case, and the characteristic velocity in the force equation is the absolute wing tip speed  $U \approx \sqrt{U_\infty^2 + U_{\text{tip}}^2}$ , where  $U_\infty$  is the body speed and  $U_{\text{tip}}$  is the wing tip speed in the body-fixed reference frame (Chapter 2) (Lentink and Dickinson, 2009b). Thus, there is no isometric prediction of flight speed, only wing tip speed overall, but increasing flight speed does contribute to weight support for the same flapping velocity. [This error likely explains why other hypothesised constraints, such as maximum range or minimum power migratory flight speeds (Pennycuick, 1969), have had little predictive success (Irschick and Garland, 2001).] In bats, RMA suggests positive allometry of flight speed, but PGLS suggests it is size-invariant.

The second important test is a direct assessment of the allometry of the lift coefficient. RMA suggests the lift coefficient is size-invariant, but PGLS supports a substantial allometry, as  $W^{0.17}$ . The positive allometry of the lift coefficient appears to be principally traced to changes in wing posture with increasing body weight, such as angle of attack. RMA also suggests that larger downstroke:upstroke ratios may contribute. PGLS also suggests wing stroke period (1/stroke

frequency) increases with body size, but less than predicted by isometry, which indicates increasing wing velocity. On the whole, our view of comparative bat kinematics and functional evolution therefore greatly depends on which statistical method is used. PGLS is prone to measurement errors and phylogenetic uncertainty, (Felsenstein, 2008; Harmon and Losos, 2005; Ives et al., 2007; Ricklefs and Starck, 1996), but RMA is not a reliable method when variables have asymmetric errors or are phylogenetically correlated (Ives et al., 2007; Smith, 2009).

To discern which set of predictions might be more reliable, I applied the force allometry principle as a diagnostic of the exponents calculated by Riskin et al. Force allometry predicts a wide divergence in the reliability of each statistical method. The RMA and PGLS methods respectively predict weight support of  $W^{1.02}$  and  $W^{1.31}$ , based on the allometry of minimum wing length in flight, or  $W^{1.08}$  and  $W^{1.42}$ , based on maximum wing length. (The estimated wing velocity does not include flight speed, which could not be examined because the exponents of body and wing velocity cannot be added.) The PGLS estimate is therefore substantially biased. The close agreement of the RMA method to the  $W^1$  summation constraint reinforces the utility of force allometry for assessing the reliability of derived exponents, and supports the use of force allometry in non-hovering conditions and with morphing wings. Rejection of the PGLS method substantially alters our interpretation of comparative bat kinematics. The RMA analysis does not uphold a substantial contribution of the lift coefficient to weight support ( $W^{0.05}$ ), but does support the increased angle of attack and flight speed. Bat flight therefore does not appear to require any substantial biomechanical innovation at larger sizes, in the sense of more lift being generated for the same morphology and kinematics. The function of the change in angle of attack is less clear than in the original analysis, but could compensate for changes in wing shape, such as a tendency

toward positive allometry of aspect ratio, or other effects due to variation in skin material properties (Swartz et al., 2006).

The best current evidence is thus that among bats, increasing weight support is provided by positive allometry of wing area (compared to the isometric prediction), balanced by increasing wing velocity. This accords well with a substantial literature pointing to wing loading (wing area/weight) as a key factor in bat ecomorphological divergence (Stockwell, 2001). However, dynamic control mechanisms are recruited to execute flight behaviours. To increase flight speed, bats consistently reduce wing cambering, lift coefficient, and stroke plane angle, whereas they increase angle of attack and decrease stroke plane angle for horizontal accelerations, and increase lift coefficient for vertical accelerations. An interesting test will be to examine if the recruitment of postural changes just to support body weight constrains the range of kinematics that can be called on to execute maneuvers at larger body sizes. It seems likely that bats increase camber to enhance lift at low air speeds (Muijres et al., 2008; Swartz et al., 1996), which suggests that the cambering found in Chapter 3 might also be a mechanism hummingbirds specifically use while hovering but reduce in forward flight. Overall, these results support my hypothesis of hummingbird evolution: evolution of wing size establishes mean intraspecific flight performance whereas evolution of dynamic wing control expands the flight performance envelope.

#### **4.3.2 Functional evolution of adhesive pads**

A conceptually nearly identical model to force allometry was applied by Labonte et al. (Labonte et al., 2016) to study the allometry of adhesive area in adhesion-based climbing animals. Animals adhere to surfaces through pads that vary in surface area and adhesive

efficiency, and increasing weight support must be provided by some, possibly clade-specific combination of both. Adhesive forces are therefore another model system to investigate the evolutionary contributions of changes in geometry and biomechanical novelty. Applying the force allometry logic, Labonte et al. relate body weight,  $W$ , to the adhesive force,  $F$ , determined by the product of pad area,  $A$ , and adhesive stress,  $\sigma=F/A$ .

$$F = W^1 = A\sigma = W^\alpha W^\beta$$

and  $\alpha + \beta = 1$ , as in Chapter 2. The functional innovations represented by adhesive efficiency are analogous to the innovations in the wing represented by the force coefficient in Chapter 2, but the stress is a dimensional measurement.

The predicted contributions to weight support of toe pad area and adhesive stress depends on taxonomic rank. At Class rank and lower, the allometry of pad area is indistinguishable from the isometric null hypothesis of conserved linear dimensions,  $W^{2/3}$ . Labonte et al. only test the allometry of adhesive stress in one frog clade, which supported the predicted allometry of  $W^{1/3}$ , suggesting adhesive efficiency increases with body size through an unknown mechanism (Labonte et al., 2016). Across all Classes (insects, reptiles, amphibians and arachnids), however, pad area allometry is  $W^1$ , suggesting that adhesive efficiency is independent of body size over the size range of all animals. I suggest that a more consistent interpretation is that weight support at the *mean* taxon size can be fully explained by differences in pad area, with evolutionary innovations in adhesive efficiency as species size moves away from the mean. This pattern could arise through independent inventions of adhesion in different groups, and convergence on a constant adhesive stress in the ancestor. A reconstruction of the ancestor size and pad function would be most illuminating (e.g., Figure 4.2).

Although the model is similar to force allometry in Chapter 2, even called ‘force scaling’, it was not formally derived (discussed in detail below), and the authors do not prove their model is sufficient. An example of a potentially missing parameter is the adhesion angle with respect to the surface,  $\theta$ , which modifies the required adhesive force for weight support (angle of attack is an equivalent non-dimensional factor in the lift equation derivation). Where  $\theta$  depends on body size, the summation constraint will no longer be unity, as in some frogs in which larger species have reduced maximum sticking angles (Barnes et al., 2006). To determine how evolution of adhesive properties is influenced by performance requirements, it will be revealing to compare routine and maximum capacities. For instance, some groups may exhibit size-invariant maximum adhesive stress, in which case a reliance on adhesive stress for weight support will result in a negative allometry of reserve adhesive strength.

### 4.3.3 Functional evolution of leaf flexibility

A framework based on the force equation was also used to identify the functional consequences of leaf reconfiguration with increasing wind speed (Vogel, 1989). Leaf shape is dynamically reconfigured with increasing drag, and so the drag coefficient,  $C_D$ , is not constant, but dependent on wind velocity. To model the nonlinear relationship between drag,  $F_D$ , and wind velocity,  $U$ , among species and leaf designs, Vogel proposed the allometric relationship,

$$F_D = \frac{1}{2} \rho U^{2-E} S C_D$$

where  $\rho$  and  $S$  are air density and leaf projected area, respectively. Although the equation is dimensionally inconsistent except for the isometric condition that  $E=-2$ , it captures two interesting properties of leaf functional (mechanical) morphology. The exponent  $E$  averaged

-0.78, meaning that in general, aeroelastic reconfiguration of leaf shape results in a scaling of  $<U^2$ , but Vogel also identifies an extreme outlier of  $E=1$ , meaning the drag increased as  $U^3$ . It is likely that this outlier corresponds to a different evolutionary strategy for dealing with the effects of drag in a different environment, representing a phylogenetic constraint [see also the constraints of macroalgal shape types, (Boller and Carrington, 2007)]. The leaves reconfigure on highly reproducible lines, indicating that the deformation patterns are an evolving property related to the venation patterns. This suggests an intriguing evolutionary and biomechanical parallel between plant leaves and animal wings, and indeed, leaves and animals can exploit similar fluid phenomena (Lentink et al., 2009). Dynamic morphology may also be driven by a common pressure to minimise drag and thus the probability of breakage (Boller and Carrington, 2007; Lentink et al., 2007; Vogel, 1989).

Vogel's model was refined to properly describe changes in size and shape of flexible organisms, such as macroalgae (Boller and Carrington, 2006; Boller and Carrington, 2007). Macroalgal shape and force coefficients are highly dynamic, a capacity driven by selection for flexibility to support the exploitation of a niche of rocky shorelines subject to intense hydrodynamic forces. The principal result of Boller and Carrington's analysis is that reconfiguration patterns are complex and dependent on major group differences in size and shape, such as blade-like species that are highly compressible and hydrodynamically streamlined, to tree-like species which are the least compressible and least streamlined (Boller and Carrington, 2007). A next step would be to understand how algae diverge within these major groups, and whether the evolutionary trajectory of flexibility is contingent on inherited features. In general, I suspect many adaptations and constraints will only be understood in the context of the specific forces (fitness) that gave rise to them.

#### 4.3.4 Allometry and estimates of maximum size

A perspective on biomechanical innovation, and therefore evolution in general, is missing from ultimate-cause models that propose a single factor constrains the size or functioning of an entire group of organisms. An ongoing debate has been the physiological factors that limit maximum size for flight. Marden found that maximum aerodynamic force scales isometrically with body mass,  $W^1$ , whereas ideal induced power scaled as  $W^{1.13}$  (Marden, 1987; Marden, 1994), so lift/power decreases as  $W^{-0.013}$ . On this basis, Marden concluded that the body size of flying animals must be limited by the maximum power required to fly, probably about the size of the largest pterosaurs. Ellington (Ellington, 1991) refuted this view by noting that under isometric morphological and kinematic conditions,  $\rho \propto M^0$ ,  $v^2 \propto M^{1/3}$ ,  $S \propto M^{2/3}$ , and  $C_V \propto M^0$ , in which case the isometrically-scaled induced power required for flight is  $W^{7/6}=W^{1.15}$ , so the available and required powers are too similar to be able to predict that power requirements limit flight.

I take a different tack, and ask, why haven't animals developed more efficient wings? The reliance on velocity (flight speed plus wing velocity) for weight support in the isometric model increases force by  $v^2$ , but power by  $v^3$ . Wouldn't it be cheaper to innovate a new wing that generates lift more efficiently, without relying on increasing speed? In the force allometry model, this corresponds to a change in evolutionary strategy from  $v^2 \propto M^{1/3}$  to  $C_V \propto M^{1/3}$ . The implications of such a switch in strategy can be studied through the force and power allometry (Chapters 2). Marden's maximum force measurements were made in takeoff flight, and both Marden and Ellington argued on the basis of an actuator disk model (ideal induced power), so the power factor,  $PF$ , is a more consistent method of equating force and power than the ratio

lift/power (Kruyt et al., 2014). Therefore, the power coefficient (Chapter 3) is,  $C_P = \frac{P}{\frac{1}{2}\rho v^3 S}$ , and

on that basis we can define the power factor,  $PF = \frac{C_V^{3/2}}{C_P}$ . The disadvantage of relying on  $v$

becomes clear from the power factor. Although increasing velocity does increase power output,

$C_V \propto M^0$  and  $C_P \propto W^0$ , resulting in constant power factor. For  $C_V \propto M^{1/3}$ , then  $C_P \propto M^{1/3}$ , and

$$PF = \frac{C_V^{3/2}}{C_P} = \frac{W^{1/3 \cdot 3/2}}{W^{1/3}} = W^{1/6}$$

The potential for a positive allometry of power factor suggests that where energetic efficiency is concerned, there can be a selective pressure for wing innovation. Can animals actually biomechanically innovate in this way, by increasing  $C_V$ ? The lift coefficient is likely restricted to a range of about 0.5–2, [higher lift coefficients are signatures of specific types of high-lift flight, such as hovering, (Hubel and Tropea, 2010; Muijres et al., 2012b; Pennycuik, 1971; Riskin et al., 2010; Tucker and Parrott, 1970; Withers, 1981)]. This range of coefficients across the approximately four orders of magnitude in bird size (Figure 1.3) suggests that the allometric exponent of  $C_V$  cannot be larger than  $\sim 0.04$ . As well, over a large range of body sizes, flying animals tend to converge on similar values of important aerodynamic numbers (Lentink and Dickinson, 2009a; Taylor et al., 2003), suggesting that lift coefficient should also converge. Over small size ranges within a clade, there can be more potential for innovations that alter power factor (efficiency). Over an order of magnitude in body sizes, the same range of  $C_V$  predicts a maximum possible allometry of 0.176, nearly identical to the exponent originally predicted in bats (Riskin et al., 2010). The potential for aerodynamic biomechanical innovation to contribute to weight within but not among taxa is similar to the proposed contribution of adhesive stress to weight support within but not among taxonomic Classes (Labonte et al., 2016).

Overall, this suggests that the *average* power factor is constant among all birds, perhaps due to similar physiological properties such as intrinsic muscle velocities (Ellington, 1991), but it could be a selective pressure within clades.

Analysing across and within groups therefore gives very different interpretations, and these can be misleading when used to extrapolate and predict maximum body size in flight. This limits the potential to extrapolate from an inhomogeneous group of extant fliers to predict the maximum size of an extinct flier. This was the error of Labonte et al. (Labonte et al., 2016), who erroneously extrapolated adhesive pad area to humans, and failed to account for evolutionary innovation (Hawkes et al., 2015). Indeed, pterosaurs were neither entirely bird- nor bat-like, but evolved novel solutions to the mechanical demands of flight (Middleton and English, 2015), so the largest pterosaur size would have been limited by specific aspects of pterosaur biology [including behaviour, (Dick and Clemente, 2017)]. This is a phylogenetic, not biomechanical, constraint. As proposed for *Patagona*, the maximum size of an animal is primarily due to the favourability of the selection gradient (Heim et al., 2015), and the (so far) absence of larger fliers can be attributed to a lack of selection. To quote Ellington, the largest extinct fliers will be relieved to learn they could fly (Ellington, 1991).

Innovations are not free, and alterations to the lift exponent will create adverse conditions such as a (potentially quadratic) increase in drag coefficient. Moreover, the applicability of this model to the largest fliers becomes problematic as their behaviour transitions from flapping to soaring flight. However, force allometry provides a framework to study the consequences of why some aerodynamic strategies are favoured, and the performance trade-offs they entail.

#### **4.4 Can the force allometry approach guide allometric research?**

I have argued that force allometry will be an especially important tool as the field moves toward understanding the functional implications of dynamic morphology. Here, I will argue that building on these foundations will lead to more powerful predictive models. Three traits of force allometry make it a useful model. First, the functional interpretation of body mass is unambiguous in the model. Second, the model uses this definition to choose an appropriate framework based on a formal and rigorously-validated equation. Finally, the method is explicitly evolutionary in origin, and we expect many possible strategies rather than a single, overarching constraint.

##### **4.4.1 Interpretation of body mass**

Among the greatest challenges in allometry is developing an integrative perspective that meaningfully relates differences among animals to the question at hand (Houle et al., 2011). The majority of studies choose body mass as the appealing reference frame (Günther et al., 1992) because this is easily measured, and the general similarity of body density means mass is approximately a function of volume (body ‘size’). This definition will be used in the following discussion. Nonetheless, the functional implications of body mass can be difficult to interpret, such as the proportion of body mass that consists of metabolically active tissue contributing to the allometry of metabolic rate. Indeed, the difference between body mass and body weight can lead to very different predictions about the allometry of metabolic rate on body size in terrestrial and aquatic environments (Platt and Silvert, 1981). The allometric model of Chapter 2 was conceived to specifically address the functional meaning of body mass in locomotion: in flight, animals must generate force and expend power sufficient to support body weight.

#### 4.4.2 A formal basis for scaling and allometry

Scaling is a rigorously developed theory in physics and engineering, in which similarity criteria define the invariance of a system with respect to a set of determining variables. These similarity criteria are derived using the formal method of dimensional analysis introduced by Buckingham, solving for dimensionless variables called  $\Pi$  groups (Buckingham, 1914; Butler et al., 1987; Fox et al., 2005). One object is said to be *dynamically scaled* from another when the dimensionless groups are equal. In aerodynamics, a small wing and large wing are dynamically scaled if the invariant  $\Pi$  groups of Reynolds number, Mach number (ignored for subsonic animal flight), lift coefficient, and angle of attack are all equal. In biology, there appear to be certain quantities which are independent of body mass, such as specific metabolic rate (Makarieva et al., 2008), which provides the motivation for allometry. In contrast to dynamic scaling through dimensionless numbers, allometric scaling is a description of the traits that change with body mass. A crucial caveat of dimensional analysis is that there are many potential dimensionless groups: the choice of invariant quantities is determined solely by the researcher (Butler et al., 1987) and accepted only after rigorous experimental validation (Buckingham, 1914; Lentink and Dickinson, 2009b; Prothero, 2002). In contrast, many allometric theories are validated by the correlations that inspired the analysis.

An allometric framework appealingly similar to the current work arises from a common form of dimensional analysis used to derive allometric exponents (Günther et al., 1992; Heusner, 1984; Morgado and Günther, 1998; Yales, 1979). Let us consider a variable,  $Q$ , in the MLT (mass-length-time) physical system,  $Q = M^\alpha L^\beta T^\gamma$ . To find an allometric function, we compare the state  $Q_I$  to a characteristic value  $Q_0$  [(Günther et al., 1992), simplified notation], and obtain,

$$\frac{Q_1}{Q_0} = \left(\frac{M_1}{M_0}\right)^\alpha \cdot \left(\frac{L_1}{L_0}\right)^\beta \cdot \left(\frac{T_1}{T_0}\right)^\gamma$$

The characteristic scale is typically 1 convenient unit (e.g., 1 kilogram) (Makarieva et al., 2008), although the concept of characteristic scales across all of biological diversity can be disputed (Banavar et al., 2003). This equation is cast in a common body mass reference frame by finding constant combinations of dimensions, in particular body density ( $ML^{-3} = 1$ ) and gravity ( $MT^{-2} = 1$ ). Taking mass to be a measure of volume ( $M = L^3$ ), the most frequent assumption in allometry, we eventually obtain the familiar basic allometric relationship and the decomposition of the exponent  $b$ ,

$$\frac{Q_1}{Q_0} = \left(\frac{M_1}{M_0}\right)^b = \left(\frac{M_1}{M_0}\right)^{\alpha+\beta/3+\gamma/6}$$

Intriguingly, by a different method from Chapter 2, we have arrived at a formulation which predicts that allometric exponents of body mass are products of multiple interacting functions.

Rather than considering the individual exponents as in Chapter 2, Günther and colleagues (Günther et al., 1992; Morgado and Günther, 1998) compare the exponent sum,  $b$ , to empirical estimates to test deviations from isometry. The strength of this method is that accounting for dimensions reveals the appropriate isometric prediction (null hypothesis), instead of applying *ad hoc* rules like isometry is implied by  $b=1$  (Pélabon et al., 2014). Basing allometric predictions in the mass-time-length system avoids assumptions like treating mass as a volume. Platt and Silvert applied this method to develop an isometric prediction for metabolic power proportional to  $W^{2/3}$  for aquatic organisms and to  $W^{3/4}$  for terrestrial organisms (Platt and Silvert, 1981). The difference was due to the suggestion that aquatic life is cheaper because buoyancy provides

weight support. Notably, by an adjustment of assumptions,  $W^{3/4}$  becomes the isometric prediction, and so an ‘allometric’ hypothesis is unnecessary (West et al., 1997).

This dimensional method suffers from two weaknesses. First, as in other null-hypothesis testing, the model provides neither rigorous validation nor functional interpretation of departures from isometry. Most importantly, it is not clear that allometric exponents derived with this dimensional method withstand careful scrutiny (Butler et al., 1987). Using formal analysis, Butler et al. derived  $\Pi$  groups for metabolic scaling, and found that the scaling of metabolic rate on mass is entirely dependent on the variables that the authors believe determine metabolic rate. Depending on which combination of specific enthalpy, body density, gravity, diffusivity, or pressure is used, metabolic rate can variously scale with body mass as  $2/3$ ,  $5/4$ ,  $7/6$ , or  $1/5$ . Butler et al. conclude that dimensional analysis is meaningless for this purpose. Thus, a critical platform for a robust allometric analysis is a formally-derived and experimentally validated theoretical basis. This criticism equally applies to the scaling of maneuverability and torque discussed above, so those predictions must be experimentally supported.

#### **4.4.3 The importance of the evolutionary framework**

An oft-neglected aspect of comparative allometric modelling is that allometric exponents develop and evolve (Pélabon et al., 2014; Shingleton et al., 2007; Uyeda et al., 2017; Voje et al., 2014). Even isometric scaling among species, such as wing length proportion to  $W^{1/3}$ , must be the product of evolution. If any aspect of development covaries with body size (e.g., genetic codetermination), then selection on body size will alter growth patterns and intraspecific (static) allometries (Pélabon et al., 2013; Tobler and Nijhout, 2010). Consequently, if species of different sizes exhibit similar intraspecific allometries, then selection must have acted to restore similar

(isometric) growth patterns and allometries. Contrary to the common view of isometry as proportional growth or a geometric constraint (Altshuler et al., 2004c; Rayner, 1988; Riskin et al., 2010), adherence to isometry should actually reveal evolutionary patterns. I think this is a more interesting hypothesis than null modelling, because it allows us to ask, what is so important about geometric similarity? From this perspective, the wing area allometry of other volant taxa closer to  $W^{2/3}$  (Figure 1.3, mindful of taxonomic inconsistencies) should indeed be seen as an evolutionary flight strategy, rather than a constraint that the hummingbirds have broken.

When do allometries actually represent constraints, and when do they represent opportunities (Gould, 1966)? A recent example of a constraint hypothesis is an allometric model that purports to explain why the maximum speed of animals increases linearly with body mass but then precipitously drops; the fastest animals are not the largest. Hirt et al. propose that the maximum time available to accelerate is constraining, and that the largest animals simply cannot accelerate for a long enough period to reach their maximum speed (Hirt et al., 2017). However, the specific allometric pattern that Hirt et al. identify across all animal groups likely occurs within taxa as well (Dick and Clemente, 2017). Maximum speed is an inverted-U function of body mass, peaking near or slightly greater than the mean taxon body size. The apparent precipitous drop in maximum speed at the largest body sizes across all animals (Hirt et al., 2017) may therefore simply be a taxonomically repeated pattern that is emphasised in the largest taxa due to the scale of the variables. Instead, the anatomical and biomechanical innovations that fuel clade radiations likely impose limits on the sizes over which those strategies remain effective (Dick and Clemente, 2017; Stanley, 1973). The pattern identified by Hirt et al. may be the biomechanical and performance signature of this limitation. A similar suggestion arises in

hummingbirds: the morphological innovation (wing area) that is enabling their success may also be limiting their maximum effective body size (adverse scaling of maneuverability).

It is easier to conceptualise a constraining, top-down, single-cause model than an evolutionary, bottom-up, multi-cause model (Darveau et al., 2002; O'Connor et al., 2007). A principal conceptual contribution of Chapter 2 is to develop an allometric framework that explicitly incorporates evolution, by allowing the exponents to vary among clades due to distinct pressures. Importantly, and generally unlike single-cause models, the force allometric model should be falsifiable by measurements of fitness, for instance a positive correlation between relative wing area and male or female reproductive success. Because multiple factors contribute to the scaling of weight support, the force allometry model is broadly a multi-cause model.

An archetype of the multi-cause models is the allometric cascade hypothesis (Darveau et al., 2002). The allometric cascade proposes that the scaling of metabolic rate arises not from a single constraint, but from summing over many metabolic processes  $b_i$  with control coefficients  $c_i$ . Among the proposed advantages of this theory was the potential to explain the allometry of both standard and maximum metabolic rates (Darveau et al., 2002; Darveau et al., 2003), which is impossible with constraint-based single-cause models. Letting  $Q$  be metabolic rate, Darveau et al. proposed  $Q = a \sum c_i M^{b_i}$ , where  $c_i$  is a physiological control coefficient of some process that has allometric coefficient  $b_i$ . The model is dimensionally inhomogeneous, but in their rebuttal West et al. (West et al., 2003) point out that a consistent version of the equation requires that  $b = \sum c_i b_i$ , subject to the constraints  $\sum c_i = 1$  and  $\sum c_i (b - b_i) = 0$ . In general, it will be difficult to distinguish the contributions of  $c_i$  and  $b_i$  unless the latter is presumed a fixed quantity. That condition would violate the general evolutionary constraint of force allometry that all parameters

should be free to vary, but could be true among closely related species. Writing instead that  $b = \sum \hat{b}_i$ , yields the expression,

$$Q = aM^b = a \prod M^{\hat{b}_i} = aM^{\hat{b}_1}M^{\hat{b}_2}M^{\hat{b}_3}M^{\hat{b}_4} \dots$$

which is the exact form of the force allometry model. Plainly, metabolic rate is the *product*, not the *sum*, of metabolic processes. This modified expression admits many, possibly species- and clade-specific allometric strategies, which is supported by multiple shifts in the metabolic rate exponent among vertebrates (Uyeda et al., 2017) and by metabolic scaling  $Q = M^1$  in plants, which is entirely controlled by nitrogen availability (Reich et al., 2006). In fact, if the metabolic rate exponent for a given group is known, then the summation  $b = \sum \hat{b}_i$  can be the basis for comparing the evolution of specific elements of the metabolic strategy among and within taxa. Evolution of the control coefficients may be possible with more rigorous definitions to separate the control coefficients from the mass exponent.

#### 4.5 Summary and prospects

In this thesis, I have emphasised the study of hummingbird physiology within the form-function-fitness paradigm (Chapter 1). Evolution depends on differential reproductive success, so biomechanical differentiation must be understood in terms of the behaviours and ecological context that contribute to fitness. In Chapter 1, I reviewed the diversity of hummingbird sexual and competitive behaviours that have likely driven their numerous and unique physiological and biomechanical specialisations. The available evidence is consistent with sexual displays, territorial competitions, and perhaps variation in behavioural strategies (guilds) as being the major factors in locomotor evolution in hummingbirds.

In Chapter 2, I developed a model termed force allometry to integrate diverse ecological, morphological, and biomechanical aspects of flight physiology. On the basis of the behaviours reviewed in Chapter 1, I proposed that hummingbirds' energetically demanding and combative lifestyles have favoured the evolution of a (so far) unique allometric strategy for weight support. This finding should provide impetus to shift from isolated morphological measurements to an integrative perspective, and application of force allometry to diverse clades will likely reveal unique evolutionary biomechanical strategies.

In Chapter 3, I investigated how behavioural and morphological flexibility enables hummingbird performance through new marker tracking methods and analyses, allowing high-resolution reconstruction of the wing surface during flight challenges. I propose that hummingbirds actively morph their wing to minimise counterproductive forces, similarly to other birds, and pointing to inherent phylogenetic constraints on hummingbirds' evolutionary convergence with insect flight. However, hummingbirds also have the capacity to morph their wings and sacrifice flight efficiency when it enables a desired goal.

On the basis of these results, in Chapter 4 I proposed that hummingbird evolution involves selection on mean wing size and shape for mean species flight performance, and dynamic shape for individual performance. Selection on flight performance is suggested to be creating a downward pressure on body size in hummingbirds. In addition, I synthesised the methods and lessons learned here with a review of the literature. Consistent with the results of this thesis, I suggested that future advances will come from multi-cause models on evolutionarily-relevant time scales (i.e., within taxa rather than across all domains of life). This perspective will enable the incorporation of biomechanical innovations into comparative analyses, to understand how evolution ultimately acts on form and function.

The results presented here suggest important directions in future research on hummingbirds.

1. How does wing morphing vary within and among individuals? In bats, greater camber is recruited to aid flight at low speeds (Iriarte-Diaz et al., 2012; Riskin et al., 2010). The cambering seen in Chapter 3 may thus also be part of the hummingbird toolkit for hovering, and then reduced in forward flight. Camber increases the lift coefficient for a given angle of attack, but the effects on aerodynamics, such as drag and stall angle, are strongly state-dependent and difficult to predict. One consequence of camber is a nose-down pitching moment, which could be destabilising (Krus, 1997); this can be beneficial or problematic depending on the task, so active control of camber might underlie a larger portion of the performance envelope and thus a wide range of behaviours. If hovering is primarily used for hovering weight support, then there is also the possibility of differences in recruitment among individuals of different sizes, which would in turn have an adverse effect on the range of potential behaviours. Likewise, do larger individuals rely on different wing postures for weight support, and does this also decrease the behavioural scope for postural modulation? Thus, further characterisation of postural and morphing parameters is a crucial next step. Potentially, wing morphing may enable sexual wing acoustic displays (Hunter and Picman, 2005), which should be maximised (e.g., loudest, highest frequencies) by the largest scope for postural changes.

2. The fitness consequences of hummingbirds' exceptionally great wing allometry must be explored. A first test would be to examine how wing loading is correlated with reproductive success in males or females. Altshuler et al. found that in competitive interactions among species, the winner was predicted by the species with a lower wing disc loading (product of wing area and stroke amplitude). This observation was inconsistent with wing disc loading theory

(Chapter 1), but is exactly predicted by Chapter 2, because lower wing disc loadings predict greater burst forces. This analysis should be extended to variation among individuals to examine territory-holding capacity, and then mating and reproductive success.

3. Hummingbirds' wing allometry must ultimately derive from altered growth patterns (Pélabon et al., 2013). Juveniles and females were included in the analyses of Chapter 2, so the extreme allometry cannot be due to different areas between life stages or sexes. Hummingbirds must either have evolved faster ontogenetic wing growth, or longer development times. The former would require novel developmental regulation, but longer fledging periods increase energetic demands for females and expose chicks to predation (Baltosser, 1986).

4. The evolution of bird wings is characterised by denser and stiffer bones (Dumont, 2010; Middleton and English, 2015). The high wing stroke frequencies of hummingbirds combined with the potential aerodynamic benefits of flexibility (Mountcastle and Combes, 2013), could favour further specialisation of wing material properties. Indeed, the evolution of hummingbirds from a common ancestor with swifts suggests that the stem hummingbirds likely had heavier and stiffer wings than extant species. A major insight into the biomechanical underpinnings of the hummingbird radiation will therefore come from a comparative analysis of dynamic morphing capacity and wing surface elastic modulus (ratio of applied force to surface deformation).

5. Finally, I have assumed in this thesis that innovations in the wing are driven by aerodynamic performance, but flight behaviours are enabled by environmental sensing of the forces acting on the body (Marshall et al., 2015; Sterbing-D'Angelo et al., 2011). The recent finding that peripheral mechanosensor sensitivity coevolves with fish fin shape (Aiello et al., 2017) suggests an entirely unexplored role of efficient mechanical feedback in dictating avian wing design.

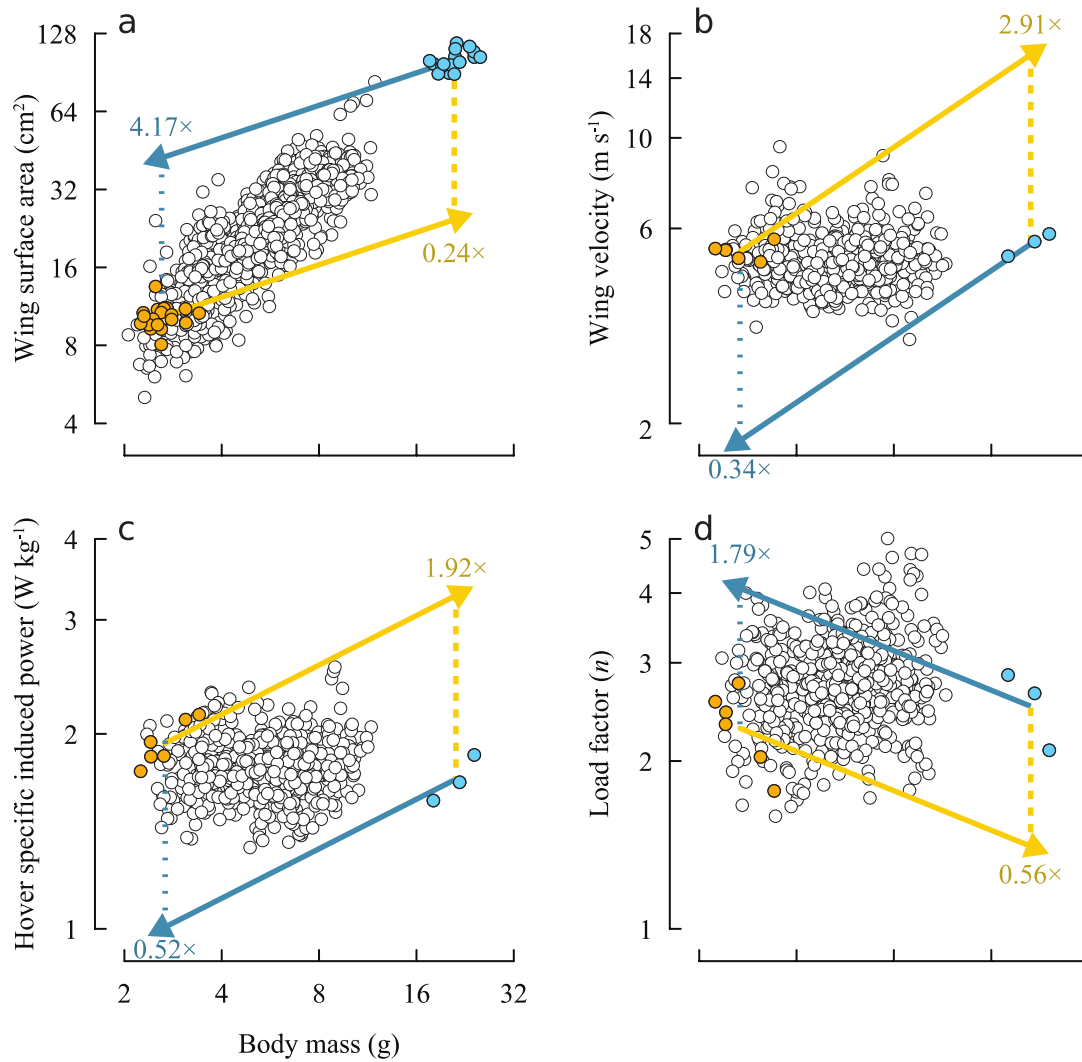


**Figure 4.1** Contrasting consequences of selection for larger and smaller body sizes, based on extrapolation of intraspecific allometry. In Chapter 2, it is suggested that small species cannot be scaled up according to intraspecific patterns to the size of large species (yellow line) without incurring undersized wings (a), excessively high wing velocities (b) and power expenditure (c), and a large decrease in burst load factor (d). The implication of this model is that evolution favours increasing body sizes, and wing areas must increase to maintain performance. If, instead, evolution favours smaller species, then the allometric extrapolation is reversed, and smaller species would benefit from scaling according to intraspecific patterns due to oversized wings (a), greatly reduced wing velocities (b) and power expenditure (c), and a large increase in burst load factor (d).

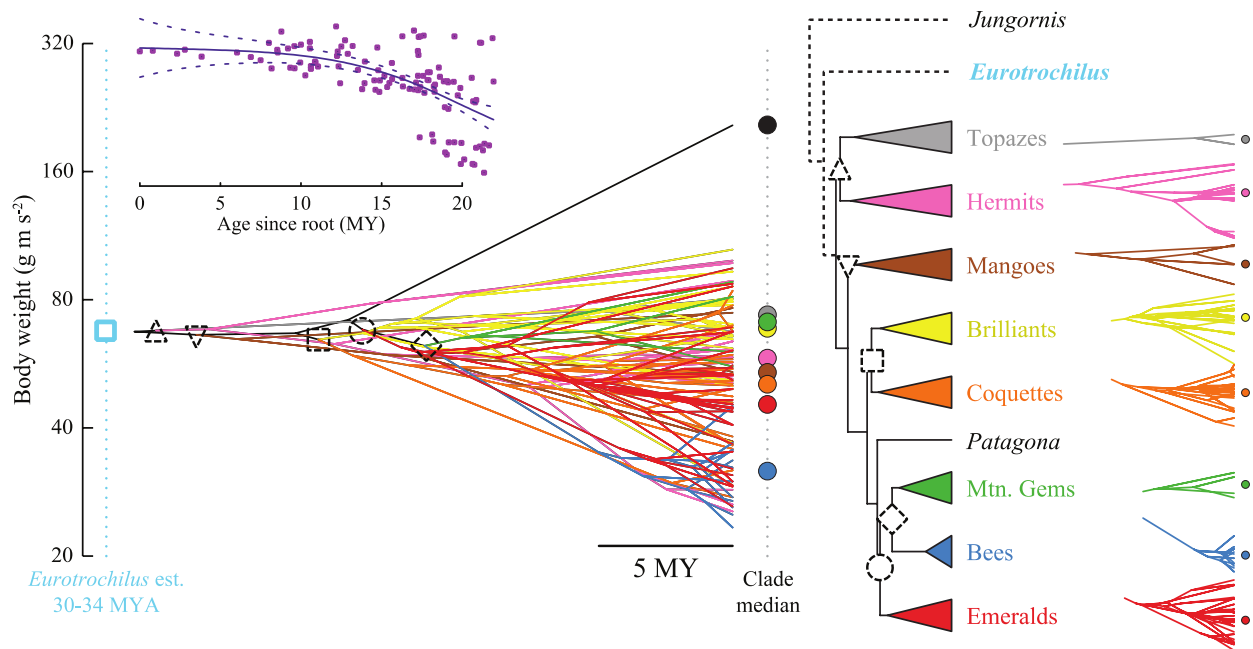


**Figure 4.2** Evolution of body size among hummingbirds. Body weight was estimated at internal nodes through a multivariate Ornstein-Uhlenbeck process based on individual and species covariance between body weight, wing area, and burst load lifting performance (correlated evolution of form and function). Each trait is highly phylogenetically correlated (>90% of trait variance). The reconstructed states are coloured by branches according to the clade in the cartoon phylogeny at right, and notable splits within the hummingbirds denoted with a dotted-line symbol. Clade median body weight is denoted with a circle. For clarity, reconstructed clades are also shown individually next to the phylogeny. In addition, I show the current placement of the stem hummingbirds *Eurotrochilus* and *Jungornis*. The estimated body weight of *Eurotrochilus* [based on similar size to *Glaucis hirsuta*, (Mayr, 2004)] is extremely close to the reconstructed ancestral body weight at the root of the crown hummingbirds. The placement of *Eurotrochilus* on the time axis is not proportional to its estimated fossil age. Inset: smoothed additive model of internal node reconstructed body weight versus the node age since the root. Millions of Years (Ago), MY(A).

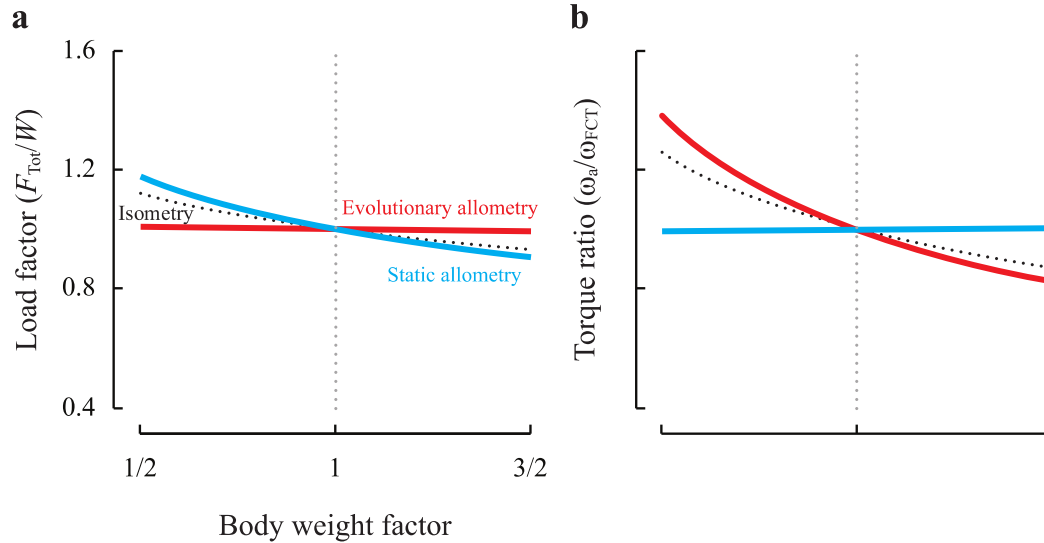


**Figure 4.3** Consequences of selection on different measures contributing to flight performance. Changes in load factor (**a**) and torque ratio (**b**) are shown relative a reference body weight (body weight factor=1). In isometrically-scaled animals, both load factor and torque ratio decline as body weights get larger, and increase as body weights get smaller. If a selective pressure results in increased body mass in hummingbirds, the resultant aerial performance will depend on whether morphological traits evolve along trajectories determined by the static (intraspecific, blue) or evolutionary allometries (interspecific, red). Increasing body size according to static allometry results in declining load factor and constant torque ratio, but according to evolutionary allometry leads to constant load factor and declining torque ratio. Regardless of the trajectory, we therefore predict declining overall flight performance with increasing body size. Decreasing body size according to static allometry results in increased load factor and constant torque ratio, but according to evolutionary allometry leads to constant load factor and a large gain in torque ratio. Regardless of the trajectory, we therefore predict that decreasing body size results in increased overall flight performance.

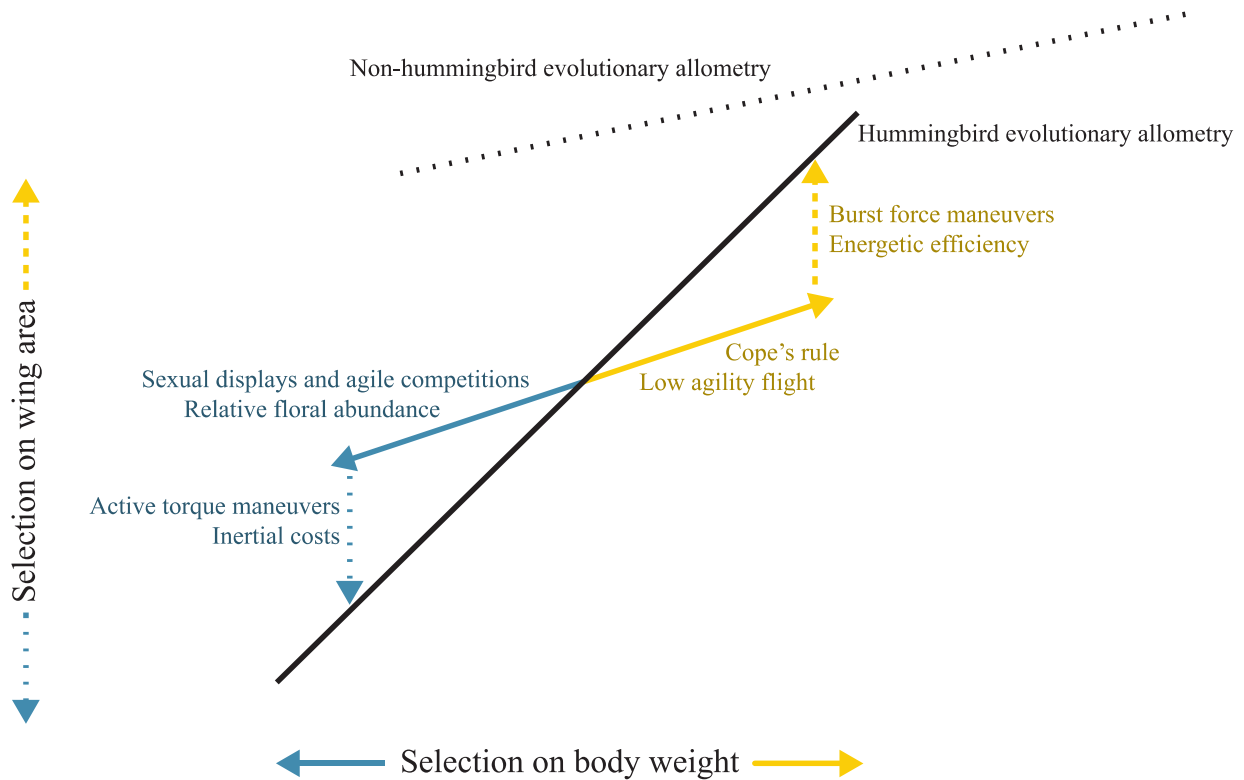
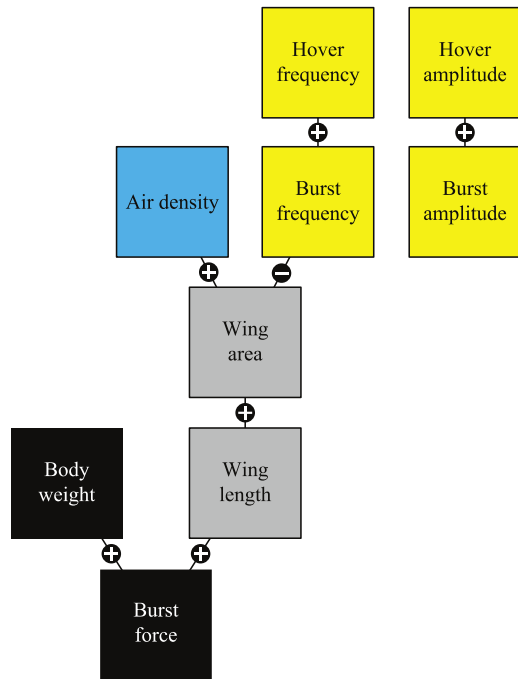


**Figure 4.4** Proposed model for correlated selection on body weight and wing area in hummingbirds. Smaller body sizes are favoured by selection for intense sexual displays and agile competitions, and for high relative floral abundance compared to individual dietary requirements. Static scaling of wing area (according to mean intraspecific exponents) with reduced body weight leads to disadvantageously large wings and high inertial costs and high frictional torque during turning. Selection therefore acts to reduce wing areas and restore constant wing loading. Larger body sizes are generally favoured by Cope's rule, and in specific cases where flight agility is low when competition is high. Static scaling of wing area results in small wings that are energetically unfavourable and result in a disadvantage in burst force production. Selection therefore acts to increase wing areas, again restoring constant wing loading. Overall, selection is likely favouring decreased body sizes in hummingbirds, which explains why hummingbird wings are smaller than expected based on the allometry of non-hummingbirds.

**a Among species**



**b Within species**

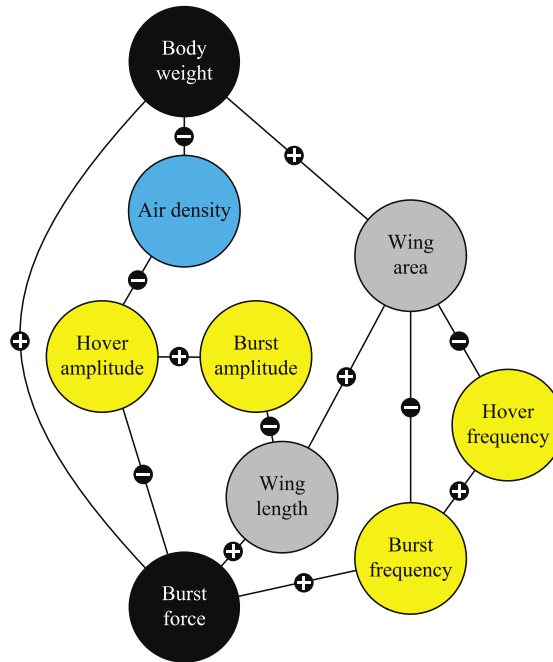


**Figure 4.5** A network integrative perspective reveals wing area is a key morphological trait in hummingbird diversification. Edges between pairs of variables among (squares; **a,c**) and within (circles; **b,d**) reflect direct associations that are not explained by covariance with other traits (up to second-order). **a** Wing area is directly correlated with air density among species, and stroke amplitudes are independent of any other factor which suggests compensatory evolution to resolve the detrimental effects of reduced air density on performance within species. Moreover, stroke amplitude during hovering and burst performance are independent of any measured factor among species, but not within species, suggesting that selection acts to maintain performance margins through stroke amplitude modulation. In **a,b**, both wing area and wing length are corrected for the second moment of area,  $r_2^2(S)$ .

## References

- Aiello, B. R., Westneat, M. W. and Hale, M. E.** (2017). Mechanosensation is evolutionarily tuned to locomotor mechanics. *Proc. Natl. Acad. Sci.* 201616839.
- Alatalo, R. V., Gustafsson, L. and Lundberg, A.** (1984). Why do young passerine birds have shorter wings than older birds? *Ibis* **126**, 410–415.
- Alben, S., Madden, P. G. and Lauder, G. V.** (2007). The mechanics of active fin-shape control in ray-finned fishes. *J. R. Soc. Interface* **4**, 243–256.
- Alerstam, T., Rosén, M., Bäckman, J., Ericson, P. G. P. and Hellgren, O.** (2007). Flight speeds among bird species: Allometric and phylogenetic effects. *PLOS Biol* **5**, e197.
- Altshuler, D. L.** (2006). Flight performance and competitive displacement of hummingbirds across elevational gradients. *Am. Nat.* **167**, 216–229.
- Altshuler, D. L. and Dudley, R.** (2002). The ecological and evolutionary interface of hummingbird flight physiology. *J. Exp. Biol.* **205**, 2325–2336.
- Altshuler, D. L. and Dudley, R.** (2003). Kinematics of hovering hummingbird flight along simulated and natural elevational gradients. *J. Exp. Biol.* **206**, 3139–3147.
- Altshuler, D. L., Stiles, F. G., Dudley, R. and Wainwright, A. E. P. C.** (2004a). Of Hummingbirds and Helicopters: Hovering Costs, Competitive Ability, and Foraging Strategies. *Am. Nat.* **163**, 16–25.
- Altshuler, D. L., Dudley, R. and Ellington, C. P.** (2004b). Aerodynamic forces of revolving hummingbird wings and wing models. *J. Zool.* **264**, 327–332.
- Altshuler, D. L., Dudley, R. and McGuire, J. A.** (2004c). Resolution of a paradox: Hummingbird flight at high elevation does not come without a cost. *Proc. Natl. Acad. Sci. U. S. A.* **101**, 17731–17736.
- Altshuler, D. L., Dickson, W. B., Vance, J. T., Roberts, S. P. and Dickinson, M. H.** (2005). Short-amplitude high-frequency wing strokes determine the aerodynamics of honeybee flight. *Proc. Natl. Acad. Sci. U. S. A.* **102**, 18213–18218.
- Altshuler, D. L., Princevac, M., Pan, H. and Lozano, J.** (2009). Wake patterns of the wings and tail of hovering hummingbirds. *Exp. Fluids* **46**, 835–846.
- Altshuler, D. L., Dudley, R., Heredia, S. M. and McGuire, J. A.** (2010). Allometry of hummingbird lifting performance. *J. Exp. Biol.* **213**, 725–734.

- Altshuler, D. L., Quicazan-Rubio, E. M., Segre, P. S. and Middleton, K. M.** (2012). Wingbeat kinematics and motor control of yaw turns in Anna's hummingbirds (*Calypte anna*). *J. Exp. Biol.* **215**, 4070–4084.
- Altshuler, D. L., Bahlman, J. W., Dakin, R., Gaede, A. H., Goller, B., Lentink, D., Segre, P. S. and Skandalis, D. A.** (2015). The biophysics of bird flight: functional relationships integrate aerodynamics, morphology, kinematics, muscles, and sensors. *Can. J. Zool.* **93**, 961–975.
- Àlvarez, J., Meseguer, J., Meseguer, E. and Pérez, A.** (2001). On the role of the alula in the steady flight of birds. *Ardeola* **48**, 161–173.
- Apol, M. E. F., Etienne, R. S. and Olf, H.** (2008). Revisiting the evolutionary origin of allometric metabolic scaling in biology. *Funct. Ecol.* **22**, 1070–1080.
- Armstrong, D. P.** (1987). Economics of Breeding Territoriality in Male Calliope Hummingbirds. *The Auk* **104**, 242–253.
- Arnold, S. J.** (1983). Morphology, Performance and Fitness. *Am. Zool.* **23**, 347–361.
- Askew, G. N.** (2014). The elaborate plumage in peacocks is not such a drag. *J. Exp. Biol.* **217**, 3237–3241.
- Bachmann, T., Blazek, S., Erlinghagen, T., Baumgartner, W. and Wagner, H.** (2012). Barn Owl Flight. In *Nature-Inspired Fluid Mechanics*, pp. 101–117. Springer.
- Badger, M., Ortega-Jimenez, V. M., Rabenau, L. von, Smiley, A. and Dudley, R.** (2015). Electrostatic Charge on Flying Hummingbirds and Its Potential Role in Pollination. *PLOS ONE* **10**, e0138003.
- Bahlman, J. W., Swartz, S. M. and Breuer, K. S.** (2013). Design and characterization of a multi-articulated robotic bat wing. *Bioinspir. Biomim.* **8**, 016009.
- Baltosser, W. H.** (1986). Nesting success and productivity of hummingbirds in southwestern New Mexico and southeastern Arizona. *Wilson Bull.* **98**, 353–367.
- Banavar, J. R., Damuth, J., Maritan, A. and Rinaldo, A.** (2003). Physiology (communication arising): Allometric cascades. *Nature* **421**, 713–714.
- Banks, R. C. and Johnson, N. K.** (1961). A Review of North American Hybrid Hummingbirds. *The Condor* **63**, 3–28.
- Barbosa, A. and Møller, A. P.** (1999). Sexual selection and tail streamers in the barn swallow: appropriate tests of the function of size-dimorphic long tails. *Behav. Ecol.* **10**, 112–114.

- Barnes, W. J. P., Oines, C. and Smith, J. M.** (2006). Whole animal measurements of shear and adhesive forces in adult tree frogs: insights into underlying mechanisms of adhesion obtained from studying the effects of size and scale. *J. Comp. Physiol. A* **192**, 1179–1191.
- Bennett, A. F.** (1987). Interindividual variability: an underutilized resource. *New Dir. Ecol. Physiol.* **15**, 147–169.
- Bennett, P. M. and Owens, I. P. F.** (1997). Variation in extinction risk among birds: chance or evolutionary predisposition? *Proc. R. Soc. Lond. B Biol. Sci.* **264**, 401–408.
- Bergou, A. J., Swartz, S. M., Vejdani, H., Riskin, D. K., Reimnitz, L., Taubin, G. and Breuer, K. S.** (2015). Falling with Style: Bats Perform Complex Aerial Rotations by Adjusting Wing Inertia. *PLOS Biol.* **13**, e1002297.
- Berman, G. J. and Wang, Z. J.** (2007). Energy-minimizing kinematics in hovering insect flight. *J. Fluid Mech.* **582**, 153–168.
- BirdLife International and NatureServe** (2014). *Bird species distribution maps of the world*. BirdLife International, Cambridge, UK and natureServe, Arlington, USA.
- Bishop, C. M., Spivey, R. J., Hawkes, L. A., Batbayar, N., Chua, B., Frappell, P. B., Milsom, W. K., Natsagdorj, T., Newman, S. H., Scott, G. R., et al.** (2015). The roller coaster flight strategy of bar-headed geese conserves energy during Himalayan migrations. *Science* **347**, 250–254.
- Blomberg, S. P., Garland, T. and Ives, A. R.** (2003). Testing for phylogenetic signal in comparative data: behavioral traits are more labile. *Evolution* **57**, 717–745.
- Bochenski, Z. and Bochenski, Z. M.** (2008). An Old World hummingbird from the Oligocene: a new fossil from Polish Carpathians. *J. Ornithol.* **149**, 211–216.
- Bokhorst, E. van, Kat, R. de, Elsinga, G. E. and Lentink, D.** (2015). Feather roughness reduces flow separation during low Reynolds number glides of swifts. *J. Exp. Biol.* **218**, 3179–3191.
- Boller, M. L. and Carrington, E.** (2006). The hydrodynamic effects of shape and size change during reconfiguration of a flexible macroalga. *J. Exp. Biol.* **209**, 1894–1903.
- Boller, M. L. and Carrington, E.** (2007). Interspecific comparison of hydrodynamic performance and structural properties among intertidal macroalgae. *J. Exp. Biol.* **210**, 1874–1884.
- Bolstad, G. H., Cassara, J. A., Márquez, E., Hansen, T. F., Linde, K. van der, Houle, D. and Pélabon, C.** (2015). Complex constraints on allometry revealed by artificial selection on the wing of *Drosophila melanogaster*. *Proc. Natl. Acad. Sci.* **112**, 13284–13289.

- Bomphrey, R. J., Taylor, G. K. and Thomas, A. L. R.** (2009). Smoke visualization of free-flying bumblebees indicates independent leading-edge vortices on each wing pair. *Exp. Fluids* **46**, 811–821.
- Bomphrey, R. J., Nakata, T., Phillips, N. and Walker, S. M.** (2017). Smart wing rotation and trailing-edge vortices enable high frequency mosquito flight. *Nature* **544**, 92–95.
- Borazjani, I. and Daghooghi, M.** (2013). The fish tail motion forms an attached leading edge vortex. *Proc. R. Soc. B Biol. Sci.* **280**,
- Borazjani, I. and Sotiropoulos, F.** (2010). On the role of form and kinematics on the hydrodynamics of self-propelled body/caudal fin swimming. *J. Exp. Biol.* **213**, 89–107.
- Bowlin, M. S. and Wikelski, M.** (2008). Pointed Wings, Low Wingloading and Calm Air Reduce Migratory Flight Costs in Songbirds. *PLoS ONE* **3**, e2154.
- Brown, J. H., Gillooly, J. F., Allen, A. P., Savage, V. M. and West, G. B.** (2004). Toward a Metabolic Theory of Ecology. *Ecology* **85**, 1771–1789.
- Buckingham, E.** (1914). On physically similar systems; illustrations of the use of dimensional equations. *Phys. Rev.* **4**, 345–376.
- Busse, R. von, Swartz, S. M. and Voigt, C. C.** (2013). Flight metabolism in relation to speed in Chiroptera: testing the U-shape paradigm in the short-tailed fruit bat *Carollia perspicillata*. *J. Exp. Biol.* **216**, 2073–2080.
- Butler, J. P., Feldman, H. A. and Fredberg, J. J.** (1987). Dimensional analysis does not determine a mass exponent for metabolic scaling. *Am. J. Physiol.-Regul. Integr. Comp. Physiol.* **253**, R195–R199.
- Byers, J., Hebets, E. and Podos, J.** (2010). Female mate choice based upon male motor performance. *Anim. Behav.* **79**, 771–778.
- Calder, W. A.** (1973). Microhabitat Selection During Nesting of Hummingbirds in the Rocky Mountains. *Ecology* **54**, 127–134.
- Careau, V. and Garland, T.** (2012). Performance, Personality, and Energetics: Correlation, Causation, and Mechanism. *Physiol. Biochem. Zool.* **85**, 543–571.
- Careau, V. and Wilson, R. S.** (2017). Performance trade-offs and ageing in the ‘world’s greatest athletes.’ *Proc R Soc B* **284**, 20171048.
- Carpenter, F. L., Paton, D. C. and Hixon, M. A.** (1983). Weight gain and adjustment of feeding territory size in migrant hummingbirds. *Proc. Natl. Acad. Sci.* **80**, 7259–7263.
- Chai, P. and Dudley, R.** (1995). Limits to vertebrate locomotor energetics suggested by hummingbirds hovering in heliox. *Nature* **377**, 722–725.

- Chai, P. and Dudley, R.** (1996). Limits to flight energetics of hummingbirds hovering in hypodense and hypoxic gas mixtures. *J. Exp. Biol.* **199**, 2285–2295.
- Chai, P. and Millard, D.** (1997). Flight and size constraints: hovering performance of large hummingbirds under maximal loading. *J. Exp. Biol.* **200**, 2757–2763.
- Chai, P., Chen, J. S. and Dudley, R.** (1997). Transient hovering performance of hummingbirds under conditions of maximal loading. *J. Exp. Biol.* **200**, 921–929.
- Chai, P., Chang, A. C. and Dudley, R.** (1998). Flight thermogenesis and energy conservation in hovering hummingbirds. *J. Exp. Biol.* **201**, 963–968.
- Chen, C. C. W. and Welch, K. C.** (2014). Hummingbirds can fuel expensive hovering flight completely with either exogenous glucose or fructose. *Funct. Ecol.* **28**, 589–600.
- Cheney, J. A., Konow, N., Middleton, K. M., Breuer, K. S., Roberts, T. J., Giblin, E. L. and Swartz, S. M.** (2014). Membrane muscle function in the compliant wings of bats. *Bioinspir. Biomim.* **9**, 025007.
- Cheng, B., Fry, S. N., Huang, Q. and Deng, X.** (2010). Aerodynamic damping during rapid flight maneuvers in the fruit fly *Drosophila*. *J. Exp. Biol.* **213**, 602–612.
- Chin, D. D., Matloff, L. Y., Stowers, A. K., Tucci, E. R. and Lentink, D.** (2017). Inspiration for wing design: how forelimb specialization enables active flight in modern vertebrates. *J. R. Soc. Interface* **14**, 20170240.
- Clark, C. J.** (2009). Courtship dives of Anna’s hummingbird offer insights into flight performance limits. *Proc. R. Soc. Lond. B Biol. Sci.* **276**, 3047–3052.
- Clark, C. J. and Dudley, R.** (2009). Flight costs of long, sexually selected tails in hummingbirds. *Proc. R. Soc. B Biol. Sci.* **276**, 2109–2115.
- Clark, C. J. and Dudley, R.** (2010). Hovering and Forward Flight Energetics in Anna’s and Allen’s Hummingbirds. *Physiol. Biochem. Zool.* **83**, 654–662.
- Clark, A. G. and Keith, L. E.** (1989). Rapid enzyme kinetic assays of individual *Drosophila* and comparisons of field-caught *D. melanogaster* and *D. simulans*. *Biochem. Genet.* **27**, 263–277.
- Clark, C. J., Elias, D. O. and Prum, R. O.** (2011). Aeroelastic Flutter Produces Hummingbird Feather Songs. *Science* **333**, 1430–1433.
- Clark, C. J., Kirschel, A. N. G., Hadjioannou, L. and Prum, R. O.** (2016). Smithornis broadbills produce loud wing song by aeroelastic flutter of medial primary wing feathers. *J. Exp. Biol.* **219**, 1069–1075.

- Colwell, R. K.** (2000). Rensch's rule crosses the line: Convergent allometry of sexual size dimorphism in hummingbirds and flower mites. *Am. Nat.* **156**, 495–510.
- Combes, S. A. and Daniel, T. L.** (2001a). Shape, flapping and flexion: Wing and fin design for forward flight. *J. Exp. Biol.* **204**, 2073–2085.
- Combes, S. A. and Daniel, T. L.** (2001b). Shape, flapping and flexion: wing and fin design for forward flight. *J. Exp. Biol.* **204**, 2073–2085.
- Corning, W. R. and Biewener, A. A.** (1998). In vivo strains in pigeon flight feather shafts: Implications for structural design. *J. Exp. Biol.* **201**, 3057–3066.
- Cornwell, W. and Nakagawa, S.** (2017). Phylogenetic comparative methods. *Curr. Biol.* **27**, R333–R336.
- Crino, O. L., Klaassen van Oorschot, B., Crandell, K. E., Breuner, C. W. and Tobalske, B. W.** (2017). Flight performance in the altricial zebra finch: Developmental effects and reproductive consequences. *Ecol. Evol.* **7**, 2316–2326.
- Cuervo, J. J., Møller, A. P. and de Lope, F.** (2003). Experimental manipulation of tail length in female barn swallows (*Hirundo rustica*) affects their future reproductive success. *Behav. Ecol.* **14**, 451–456.
- Dakin, R., Fellows, T. K. and Altshuler, D. L.** (2016). Visual guidance of forward flight in hummingbirds reveals control based on image features instead of pattern velocity. *Proc. Natl. Acad. Sci.* **113**, 8849–8854.
- Dale, J., Dey, C. J., Delhey, K., Kempnaers, B. and Valcu, M.** (2015). The effects of life history and sexual selection on male and female plumage colouration. *Nature* **527**, 367–370.
- Daniel, T. L.** (1984). Unsteady Aspects of Aquatic Locomotion. *Am. Zool.* **24**, 121–134.
- Darveau, C.-A., Suarez, R. K., Andrews, R. D. and Hochachka, P. W.** (2002). Allometric cascade as a unifying principle of body mass effects on metabolism. *Nature* **417**, 166–170.
- Darveau, C.-A., Suarez, R. K., Andrews, R. D. and Hochachka, P. W.** (2003). Physiology (communication arising (reply): Why does metabolic rate scale with body size?/Allometric cascades. *Nature* **421**, 714–714.
- Darveau, C.-A., Hochachka, P. W., Welch, K. C., Roubik, D. W. and Suarez, R. K.** (2005a). Allometric scaling of flight energetics in Panamanian orchid bees: a comparative phylogenetic approach. *J. Exp. Biol.* **208**, 3581–3591.

- Darveau, C.-A., Hochachka, P. W., Roubik, D. W. and Suarez, R. K.** (2005b). Allometric scaling of flight energetics in orchid bees: evolution of flux capacities and flux rates. *J. Exp. Biol.* **208**, 3593–3602.
- de la Fuente, A., Bing, N., Hoeschele, I. and Mendes, P.** (2004). Discovery of meaningful associations in genomic data using partial correlation coefficients. *Bioinforma. Oxf. Engl.* **20**, 3565–3574.
- de Villemereuil, P. de, Wells, J. A., Edwards, R. D. and Blomberg, S. P.** (2012). Bayesian models for comparative analysis integrating phylogenetic uncertainty. *BMC Evol. Biol.* **12**, 102.
- Dearborn, D. C.** (1998). Interspecific territoriality by a Rufous-tailed hummingbird (*Amazilia tzacatl*): Effects of intruder size and resource value. *Biotropica* **30**, 306–313.
- Deetjen, M. E., Biewener, A. A. and Lentink, D.** (2017). High-speed surface reconstruction of a flying bird using structured light. *J. Exp. Biol.* **220**, 1956–1961.
- Dial, K.** (1992). Avian forelimb muscles and nonsteady flight. *The Auk* **109**, 874–885.
- Dial, K. P.** (2003). Wing-Assisted Incline Running and the Evolution of Flight. *Science* **299**, 402–404.
- Dial, K. P., Biewener, A. A., Tobalske, B. W. and Warrick, D. R.** (1997). Mechanical power output of bird flight. *Nat. Lond.* **390**, 67–70.
- Dial, K. P., Jackson, B. E. and Segre, P.** (2008). A fundamental avian wing-stroke provides a new perspective on the evolution of flight. *Nature* **451**, 985–989.
- Dial, T. R., Heers, A. M. and Tobalske, B. W.** (2012). Ontogeny of aerodynamics in mallards: comparative performance and developmental implications. *J. Exp. Biol.* **215**, 3693–3702.
- Dick, T. J. M. and Clemente, C. J.** (2017). Where Have All the Giants Gone? How Animals Deal with the Problem of Size. *PLOS Biol.* **15**, e2000473.
- Donley, J. M., Sepulveda, C. A., Konstantinidis, P., Gemballa, S. and Shadwick, R. E.** (2004). Convergent evolution in mechanical design of lamnid sharks and tunas. *Nature* **429**, 61–65.
- Donovan, E. R., Keeney, B. K., Kung, E., Makan, S., Wild, J. M. and Altshuler, D. L.** (2013). Muscle Activation Patterns and Motor Anatomy of Anna’s Hummingbirds *Calypste anna* and Zebra Finches *Taeniopygia guttata*. *Physiol. Biochem. Zool.* **86**, 27–46.
- Dryden, I. L. and Mardia, K. V.** (2016). *Statistical Shape Analysis, with Applications in R.* John Wiley & Sons, Ltd.

- Du, G. and Sun, M.** (2010). Effects of wing deformation on aerodynamic forces in hovering hoverflies. *J. Exp. Biol.* **213**, 2273–2283.
- Duckworth, R. A. and Badyaev, A. V.** (2007). Coupling of dispersal and aggression facilitates the rapid range expansion of a passerine bird. *Proc. Natl. Acad. Sci.* **104**, 15017–15022.
- Dudley, R.** (1990). Biomechanics of Flight in Neotropical Butterflies: Morphometrics and Kinematics. *J. Exp. Biol.* **150**, 37–53.
- Dudley, R.** (1991). Biomechanics of Flight in Neotropical Butterflies: Aerodynamics and Mechanical Power Requirements. *J. Exp. Biol.* **159**, 335–357.
- Dumont, E. R.** (2010). Bone density and the lightweight skeletons of birds. *Proc. R. Soc. B Biol. Sci.* **277**, 2193–2198.
- Eliason, E. J., Clark, T. D., Hague, M. J., Hanson, L. M., Gallagher, Z. S., Jeffries, K. M., Gale, M. K., Patterson, D. A., Hinch, S. G. and Farrell, A. P.** (2011). Differences in Thermal Tolerance Among Sockeye Salmon Populations. *Science* **332**, 109–112.
- Ellington, C. P.** (1984a). The aerodynamics of hovering insect flight. VI. Lift and power requirements. *Philos. Trans. R. Soc. Lond. B Biol. Sci.* **305**, 145–181.
- Ellington, C. P.** (1984b). The aerodynamics of hovering insect flight. III. Kinematics. *Philos. Trans. R. Soc. Lond. B Biol. Sci.* **305**, 41–78.
- Ellington, C. P.** (1984c). The aerodynamics of hovering insect flight. I. The quasi-steady analysis. *Philos. Trans. R. Soc. Lond. B Biol. Sci.* **305**, 1–15.
- Ellington, C. P.** (1984d). The aerodynamics of hovering insect flight. II. Morphological parameters. *Philos. Trans. R. Soc. Lond. B Biol. Sci.* **305**, 17–40.
- Ellington, C. P.** (1984e). The aerodynamics of hovering insect flight. IV. Aerodynamic mechanisms. *Philos. Trans. R. Soc. Lond. B Biol. Sci.* **305**, 79–113.
- Ellington, C. P.** (1991). Limitations on animal flight performance. *J. Exp. Biol.* **160**, 71–91.
- Ellington, C. P.** (2006). Insects versus birds: the great divide. In *44th AIAA aerospace sciences meeting and exhibit*, pp. 1–6.
- Ellington, C. P., Machin, K. E. and Casey, T. M.** (1990). Oxygen consumption of bumblebees in forward flight. *Nature* **347**, 472–473.
- Ellington, C. P., van den Berg, C., Willmott, A. P. and Thomas, A. L. R.** (1996). Leading-edge vortices in insect flight. *Nature* **384**, 626–630.

- Elliott, K. H., Ricklefs, R. E., Gaston, A. J., Hatch, S. A., Speakman, J. R. and Davoren, G. K.** (2013). High flight costs, but low dive costs, in auks support the biomechanical hypothesis for flightlessness in penguins. *Proc. Natl. Acad. Sci.* **110**, 9380–9384.
- Ennos, A. R.** (1988). The Importance of Torsion in the Design of Insect Wings. *J. Exp. Biol.* **140**, 137–160.
- Epting, R. J.** (1980). Functional Dependence of the Power for Hovering on Wing Disc Loading in Hummingbirds. *Physiol. Zool.* **53**, 347–357.
- Epting, R. J. and Casey, T. M.** (1973). Power Output and Wing Disc Loading in Hovering Hummingbirds. *Am. Nat.* **107**, 761–765.
- Evans, M. R.** (1998). Selection on swallow tail streamers. *Nature* **394**, 233–234.
- Evans, M. R. and Thomas, A. L. R.** (1992). The aerodynamic and mechanical effects of elongated tails in the scarlet-tufted malachite sunbird: measuring the cost of a handicap. *Anim. Behav.* **43**, 337–347.
- Ewald, P. W. and Bransfield, R. J.** (1987). Territory quality and territorial behavior in two sympatric species of hummingbirds. *Behav. Ecol. Sociobiol.* **20**, 285–293.
- Ewald, P. W. and Orians, G. H.** (1983). Effects of resource depression on use of inexpensive and escalated aggressive behavior: experimental tests using Anna hummingbirds. *Behav. Ecol. Sociobiol.* **12**, 95–101.
- Ewald, P. W. and Rohwer, S.** (1980). Age, coloration and dominance in nonbreeding hummingbirds: A test of the asymmetry hypothesis. *Behav. Ecol. Sociobiol.* **7**, 273–279.
- Feinsinger, P. and Chaplin, S. B.** (1975). On the Relationship between Wing Disc Loading and Foraging Strategy in Hummingbirds. *Am. Nat.* **109**, 217–224.
- Feinsinger, P. and Colwell, R. K.** (1978). Community Organization among Neotropical Nectar-Feeding Birds. *Am. Zool.* **18**, 779–795.
- Feinsinger, P., Colwell, R. K., Terborgh, J. and Chaplin, S. B.** (1979). Elevation and the Morphology, Flight Energetics, and Foraging Ecology of Tropical Hummingbirds. *Am. Nat.* **113**, 481–497.
- Felsenstein, J.** (1985). Phylogenies and the Comparative Method. *Am. Nat.* **125**, 1–15.
- Felsenstein, J.** (2008). Comparative Methods with Sampling Error and Within-Species Variation: Contrasts Revisited and Revised. *Am. Nat.* **171**, 713–725.
- Fernández, M. J., Dudley, Robert and Bozinovic, F.** (2011). Comparative energetics of the Giant hummingbird (Patagona gigas). *Physiol. Biochem. Zool.* **84**, 333–340.

- Fierro-Calderón, K. and Martin, T. E.** (2007). Reproductive Biology of the Violet-Chested Hummingbird in Venezuela and Comparisons with Other Tropical and Temperate Hummingbirds. *The Condor* **109**, 680–685.
- Fox, R. W., McDonald, A. T. and Pritchard, P. J.** (2005). *Introduction to Fluid Mechanics*. 6 edition. Hoboken, NJ: Wiley.
- Fox Keller, E.** (2007). A clash of two cultures. *Nature* **445**, 603–603.
- Gaede, A. H., Goller, B., Lam, J. P. M., Wylie, D. R. and Altshuler, D. L.** (2017). Neurons Responsive to Global Visual Motion Have Unique Tuning Properties in Hummingbirds. *Curr. Biol.* **27**, 279–285.
- Garamszegi, L. Z.** (2014). Uncertainties Due to Within-Species Variation in Comparative Studies: Measurement Errors and Statistical Weights. In *Modern Phylogenetic Comparative Methods and Their Application in Evolutionary Biology* (ed. Garamszegi, L. Z.), pp. 157–199. Springer Berlin Heidelberg.
- Garamszegi, L. Z. and Møller, A. P.** (2010). Effects of sample size and intraspecific variation in phylogenetic comparative studies: a meta-analytic review. *Biol. Rev.* **85**, 797–805.
- Garland, T. and Adolph, S. C.** (1994). Why Not to Do Two-Species Comparative Studies: Limitations on Inferring Adaptation. *Physiol. Zool.* **67**, 797–828.
- Garland, T. and Losos, J. B.** (1994). Ecological morphology of locomotor performance in squamate reptiles. In *Ecological morphology: integrative organismal biology* (ed. Wainwright, P. C. and Reilly, S. M.), pp. 240–302. Chicago: University of Chicago Press.
- Gass, C. L.** (1978). Rufous hummingbird feeding territoriality in a suboptimal habitat. *Can. J. Zool.* **56**, 1535–1539.
- Gaston, K. J. and Blackburn, T. M.** (1995). Birds, body size and the threat of extinction. *Phil Trans R Soc Lond B* **347**, 205–212.
- Gelman, A.** (2006). Prior distributions for variance parameters in hierarchical models. *Bayesian Anal.* **1**, 515–534.
- Gerritsen, H.** (2014). *mapplots: Data Visualisation on Maps*. <https://CRAN.R-project.org/package=mapplots>
- Gillies, J. A., Thomas, A. L. R. and Taylor, G. K.** (2011). Soaring and manoeuvring flight of a steppe eagle *Aquila nipalensis*. *J. Avian Biol.* **42**, 377–386.
- Goller, B. and Altshuler, D. L.** (2014). Hummingbirds control hovering flight by stabilizing visual motion. *Proc. Natl. Acad. Sci.* **111**, 18375–18380.

- Goolsby, E. W., Bruggeman, J. and Ané, C.** (2017). Rphylopars : fast multivariate phylogenetic comparative methods for missing data and within-species variation. *Methods Ecol. Evol.* **8**, 22–27.
- Gould, S. J.** (1966). Allometry and Size in Ontogeny and Phylogeny. *Biol. Rev.* **41**, 587–638.
- Graham, C. H., Parra, J. L., Rahbek, C. and McGuire, J. A.** (2009). Phylogenetic structure in tropical hummingbird communities. *Proc. Natl. Acad. Sci.* **106**, 19673–19678.
- Grant, P. R. and Grant, B. R.** (2006). Evolution of Character Displacement in Darwin's Finches. *Science* **313**, 224–226.
- Graves, G. R., Dittmann, D. L. and Cardiff, S. W.** (2016). Diagnoses of hybrid hummingbirds (Aves: Trochilidae). 17. Documentation of the intrageneric hybrid (*Archilochus colubris* × *Archilochus alexandri*). *Proc. Biol. Soc. Wash.* **129**, 1–9.
- Green, A. J., Figuerola, J. and King, R.** (2001). Comparing interspecific and intraspecific allometry in the Anatidae. *J. Für Ornithol.* **142**, 321–334.
- Greenewalt, C. H.** (1962). *Dimensional relationships for flying animals*. Washington: Smithsonian Institution.
- Groom, D. J. E., Toledo, M. C. B. and Welch, K. C.** (2017). Wingbeat kinematics and energetics during weightlifting in hovering hummingbirds across an elevational gradient. *J. Comp. Physiol. B* **187**, 165–182.
- Günther, B., González, U. and Morgado, E.** (1992). Biological similarity theories: a comparison with the empirical allometric equations. *Biol Res* **25**, 7–13.
- Gutierrez, E., Quinn, D. B., Chin, D. D. and Lentink, D.** (2017). Lift calculations based on accepted wake models for animal flight are inconsistent and sensitive to vortex dynamics. *Bioinspir. Biomim.* **12**, 016004.
- Hadfield, J. D.** (2010). MCMC methods for multi-response generalized linear mixed models: the MCMCglmm R package. *J. Stat. Softw.* **33**, 1–22.
- Hadfield, J. D. and Nakagawa, S.** (2010). General quantitative genetic methods for comparative biology: phylogenies, taxonomies and multi-trait models for continuous and categorical characters. *J. Evol. Biol.* **23**, 494–508.
- Hainsworth, F. R. and Wolf, L. L.** (1970). Regulation of Oxygen Consumption and Body Temperature during Torpor in a Hummingbird, *Eulampis jugularis*. *Science* **168**, 368–369.
- Harmon, L. J. and Losos, J. B.** (2005). The effect of intraspecific sample size on type i and type ii error rates in comparative studies. *Evolution* **59**, 2705–2710.

- Harrison, J. F., Fewell, J. H., Roberts, S. P. and Hall, H. G.** (1996). Achievement of Thermal Stability by Varying Metabolic Heat Production in Flying Honeybees. *Science* **274**, 88–90.
- Hawkes, L. A., Balachandran, S., Batbayar, N., Butler, P. J., Frappell, P. B., Milsom, W. K., Tseveenmyadag, N., Newman, S. H., Scott, G. R., Sathiyaselvam, P., et al.** (2011). The trans-Himalayan flights of bar-headed geese (*Anser indicus*). *Proc. Natl. Acad. Sci.* **108**, 9516–9519.
- Hawkes, E. W., Eason, E. V., Christensen, D. L. and Cutkosky, M. R.** (2015). Human climbing with efficiently scaled gecko-inspired dry adhesives. *J. R. Soc. Interface* **12**, 20140675.
- Hedenström, A. and Lindström, Å.** (2017). Wind tunnel as a tool in bird migration research. *J. Avian Biol.* **48**, 37–48.
- Hedrick, T. L.** (2008). Software techniques for two- and three-dimensional kinematic measurements of biological and biomimetic systems. *Bioinspir. Biomim.* **3**, 034001.
- Hedrick, T. L.** (2011). Damping in flapping flight and its implications for manoeuvring, scaling and evolution. *J. Exp. Biol.* **214**, 4073–4081.
- Hedrick, T. L. and Daniel, T. L.** (2006). Flight control in the hawkmoth *Manduca sexta*: the inverse problem of hovering. *J. Exp. Biol.* **209**, 3114–3130.
- Hedrick, T. L., Tobalske, B. W. and Biewener, A. A.** (2002). Estimates of circulation and gait change based on a three-dimensional kinematic analysis of flight in cockatiels (*Nymphicus hollandicus*) and ringed turtle-doves (*Streptopelia risoria*). *J. Exp. Biol.* **205**, 1389–1409.
- Hedrick, T. L., Cheng, B. and Deng, X.** (2009). Wingbeat Time and the Scaling of Passive Rotational Damping in Flapping Flight. *Science* **324**, 252–255.
- Hedrick, T. L., Tobalske, B. W., Ros, I. G., Warrick, D. R. and Biewener, A. A.** (2012). Morphological and kinematic basis of the hummingbird flight stroke: scaling of flight muscle transmission ratio. *Proc. R. Soc. B Biol. Sci.* **279**, 1986–1992.
- Hedrick, T. L., Combes, S. A. and Miller, L. A.** (2015). Recent developments in the study of insect flight. *Can. J. Zool.* **93**, 925–943.
- Heers, A. M., Tobalske, B. W. and Dial, K. P.** (2011). Ontogeny of lift and drag production in ground birds. *J. Exp. Biol.* **214**, 717–725.
- Heim, N. A., Knope, M. L., Schaal, E. K., Wang, S. C. and Payne, J. L.** (2015). Cope's rule in the evolution of marine animals. *Science* **347**, 867–870.

- Heinold, M. and Kähler, C. J.** (2015). Wing-Surface Reconstruction of a Lanner-Falcon in Free Flapping Flight with Multiple Cameras. In *Image and Video Technology*, pp. 392–403. Springer, Cham.
- Henderson, J., Hurly, T. A., Bateson, M. and Healy, S. D.** (2006). Timing in Free-Living Rufous Hummingbirds, *Selasphorus rufus*. *Curr. Biol.* **16**, 512–515.
- Henningsson, P., Muijres, F. T. and Hedenström, A.** (2011). Time-resolved vortex wake of a common swift flying over a range of flight speeds. *J. R. Soc. Interface* **8**, 807–816.
- Henningsson, P., Hedenström, A. and Bomphrey, R. J.** (2014). Efficiency of Lift Production in Flapping and Gliding Flight of Swifts. *PLoS ONE* **9**, e90170.
- Hesselberg, T. and Lehmann, F.-O.** (2007). Turning behaviour depends on frictional damping in the fruit fly *Drosophila*. *J. Exp. Biol.* **210**, 4319–4334.
- Hesselberg, T. and Lehmann, F.-O.** (2009). The role of experience in flight behaviour of *Drosophila*. *J. Exp. Biol.* **212**, 3377–3386.
- Heusner, A. A.** (1984). Biological similitude: statistical and functional relationships in comparative physiology. *Am. J. Physiol.-Regul. Integr. Comp. Physiol.* **246**, R839–R846.
- Higginson, D. M., Badyaev, A. V., Segraves, K. A. and Pitnick, S.** (2015). Causes of Discordance between Allometries at and above Species Level: An Example with Aquatic Beetles. *Am. Nat.* **186**, 176–186.
- Hijmans, R. J.** (2015). *raster: Geographic Data Analysis and Modeling*. <https://CRAN.R-project.org/package=raster>
- Hirt, M. R., Jetz, W., Rall, B. C. and Brose, U.** (2017). A general scaling law reveals why the largest animals are not the fastest. *Nat. Ecol. Evol.* **1**, 1116.
- Hou, L. and Welch, K. C.** (2016). Premigratory ruby-throated hummingbirds, *Archilochus colubris*, exhibit multiple strategies for fuelling migration. *Anim. Behav.* **121**, 87–99.
- Hou, L., Verdirame, M. and Welch, K. C.** (2015). Automated tracking of wild hummingbird mass and energetics over multiple time scales using radio frequency identification (RFID) technology. *J. Avian Biol.* **46**, 1–8.
- Houle, D., Govindaraju, D. R. and Omholt, S.** (2010). Phenomics: the next challenge. *Nat. Rev. Genet.* **11**, 855–866.
- Houle, D., Pélabon, C., Wagner, G. P. and Hansen, T. F.** (2011). Measurement and Meaning in Biology. *Q. Rev. Biol.* **86**, 3–34.
- Hubel, T. Y. and Tropea, C.** (2010). The importance of leading edge vortices under simplified flapping flight conditions at the size scale of birds. *J. Exp. Biol.* **213**, 1930–1939.

- Hunter, T. A.** (2008). On the role of wing sounds in hummingbird communication. *The Auk* **125**, 532–541.
- Hunter, T. A. and Picman, J.** (2005). Characteristics of the Wing Sounds of Four Hummingbird Species That Breed in Canada. *The Condor* **107**, 570–582.
- Husak, J. F.** (2006). Does survival depend on how fast you can run or how fast you do run? *Funct. Ecol.* **20**, 1080–1086.
- Husak, J. F., Irschick, D. J., McCormick, S. D. and Moore, I. T.** (2009). Hormonal regulation of whole-animal performance: Implications for selection. *Integr. Comp. Biol.* **49**, 349–353.
- Iriarte-Diaz, J., Riskin, D. K., Breuer, K. S. and Swartz, S. M.** (2012). Kinematic Plasticity during Flight in Fruit Bats: Individual Variability in Response to Loading. *PLoS ONE* **7**, e36665.
- Irschick, D. J. and Garland, T.** (2001). Integrating Function and Ecology in Studies of Adaptation: Investigations of Locomotor Capacity as a Model System. *Annu. Rev. Ecol. Syst.* **32**, 367–396.
- Irschick, D. J., Meyers, J. J., Husak, J. F. and Le Galliard, J.-F.** (2008). How does selection operate on whole-organism functional performance capacities? A review and synthesis. *Evol. Ecol. Res.* **10**, 177–196.
- Ives, A. R., Midford, P. E. and Garland, T.** (2007). Within-Species Variation and Measurement Error in Phylogenetic Comparative Methods. *Syst. Biol.* **56**, 252–270.
- Iwamoto, H., Inoue, K. and Yagi, N.** (2006). Evolution of long-range myofibrillar crystallinity in insect flight muscle as examined by X-ray cryomicrodiffraction. *Proc. R. Soc. B Biol. Sci.* **273**, 677–685.
- Iwaniuk, A. N. and Wylie, D. R. W.** (2007). Neural specialization for hovering in hummingbirds: Hypertrophy of the pretectal nucleus lentiformis mesencephali. *J. Comp. Neurol.* **500**, 211–221.
- Jetz, W., Thomas, G. H., Joy, J. B., Hartmann, K. and Mooers, A. O.** (2012). The global diversity of birds in space and time. *Nature* **491**, 444–448.
- Johansson, L. C., Engel, S., Kelber, A., Heerenbrink, M. K. and Hedenström, A.** (2013). Multiple leading edge vortices of unexpected strength in freely flying hawkmoth. *Sci. Rep.* **3**,.
- Jombart, T., Kendall, M., Almagro-Garcia, J. and Colijn, C.** (2017). treespace: Statistical exploration of landscapes of phylogenetic trees. <https://CRAN.R-project.org/package=treespace>

- Kalisch, M., Mächler, M., Colombo, D., Maathuis, M. H., Bühlmann, P. and others** (2012). Causal inference using graphical models with the R package pcalg. *J. Stat. Softw.* **47**, 1–26.
- Kendall, M. and Colijn, C.** (2016). Mapping Phylogenetic Trees to Reveal Distinct Patterns of Evolution. *Mol. Biol. Evol.* **33**, 2735–2743.
- Kim, E. J., Wolf, M., Ortega-Jimenez, V. M., Cheng, S. H. and Dudley, R.** (2014). Hovering performance of Anna’s hummingbirds (*Calypte anna*) in ground effect. *J. R. Soc. Interface* **11**, 20140505.
- Kingsolver, J. G., Pfennig, D. W. and Phillips, P.** (2004). Individual-level selection as a cause of Cope’s rule of phyletic size increase. *Evolution* **58**, 1608–1612.
- KleinHeerenbrink, M., Johansson, L. C. and Hedenström, A.** (2017). Multi-cored vortices support function of slotted wing tips of birds in gliding and flapping flight. *J. R. Soc. Interface* **14**, 20170099.
- Kodric-Brown, A. and Brown, J. H.** (1978). Influence of Economics, Interspecific Competition, and Sexual Dimorphism on Territoriality of Migrant Rufous Hummingbirds. *Ecology* **59**, 285–296.
- Koehler, C., Liang, Z., Gaston, Z., Wan, H. and Dong, H.** (2012). 3D reconstruction and analysis of wing deformation in free-flying dragonflies. *J. Exp. Biol.* **215**, 3018–3027.
- Konow, N., Cheney, J. A., Roberts, T. J., Iriarte-Díaz, J., Breuer, K. S., Waldman, J. R. S. and Swartz, S. M.** (2017). Speed-dependent modulation of wing muscle recruitment intensity and kinematics in two bat species. *J. Exp. Biol.* **220**, 1820–1829.
- Krus, P.** (1997). Natural methods for flight stability in birds. *AIAA Papers* 97–5653.
- Kruschke, J. K.** (2013). Bayesian Estimation Supersedes the t Test. *J. Exp. Psychol.-Gen.* **142**, 573–603.
- Kruyt, J. W., Quicazán-Rubio, E. M., Heijst, G. F. van, Altshuler, D. L. and Lentink, D.** (2014). Hummingbird wing efficacy depends on aspect ratio and compares with helicopter rotors. *J. R. Soc. Interface* **11**, 20140585.
- Kruyt, J. W., Heijst, G. F. van, Altshuler, D. L. and Lentink, D.** (2015). Power reduction and the radial limit of stall delay in revolving wings of different aspect ratio. *J. R. Soc. Interface* **12**, 20150051.
- Ksepka, D. T., Clarke, J. A., Nesbitt, S. J., Kulp, F. B. and Grande, L.** (2013). Fossil evidence of wing shape in a stem relative of swifts and hummingbirds (Aves, Pan-Apodiformes). *Proc. R. Soc. B Biol. Sci.* **280**, 20130580–20130580.

- Kuznetsova, A., Bruun Brockhoff, P. and Haubo Bojesen Christensen, R.** (2016). *lmerTest: Tests in Linear Mixed Effects Models*. <https://CRAN.R-project.org/package=lmerTest>
- Labonte, D., Clemente, C. J., Dittrich, A., Kuo, C.-Y., Crosby, A. J., Irschick, D. J. and Federle, W.** (2016). Extreme positive allometry of animal adhesive pads and the size limits of adhesion-based climbing. *Proc. Natl. Acad. Sci.* **113**, 1297–1302.
- Lack, J. B., Monette, M. J., Johannig, E. J., Sprengelmeyer, Q. D. and Pool, J. E.** (2016). Decanalization of wing development accompanied the evolution of large wings in high-altitude *Drosophila*. *Proc. Natl. Acad. Sci.* **113**, 1014–1019.
- Le, T. Q., Truong, T. V., Park, S. H., Truong, T. Q., Ko, J. H., Park, H. C. and Byun, D.** (2013). Improvement of the aerodynamic performance by wing flexibility and elytra–hind wing interaction of a beetle during forward flight. *J. R. Soc. Interface* **10**,.
- Le Galliard, J.-F., Clobert, J. and Ferrière, R.** (2004). Physical performance and darwinian fitness in lizards. *Nature* **432**, 502–505.
- Lee, S., Kim, J., Park, H., Jabłoński, P. G. and Choi, H.** (2015). The Function of the Alula in Avian Flight. *Sci. Rep.* **5**, srep09914.
- Lehmann, F.-O.** (2012). Wake structure and vortex development in flight of fruit flies using high-speed particle image velocimetry. In *Nature-Inspired Fluid Mechanics*, pp. 65–79. Springer.
- Lehmann, F. O. and Dickinson, M. H.** (1997). The changes in power requirements and muscle efficiency during elevated force production in the fruit fly *Drosophila melanogaster*. *J. Exp. Biol.* **200**, 1133–1143.
- Lehmann, F.-O., Gorb, S., Nasir, N. and Schützner, P.** (2011). Elastic deformation and energy loss of flapping fly wings. *J. Exp. Biol.* **214**, 2949–2961.
- Leishman, J. G.** (2000). *Principles of Helicopter Aerodynamics*. Cambridge: Cambridge University Press.
- Lenth, R. V.** (2016). Least-Squares Means: The R Package lsmeans. *J. Stat. Softw.* **69**. <https://CRAN.R-project.org/package=lsmeans>
- Lentink, D. and Dickinson, M. H.** (2009a). Rotational accelerations stabilize leading edge vortices on revolving fly wings. *J. Exp. Biol.* **212**, 2705–2719.
- Lentink, D. and Dickinson, M. H.** (2009b). Biofluiddynamic scaling of flapping, spinning and translating fins and wings. *J. Exp. Biol.* **212**, 2691–2704.
- Lentink, D., Müller, U. K., Stamhuis, E. J., de Kat, R., van Gestel, W., Veldhuis, L. L. M., Henningson, P., Hedenström, A., Videler, J. J. and van Leeuwen, J. L.** (2007). How swifts control their glide performance with morphing wings. *Nature* **446**, 1082–1085.

- Lentink, D., Dickson, W. B., Leeuwen, J. L. van and Dickinson, M. H.** (2009). Leading-Edge Vortices Elevate Lift of Autorotating Plant Seeds. *Science* **324**, 1438–1440.
- Lislevand, T., Figuerola, J. and Székely, T.** (2007). Avian Body Sizes in Relation to Fecundity, Mating System, Display Behavior, and Resource Sharing. *Ecology* **88**, 1605–1605.
- Lockwood, R., Swaddle, J. P. and Rayner, J. M. V.** (1998). Avian wingtip shape reconsidered: Wingtip shape indices and morphological adaptations to migration. *J. Avian Biol.* **29**, 273–292.
- Losos, J. B., Schoener, T. W., Langerhans, R. B. and Spiller, D. A.** (2006). Rapid Temporal Reversal in Predator-Driven Natural Selection. *Science* **314**, 1111–1111.
- Ma, Y., Ning, J. G., Ren, H. L., Zhang, P. F. and Zhao, H. Y.** (2015). The function of resilin in honeybee wings. *J. Exp. Biol.* **218**, 2136–2142.
- Mahalingam, S. and Welch, K. C.** (2013). Neuromuscular control of hovering wingbeat kinematics in response to distinct flight challenges in the ruby-throated hummingbird, *Archilochus colubris*. *J. Exp. Biol.* **216**, 4161–4171.
- Mahler, D. L., Ingram, T., Revell, L. J. and Losos, J. B.** (2013). Exceptional Convergence on the Macroevolutionary Landscape in Island Lizard Radiations. *Science* **341**, 292–295.
- Makarieva, A. M., Gorshkov, V. G., Li, B.-L., Chown, S. L., Reich, P. B. and Gavrilov, V. M.** (2008). Mean mass-specific metabolic rates are strikingly similar across life's major domains: evidence for life's metabolic optimum. *Proc. Natl. Acad. Sci.* **105**, 16994–16999.
- Marden, J. H.** (1987). Maximum Lift Production During Takeoff in Flying Animals. *J. Exp. Biol.* **130**, 235–258.
- Marden, J. H.** (1989). Bodybuilding Dragonflies: Costs and Benefits of Maximizing Flight Muscle. *Physiol. Zool.* **62**, 505–521.
- Marden, J. H.** (1994). From damselflies to pterosaurs: how burst and sustainable flight performance scale with size. *Am. J. Physiol.-Regul. Integr. Comp. Physiol.* **266**, R1077–R1084.
- Marshall, K. L., Chadha, M., deSouza, L. A., Sterbing-D'Angelo, S. J., Moss, C. F. and Lumpkin, E. A.** (2015). Somatosensory Substrates of Flight Control in Bats. *Cell Rep.* **11**, 851–858.
- Martin, T. E.** (2015). Age-related mortality explains life history strategies of tropical and temperate songbirds. *Science* **349**, 966–970.

- Martínez, F., Manzanera, A. and Romero, E.** (2015). Automatic analysis and characterization of the hummingbird wings motion using dense optical flow features. *Bioinspir. Biomim.* **10**, 016006.
- Martins, E. P. and Hansen, T. F.** (1997). Phylogenies and the Comparative Method: A General Approach to Incorporating Phylogenetic Information into the Analysis of Interspecific Data. *Am. Nat.* **149**, 646–667.
- Mayr, G.** (2003). Phylogeny of early tertiary swifts and hummingbirds (Aves: Apodiformes). *The Auk* **120**, 145–151.
- Mayr, G.** (2004). Old World Fossil Record of Modern-Type Hummingbirds. *Science* **304**, 861–864.
- McCarthy, E. M.** (2006). *Handbook of Avian Hybrids of the World*. New York, NY: Oxford University Press, Inc.
- McGuire, J. A., Witt, C. C., Remsen, J. V., Corl, A., Rabosky, D. L., Altshuler, D. L. and Dudley, R.** (2014). Molecular phylogenetics and the diversification of hummingbirds. *Curr. Biol.*
- McMahon, T.** (1973). Size and shape in biology. *Science* **179**, 1201–1204.
- Middleton, K. M. and English, L. T.** (2015). Challenges and advances in the study of pterosaur flight. *Can. J. Zool.* **93**, 945–959.
- Miller, R. S. and Gass, C. L.** (1985). Survivorship in Hummingbirds: Is Predation Important? *Auk* **102**, 175–178.
- Moens, M. A. J., Valkiūnas, G., Paca, A., Bonaccorso, E., Aguirre, N. and Pérez-Tris, J.** (2016). Parasite specialization in a unique habitat: hummingbirds as reservoirs of generalist blood parasites of Andean birds. *J. Anim. Ecol.* **85**, 1234–1245.
- Møller, A. P.** (1988). Female choice selects for male sexual tail ornaments in the monogamous swallow. *Nature* **332**, 640–642.
- Møller, A. P.** (1992). Female swallow preference for symmetrical male sexual ornaments. *Nature* **357**, 238–240.
- Møller, A. P.** (1995). Sexual selection in the barn swallow (*Hirundo rustica*). V. Geographic variation in ornament size. *J. Evol. Biol.* **8**, 3–19.
- Møller, A. P. and Alatalo, R. V.** (1999). Good-Genes Effects in Sexual Selection. *Proc. Biol. Sci.* **266**, 85–91.
- Møller, A. P., De Lope, F. and Saino, N.** (1995a). Sexual selection in the barn swallow *Hirundo rustica*. VI. Aerodynamic adaptations. *J. Evol. Biol.* **8**, 671–687.

- Møller, A. P., Lope, F. de and Caballero, J. M. L.** (1995b). Foraging costs of a tail ornament: Experimental evidence from two populations of barn swallows *Hirundo rustica* with different degrees of sexual size dimorphism. *Behav. Ecol. Sociobiol.* **37**, 289–295.
- Moore, R. T.** (1947). Habits of male hummingbirds near their nests. *Wilson Bull.* **59**, 21–25.
- Morgado, E. and Günther, B.** (1998). Dimensional analysis and allometric equations concerning Cope's rule. *Rev. Chil. Hist. Nat.* **71**, 331–335.
- Mountcastle, A. M. and Combes, S. A.** (2013). Wing flexibility enhances load-lifting capacity in bumblebees. *Proc. R. Soc. B Biol. Sci.* **280**, 20130531.
- Mountcastle, A. M. and Combes, S. A.** (2014). Biomechanical strategies for mitigating collision damage in insect wings: structural design versus embedded elastic materials. *J. Exp. Biol.* **217**, 1108–1115.
- Muijres, F. T., Johansson, L. C., Barfield, R., Wolf, M., Spedding, G. R. and Hedenström, A.** (2008). Leading-Edge Vortex Improves Lift in Slow-Flying Bats. *Science* **319**, 1250–1253.
- Muijres, F. T., Johansson, L. C., Bowlin, M. S., Winter, Y. and Hedenström, A.** (2012a). Comparing Aerodynamic Efficiency in Birds and Bats Suggests Better Flight Performance in Birds. *PLOS ONE* **7**, e37335.
- Muijres, F. T., Johansson, L. C. and Hedenström, A.** (2012b). Leading edge vortex in a slow-flying passerine. *Biol. Lett.* **8**, 554–557.
- Nagarajan, R., Scutari, M. and Lèbre, S.** (2013). *Bayesian Networks in R*. New York, NY: Springer New York.
- Nakagawa, S. and Freckleton, R. P.** (2008). Missing inaction: the dangers of ignoring missing data. *Trends Ecol. Evol.* **23**, 592–596.
- Nakagawa, S. and Schielzeth, H.** (2013). A general and simple method for obtaining  $R^2$  from generalized linear mixed-effects models. *Methods Ecol. Evol.* **4**, 133–142.
- Norberg, R. Å.** (1994). Swallow tail streamer is a mechanical device for self-deflection of tail leading edge, enhancing aerodynamic efficiency and flight manoeuvrability. *Proc R Soc Lond B* **257**, 227–233.
- Norberg, U. M. and Rayner, J. M. V.** (1987). Ecological Morphology and Flight in Bats (Mammalia; Chiroptera): Wing Adaptations, Flight Performance, Foraging Strategy and Echolocation. *Philos. Trans. R. Soc. Lond. B. Biol. Sci.* **316**, 335–427.
- Nowak, M. A.** (2006). Five rules for the evolution of cooperation. *science* **314**, 1560–1563.
- Nudds, R. L.** (2007). Wing-bone length allometry in birds. *J. Avian Biol.* **38**, 515–519.

- Nyffeler, M., Maxwell, M. R. and Remsen Jr, J. V.** (2017). Bird Predation By Praying Mantises: A Global Perspective. *Wilson J. Ornithol.* **129**, 331–344.
- O'Connor, M. P., Kemp, S. J., Agosta, S. J., Hansen, F., Sieg, A. E., Wallace, B. P., McNair, J. N. and Dunham, A. E.** (2007). Reconsidering the mechanistic basis of the metabolic theory of ecology. *Oikos* **116**, 1058–1072.
- Opazo, J. C., Soto-Gamboa, M. and Fernández, M. J.** (2005). Cell size and basal metabolic rate in hummingbirds. *Rev. Chil. Hist. Nat.* **78**,.
- Ortega-Jimenez, V. M. and Dudley, R.** (2013). Spiderweb deformation induced by electrostatically charged insects. *Sci. Rep.* **3**,.
- Ortega-Jimenez, V. M., Badger, M., Wang, H. and Dudley, R.** (2016). Into rude air: hummingbird flight performance in variable aerial environments. *Phil Trans R Soc B* **371**, 20150387.
- Oufiero, C. E. and Garland, T.** (2007). Evaluating performance costs of sexually selected traits. *Funct. Ecol.* **21**, 676–689.
- Pagel, M.** (1999). Inferring the historical patterns of biological evolution. *Nature* **401**, 877–884.
- Paradis, E., Claude, J. and Strimmer, K.** (2004). APE: Analyses of phylogenetics and evolution in R language. *Bioinformatics* **20**, 289–290.
- Park, T. J., Reznick, J., Peterson, B. L., Blass, G., Omerbašić, D., Bennett, N. C., Kuich, P. H. J. L., Zasada, C., Browe, B. M., Hamann, W., et al.** (2017). Fructose-driven glycolysis supports anoxia resistance in the naked mole-rat. *Science* **356**, 307–311.
- Paton, D. C. and Carpenter, F. L.** (1984). Peripheral Foraging by Territorial Rufous Hummingbirds: Defense by Exploitation. *Ecology* **65**, 1808–1819.
- Pebesma, E. J. and Bivand, R. S.** (2005). Classes and methods for spatial data in R. *R News* **5**, 9–13.
- Pélabon, C., Bolstad, G. H., Egset, C. K., Cheverud, J. M., Pavlicev, M. and Rosenqvist, G.** (2013). On the Relationship between Ontogenetic and Static Allometry. *Am. Nat.* **181**, 195–212.
- Pélabon, C., Firmat, C., Bolstad, G. H., Voje, K. L., Houle, D., Cassara, J., Rouzic, A. L. and Hansen, T. F.** (2014). Evolution of morphological allometry. *Ann. N. Y. Acad. Sci.* **1320**, 58–75.
- Pennycuik, C. J.** (1969). The Mechanics of Bird Migration. *Ibis* **111**, 525–556.
- Pennycuik, C. J.** (1971). Gliding Flight of the White-Backed Vulture *Gyps Africanus*. *J. Exp. Biol.* **55**, 13–38.

- Pennycuik, C. J.** (1990). Predicting Wingbeat Frequency and Wavelength of Birds. *J. Exp. Biol.* **150**, 171–185.
- Phan, H. V., Truong, Q. T. and Park, H. C.** (2017). An experimental comparative study of the efficiency of twisted and flat flapping wings during hovering flight. *Bioinspir. Biomim.* **12**, 036009.
- Phillips, N., Knowles, K. and Bomphrey, R. J.** (2015). The effect of aspect ratio on the leading-edge vortex over an insect-like flapping wing. *Bioinspir. Biomim.* **10**, 056020.
- Pinheiro, J. C., Bates, D., DebRoy, S., Sarkar, D. and R Core Team** (2016). *nlme: Linear and Nonlinear Mixed Effects Models*. <https://CRAN.R-project.org/package=nlme>
- Platt, T. and Silvert, W.** (1981). Ecology, physiology, allometry and dimensionality. *J. Theor. Biol.* **93**, 855–860.
- Plummer, M.** (2003). JAGS: A program for analysis of Bayesian graphical models using Gibbs sampling. In *Proceedings of the 3rd international workshop on distributed statistical computing*, p. 125. Vienna.
- Plummer, M.** (2016). *rjags: Bayesian Graphical Models using MCMC*. <https://CRAN.R-project.org/package=rjags>
- Pournazeri, S., Segre, P. S., Princevac, M. and Altshuler, D. L.** (2013). Hummingbirds generate bilateral vortex loops during hovering: evidence from flow visualization. *Exp. Fluids* **54**, 1439.
- Powers, D. R.** (1987). Effects of Variation in Food Quality on the Breeding Territoriality of the Male Anna’s Hummingbird. *The Condor* **89**, 103–111.
- Projecto-Garcia, J., Natarajan, C., Moriyama, H., Weber, R. E., Fago, A., Cheviron, Z. A., Dudley, R., McGuire, J. A., Witt, C. C. and Storz, J. F.** (2013). Repeated elevational transitions in hemoglobin function during the evolution of Andean hummingbirds. *Proc. Natl. Acad. Sci.* **110**, 20669–20674.
- Prothero, J.** (2002). Perspectives on Dimensional Analysis in Scaling Studies. *Perspect. Biol. Med.* **45**, 175–189.
- Purcell, E. M.** (1977). Life at low Reynolds number. *Am. J. Phys.* **45**, 3–11.
- R Core Team** (2017). *R: A language and environment for statistical computing*. Vienna, Austria: R Foundation for Statistical Computing.
- Rangel, T. F., Colwell, R. K., Graves, G. R., Fučíková, K., Rahbek, C. and Diniz-Filho, J. A. F.** (2015). Phylogenetic uncertainty revisited: Implications for ecological analyses. *Evolution* **69**, 1301–1312.

- Rattenborg, N. C., Voirin, B., Cruz, S. M., Tisdale, R., Dell’Omo, G., Lipp, H.-P., Wikelski, M. and Vyssotski, A. L.** (2016). Evidence that birds sleep in mid-flight. *Nat. Commun.* **7**, 12468.
- Ray, R. P., Nakata, T., Henningson, P. and Bompfrey, R. J.** (2016). Enhanced flight performance by genetic manipulation of wing shape in *Drosophila*. *Nat. Commun.* **7**, ncomms10851.
- Rayner, J. M. V.** (1988). Form and Function in Avian Flight. In *Current Ornithology* (ed. Johnston, R. F.), pp. 1–66. Springer US.
- Read, T. J. G., Segre, P. S., Middleton, K. M. and Altshuler, D. L.** (2016). Hummingbirds control turning velocity using body orientation and turning radius using asymmetrical wingbeat kinematics. *J. R. Soc. Interface* **13**,.
- Reich, P. B., Tjoelker, M. G., Machado, J.-L. and Oleksyn, J.** (2006). Universal scaling of respiratory metabolism, size and nitrogen in plants. *Nature* **439**, 457–461.
- Reiser, P. J., Welch, K. C., Suarez, R. K. and Altshuler, D. L.** (2013). Very low force-generating ability and unusually high temperature dependency in hummingbird flight muscle fibers. *J. Exp. Biol.* **216**, 2247–2256.
- Revell, L. J.** (2012). phytools: an R package for phylogenetic comparative biology (and other things). *Methods Ecol. Evol.* **3**, 217–223.
- Reynolds, K. V., Thomas, A. L. R. and Taylor, G. K.** (2014). Wing tucks are a response to atmospheric turbulence in the soaring flight of the steppe eagle *Aquila nipalensis*. *J. R. Soc. Interface* **11**, 20140645.
- Rezende, E. L., Gomes, F. R., Chappell, M. A. and Garland Jr., T.** (2009). Running Behavior and Its Energy Cost in Mice Selectively Bred for High Voluntary Locomotor Activity. *Physiol. Biochem. Zool.* **82**, 662–679.
- Ricklefs, R. E. and Starck, J. M.** (1996). Applications of Phylogenetically Independent Contrasts: A Mixed Progress Report. *Oikos* **77**, 167–172.
- Rico-Guevara, A. and Araya-Salas, M.** (2015). Bills as daggers? A test for sexually dimorphic weapons in a lekking hummingbird. *Behav. Ecol.* **26**, 21–29.
- Riskin, D. K., Iriarte-Díaz, J., Middleton, K. M., Breuer, K. S. and Swartz, S. M.** (2010). The effect of body size on the wing movements of pteropodid bats, with insights into thrust and lift production. *J. Exp. Biol.* **213**, 4110–4122.
- Riskin, D. K., Bergou, A., Breuer, K. S. and Swartz, S. M.** (2012). Upstroke wing flexion and the inertial cost of bat flight. *Proc. R. Soc. B Biol. Sci.* rspb20120346.

- Ristroph, L., Bergou, A. J., Ristroph, G., Coumes, K., Berman, G. J., Guckenheimer, J., Wang, Z. J. and Cohen, I.** (2010). Discovering the flight autostabilizer of fruit flies by inducing aerial stumbles. *Proc. Natl. Acad. Sci.* **107**, 4820–4824.
- Rummer, J. L., McKenzie, D. J., Innocenti, A., Supuran, C. T. and Brauner, C. J.** (2013). Root Effect Hemoglobin May Have Evolved to Enhance General Tissue Oxygen Delivery. *Science* **340**, 1327–1329.
- Sachs, G.** (2005). Aerodynamic yawing moment characteristics of bird wings. *J. Theor. Biol.* **234**, 471–478.
- Sandell, L. and Otto, S. P.** (2016). Probing the Depths of Biological Diversity During the Second Century of GENETICS. *Genet. Bethesda* **204**, 395–400.
- Sane, S. P. and Dickinson, M. H.** (2001). The control of flight force by a flapping wing: lift and drag production. *J. Exp. Biol.* **204**, 2607–2626.
- Sane, S. P. and Dickinson, M. H.** (2002). The aerodynamic effects of wing rotation and a revised quasi-steady model of flapping flight. *J. Exp. Biol.* **205**, 1087–1096.
- Sapir, N. and Dudley, R.** (2012). Backward flight in hummingbirds employs unique kinematic adjustments and entails low metabolic cost. *J. Exp. Biol.* **215**, 3603–3611.
- Sapir, N. and Dudley, R.** (2013). Implications of floral orientation for flight kinematics and metabolic expenditure of hover-feeding hummingbirds. *Funct. Ecol.* **27**, 227–235.
- Schlager, S.** (2017). Morpho and Rvcg – Shape Analysis in R: R-Packages for Geometric Morphometrics, Shape Analysis and Surface Manipulations. In *Statistical Shape and Deformation Analysis*, pp. 217–256. Academic Press.
- Schluter, D.** (1994). Experimental Evidence That Competition Promotes Divergence in Adaptive Radiation. *Science* **266**, 798–801.
- Schuchmann, K. L.** (1999). Family Trochilidae (Hummingbirds). In *Handbook of the Birds of the World, Vol. 5: Barn Owls to Hummingbirds* (ed. Hoyo, J. del, Elliott, A.), and Sargatal, J.), p. Barcelona: Lynx Edicions.
- Scutari, M. and Nagarajan, R.** (2013). Identifying significant edges in graphical models of molecular networks. *Artif. Intell. Med.* **57**, 207–217.
- Segre, P. S., Dakin, R., Zordan, V. B., Dickinson, M. H., Straw, A. D. and Altshuler, D. L.** (2015). Burst muscle performance predicts the speed, acceleration, and turning performance of Anna’s hummingbirds. *eLife* e11159.
- Segre, P. S., Dakin, R., Read, T. J. G., Straw, A. D. and Altshuler, D. L.** (2016). Mechanical Constraints on Flight at High Elevation Decrease Maneuvering Performance of Hummingbirds. *Curr. Biol.* **26**, 3368–3374.

- Sherry, D. F. and Hoshooley, J. S.** (2010). Seasonal hippocampal plasticity in food-storing birds. *Philos. Trans. R. Soc. B Biol. Sci.* **365**, 933–943.
- Shingleton, A. W., Frankino, W. A., Flatt, T., Nijhout, H. F. and Emlen, D. J.** (2007). Size and shape: the developmental regulation of static allometry in insects. *BioEssays* **29**, 536–548.
- Shipley, B.** (2000). *Cause and Correlation in Biology: A User's Guide to Path Analysis, Structural Equations and Causal Inference*. Cambridge: Cambridge University Press.
- Shipley, B.** (2004). Analysing the allometry of multiple interacting traits. *Perspect. Plant Ecol. Evol. Syst.* **6**, 235–241.
- Sholtis, K. M., Shelton, R. M. and Hedrick, T. L.** (2015). Field flight dynamics of hummingbirds during territory encroachment and defense. *PLoS ONE* **10**, e0125659.
- Sibly, R. M., Witt, C. C., Wright, N. A., Venditti, C., Jetz, W. and Brown, J. H.** (2012). Energetics, lifestyle, and reproduction in birds. *Proc. Natl. Acad. Sci.* **109**, 10937–10941.
- Skandalis, D. A. and Darveau, C.-A.** (2012). Morphological and Physiological Idiosyncrasies Lead to Interindividual Variation in Flight Metabolic Rate in Worker Bumblebees (*Bombus impatiens*). *Physiol. Biochem. Zool.* **85**, 657–670.
- Smith, R. J.** (2009). Use and misuse of the reduced major axis for line-fitting. *Am. J. Phys. Anthropol.* **140**, 476–486.
- Socha, J. J., Jafari, F., Munk, Y. and Byrnes, G.** (2015). How animals glide: from trajectory to morphology. *Can. J. Zool.* **93**, 901–924.
- Song, J., Luo, H. and Hedrick, T. L.** (2014). Three-dimensional flow and lift characteristics of a hovering ruby-throated hummingbird. *J. R. Soc. Interface* **11**, 20140541.
- Song, J., Luo, H. and Hedrick, T. L.** (2015a). Wing-pitching mechanism of hovering Ruby-throated hummingbirds. *Bioinspir. Biomim.* **10**, 016007.
- Song, J., Luo, H. and Hedrick, T. L.** (2015b). Performance of a quasi-steady model for hovering hummingbirds. *Theor. Appl. Mech. Lett.* **5**, 50–53.
- Song, J., Tobalske, B. W., Powers, D. R., Hedrick, T. L. and Luo, H.** (2016). Three-dimensional simulation for fast forward flight of a calliope hummingbird. *R. Soc. Open Sci.* **3**, 160230.
- South, A.** (2011). rworldmap: A New R package for Mapping Global Data. *R J.* **3**, 35–43.
- Srygley, R. B. and Thomas, A. L. R.** (2002). Unconventional lift-generating mechanisms in free-flying butterflies. *Nature* **420**, 660–664.

- Stanley, S. M.** (1973). An Explanation for Cope's Rule. *Evolution* **27**, 1–26.
- Sterbing-D'Angelo, S., Chadha, M., Chiu, C., Falk, B., Xian, W., Barcelo, J., Zook, J. M. and Moss, C. F.** (2011). Bat wing sensors support flight control. *Proc. Natl. Acad. Sci.* **108**, 11291–11296.
- Stiles, F. G.** (1971). Time, Energy, and Territoriality of the Anna Hummingbird (*Calypte anna*). *Science* **173**, 818–821.
- Stiles, F. G.** (1973). *Food supply and the annual cycle of the Anna hummingbird*. Berkeley : University of California Press.
- Stiles, F. G.** (1978). Possible Specialization for Hummingbird-Hunting in the Tiny Hawk. *The Auk* **95**, 550–553.
- Stiles, F. G.** (1982). Aggressive and courtship displays of the male Anna's hummingbird. *Condor* 208–225.
- Stiles, F. G.** (1995). Behavioral, Ecological and Morphological Correlates of Foraging for Arthropods by the Hummingbirds of a Tropical Wet Forest. *The Condor* **97**, 853–878.
- Stiles, F. G.** (2008). Ecomorphology and phylogeny of hummingbirds: Divergence and convergence in adaptations to high elevations. *Ornitol. Neotropical* **19**, 511–520.
- Stiles, F. G. and Wolf, L. L.** (1979). Ecology and Evolution of Lek Mating Behavior in the Long-Tailed Hermit Hummingbird. *Ornithol. Monogr.* 1–78.
- Stiles, F. G., Altshuler, D. L. and Smith, K. G.** (2004). Conflicting terminology for wing measurements in ornithology and aerodynamics. *The Auk* **121**, 973–976.
- Stiles, F. G., Altshuler, D. L., Dudley, R. and Johnson, K. P.** (2005). Wing morphology and flight behavior of some North American hummingbird species. *The Auk* **122**, 872–886.
- Stockwell, E. F.** (2001). Morphology and flight manoeuvrability in New World leaf-nosed bats (Chiroptera: Phyllostomidae). *J. Zool.* **254**, 505–514.
- Su, Y.-S. and Yajima, M.** (2014). *R2jags: A Package for Running jags from R*. <https://CRAN.R-project.org/package=R2jags>
- Suarez, R. K. and Gass, C. L.** (2002). Hummingbird foraging and the relation between bioenergetics and behaviour. *Comp. Biochem. Physiol. A. Mol. Integr. Physiol.* **133**, 335–343.
- Suarez, R. K. and Welch, K. C.** (2017). Sugar Metabolism in Hummingbirds and Nectar Bats. *Nutrients* **9**, 743.

- Suarez, R. K., Lighton, J. R. B., Moyes, C. D., Brown, G. S., Gass, C. L. and Hockachka, P. W.** (1990). Fuel Selection in Rufous Hummingbirds: Ecological Implications of Metabolic Biochemistry. *Proc. Natl. Acad. Sci. U. S. A.* **87**, 9207–9210.
- Suarez, R. K., Lighton, J. R. B., Brown, G. S. and Mathieu-Costello, O.** (1991). Mitochondrial respiration in hummingbird flight muscles. *Proc. Natl. Acad. Sci. U. S. A.* **88**, 4870–4873.
- Suarez, R. K., M, L. G. H. and Welch, K. C.** (2011). The sugar oxidation cascade: aerial refueling in hummingbirds and nectar bats. *J. Exp. Biol.* **214**, 172–178.
- Swartz, S. M., Groves, M. S., Kim, H. D. and Walsh, W. R.** (1996). Mechanical properties of bat wing membrane skin. *J. Zool.* **239**, 357–378.
- Swartz, S. M., Bishop, K. and Ismael Aguirre, M.-F.** (2006). Dynamic Complexity of Wing Form in Bats: Implications for Flight Performance. In *Functional and Evolutionary Ecology of Bats* (ed. Zubaid, A.), McCracken, G. F.), and Kunz, Thomas H.), pp. 110–130. Oxford, UK: Oxford University Press.
- Székely, T., Reynolds, J. D. and Figuerola, J.** (2000). Sexual Size Dimorphism in Shorebirds, Gulls, and Alcids: The Influence of Sexual and Natural Selection. *Evolution* **54**, 1404–1413.
- Székely, T., Freckleton, R. P. and Reynolds, J. D.** (2004). Sexual selection explains Rensch's rule of size dimorphism in shorebirds. *Proc. Natl. Acad. Sci. U. S. A.* **101**, 12224–12227.
- Tamm, S.** (1985). Breeding territory quality and agonistic behavior: effects of energy availability and intruder pressure in hummingbirds. *Behav. Ecol. Sociobiol.* **16**, 203–207.
- Tanaka, H., Suzuki, H., Kitamura, I., Maeda, M. and Liu, H.** (2013). Lift generation of hummingbird wing models with flexible loosened membranes. In *Intelligent Robots and Systems (IROS), 2013 IEEE/RSJ International Conference on*, pp. 3777–3783.
- Tarka, M., Åkesson, M., Hasselquist, D. and Hansson, B.** (2014). Intralocus Sexual Conflict over Wing Length in a Wild Migratory Bird. *Am. Nat.* **183**, 62–73.
- Taylor, G. K., Nudds, R. L. and Thomas, A. L. R.** (2003). Flying and swimming animals cruise at a Strouhal number tuned for high power efficiency. *Nature* **425**, 707–711.
- Taylor, G. K., Reynolds, K. V. and Thomas, A. L. R.** (2016). Soaring energetics and glide performance in a moving atmosphere. *Phil Trans R Soc B* **371**, 20150398.
- Temeles, E. J. and Kress, W. J.** (2003). Adaptation in a Plant-Hummingbird Association. *Science* **300**, 630–633.

- Theriault, D. H., Fuller, N. W., Jackson, B. E., Bluhm, E., Evangelista, D., Wu, Z., Betke, M. and Hedrick, T. L.** (2014). A protocol and calibration method for accurate multi-camera field videography. *J. Exp. Biol.* **217**, 1843–1848.
- Thomas, A. L. R.** (1993). On the aerodynamics of birds' tails. *Phil Trans R Soc Lond B* **340**, 361–380.
- Thomas, A. L. R.** (1996). The Flight of Birds that have Wings and a Tail: Variable Geometry Expands the Envelope of Flight Performance. *J. Theor. Biol.* **183**, 237–245.
- Tobalske, B. W., Hedrick, T. L., Dial, K. P. and Biewener, A. A.** (2003). Comparative power curves in bird flight. *Nature* **421**, 363–366.
- Tobalske, B. W., Warrick, D. R., Clark, C. J., Powers, D. R., Hedrick, T. L., Hyder, G. A. and Biewener, A. A.** (2007a). Three-dimensional kinematics of hummingbird flight. *J. Exp. Biol.* **210**, 2368–2382.
- Tobalske, B. W., Warrick, D. R., Clark, C. J., Powers, D. R., Hedrick, T. L., Hyder, G. A. and Biewener, A. A.** (2007b). Three-dimensional kinematics of hummingbird flight. *J. Exp. Biol.* **210**, 2368–2382.
- Tobalske, B. W., Hearn, J. W. D. and Warrick, D. R.** (2009). Aerodynamics of intermittent bounds in flying birds. *Exp. Fluids* **46**, 963–973.
- Tobalske, B. W., Biewener, A. A., Warrick, D. R., Hedrick, T. L. and Powers, D. R.** (2010). Effects of flight speed upon muscle activity in hummingbirds. *J. Exp. Biol.* **213**, 2515–2523.
- Tobler, A. and Nijhout, H. F.** (2010). Developmental constraints on the evolution of wing-body allometry in *Manduca sexta*. *Evol. Dev.* **12**, 592–600.
- Truong, Q. T., Nguyen, Q. V., Truong, V. T., Park, H. C., Byun, D. Y. and Goo, N. S.** (2011). A modified blade element theory for estimation of forces generated by a beetle-mimicking flapping wing system. *Bioinspir. Biomim.* **6**, 036008.
- Tucker, V. A. and Parrott, G. C.** (1970). Aerodynamics of Gliding Flight in a Falcon and Other Birds. *J. Exp. Biol.* **52**, 345–367.
- Usherwood, J. R.** (2009). Inertia may limit efficiency of slow flapping flight, but mayflies show a strategy for reducing the power requirements of loiter. *Bioinspir. Biomim.* **4**, 015003.
- Usherwood, J. R. and Ellington, C. P.** (2002). The aerodynamics of revolving wings II. Propeller force coefficients from mayfly to quail. *J. Exp. Biol.* **205**, 1565–1576.
- Uyeda, J. C., Pennell, M. W., Miller, E. T., Maia, R. and McClain, C. R.** (2017). The Evolution of Energetic Scaling across the Vertebrate Tree of Life. *Am. Nat.* **190**, 185–199.

- van Buuren, S. and Groothuis-Oudshoorn, K.** (2011). Multivariate imputation by chained equations in R. *J. Stat. Softw.* **45**, 1–67.
- van de Pol, M. and Wright, J.** (2009). A simple method for distinguishing within- versus between-subject effects using mixed models. *Anim. Behav.* **77**, 753–758.
- Voelkl, B., Portugal, S. J., Unsöld, M., Usherwood, J. R., Wilson, A. M. and Fritz, J.** (2015). Matching times of leading and following suggest cooperation through direct reciprocity during V-formation flight in ibis. *Proc. Natl. Acad. Sci.* **112**, 2115–2120.
- Vogel, S.** (1989). Drag and reconfiguration of broad leaves in high winds. *J. Exp. Bot.* **40**, 941–948.
- Voigt, C. C.** (2000). Intraspecific scaling of flight power in the bat *Glossophaga soricina* (Phyllostomidae). *J. Comp. Physiol. B* **170**, 403–410.
- Voigt, C. C., Heckel, G. and Mayer, F.** (2005). Sexual selection favours small and symmetric males in the polygynous greater sac-winged bat *Saccopteryx bilineata* (Emballonuridae, Chiroptera). *Behav. Ecol. Sociobiol.* **57**, 457–464.
- Voje, K. L., Hansen, T. F., Egset, C. K., Bolstad, G. H. and Pélabon, C.** (2014). Allometric Constraints and the Evolution of Allometry. *Evolution* **68**, 866–885.
- Walker, J. A.** (2002). Rotational lift: something different or more of the same? *J. Exp. Biol.* **205**, 3783–3792.
- Walker, J. A. and Westneat, M. W.** (2000). Mechanical performance of aquatic rowing and flying. *Proc. R. Soc. Lond. B Biol. Sci.* **267**, 1875–1881.
- Walker, S. M., Thomas, A. L. R. and Taylor, G. K.** (2009). Photogrammetric reconstruction of high-resolution surface topographies and deformable wing kinematics of tethered locusts and free-flying hoverflies. *J. R. Soc. Interface* **6**, 351–366.
- Waller, J. T. and Svensson, E. I.** (2017). Body size evolution in an old insect order: No evidence for Cope’s Rule in spite of fitness benefits of large size. *Evolution* **71**, 2178–2193.
- Wang, H., Zeng, L. and Yin, C.** (2002). Measuring the body position, attitude and wing deformation of a free-flight dragonfly by combining a comb fringe pattern with sign points on the wing. *Meas. Sci. Technol.* **13**, 903.
- Ward, B. J., Day, L. B., Wilkening, S. R., Wylie, D. R., Saucier, D. M. and Iwaniuk, A. N.** (2012). Hummingbirds have a greatly enlarged hippocampal formation. *Biol. Lett.* **8**, 657–659.
- Warrick, D. R., Bundle, M. W. and Dial, K. P.** (2002). Bird maneuvering flight: Blurred bodies, clear heads. *Integr. Comp. Biol.* **42**, 141–148.

- Warrick, D. R., Tobalske, B. W. and Powers, D. R.** (2005). Aerodynamics of the hovering hummingbird. *Nature* **435**, 1094–1097.
- Warrick, D. R., Tobalske, B. W. and Powers, D. R.** (2009). Lift production in the hovering hummingbird. *Proc. R. Soc. B Biol. Sci.* **276**, 3747–3752.
- Warrick, D., Hedrick, T., Fernandez, M. J., Tobalske, B. and Biewener, A.** (2012). Hummingbird flight. *Curr. Biol.* **22**, R472–R477.
- Weimerskirch, H., Bishop, C., Jeanniard-du-Dot, T., Prudor, A. and Sachs, G.** (2016). Frigate birds track atmospheric conditions over months-long transoceanic flights. *Science* **353**, 74–78.
- Weis-Fogh, T.** (1972). Energetics of hovering flight in hummingbirds and in *Drosophila*. *J. Exp. Biol.* **56**, 79–104.
- Welch, K. C. and Altshuler, D. L.** (2009). Fiber type homogeneity of the flight musculature in small birds. *Comp. Biochem. Physiol. B-Biochem. Mol. Biol.* **152**, 324–331.
- Welch, K. C., Altshuler, D. L. and Suarez, R. K.** (2007). Oxygen consumption rates in hovering hummingbirds reflect substrate-dependent differences in P/O ratios: carbohydrate as a 'premium fuel'. *J. Exp. Biol.* **210**, 2146–2153.
- Welch, K. C., Allalou, A., Sehgal, P., Cheng, J. and Ashok, A.** (2013). Glucose Transporter Expression in an Avian Nectarivore: The Ruby-Throated Hummingbird (*Archilochus colubris*). *PLOS ONE* **8**, e77003.
- Welch, K. C., Chen, C. C. and W** (2014). Sugar flux through the flight muscles of hovering vertebrate nectarivores: a review. *J. Comp. Physiol. B Biochem. Syst. Environ. Physiol. Heidelberg.* **184**, 945–959.
- Wells, D. J.** (1993a). Ecological correlates of hovering flight of hummingbirds. *J. Exp. Biol.* **178**, 59–70.
- Wells, D. J.** (1993b). Muscle performance in hovering hummingbirds. *J. Exp. Biol.* **178**, 39–57.
- Wells, S. and Baptista, L. F.** (1979). Displays and Morphology of an Anna × Allen Hummingbird Hybrid. *Wilson Bull.* **91**, 524–532.
- Wells, S., Bradley, R. A. and Baptista, L. F.** (1978). Hybridization in Calypte Hummingbirds. *The Auk* **95**, 537–549.
- West, G. B., Brown, J. H. and Enquist, B. J.** (1997). A General Model for the Origin of Allometric Scaling Laws in Biology. *Science* **276**, 122–126.

- West, G. B., Savage, V. M., Gillooly, J., Enquist, B. J., Woodruff, W. H. and Brown, J. H.** (2003). Physiology (communication arising): Why does metabolic rate scale with body size? *Nature* **421**, 713–713.
- Wester, P.** (2014). Feeding on the wing: hovering in nectar-drinking Old World birds – more common than expected. *Emu* **114**, 171–183.
- Wickham, H. and Francois, R.** (2015). *dplyr: A Grammar of Data Manipulation*.  
<https://CRAN.R-project.org/package=dplyr>
- Withers, P. C.** (1981). An Aerodynamic Analysis of Bird Wings as Fixed Aerofoils. *J. Exp. Biol.* **90**, 143–162.
- Wolf, L. L.** (1969). Female Territoriality in a Tropical Hummingbird. *The Auk* **86**, 490–504.
- Wolf, L. L.** (1975). “Prostitution” Behavior in a Tropical Hummingbird. *The Condor* **77**, 140–144.
- Wolf, L. L. and Stiles, F. G.** (1970). Evolution of Pair Cooperation in a Tropical Hummingbird. *Evolution* **24**, 759–773.
- Wolf, L. L., Hainsworth, F. R. and Stiles, F. G.** (1972). Energetics of Foraging: Rate and Efficiency of Nectar Extraction by Hummingbirds. *Science* **176**, 1351–1352.
- Wolf, M., Ortega-Jimenez, V. M. and Dudley, R.** (2013). Structure of the vortex wake in hovering Anna’s hummingbirds (*Calypte anna*). *Proc. R. Soc. B Biol. Sci.* **280**, 20132391–20132391.
- Wood, S. N.** (2004). Stable and Efficient Multiple Smoothing Parameter Estimation for Generalized Additive Models. *J. Am. Stat. Assoc.* **99**, 673–686.
- Xiao, X., White, E. P., Hooten, M. B. and Durham, S. L.** (2011). On the use of log-transformation vs. nonlinear regression for analyzing biological power laws. *Ecology* **92**, 1887–1894.
- Yales, F. E.** (1979). Comparative physiology: compared to what? *Am. J. Physiol.-Regul. Integr. Comp. Physiol.* **237**, R1–R2.
- Yanega, G. M. and Rubega, M. A.** (2004). Feeding mechanisms: Hummingbird jaw bends to aid insect capture. *Nature* **428**, 615–615.
- Young, J., Walker, S. M., Bomphrey, R. J., Taylor, G. K. and Thomas, A. L. R.** (2009a). Details of Insect Wing Design and Deformation Enhance Aerodynamic Function and Flight Efficiency. *Science* **325**, 1549–1552.

**Young, J., Walker, S. M., Bomphrey, R. J., Taylor, G. K. and Thomas, A. L. R.** (2009b). Details of Insect Wing Design and Deformation Enhance Aerodynamic Function and Flight Efficiency. *Science* **325**, 1549–1552.

**Zenzal, T. J., Fish, A. C., Jones, T. M., Ospina, E. A. and Moore, F. R.** (2013). Observations of Predation and Anti-Predator Behavior of Rubythroated Hummingbirds During Migratory Stopover. *Southeast. Nat.* **12**, N21–N25.

**Zheng, L., Hedrick, T. L. and Mittal, R.** (2013). Time-Varying Wing-Twist Improves Aerodynamic Efficiency of Forward Flight in Butterflies. *PLOS ONE* **8**, e53060.

## Appendix A Species naming decisions

The following decisions on species naming and phylogenetic placement were made:

1. It is not established that *Eriocnemis sapphiropygia* is distinct from *E. luciani*, so we use the *E. luciani* position in the tree for analyzing *E. sapphiropygia* data.
2. It is not established that *Threnetes niger* is distinct from *T. leucurus*, so we use the *T. leucurus* position for *T. niger*.
3. *Haplophaedia assimilis* is not present in the phylogeny but is a recent split from *H. aeureliae*, and we therefore use the position of *H. aureliae*.
4. The data for *Eugenes fulgens* is obtained from the *E. fulgens fulgens* subspecies, but the phylogenetic placement on the tree is for *E. fulgens spectabilis*. However, because they are certainly sister taxa, we use the tip position of *E. f. spectabilis*.
5. The phylogenetic hypothesis suggests that the two subspecies of *Amazilia saucerrottei*, *A. s. hoffmanni* and *A. s. saucerrottei*, are actually distinct species; our single specimen is of *A. s. hoffmanni*.
6. Specimens labelled *Acestrura mulstant* were renamed *Chaetocercus mulsant* to match the current phylogenetic hypothesis.
7. Specimens labelled *Leucippus chionogaster* were renamed *Amazilia chionogaster* to match the current phylogenetic hypothesis.
8. Specimens labelled *Saucerottia edward* were renamed *Amazilia edward* to match the current phylogenetic hypothesis.
9. *Chlorestes notatus* can take two possible positions on the tree (McGuire et al., 2014) but is likely sister to *Damophila julie*. This uncertainty is included in the analysis by including both positions in the posterior distribution of the phylogenetic hypothesis.